Adaptive interference suppression algorithms for DS-UWB systems

This thesis is submitted in partial fulfilment of the requirements for Doctor of Philosophy (Ph.D.)

Sheng Li
Communications Research Group
Department of Electronics
University of York

October 2010

ABSTRACT

In multiuser ultra-wideband (UWB) systems, a large number of multipath components (MPCs) are introduced by the channel. One of the main challenges for the receiver is to effectively suppress the interference with affordable complexity. In this thesis, we focus on the linear adaptive interference suppression algorithms for the direct-sequence ultra-wideband (DS-UWB) systems in both time-domain and frequency-domain.

In the time-domain, symbol by symbol transmission multiuser DS-UWB systems are considered. We first investigate a generic reduced-rank scheme based on the concept of joint and iterative optimization (JIO) that jointly optimizes a projection vector and a reduced-rank filter by using the minimum mean-squared error (MMSE) criterion. A low-complexity scheme, named Switched Approximations of Adaptive Basis Functions (SAABF), is proposed as a modification of the generic scheme, in which the complexity reduction is achieved by using a multi-branch framework to simplify the structure of the projection vector. Adaptive implementations for the SAABF scheme are developed by using least-mean squares (LMS) and recursive least-squares (RLS) algorithms. We also develop algorithms for selecting the branch number and the model order of the SAABF scheme. Secondly, a novel linear reduced-rank blind adaptive receiver based on JIO and the constrained constant modulus (CCM) design criterion is proposed that offers higher spectrum efficiency. Adaptive implementations for the blind JIO receiver are developed by using the normalized stochastic gradient (NSG) and RLS algorithms. In order to obtain a low-complexity scheme, the columns of the projection matrix with the RLS algorithm are updated individually. Blind channel estimation algorithms for both versions (NSG and RLS) are implemented. Assuming the perfect timing, the JIO receiver only requires the knowledge of the spreading code of the desired user and the received data.

In the frequency-domain, we propose two adaptive detection schemes based on single-carrier frequency domain equalization (SC-FDE) for the block by block transmission multiuser DS-UWB systems, which are termed structured channel estimation (SCE) and direct adaptation (DA). Both schemes use the MMSE linear detection strategy and employ a cyclic prefix. In the SCE scheme, we perform the adaptive channel estimation in the frequency-domain and implement the despreading in the time-domain after the FDE. In

this scheme, the MMSE detection requires the knowledge of the number of users and the noise variance. For this purpose, we propose low-complexity algorithms for estimating these parameters. In the DA scheme, the interference suppression task is fulfilled with only one adaptive filter in the frequency-domain and a new signal expression is adopted to simplify the design of such a filter. LMS, RLS and conjugate gradient (CG) adaptive algorithms are then developed for both schemes.

Another strand of investigation considers adaptive detectors and frequency domain equalization for multiuser DS-UWB systems with block transmissions and biased estimation methods. Biased estimation techniques can provide performance improvements to the existing unbiased estimation algorithms. In this work, biased adaptive estimation techniques based on shrinkage estimators are devised and incorporated into RLS-type algorithms. For the SCE scheme, automatic shrinkage factor mechanisms are proposed and incorporated into RLS estimators, obtaining a lower MSE of the channel estimation. For the DA scheme, the automatic shrinkage factors are incorporated directly to the adaptive receiver weights. The results show that a shorter data support is required by the proposed biased DA-RLS technique. An analysis of fundamental estimation limits of the proposed frequency domain biased estimators is included along with the derivation of appropriate Cramér-Rao lower bounds (CRLB).

CONTENTS

Acknowledgements

Firstly, I would like to express my most sincere gratitude to my supervisor, Dr. Rodrigo C. de Lamare, for his help and valuable supervision with my research, without which much of this work would not have been possible.

Further thanks go to all members of the Communications Research Group, for their support throughout my Ph.D. research.

Finally, my deep gratitude goes to my parents and my wife Xiaolei Zhang for their unconditional support, end-less love and encouragement.

Declaration

Some of the research presented in this thesis has resulted in some publications. These publications are listed at the end of Chapter 1.

All work presented in this thesis as original is so, to the best knowledge of the author. References and acknowledgements to other researchers have been given as appropriate.

Glossary

ADC	Analog-to-Digital Converters
AT	Automatic Tuning
AVF	Auxiliary Vector Filtering
AWGN	Additive White Gaussian Noise
BCG	Block Conjugate Gradient
BER	Bit Error Rate
BOK	Bi-Orthogonal Keying (4BOK)
BPAM	Binary Pulse Amplitude Modulation
BPSK	Binary Phase Shift Keying
CCM	Constrained Constant Modulus
CDMA	Code-Division Multiple Access
CG	Conjugate Gradient
CM	Constant Modulus
CMF	Chip-Matched Filter
CMV	Constrained Minimum Variance
CP	Cyclic-Prefixed
CRLB	Cramér-Rao Lower Bound
DA	Direct Adaptation
DFT	Discrete Fourier Transform
DS-UWB	Direct-sequence Ultra-wideband
EB	Estimator Based
FCC	Federal Communications Commission
FIR	Finite Impulse Response
FR	Full-Rank
GPS	Global Positioning System
IBI	Inter Block Interference
ISI	Inter-symbol Interference
JIO	Joint Iterative Optimization
LDPC	Low-Density Parity-Check
LMS	Least-mean Squares
LS	Least Squares
MAI	Multiple Access Interference
ML	Maximum Likelihood
MMSE	Minimum Mean-squared Error
MPCs	Multipath Components
MSE	Mean-squared Error
MSWF	Multistage Wiener Filter

MVUE	Minimum Variance Unbiased Estimator
NBI	Narrow Band Interference
NLOS	Non-line of Sight
NSG	Normalized Stochastic Gradient
OFDM	Orthogonal Frequency-Division Multiplexing
OOK	On-Off Keying
PC	Principle Component
PPM	Pulse Position Modulation
PSM	Pulse shape modulation
RLS	Recursive Least Squares
RR	Reduced-Rank
RRC	Root-Raised Cosine
SAABF	Switched Approximations of Adaptive Basis Functions
SCE	Structured Channel Estimation
SC-FDE	Single-carrier Frequency Domain Equalization
SG	Stochastic Gradient
SINR	Signal-plus-Interference-to-Noise Ratio
SIR	Signal-to-Interference Ratio
SNR	Signal-to-Noise Ratio
SVD	Singular Value Decomposition
TH-UWB	Time-hopping UWB
UFZ	UWB Friendly Zone
UWB	Ultra-wideband
WPANs	Wireless Personal Area Networks

List of Symbols

∇	Gradient
$O(\cdot)$	Complexity
$\mathbb{E}[\cdot]$	Expectation
∞	Infinity
$\mathfrak{R}(\cdot)$	Real part
$\mathfrak{C}(\cdot)$	Imaginary part
Π	Product
$\sum$	Sum
$\|\cdot\|$	Euclidean norm
$\|\cdot\|$	Absolute
$\mathrm{diag}(\mathbf{a})$	A diagonal matrix with the diagonal vector equals to $\mathbf{a}$
trace$(\cdot)$	Trace of a matrix
$\boldsymbol{I}$	Identity matrix
span$(\cdot)$	Span a space
$\mathbb{C}^{m\times q}$	space of complex valued matrices of size m by q
$\mathbb{R}^{m\times q}$	space of real valued matrices of size m by q

LIST OF FIGURES

LIST OF TABLES

1. INTRODUCTION

Contents

1.1 UWB Systems

Ultra-wideband (UWB) technology is a promising short-range wireless communication technique. The research on impulse radio by Win and Scholtz [1]- [3], has placed UWB as a potentially very fast communication scheme. In 2002, the Federal Communications Commission (FCC) in the US release a $7.5GHz$ ($3.1GHz - 10.6GHz$) huge bandwidth for unlicensed use of UWB systems [4]- [10]. This permit boosts the development of the UWB communications for commercial applications. Using extremely short pulses, UWB can be considered as a multipath immunity communication. This is because the multipath components (MPCs) in UWB systems whose path lengths differ by only a few centimeters, e.g., 10 cm for a signal bandwidth of 3 GHz, are resolvable at the receiver [10], [11].

The advantages of UWB systems on the aspect of engineering can be summarized by examining Shannon's capacity equation as shown in [6]- [10]. The channel capacity of communications systems can be improved by increasing the channel bandwidth or the signal to noise ratio (SNR). With the huge bandwidth, UWB communications could have high capacity of the channel. Another way to summarize the benefits of UWB is to consider the degree of diversity at the receiver [9]. For UWB systems, the huge transmission bandwidths introduce a large number of resolvable MPCs at the receiver, and hence, a high degree of diversity is available [11]. Receivers for UWB systems are required to

efficiently suppress the severe inter-symbol interference (ISI) that is caused by the dense multipath channel and the multiple-access interference (MAI) that is caused by the lack of orthogonality between signals at the receiver in multiuser communications.

In this section, some basic aspects of the UWB systems are introduced. Parameters and the technologies that are adopted in our system model are presented and discussed.

1.1.1 UWB Pulse-Shaping

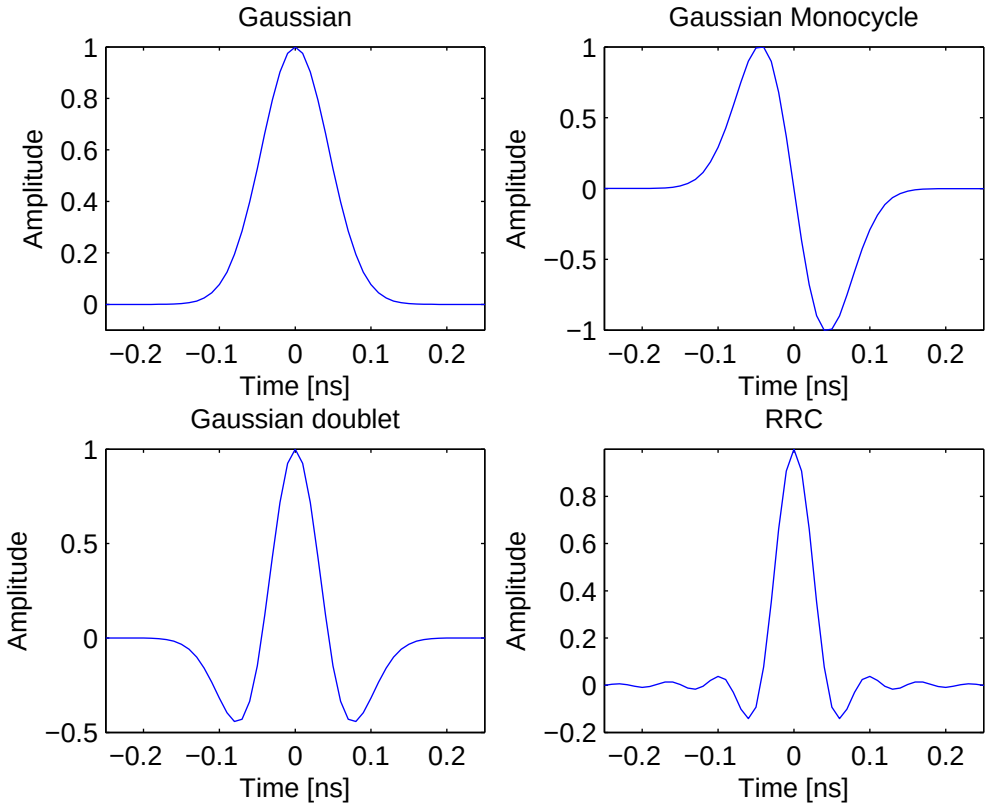

Fig. 1.1: Typical UWB waveforms

The extremely short pulses make the UWB a unique technique, the pulse shaping is an important aspect of designing a UWB communication systems. In the document [4], the UWB signal has been described with the following characteristics: the maximum transmission power is $-41.3dBm/MHz$; the minimum $-10dB$ bandwidth is $500MHz$ and the power level beyond $-20dB$ bandwidth must at least $20dB$ lower than the maximum transmission power.

It should be noted that due to the pressure from other wireless groups such as the

global positioning system (GPS), the allowed maximum power level $-41.3dBm/MHz$ is a conservative limitation [10]. For example, in the UWB Friendly Zone (UFZ) of Singapore, the maximum power level allowed is $-35.3dB/MHz$ [7].

A typical class of UWB pulses is the Gaussian waveforms which consist of the Gaussian pulse, the Gaussian monocycle and the Gaussian doublet [10]. Another class of pulse shaping technology that is widely used is the raised-cosine pulse shaping and the root-raised cosine (RRC) pulse shaping [7], [12]. The traditional rectangular waveform which is used for code-division multiple access (CDMA) systems cannot be adopted for UWB systems since the power level of the sidelobe of this kind of pulse is too high. In this thesis, the pulse waveform is modeled as the RRC pulse with a roll-off factor of 0.5 [12]. Fig.1.1 shows the Gaussian waveforms and the RRC waveform. The main advantage of these typical UWB pulses is that they can be generated easily [10], the main drawback of them is the poor fitness of the spectral mask [14].

The design of orthogonal waveforms have been described in [10] and some new waveforms that can fit the FCC spectral mask have been proposed in [13] and [14]. These waveforms could improve the performance of the UWB communications. However, the adoption of these technologies will increase the complexity of the hardware design.

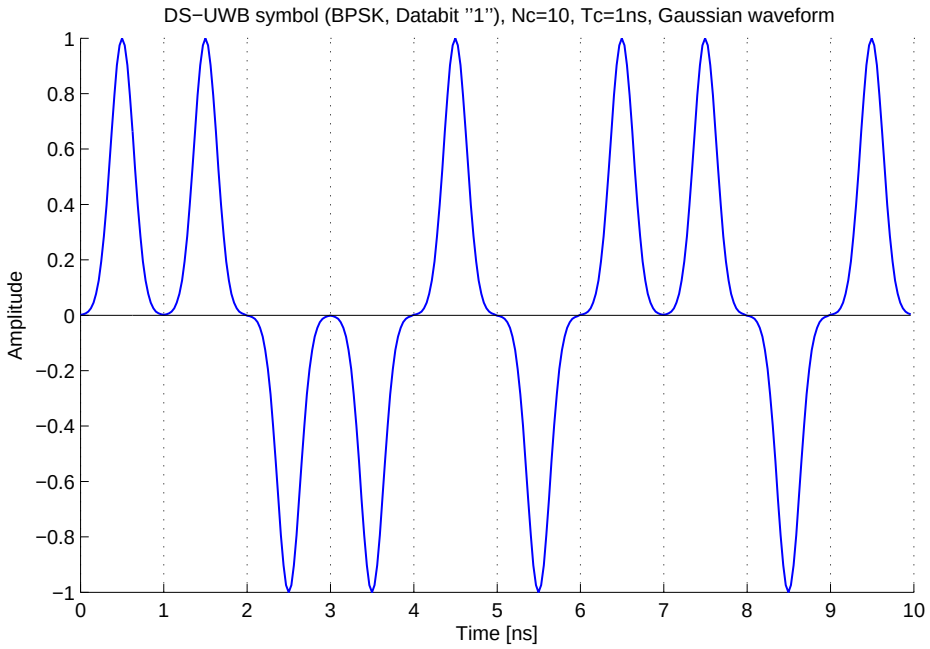

Fig. 1.2: Time window of transmitted data bit '1' in a BPSK DS-UWB system.

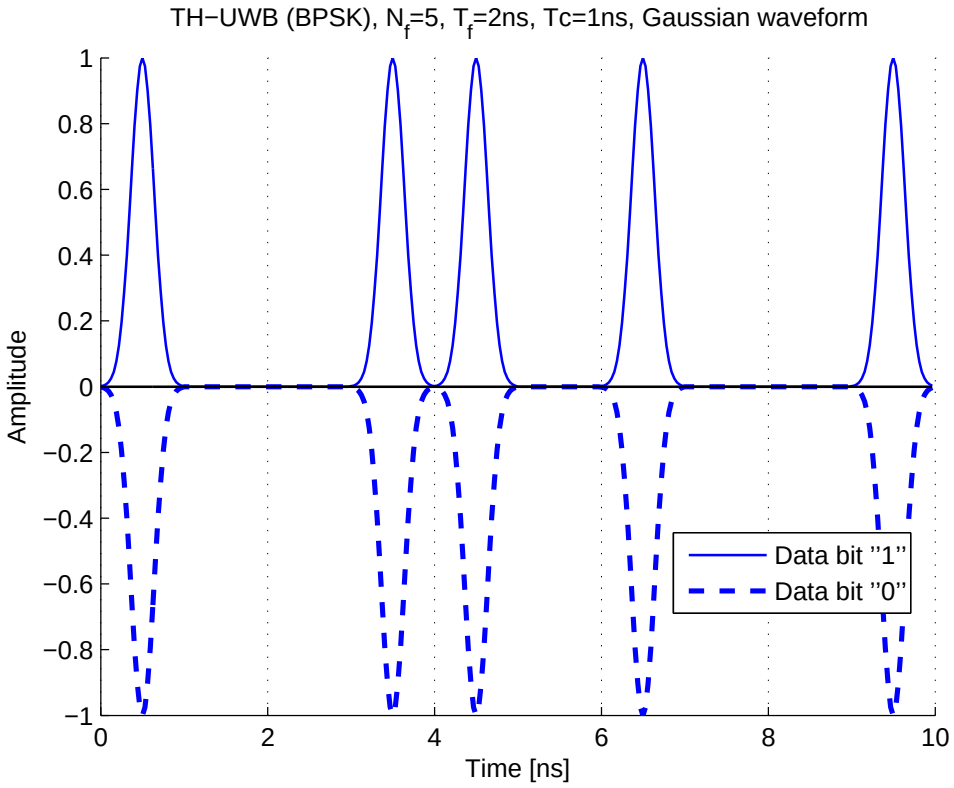

Fig. 1.3: Time window of transmitted data bits in a BPSK TH-UWB system.

1.1.2 Spread-Spectrum Techniques in UWB

There are two popular spread-spectrum techniques in UWB communications, namely Direct-sequence UWB (DS-UWB) and Time-hopping UWB (TH-UWB) [6]. In the DS-UWB system, the information symbols are spread by a pseudo-random (PR) code and the pulses are transmitted continuously [6]. In Fig.1.2, the transmitted data bit '1' in a BPSK DS-UWB system is presented. The spreading code is $\mathbf{s} = [1, 1, -1, -1, 1, -1, 1, 1, -1, 1]$ and the spreading gain equals to 10. The TH-UWB uses a PR code to define the pulse transmitting time [3]. In Fig. 1.3, the transmitted data bits in a BPSK TH-UWB system are presented. In this example, the number of frames is set to 5 and the number of chips in each frame is set to 2. The spreading gain equals to 10 which is the same as the example in Fig. 1.2.

The TH-UWB has been chosen for low-data rate applications such as ranging and localization [15]. Due to the sensitiveness of the synchronization in TH-UWB system, DS-UWB performs better for high-speed indoor links [16]. In 2005, direct-sequence DS-UWB was proposed as a possible standard physical layer technology for wireless personal area networks (WPANs) and it has the potential to provide high data rates ranging from

$28Mbps$ to $1.32Gbps$ [12], [17]. In this thesis, the target operate environment is assumed to be non-line of sight (NLOS) indoor links with high data rate, so the DS-UWB system is adopted. We remark that the adaptive receivers proposed in this thesis are general schemes, which means they can work not only in the DS-UWB systems, but also in the TH-UWB systems and other wireless communication systems.

1.1.3 UWB Modulation

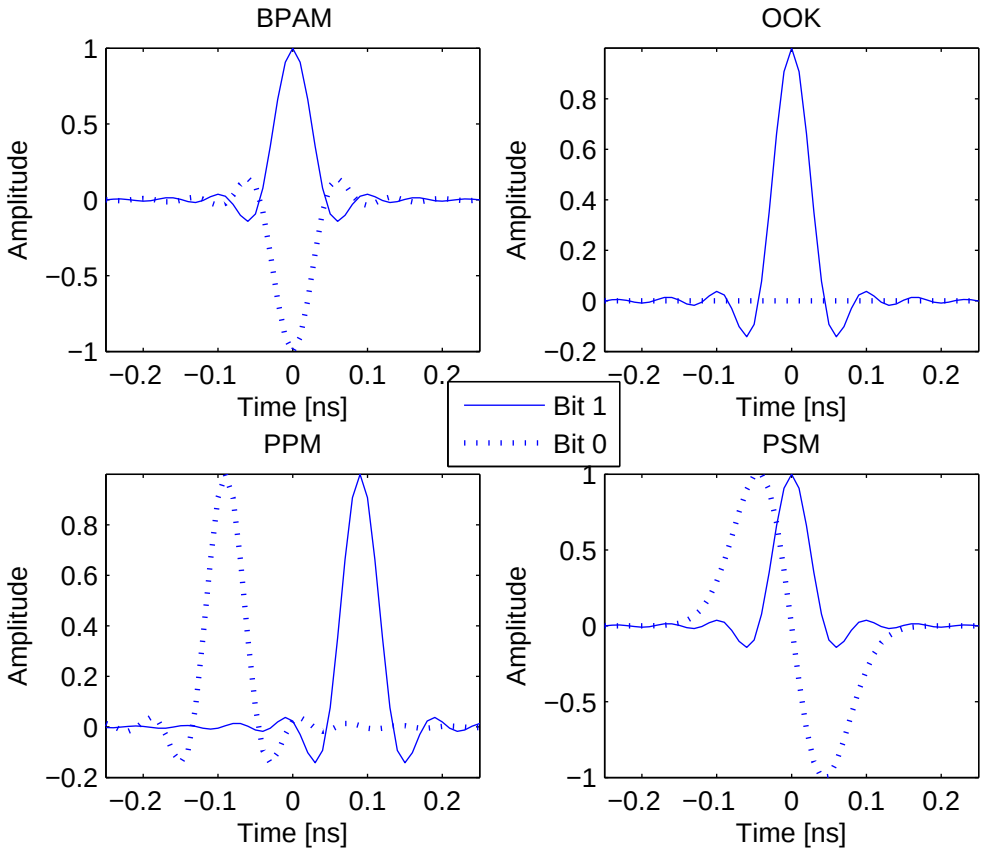

Fig. 1.4: UWB modulation schemes

In Binary Pulse Amplitude Modulation (BPAM), the data bits are represented by using different amplitudes [6]. Let us denote the pulse waveform as $p_t(t)$. If we use $+p_t(t)$ and $-p_t(t)$ to represents the data bit of $+1$ and 0 respectively, then the BPAM is equivalent to the Binary Phase-Shift Keying (BPSK) [7]. On-Off Keying (OOK), using $+p_t(t)$ and 0 to represents the data bit of $+1$ and 0 respectively. It is a simple scheme but requires higher accuracy on the synchronization. The Pulse Position Modulation (PPM), which distinguishes data bits by adding different time shifts on the same pulse waveform, is a kind of modulation which is very sensitive to the synchronization of the communication

systems. The Pulse shape modulation (PSM) uses different waveforms to presents different data bits. This scheme require more than one pulse generater and hence has higher complexity.

The pulse shapes for these four typical data modulation schemes are shown in Fig.1.4 [6]. It should be noted that these schemes could change to M-ary modulation schemes to improve power efficiency or increase the data rate, but the systems complexity will become higher. The comparison of performance of BPAM, OOK and PPM in AWGN channel in presence of jamming is shown in [18], where BPAM outperforms OOK and PPM in both TH-UWB and DS-UWB systems. In [19], BPAM (or BPSK) is preferred for its high power efficiency and smooth spectrum. It should be noted that as required in [12], the high data rate of the DS-UWB systems is achieved with BPSK and 4-ary bi-orthogonal keying (4BOK) modulation. All the compliant devices of DS-UWB communications must support BPSK modulation, while the 4BOK modulation scheme is optional [17]. In this thesis, we will focus on the BPSK modulation.

1.1.4 UWB Channel Model

The first work on statistical UWB channel models came out in 2001 [20], [21], and the standardized channel models of IEEE 802.15.3a and 802.15.4a groups were developed in 2003 and 2005, respectively [22], [23].

The standard channel model developed by the IEEE 802.15.3a group was the first standard model for UWB communications. However, this model only considered the office and residential indoor environments with a range of less than $10m$ [25]. With more measurements, a more general standard channel model was determined by the 802.15.4a group [24]. The 4a model was proposed for UWB systems in more operate environments such as office indoor, residential indoor, industrial, outdoor, and farm environments [23]. It should be noted that the IEEE 802.15.4a group was established to recognize some low ($< 1Mbps$) data rates applications such as the UWB sensor networks, but the 4a standard channel model is valid for UWB systems irrespective of the data rate and the modulation format [25]. In this thesis, we adopt the more flexible IEEE 802.15.4a standard channel model for the indoor residential non-line of sight (NLOS) environment. An example realization of the 4a channel model is shown in Fig 1.5. This realization is adopted in Chapter 3 for the desired user. It should be noted that for a wireless communication system, the channel changes as a function of time and frequency. Coherence time and coherence bandwidth indicate how quickly the channel changes in time and frequency, respectively [9]. In this thesis, the focus is on the development of the adaptive algorithms

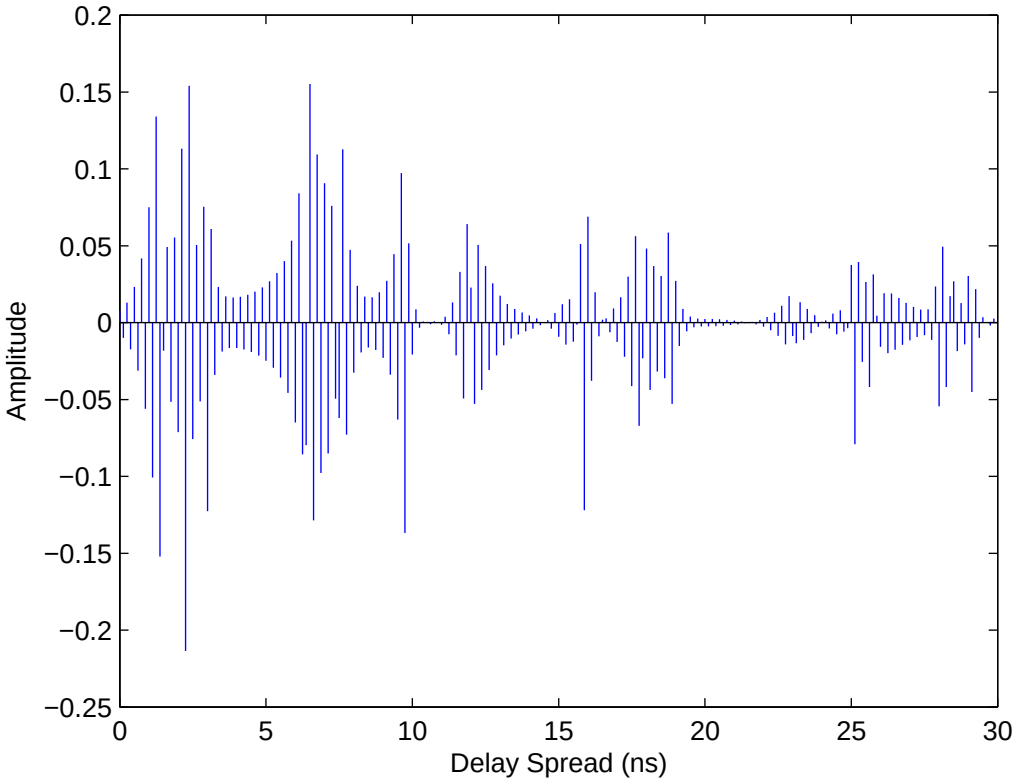

Fig. 1.5: One realization of the IEEE 8020.15.4a channel model

and it is assumed the transmission time for each experiment is smaller than the coherence time, hence the channel is assumed to be static or constant during the transmission.

1.2 Adaptive Filtering and Estimation Algorithms

An estimator or filter is known as the system that can be employed to infer or extract information from the noisy received data [26]. In this thesis, the linear filter is designed by applying the criteria of the minimum mean square error (MMSE) and the constrained constant modulus (CCM). Assuming that the received signal is stationary, the optimum designs require the statistics information of the received signal. However, when the information of the statistics is unavailable or the signal to be processed is nonstationary, the design of the optimum filters become impossible. In these situations, adaptive filtering technologies must be employed in order to learn about the statistics of the environment [26].

In this section, the MMSE design criterion based adaptive algorithms such as the least-mean square (LMS), recursive least-squares (RLS) and the conjugate gradient (CG) are introduced.

1.2.1 The Least-Mean Square Algorithm

The major advantage of the LMS algorithm is its simplicity and this feature makes the LMS as a standard against other linear adaptive algorithms [26]. The LMS algorithm can be developed from the MSE cost function:

$$\mathbf{J}_{MSE} = E[|e(i)|^2], \tag{1.1}$$

where the error signal $e(i)$ equals to the difference between the desired signal $d(i)$ and the output signal is $y(i)$. The output signal $y(i) = \mathbf{w}^H(i)\mathbf{r}(i)$, where $\mathbf{w}(i)$ is the filter represented by a M-by-1 weight vector and $\mathbf{r}(i)$ is the M-by-1 received signal. The gradient vector of $\mathbf{J}_{MSE}$ with respect to $\mathbf{w}(i)$ can be expressed as:

$$\mathbf{g}(i) = -\mathbf{p} + \mathbf{R}\mathbf{w}(i), \tag{1.2}$$

where $\mathbf{R} = E[\mathbf{r}(i)\mathbf{r}^H(i)]$ is the correlation matrix of the received signal and $\mathbf{p} = E[\mathbf{r}(i)d^*(i)]$ is the cross-correlation vector between the received signal and the desired signal. The optimum solution of such a linear filter is known as the Wiener solution that is given by

$$\mathbf{w}_o = \mathbf{R}^{-1}\mathbf{p}. \tag{1.3}$$

Since $\mathbf{R}$ and $\mathbf{p}$ are statistics of the received signal and are not given for the adaptive algorithms, these information must be estimated. LMS algorithms adopt the simplest estimator that use the instantaneous estimates for $\mathbf{R}$ and $\mathbf{p}$ [26], which can be expressed mathematically as $\hat{\mathbf{R}}(i) = \mathbf{r}(i)\mathbf{r}^H(i)$ and $\hat{\mathbf{p}}(i) = \mathbf{r}(i)d^*(i)$. The basic idea behind the LMS adaptive method is to approach the optimum filter solution by adjusting the filter weight vector in the direction of the inverse of the gradient vector. Hence, the adaptation of weight vector of LMS can be expressed as

$$\begin{aligned}\mathbf{w}(i+1) &= \mathbf{w}(i) + \mu(-\hat{\mathbf{g}}(i)) = \mathbf{w}(i) + \mu(-\hat{\mathbf{p}}(i) + \hat{\mathbf{R}}(i)\mathbf{w}(i)) \\ &= \mathbf{w}(i) + \mu\mathbf{r}(i)[d^*(i) - \mathbf{r}^H(i)\mathbf{w}(i)] = \mathbf{w}(i) + \mu\mathbf{r}(i)e^*(i),\end{aligned} \tag{1.4}$$

where μ is known as the step-size parameter. A necessary and sufficient condition for the

convergence of the LMS algorithms is given in [26] as:

$$0 < \mu < \frac{2}{MS_{max}}, \tag{1.5}$$

where M is the length of the filter and S_{max} is the maximum value of the power spectral density (PSD) of the received vector. The complexity of the LMS algorithm is $O(M)$.

1.2.2 The Recursive Least-Squares Algorithm

The advantage of the RLS algorithms is its faster convergence rate than the LMS algorithms. However, the RLS algorithms have higher computational complexity. The RLS algorithms use a recursive strategy to compute the LS estimators for the correlation matrix $\mathbf{R}$ and the cross-correlation vector $\mathbf{p}$, and adopt the matrix inversion lemma to compute the inverse of the estimate of correlation matrix.

We can develop a RLS adaptive algorithm via the cost function:

$$\mathbf{J}_{LS} = \sum_{j=1}^{i} \lambda^{i-j} |d(i) - \mathbf{w}^H(i)\mathbf{r}(i)|^2,$$

where $\mathbf{w}(i)$ is the filter represented by a M-by-1 weight vector and $\mathbf{r}(i)$ is the M-by-1 received signal. The forgetting factor λ is a positive constant which is smaller but close to 1 [26]. The optimum LS solution of the filter weight vector is

$$\mathbf{w}_{LS}(i) = \mathbf{R}_{rls}^{-1}(i)\mathbf{p}_{rls}(i), \tag{1.6}$$

where $\mathbf{R}_{rls}(i) = \sum_{j=1}^{i} \lambda^{i-j}\mathbf{r}(j)\mathbf{r}^H(j)$ and $\mathbf{p}_{rls}(i) = \sum_{j=1}^{i} \lambda^{i-j}d^*(j)\mathbf{r}(j)$. We use the matrix inversion lemma to computer the term of $\mathbf{R}_{rls}^{-1}(i)$ and obtain an recursive expression for the filter weight vector. The adaption equations of RLS algorithms are summarized as follows:

$$\begin{aligned}
&\mathbf{M}_{rls}(i) = \mathbf{R}_{rls}^{-1}(i-1)\mathbf{r}(i),\\
&\mathbf{K}_{rls}(i) = \frac{\mathbf{M}_{rls}(i)}{\lambda + \mathbf{r}^H(i)\mathbf{M}_{rls}(i)},\\
&e(i) = d(i) - \mathbf{w}^H(i-1)\mathbf{r}(i),\\
&\mathbf{w}(i) = \mathbf{w}(i-1) + \mathbf{K}_{rls}(i)e^*(i),\\
&\mathbf{R}_{rls}^{-1}(i) = \frac{\mathbf{R}_{rls}^{-1}(i-1) - \mathbf{K}_{rls}(i)\mathbf{r}^H(i)\mathbf{R}_{rls}^{-1}(i-1)}{\lambda}.
\end{aligned}$$

The complexity of the RLS algorithm is $O(M^2)$.

1.2.3 Conjugate Gradient Algorithm

The conjugate gradient (CG) algorithm is well known for its faster convergence rate than the LMS algorithm and lower computational complexity than the RLS algorithm [27] - [31]. For the adaptive filtering technique, the CG algorithm is developed to solve the problem

$$\mathbf{R}\mathbf{w} = \mathbf{p}, \tag{1.7}$$

where $\mathbf{R}$ is the M-by-M correlation matrix of the received signal and $\mathbf{p}$ is the M-by-1 cross-correlation vector. The CG algorithm provide an iterative way to calculate $\mathbf{w}$ without inverting $\mathbf{R}$. The basic CG algorithm can be expressed as follows [29], [31] by defining c as the index of the iterations

Initialization:

$$\mathbf{w}_0 = \mathbf{0}\ ;\ \mathbf{d}_0 = \mathbf{g}_0 = \mathbf{p}\ ;\ \rho_0 = \mathbf{g}_0^H \mathbf{g}_0.$$

For $c = 1, 2, \ldots, c_{\max}$

$$\begin{aligned}
&\alpha_c = \rho_{c-1} / \mathbf{d}_c^H \mathbf{R} \mathbf{d}_c, \\
&\mathbf{w}_c = \mathbf{w}_{c-1} + \alpha_c \mathbf{d}_c, \\
&\mathbf{g}_c = \mathbf{g}_{c-1} - \alpha_c \mathbf{R} \mathbf{d}_c, \\
&\rho_c = \mathbf{g}_c^H \mathbf{g}_c, \\
&\beta_c = \rho_c / \rho_{c-1}, \\
&\mathbf{d}_{c+1} = \mathbf{g}_c + \beta_c \mathbf{d}_c, \\
&c = c + 1.
\end{aligned}$$

End

$$\mathbf{w} = \mathbf{w}_{c_{\max}},$$

where α_c is the step size that minimizes the cost function (1.1), $\mathbf{d}_c$ is the direction vectors and $\mathbf{g}_c$ is defined as the inverse of the gradient vector of the cost function with respect to $\mathbf{w}$.

The adaptive CG algorithms require several iterations for each input data vector, but the adaptation time approaches 1 as the index of data vector increases [28]. The CG adaptive algorithm can also be used in block-by-block transmission systems. Assuming that a set of linearly independent direction vectors $\mathbf{d}_0, \mathbf{d}_1, \ldots, \mathbf{d}_{N-1}$ is given, where N is the block length. And these vectors are mutually conjugate with respect to the correlation matrix $\mathbf{R}$ [28], that means the scalar term of $\mathbf{d}_i^H \mathbf{R} \mathbf{d}_j$ is larger than zero only in the case when $i = j$, otherwise the value of this term is 0. For each iteration, the filter weight vector is adapted along the corresponding direction vector and the convergence can be obtained with at most N iterations [27]. The complexity of the CG algorithm is $O(M^2)$. Note that although the complexity is at the same level as the RLS algorithm, the number of operations measured in terms of arithmetic of the CG algorithm is lower than the traditional RLS algorithm [29].

1.3 Motivation

In UWB communications, the major challenges include the interference mitigation, synchronization and network design [6]- [8]. In this thesis, we focus on the linear adaptive solutions for the interference mitigation problem in multiuser DS-UWB systems. In time-domain symbol by symbol transmission systems, novel reduced-rank receivers are proposed. We also develop the adaptive receivers for single-carrier frequency domain equalization (SC-FDE) in the block by block transmission systems. It should be noted that the techniques developed for SC-FDE can also be used for multiband UWB systems that are based on orthogonal frequency-division multiplexing (OFDM) [67].

1.3.1 Motivation for Time-Domain Signal Processing

For DS-UWB communications, the major challenge for the adaptive interference suppression schemes is to achieve the robustness against narrow band interference and obtain fast convergence with satisfactory steady state performance in dense-multipath environments. Due to the long channel delay spread in UWB systems, the received signal length is large and the interference sensitive full-rank adaptive schemes experience slow convergence rate and are subject to significant performance degradation in the presence of interference that can be of various types, namely, multiple access interference (MAI), inter-symbol interference (ISI) and narrow band interference (NBI). Reduced-rank algorithms can be adopted to accelerate the convergence and provide an increased robustness against interference and noise. Recently, reduced-rank schemes have been considered

for UWB systems in [32]- [37]. A reduced-order finger selection linear MMSE receiver with RAKE-based structures have been proposed in [32], which requires the knowledge of the channel and the noise variance. Solutions for reduced-rank channel estimation and synchronization in single-user UWB systems have been proposed in [33]. For multiuser detection in UWB communications, reduced-rank schemes have been developed in [34]-[36] requiring knowledge of the multipath channel. In [37], the reduced-rank multiuser detector is proposed for hybrid direct-sequence time-hopping ultrawide bandwidth (DS-TH UWB) systems. The reduced-rank filtering techniques have faster convergence and increased robustness than the full-rank algorithms [38]- [51]. The well-known reduced-rank techniques include the eigen-decomposition methods such as the principal components (PC) [40] and the cross-spectral metric (CSM) [41], the Krylov subspace methods such as the powers of R (POR) [39], the multistage Wiener filter (MSWF) [42], [44] and the auxiliary vector filtering (AVF) [46]. Eigen-decomposition methods are based on the eigen-decomposition of the estimated covariance matrix of the received signal. The optimal representation of the input data can be obtained by the eigen-decomposition of the covariance matrix $\mathbf{R}$ [44]. However, $\mathbf{R}$ is unknown and must be estimated. In addition, these methods have very high computational complexity and the performance is often poor in heavily loaded communication systems [42]. Compared with the full-rank linear filtering techniques, the MSWF and AVF methods have faster convergence speed with a much smaller filter size. However, their computational complexity is still very high. In Chapter 3, we firstly investigate a generic reduced-rank scheme with joint and iterative optimization (JIO) of a projection vector and a reduced-rank linear estimator to minimize the MSE cost function. Since information is exchanged between the projection vector and the reduced-rank filter for each adaptation, this generic scheme outperforms other existing reduced-rank schemes. However, in this generic scheme, a large projection vector is required to be updated for each time instant and hence introduces high complexity. In order to obtain a low-complexity configuration of the generic scheme and maintain the performance, we propose the novel switched approximation of adaptive basis functions (SAABF) scheme. The basic idea of the SAABF scheme is to simplify the design of the projection vector by using a multiple-branch framework such that the number of coefficients to be adapted in the projection vector is reduced and hence achieve the complexity reduction. The LMS and RLS adaptive algorithms are then developed for the joint adaptation of the shortened projection vector and the reduced-rank filter. We also propose adaptive algorithms for branch number selection and model order adaptation.

Blind adaptive linear receivers [52]- [58] are efficient schemes for interference suppression as they offer higher spectrum efficiency than the adaptive schemes that require a training stage. Low complexity blind receiver designs can be obtained by solving constrained optimization problems based on the constrained constant modulus (CCM) or

constrained minimum variance (CMV) criterion [56], [59]. The blind receiver designs based on the CCM criterion have shown better performance and increased robustness against signature mismatch over the CMV approaches [56], [58]. Recently, blind full-rank SG and RLS adaptive filters based on the constrained optimization have been proposed for multiuser detection in DS-UWB communications [59], [60]. In [61], a blind subspace multiuser detection scheme is proposed for UWB systems which requires the eigen-decomposition of the covariance matrix of the received signal. In chapter 4, a novel CCM based joint iterative optimization (JIO) blind reduced-rank receiver is proposed. A projection matrix and a reduced-rank filter construct the proposed receiver and they are updated jointly and iteratively to minimize the CM cost function subject to a constraint. Note that the constraint is necessary since it enables us to avoid the undesired local minima. The adaptive NSG and RLS algorithms are developed for the JIO receiver. In the NSG version, a low-complexity leakage SG channel estimator that was proposed in [64] is adopted. Applying an approximation to the covariance matrix of the received signal, the RLS channel estimator proposed in [64] is modified for the proposed JIO-RLS with reduced complexity. Since each column of the projection matrix can be considered as a direction vector on one dimension of the subspace, we update the projection matrix column by column to achieve a better representation of the projection procedure in the JIO-RLS.

1.3.2 Motivation for Frequency-Domain Signal Processing

Compared to time-domain equalization techniques, the frequency-domain equalizers are able to provide better tradeoffs between the performance and complexity [65], [66]. It should be noted that in the frequency-domain, a single MMSE filter can be used for all bits in a transmitted block while in the time-domain, different set of equalizer parameters can be used for each bit. This feature of the frequency-domain equalizers leads to lower computational complexity but also introduces some performance degradation [65]. In addition, a cyclic prefix is included in the SC-FDE systems to avoid the IBI which will reduce the bandwidth efficiency compare to the time-domain detectors.

In order to operate in dense multipath environments with low complexity, SC-FDE systems with a cyclic prefix have been recently applied to DS-UWB communications [65]-[71]. In [65], frequency-domain minimum mean-square error (MMSE) turbo equalization scheme is proposed for single-user DS-UWB systems. For multiuser communications, the frequency-domain detector is obtained by combining the turbo equalizer with a soft interference canceller. In [66], the performance of the linear MMSE detector in SC-FDE and OFDM systems are compared over UWB channels and the simulation results show

that the SC-FDE system is reasonably robust in the presents of carrier frequency offset and sampling time offset. In [67], a low-complexity channel estimation algorithm is proposed for single user communication. A new SC block transmission structure was proposed in [68], where a novel despreading scheme was employed in the frequency-domain before channel estimation and equalization. In [69]- [71], frequency-domain linear multiuser detection and channel estimation was performed and a linear MMSE equalization scheme was described. However, in [65]- [71], $prior$ knowledge of the channel and the received signal is required and the parameter estimation problem was not considered in detail.

Adaptive techniques are effective tools for estimating parameters and are able to deal with channel variations [26]. In the frequency-domain, adaptive algorithms are usually more stable and converge faster than in the time-domain [72]. To the best of our knowledge, these techniques have not been thoroughly investigated for UWB communications yet. In this thesis, adaptive algorithms based on LMS, RLS and CG techniques are developed for frequency-domain detectors in multiuser DS-UWB communications. The major advantage of the LMS algorithm is its simplicity and this feature makes the LMS a standard against other linear adaptive algorithms [26]. The RLS algorithm converges faster than the LMS algorithm but usually requires much higher computation complexity. The CG method is the most important conjugate direction (CD) method that is able to generate the direction vectors simply and iteratively [73]. With faster convergence speed than stochastic gradient techniques and lower complexity than recursive least squares (RLS) algorithms, CG methods are known as powerful tools in computational systems [27]- [31] and hence, suitable for the DS-UWB communications.

In chapter 5, we present two adaptive detection schemes in the frequency-domain and apply them to SC-FDE in multiuser DS-UWB systems. In the first scheme, a structured channel estimation (SCE) approach that extends [72] to multiuser UWB systems is carried out separately in the frequency-domain and the estimated channel impulse response (CIR) is substituted into the expression of the MMSE detector to suppress the ISI. After the frequency-domain processing, the despreading is performed in the time-domain to eliminate the MAI. The LMS and RLS adaptive algorithms for the SCE with single user SC systems were proposed in [72] and we extend them to multiuser scenarios. However, the SCE-RLS has very high complexity because there is an inversion of matrix that must be computed directly [72]. This problem motivates us to develop the SCE-CG algorithm, which will be shown later, has much lower complexity than the SCE-RLS while performing better than the SCE-LMS and comparable to the SCE-RLS. In this scheme, the MMSE detector requires the knowledge of the noise variance and the number of active users. We estimate the noise variance via the maximum likelihood (ML) method.

With a relationship between the input signal power and the number of users, we propose a simple and effective approach to estimating the users number. In the second scheme, which is termed direct adaptation (DA), only one filter is implemented in the frequency-domain to suppress the interference. It is important to note that with the traditional signal expression for the multiuser block transmission systems, the DA scheme requires a matrix-structured adaptive filter in the frequency-domain which leads to prohibitive complex solutions. In the literature, the adaptive DA scheme in multiuser UWB systems has not been investigated in detail. Prior work on adaptive frequency-domain algorithms is limited to single-user systems [74] and do not exploit the structure created by multiuser UWB systems with a cyclic prefix. In order to obtain a simplified filter design, we adopt the signal expression described in [68] and extend it into an adaptive parameter estimation implementation. After obtaining the matrix form of the MMSE design of such a filter, we convert it into a vector form and develop LMS, RLS and CG algorithms in the frequency-domain that enables the linear suppression of ISI and MAI. In our proposed DA scheme, a low complexity RLS algorithm, termed DA-RLS, is obtained with the new signal expression. The proposed DA-RLS algorithm is suitable for multiuser block transmission systems. With faster convergence rate than the DA-LMS and DA-CG, the complexity of the DA-RLS in the multiuser cases is comparable to the DA-CG. In the single user scenario, the complexity of the DA-RLS is reduced to the level of the DA-LMS.

The RLS versions that are developed in chapter 5 estimate the least-square (LS) solutions, which are minimum variance unbiased estimators (MVUE) [84]. However, the MSE performance of the LS solution can be improved in certain scenarios by adding appropriately chosen bias to the conventional LS estimators [85]- [92]. The biased estimation has shown its ability to outperform the existing estimators especially in the low signal-to-noise ratios (SNR) and/or short data records [86]. In chapter 6, biased adaptive estimation techniques based on shrinkage estimators are devised and incorporated into RLS versions that are developed in chapter 5. For the SCE scheme, automatic shrinkage factor mechanisms are proposed and incorporated into RLS estimators, obtaining a lower MSE of the channel estimation. For the DA scheme, the automatic shrinkage factors are incorporated directly to the adaptive receiver weights. The results show that a shorter data support is required by the proposed biased DA-RLS technique. An analysis of fundamental estimation limits of the proposed frequency domain biased estimators is included along with the derivation of appropriate Cramér-Rao lower bounds (CRLB).

1.4 Thesis Outline

The structure of the thesis is as follows:

- In Chapter 2, the time-domain and the frequency-domain DS-UWB system models are detailed.
- In Chapter 3, a generic reduced-rank scheme based on the joint and iterative optimization (JIO) and the novel low-complex SAABF scheme are proposed for interference suppression for DS-UWB systems in the time-domain.
- In Chapter 4, blind reduced-rank adaptive receivers based on JIO and CCM design criterion are proposed for DS-UWB Systems in the time-domain.
- In Chapter 5, we develop the frequency-domain adaptive detectors for SC-FDE in multiuser DS-UWB systems based on structured channel estimation and direct adaptation.
- In Chapter 6, biased estimators with shrinkage factors are developed to improve the RLS schemes that are proposed in Chapter 5.
- In Chapter 7, conclusions and a discussion on possibilities for future work are presented.

1.5 List of Publications

Some of the research presented in this thesis has been published, accepted, submitted, or will be submitted to some publications at the time of submission of this thesis.

Journal Papers

1. S. Li and R. C. de Lamare, "Frequency Domain Adaptive Detectors for SC-FDE in Multiuser DS-UWB Systems Based on Structured Channel Estimation and Direct Adaptation," *IET Communications*, vol. 4, issue. 13, pp. 1636-1650, 2010.
2. S. Li, R. C. de Lamare and R. Fa, "Reduced-Rank Linear Interference Suppression for DS-UWB Systems Based on Switched Approximations of Adaptive Basis Functions," (submitted) *IEEE Trans. Vehicular Technology*, 2010.

3. S. Li and R. C. de Lamare, "Blind Reduced-rank Adaptive Receivers for DS-UWB Systems Based on Joint Iterative Optimization and the Constrained Constant Modulus Criterion," (submitted) *IEEE Trans. Vehicular Technology*, 2010.

4. S. Li and R. C. de Lamare, "Biased estimators for SC-FDE in Multiuser DS-UWB Systems," (under preparation) *IEEE Trans. Signal processing*, 2010.

Conference Papers

1. S. Li, R. C. de Lamare and D. Z. Filho, "Adaptive Reduced-Rank Interference Suppression for DS-UWB Systems Based on Switched Approximation of Basis Functions," Proc. IEEE Asilomar Conference on Signals, Systems and Computers, Pacific Grove, USA, October 2008.

2. S. Li and R. C. de Lamare, "Adaptive Linear Interference Suppression Based on Block Conjugate Gradient Method in Frequency Domain for DS-UWB Systems," Proc. IEEE International Symposium on Wireless Communications Systems, Siena, Italy, September 2009.

3. S. Li and R. C. de Lamare, "Adaptive Detector for SC-FDE in Multiuser DS-UWB Systems Based on Structured Channel Estimation with Conjugate Gradient Algorithm," Proc. IEEE Vehicular Technology Conference, VTC - Spring, Taipei, Taiwan, 2010.

4. S. Li and R. C. de Lamare, "Low-complexity Reduced-Rank Interference Mitigation Algorithms for DS-UWB Systems," Proc. IEEE Vehicular Technology Conference, VTC - Spring, Taipei, Taiwan, 2010.

5. S. Li and R. C. de Lamare, "Blind Joint Iterative Optimization Reduced-rank Adaptive Receiver for DS-UWB Systems Based on Constrained Constant Modulus Criterion," Proc. IEEE International Symposium on Wireless Communications Systems, York, UK, September 2010.

6. R. Fa, R. C. de Lamare and S. Li, "Reduced-Rank STAP Algorithm for Adaptive Radar Based on Basis-Functions Approximation," Proc. IEEE International Workshop on Statistical Signal Processing, Cardiff, September 2009.

7. R. C. de Lamare and S. Li , "Joint Iterative Power Allocation and Interference Suppression Algorithms for Cooperative Spread Spectrum Networks," Proc. IEEE Vehicular Technology Conference, VTC - Spring, Taipei, Taiwan, 2010.

8. S. Li and R. C. de Lamare, “Blind Reduced-rank Adaptive Receiver for DS-UWB Systems Based on Joint Iterative Optimization with Column Adaptation of the Constrained Constant Modulus Criterion,” (under preparation) for VTC - Fall, 2010.

9. S. Li and R. C. de Lamare, “Adaptive Shrinkage Estimator for SC-FDE in Multiuser DS-UWB Systems based on Structured Channel Estimation,” (under preparation) for ICASSP, 2010.

2. DS-UWB SYSTEM AND SIGNAL MODELS

Contents

In this chapter, the DS-UWB system and signal models in both time-domain and frequency domain are detailed. It should be noted that, the novel adaptive reduced-rank algorithms that will be presented in Chapter 3 and Chapter 4 use the same time-domain system model, while the frequency-domain signal processing algorithms developed in Chapter 5 and Chapter 6 share the same frequency-domain model.

2.1 Time-Domain System and Signal Model

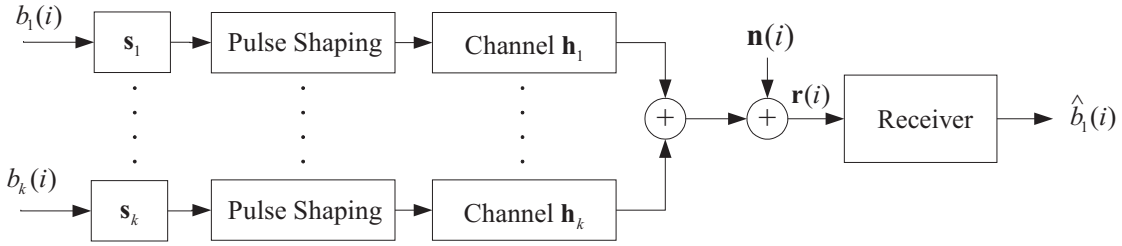

Fig. 2.1: Block diagram of the time-domain system model.

For the time-domain adaptive interference suppression, we consider the uplink of a synchronous binary phase-shift keying (BPSK) DS-UWB system with K users. The block diagram of the system model is shown in Fig. 2.1, in which user 1 is assumed to be the desired user. A random spreading code $\mathbf{s}_k$ is assigned to the k-th user. The spreading gain is $N_c = T_s/T_c$, where T_s and T_c denote the symbol duration and chip duration, respectively. The transmit signal of the k-th user, $k = 1, 2, \ldots, K$, can be expressed as

$$x^{(k)}(t) = \sqrt{E_k} \sum_{i=-\infty}^{\infty} \sum_{j=0}^{N_c-1} p_t(t - iT_s - jT_c) s_k(j) b_k(i), \tag{2.1}$$

where $b_k(i) \in \{\pm 1\}$ denotes the BPSK symbol for the k-th user at the i-th time instant, $s_k(j)$ denotes the j-th chip of the spreading code $\mathbf{s}_k$. E_k denotes the transmission energy. $p_t(t)$ is the pulse waveform of width T_c. The target data rate for the DS-UWB communication systems are in the range of $28Mbps$ to $1.32Gbps$ [12]. In this thesis, the data rate for the time-domain DS-UWB systems is set to 83 $Mbps$. For UWB communications, widely used pulse shapes include the Gaussian waveforms, raised-cosine pulse shaping and root-raised cosine (RRC) pulse shaping [7], [12]. Throughout this thesis, the pulse waveform $p_t(t)$ is modeled as the RRC pulse with a roll-off factor of 0.5 [12], [17] and [67].

The channel model considered is the IEEE 802.15.4a standard channel model for the indoor residential non-line of sight (NLOS) environment [23]. This standard channel model includes some generalizations of the Saleh-Valenzuela model and takes the frequency dependence of the path gain into account [25]. In addition, the 15.4a channel model is valid for both low-data-rate and high-data-rate UWB systems [25]. For the k-th user, the channel impulse response (CIR) of the standard channel model is

$$h_k(t) = \sum_{u=0}^{L_c-1} \sum_{v=0}^{L_r-1} \alpha_{u,v} e^{j\phi_{u,v}} \delta(t - T_u - T_{u,v}), \tag{2.2}$$

where L_c denotes the number of clusters, L_r is the number of multipath components (MPCs) in one cluster. $\alpha_{u,v}$ is the fading gain of the v-th MPC in the u-th cluster, $\phi_{u,v}$ is uniformly distributed in $[0, 2\pi)$. T_u is the arrival time of the u-th cluster and $T_{u,v}$ denotes the arrival time of the v-th MPC in the u-th cluster. For the sake of simplicity, we express the CIR as

$$h_k(t) = \sum_{l=0}^{L-1} h_{k,l} \delta(t - lT_\tau), \tag{2.3}$$

where $h_{k,l}$ and lT_τ present the complex-valued fading factor and the arrival time of the l-th MPC ($l = uL_c + v$), respectively. $L = T_{DS}/T_\tau$ denotes the total number of MPCs where T_{DS} is the channel delay spread. Note that, in order to achieve high data-rate communications, the channel delay spread is assumed significantly larger than one symbol duration. Hence, the received signal encounters severe ISI.

Assuming that the timing is acquired, the received signal can be expressed as

$$z(t) = \sum_{k=1}^{K} \sum_{l=0}^{L-1} h_{k,l} x^{(k)}(t - lT_\tau) + n(t),$$

where $n(t)$ is the additive white gaussian noise (AWGN) with zero mean and a variance of σ_n^2. The received signal is first passed through a chip-matched filter (CMF) and then

sampled at the chip rate. For high data rate UWB systems, the pulse width is typically on the order of $1ns$ or less [76]. In this thesis, T_c is set to $0.375ns$ and the sampling frequency at the receiver is $2.67GHz$. This sampling rate is lower than $4GHz$ and cheap Analog-to-Digital Converters (ADC) can be implemented [77]. We select a total number of $M = (T_s + T_{DS})/T_c$ observation samples for the detection of each data bit, where T_s is the symbol duration, T_{DS} is the channel delay spread and T_c is the chip duration. Assuming the sampling starts at the zero-th time instant, then the m-th sample can be expressed as

$$r_m = \int_{mT_c}^{(m+1)T_c} z(t)p_r(t)\,dt, \tag{2.4}$$

where $m = 1, 2, \ldots, M$, $p_r(t) = p_t^*(-t)$ denotes the CMF and $(\cdot)^*$ denotes the complex conjugation. After the chip-rate sampling, the discrete-time received signal for the i-th data bit can be expressed as $\mathbf{r}(i) = [r_1(i), r_2(i), \ldots, r_M(i)]^T$, where $(\cdot)^T$ is the transposition. We can further express it in a matrix form as

$$\mathbf{r}(i) = \sum_{k=1}^{K} \sqrt{E_k}\mathbf{P}_r\mathbf{H}_k\mathbf{P}_t\mathbf{s}_k b_k(i) + \boldsymbol{\eta}(i) + \mathbf{n}(i), \tag{2.5}$$

where $\mathbf{H}_k$ is the Toeplitz channel matrix for the k-th user with the first column being the CIR of $\mathbf{h}_k = [h_k(0), h_k(1), \ldots, h_k(L-1)]^T$ zero-padded to length $M_H = (T_s/T_\tau) + L - 1$. Matrix $\mathbf{P}_r$ represents the CMF and chip-rate sampling with the size M-by-M_H. $\mathbf{P}_t$ denotes the (T_s/T_τ)-by-N_c pulse shaping matrix. The vector $\boldsymbol{\eta}(i)$ denotes the ISI from $2G$ adjacent symbols, where G denotes the minimum integer that is larger than or equal to the scalar term T_{DS}/T_s. Here, we express the ISI vector in a general form that is given by

$$\begin{aligned}\boldsymbol{\eta}(i) = &\sum_{k=1}^{K}\sum_{g=1}^{G} \sqrt{E_k}\mathbf{P}_r\mathbf{H}_k^{(-g)}\mathbf{P}_t\mathbf{s}_k b_k(i-g) \\ &+ \sum_{k=1}^{K}\sum_{g=1}^{G} \sqrt{E_k}\mathbf{P}_r\mathbf{H}_k^{(+g)}\mathbf{P}_t\mathbf{s}_k b_k(i+g),\end{aligned} \tag{2.6}$$

where the channel matrices for the ISI are given by

$$\mathbf{H}_k^{(-g)} = \begin{bmatrix}\mathbf{0} & \mathbf{H}_k^{(u,g)} \\ \mathbf{0} & \mathbf{0}\end{bmatrix} \;;\; \mathbf{H}_k^{(+g)} = \begin{bmatrix}\mathbf{0} & \mathbf{0} \\ \mathbf{H}_k^{(l,g)} & \mathbf{0}\end{bmatrix}. \tag{2.7}$$

Note that the matrices $\mathbf{H}_k^{(u,g)}$ and $\mathbf{H}_k^{(l,g)}$ have the same size as $\mathbf{H}_k$, which is M_H-by-(T_s/T_τ), and can be considered as the partitions of an upper triangular matrix $\mathbf{H}_{\text{up}}$ and a

lower triangular matrix $\mathbf{H}_{\text{low}}$, respectively, where

$$\mathbf{H}_{\text{up}} = \begin{bmatrix} h_k(L-1) & \dots & h_k(L-\frac{T_{DS}-(g-1)T_s}{T_\tau}) \\ & \ddots & \vdots \\ & & h_k(L-1) \end{bmatrix};$$

$$\mathbf{H}_{\text{low}} = \begin{bmatrix} h_k(0) & & \\ \vdots & \ddots & \\ h_k(\frac{T_{DS}-(g-1)T_s}{T_\tau}-2) & \dots & h_k(0) \end{bmatrix}.$$

These triangular matrices have the row-dimension of $[T_{DS}-(g-1)T_s]/T_\tau - 1 = L - (g-1)T_s/T_\tau - 1$. Note that when the channel delay spread is large, the row-dimension of these triangular matrices could surpass the column dimension of the matrix $\mathbf{H}_k$, which is T_s/T_τ. Hence, in case of

$$\begin{aligned} &L-(g-1)T_s/T_\tau - 1 > T_s/T_\tau, \\ &i.e.\ \ L > gT_s/T_\tau + 1, \end{aligned} \tag{2.8}$$

the matrix $\mathbf{H}_k^{(u,g)}$ is the last T_s/T_τ columns of the upper triangular matrix $\mathbf{H}_{\text{up}}$ and $\mathbf{H}_k^{(l,g)}$ is the first T_s/T_τ columns of the lower triangular matrix $\mathbf{H}_{\text{low}}$. When $L < gT_s/T_\tau + 1$, $\mathbf{H}_k^{(u,g)} = \mathbf{H}_{\text{up}}$ and $\mathbf{H}_k^{(l,g)} = \mathbf{H}_{\text{low}}$. It is interesting to review the expression of the ISI vector via its physical meaning, since the row-dimension of the matrices $\mathbf{H}_k^{(u,g)}$ and $\mathbf{H}_k^{(l,g)}$, which is $L-(g-1)T_s/T_\tau - 1$, reflects the time-domain overlap between the data symbol $b(i)$ and the adjacent symbols of $b(i-g)$ and $b(i+g)$.

The time-domain interference suppression adaptive algorithms are required to recover the data bit from the noisy received signal that is given in (2.5). The full-rank adaptive filters experience slow convergence rate in DS-UWB systems because of the long channel delay spread. In order to accelerate the convergence and increase the robustness against interference, in Chapter 3 and Chapter 4, novel reduced-rank adaptive algorithms are proposed based on the MMSE design criterion and the CCM design criterion, respectively.

2.2 Frequency-Domain System and Signal Model

For the frequency-domain adaptive interference suppression,we consider a synchronous downlink block-by-block transmission BPSK DS-UWB system with K users. The block diagram of the frequency-domain system model is shown in Fig. 2.2, where user 1 is assumed to be the desired user. An N_c-by-1 Walsh spreading code $\mathbf{s}_k$ is assigned to the k-th user. The spreading gain is $N_c = T_s/T_c$, where T_s and T_c denote the symbol

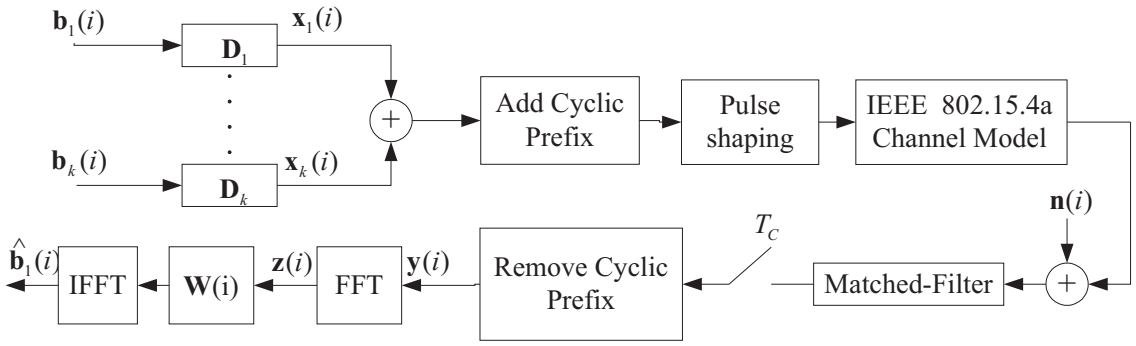

Fig. 2.2: Block diagram of the frequency-domain system model.

duration and chip duration, respectively. At each time instant, an N-dimensional data vector $\mathbf{b}_k(i)$ is transmitted by the k-th user. The target data rate for the DS-UWB communication systems are in the range of $28Mbps$ to $1.32Gbps$ [12]. In this thesis, the data rate for the frequency-domain DS-UWB systems is set to 293 $Mbps$. We define the signal after spreading as $\mathbf{x}_k(i)$ and express it in a matrix form as

$$\mathbf{x}_k(i) = \mathbf{D}_k \mathbf{b}_k(i), \tag{2.9}$$

where the M-by-N ($M = N \times N_c$) block diagonal matrix $\mathbf{D}_k$ is performing the spreading of the data block and can be expressed as

$$\mathbf{D}_k = \begin{bmatrix} \mathbf{s}_k & & & \\ & \mathbf{s}_k & & \\ & & \ddots & \\ & & & \mathbf{s}_k \end{bmatrix}. \tag{2.10}$$

In order to prevent inter block interference (IBI), a cyclic-prefixed (CP) guard interval is added and the length of the CP is assumed larger than the CIR. With the insertion of the CP at the transmitter and its removal at the receiver, the Toeplitz channel matrix could be transformed into an equivalent circulant channel matrix [70]. We adopt the IEEE 802.15.4a standard channel model for the indoor residential non-line of sight (NLOS) environment [23]. This standard channel model is valid for both low-data-rate and high-data-rate UWB systems [25]. We assume that the timing is perfect and focus on the channel estimation and interference suppression tasks. At the receiver, a CMF is applied and the received sequence is then sampled at chip-rate and organized in an M-dimensional vector $\mathbf{y}(i)$. For high data rate UWB systems, the pulse width is typically on the order of $1ns$ or less [76]. In this thesis, T_c is set to $0.375ns$ and the sampling frequency at the receiver is $2.67GHz$. The equivalent channel is denoted as an M-by-M circulant Toeplitz

matrix $\mathbf{H}_{\text{equ}}$, whose first column is structured with $\mathbf{h}_{\text{equ}}$ zero-padded to length M, where $\mathbf{h}_{\text{equ}} = [h(0), h(1), \ldots, h(L-1)]$ is the equivalent CIR. The time-domain received signal at the i-th time instant can be expressed as

$$\mathbf{y}(i) = \sum_{k=1}^{K} \mathbf{H}_{\text{equ}} \mathbf{x}_k(i) + \mathbf{n}(i), \tag{2.11}$$

where $\mathbf{n}(i)$ denotes the additive white Gaussian noise (AWGN). After the discrete Fourier transform (DFT), the frequency-domain received signal $\mathbf{z}(i)$ is expressed as

$$\mathbf{z}(i) = \mathbf{F}\mathbf{y}(i), \tag{2.12}$$

where $\mathbf{F}$ represents the M-by-M DFT matrix and its (a, b)-th entry can be expressed as

$$\mathrm{F}_{a,b} = (1/\sqrt{M})\exp\{-j(2\pi/M)ab\}, \tag{2.13}$$

where $a, b \in \{0, M-1\}$.

Given the frequency-domain received signal as shown in (2.12), the frequency-domain detectors are implemented to recover the original data vector. In Chapter 5, we propose two MMSE based detection schemes, named structured channel estimation (SCE) and direct adaptation (DA), respectively. The SCE scheme explicitly perform the channel estimation in the frequency-domain, the detection with the estimated channel coefficients, and finally carry out despreading in the time-domain. The DA scheme implicitly estimates the channel and suppresses the ISI and MAI together with only one filter and has simpler structure than the SCE scheme. In Chapter 6, the RLS versions of the SCE and DA schemes will be equipped with adaptive shrinkage factors to improve the MSE performance.

3. REDUCED-RANK INTERFERENCE SUPPRESSION SCHEMES BASED ON JOINT AND ITERATIVE OPTIMIZATION AND SWITCHING

Contents

3.1 Introduction

In this chapter, we firstly investigate a generic reduced-rank scheme with joint and iterative optimization of a projection vector and a reduced-rank linear estimator to minimize the mean square error (MSE) cost function. Since information is exchanged between the projection matrix and the reduced-rank filter for each adaptation, this generic scheme outperforms other existing reduced-rank schemes. However, in this generic scheme, a large projection vector is required to be updated for each time instant and hence introduces high complexity. In order to obtain a low-complexity configuration of the generic scheme and maintain the performance, we propose the novel switched approximation of adaptive basis functions (SAABF) scheme. The basic idea of the SAABF scheme is to simplify the design of the projection vector by using a multiple-branch framework such that the number of coefficients to be adapted in the projection vector is reduced and hence achieve the complexity reduction. The LMS and RLS adaptive algorithms are then developed for

the joint adaptation of the shortened projection vector and the reduced-rank filter. We also propose adaptive algorithms for branch number selection and model order adaptation.

The main contributions of this chapter are listed below.

- A novel low-complexity reduced-rank scheme is proposed for interference suppression in DS-UWB system.
- LMS and RLS adaptive algorithms are developed for the proposed scheme.
- Algorithms for selecting the scheme parameters are proposed.
- The relationships between the proposed SAABF scheme, the generic scheme and the full-rank scheme are established.
- Simulations are performed with the IEEE 802.15.4a channel model and severe ISI and MAI are assumed for the evaluation of the proposed scheme.

The rest of this chapter is structured as follows. Section 3.2 presents the full-rank MMSE design and the problem statement. In Section 3.3, the design of the generic reduced-rank scheme is detailed. The proposed SAABF scheme is described in Section 3.4 and the adaptive algorithms and the complexity analysis are presented in Section 3.5. The proposed adaptive algorithms for selecting the key parameters of the SAABF scheme are described in Section 3.6. Simulations results are shown in Section 3.7 and conclusions are drawn in Section 3.8.

3.2 Problem Statement

Recalling the time-domain DS-UWB system model described in Section 2.1. In order to estimate the data bit from the noisy received signal $\mathbf{r}(i)$ which is shown in (2.5), an M-dimensional full-rank filter $\mathbf{w}(i)$ can be employed to minimize the MSE cost function:

$$\mathbf{J}_{\mathrm{MSE}}(\mathbf{w}(i)) = E[|d(i) - \mathbf{w}^H(i)\mathbf{r}(i)|^2], \tag{3.1}$$

where $d(i)$ is the desired signal, $(\cdot)^H$ denotes the Hermitian transpose and $E[\cdot]$ represents the expected value. Without loss of generality, we consider user 1 as the desired user and omit the subscript of this user for simplicity. The optimal solution that minimizes (3.1) is given by

$$\mathbf{w}_{\mathrm{o}} = \mathbf{R}^{-1}\mathbf{p}, \tag{3.2}$$

where $\mathbf{R} = E[\mathbf{r}(i)\mathbf{r}^H(i)]$ is the correlation matrix of the discrete-time received signal $\mathbf{r}(i)$ and $\mathbf{p} = E[d^*(i)\mathbf{r}(i)]$ is the cross-correlation vector between $\mathbf{r}(i)$ and $d(i)$. Assuming that $\mathbf{r}(i)$, $\boldsymbol{\eta}(i)$ and $\mathbf{n}(i)$ are uncorrelated to each other, we have

$$\begin{aligned}
\mathbf{R} &= \sum_{k=1}^{K} \mathbf{P}_r \mathbf{H}_k \mathbf{P}_t \mathbf{s}_k \mathbf{s}_k^H \mathbf{P}_t^H \mathbf{H}_k^H \mathbf{P}_r^H \\
&\quad + \sum_{k=1}^{K} \sum_{g=1}^{G} \mathbf{P}_r \mathbf{H}_k^{(-g)} \mathbf{P}_t \mathbf{s}_k \mathbf{s}_k^H \mathbf{P}_t^H \left(\mathbf{H}_k^{(-g)}\right)^H \mathbf{P}_r^H \\
&\quad + \sum_{k=1}^{K} \sum_{g=1}^{G} \mathbf{P}_r \mathbf{H}_k^{(+g)} \mathbf{P}_t \mathbf{s}_k \mathbf{s}_k^H \mathbf{P}_t^H \left(\mathbf{H}_k^{(+g)}\right)^H \mathbf{P}_r^H + \sigma^2 \mathbf{I}_M, \\
\mathbf{p} &= \mathbf{P}_r \mathbf{H} \mathbf{P}_t \mathbf{s},
\end{aligned} \tag{3.3}$$

where $\mathbf{I}_M$ denotes the M-by-M identity matrix.

The corresponding MMSE can be expressed as:

$$\mathbf{MMSE}_{\mathrm{f}} = \sigma_d^2 - \mathbf{p}^H \mathbf{R}^{-1} \mathbf{p}, \tag{3.4}$$

where σ_d^2 is the variance of the desired signal. Full-rank adaptive algorithms can update $\mathbf{w}(i)$ to approach the optimal solution in (3.2). The final decision is made by $\hat{b}(i) = \mathrm{sign}(\Re[\mathbf{w}^{\mathrm{H}}(i)\mathbf{r}(i)])$, where $\mathrm{sign}(\cdot)$ is the algebraic sign function and $\Re(\cdot)$ represents the real part of a complex number. The full-rank adaptive filters experience slow convergence rate in DS-UWB systems because of the long channel delay spread. In order to accelerate the convergence and increase the robustness against interference, we propose a generic reduced-rank scheme in what follows.

3.3 Generic Reduced-Rank Scheme and Problem Statement

Reduced-rank signal processing can be divided into two parts: an M-by-D projection matrix that projects the M-dimensional received signal onto a D-dimensional subspace (where $D \ll M$), and a D-dimensional reduced-rank linear filter that produces the output.

The projection stage of the reduced-rank schemes is given by

$$\bar{\mathbf{r}}(i) = \mathbf{T}^H(i)\mathbf{r}(i), \tag{3.5}$$

where $\bar{\mathbf{r}}(i)$ is the reduced-rank signal and $\mathbf{T}(i)$ is the projection matrix that can be expressed as

$$\mathbf{T}(i) = [\boldsymbol{\phi}_1(i), \cdots, \boldsymbol{\phi}_d(i), \cdots \boldsymbol{\phi}_D(i)], \tag{3.6}$$

where $\{\boldsymbol{\phi}_d(i)|\ d = 1, \ldots, D\}$ are the M-dimensional basis vectors. The vector $\bar{\mathbf{r}}(i)$ is then passed through a D-dimensional linear filter. The MMSE solution of such a filter is

$$\bar{\mathbf{w}}_{\mathrm{o}} = \bar{\mathbf{R}}^{-1}\bar{\mathbf{p}}, \tag{3.7}$$

where $\bar{\mathbf{R}} = E[\bar{\mathbf{r}}(i)\bar{\mathbf{r}}^H(i)]$ and $\bar{\mathbf{p}} = E[d^*(i)\bar{\mathbf{r}}(i)]$.

In reduced-rank schemes, the main challenge is how to effectively design the projection matrix $\mathbf{T}(i)$. In order to simplify the expression of the proposed SAABF scheme in later sections, the reduced-rank signal is expressed as

$$\bar{\mathbf{r}}(i) = \mathbf{T}^H(i)\mathbf{r}(i) = \begin{bmatrix} \mathbf{r}^T(i) & & & \\ & \mathbf{r}^T(i) & & \\ & & \ddots & \\ & & & \mathbf{r}^T(i) \end{bmatrix}_{D\times MD} \begin{bmatrix} \boldsymbol{\phi}_1(i) \\ \boldsymbol{\phi}_2(i) \\ \vdots \\ \boldsymbol{\phi}_D(i) \end{bmatrix}^*_{MD\times 1} = \mathbf{R}_{\mathrm{in}}(i)\mathbf{t}(i), \tag{3.8}$$

where the projection matrix is transformed into a vector form, and $\mathbf{t}(i)$ is called projection vector in what follows. It can be shown that the d-th element in the reduced-rank signal is $\bar{r}_d(i) = \mathbf{r}^T(i)\boldsymbol{\phi}_d^*(i)$, where $d = 1, \ldots, D$. The generic reduced-rank scheme is proposed to jointly and iteratively adapt the projection vector and the reduced-rank linear estimator to minimize the MSE cost function

$$\mathbf{J}_{\mathrm{MSE}}(\bar{\mathbf{w}}(i), \mathbf{t}(i)) = E[|d(i) - \bar{\mathbf{w}}^H(i)\mathbf{R}_{\mathrm{in}}(i)\mathbf{t}(i)|^2]. \tag{3.9}$$

The MMSE solution of the reduced-rank filter in the generic scheme has the same form as (3.7). By setting the gradient vector of (3.9) with respect to $\mathbf{t}(i)$ to a null vector, The optimum projection vector is given by

$$\mathbf{t}_{\mathrm{opt}} = \mathbf{R}_w^{-1}\mathbf{p}_w. \tag{3.10}$$

where $\mathbf{R}_w = E[\mathbf{R}_{\mathrm{in}}^H(i)\bar{\mathbf{w}}(i)\bar{\mathbf{w}}^H(i)\mathbf{R}_{\mathrm{in}}(i)]$ and $\mathbf{p}_w = E[d(i)\mathbf{R}_{\mathrm{in}}^H(i)\bar{\mathbf{w}}(i)]$. The MMSE of

the generic scheme can be expressed as:

$$\mathbf{MMSE}_{\mathrm{g}} = \sigma_d^2 - \bar{\mathbf{p}}^H \bar{\mathbf{R}}^{-1} \bar{\mathbf{p}}. \tag{3.11}$$

Note that when adaptive algorithms are implemented to estimate $\bar{\mathbf{w}}_{\mathrm{o}}$ and $\mathbf{t}_{\mathrm{opt}}$, $\bar{\mathbf{w}}(i)$ is a function of $\mathbf{t}(i)$ and $\mathbf{t}(i)$ is a function of $\bar{\mathbf{w}}(i)$. Thus, the joint MMSE design is not in a closed form and one possible solution for such optimization problem is to jointly and iteratively adapt these two parts with an initial guess. The joint-adaptation is operated as follow: for the i-th time instant, $\bar{\mathbf{w}}(i)$ is obtained with the knowledge of $\mathbf{t}(i-1)$ and $\bar{\mathbf{w}}(i-1)$, then $\mathbf{t}(i)$ is updated with $\mathbf{t}(i-1)$ and $\bar{\mathbf{w}}(i)$. The iterative-adaptation is to repeat the joint-adaptation until the satisfactory estimates are obtained. Hence, the number of iterations are environment dependent. Compared with existing reduced-rank schemes such as the MSWF [45] and the AVF [47], this generic scheme enables the projection vector and the reduced-rank filter to exchange information at each iteration. This feature leads to a more effective operation of the adaptive algorithms. However, the drawback of such a feature is that we cannot obtain a closed form design. It will be illustrated by the simulation results that this generic scheme outperforms the MSWF [45] and AVF [47] with a few iterations.

Note that in DS-UWB systems where the length of the full-rank received signal M is large, the complexity of updating the MD-dimensional projection vector is very high. In order to reduce the complexity of this generic scheme,we propose the following switched approximation of adaptive basis functions (SAABF) scheme.

3.4 Proposed SAABF Scheme and Filter Design

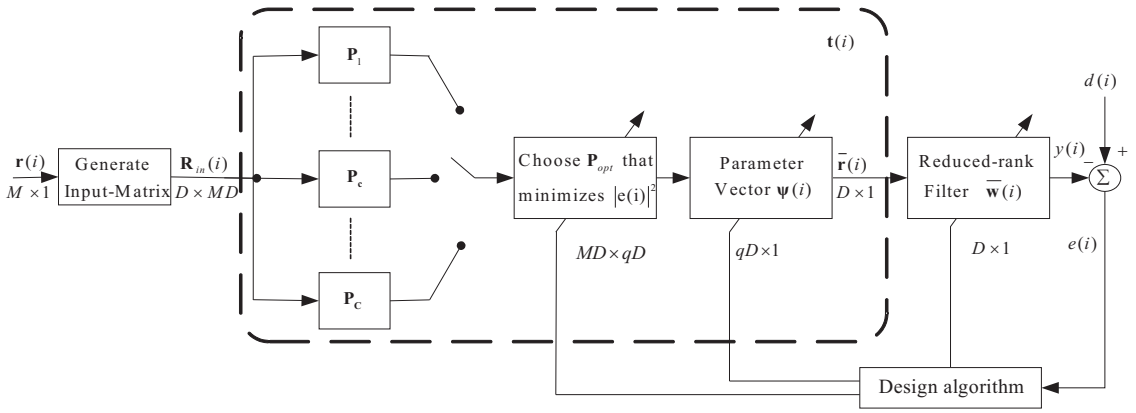

Fig. 3.1: Block diagram of the proposed reduced-rank linear receiver using the SAABF scheme.

In this section we detail the proposed SAABF scheme, whose primary idea is to constrain the structure of the MD-dimensional projection vector $\mathbf{t}(i)$, using a multiple-branch framework such that the number of coefficients to be computed is substantially reduced. The block diagram of the proposed SAABF scheme is shown in Fig.3.1. There are C branches in the SAABF scheme. For each branch, a projection vector is equivalent to a projection matrix $\mathbf{T}_c(i) = [\boldsymbol{\phi}_{c,1}(i), \cdots, \boldsymbol{\phi}_{c,d}(i), \cdots \boldsymbol{\phi}_{c,D}(i)]$, where $c = [1, 2, \cdots, C]$, $d = [1, 2, \cdots, D]$ and the M-dimensional adaptive basis function is given by

$$\boldsymbol{\phi}_{c,d}(i) = \begin{bmatrix} \mathbf{0}_{z_{c,d}\times q} \\ \mathbf{I}_q \\ \mathbf{0}_{(M-q-z_{c,d})\times q} \end{bmatrix}_{M\times q} \quad \boldsymbol{\varphi}_d(i) = \mathbf{Z}_{c,d}\boldsymbol{\varphi}_d(i), \tag{3.12}$$

where $z_{c,d}$ is the number of zeros before the q-by-1 function $\boldsymbol{\varphi}_d(i)$ (where $q \ll M$), which is called the inner function in what follows. The matrix $\mathbf{Z}_{c,d}$ consists of zeros and ones. With a q-by-q identity matrix $\mathbf{I}_q$ in the middle, the zero matrices have the size of $z_{c,d}$-by-q and $(M - q - z_{c,d})$-by-q, respectively. Hence, we can express the projection vector as

$$\mathbf{t}_c(i) = \left[\boldsymbol{\phi}_{c,1}^T(i), \boldsymbol{\phi}_{c,2}^T(i), \cdots, \boldsymbol{\phi}_{c,D}^T(i)\right]^H = \begin{bmatrix} \mathbf{Z}_{c,1} & & & \\ & \mathbf{Z}_{c,2} & & \\ & & \ddots & \\ & & & \mathbf{Z}_{c,D} \end{bmatrix} \begin{bmatrix} \boldsymbol{\varphi}_1(i) \\ \boldsymbol{\varphi}_2(i) \\ \vdots \\ \boldsymbol{\varphi}_D(i) \end{bmatrix}^* = \mathbf{P}_c\boldsymbol{\psi}(i), \tag{3.13}$$

where the MD-by-qD block diagonal matrix $\mathbf{P}_c$ is called position matrix which determines the positions of the q-dimensional inner functions and $\boldsymbol{\psi}(i)$ denotes the qD-dimensional projection vector which is constructed by the inner functions. For each time instant, the rank-reduction in the SAABF scheme is achieved by selecting the position matrix $\mathbf{P}(i)$ instantaneously from a set of pre-stored position matrices $\mathbf{P}_c$, where $c = 1, \ldots, C$, and updating the $\boldsymbol{\psi}(i)$. Compared with (3.8), equation (3.13) shows the constraint we use in the SAABF scheme. With the multi-branch structure, the dimension of the projection vector is shortened from MD to qD.

For simplicity, we denote the proposed scheme with its main parameters as 'SAABF (C,D,q)', where C is the number of branches, D is the length of the reduced-rank filter and q is the length of the inner function. Note that in the case of the SAABF (1,D,M), where $C = 1$ and $q = M$, the proposed scheme is equivalent to the generic scheme described in Section 3.3. For the SAABF (1,1,M), where $C = 1$, $D = 1$ and $q = M$, the proposed scheme can be considered to be a full-rank scheme. All these equivalences are proved in the appendix A, which shows that the optimal solutions in these scenarios will lead to the same MMSE.

It is interesting to note that the adaptation in the proposed SAABF scheme can be considered a hybrid adaptive technique, which includes a discrete parameter optimization for choosing the instantaneous position matrix and a continuous filter design for adapting the projection vector and the reduced-rank filter. In what follows, we detail the discrete parameter optimization and the filter design.

3.4.1 Discrete Parameter Optimization

In this section, the selection rule for choosing $\mathbf{P}(i)$ is introduced and the designs of the pre-stored position matrices $\mathbf{P}_c$ are detailed. The problem of computing the optimal $\mathbf{P}(i)$ is a discrete optimization problem since $\mathbf{P}(i)$ can be considered as a time independent parameter which is selected from a set of pre-stored matrices at each time instant for minimizing the instantaneous squared error. The output signal of each branch is given by

$$y_c(i) = \bar{\mathbf{w}}^H(i)\mathbf{R}_{\text{in}}(i)\mathbf{t}_c(i) = \bar{\mathbf{w}}^H(i)\mathbf{R}_{\text{in}}(i)\mathbf{P}_c\boldsymbol{\psi}(i),$$

where the corresponding error signal is $e_c(i) = d(i) - y_c(i)$. Hence, the selection rule can be expressed as

$$c_{\text{opt}} = \arg \min_{c\in\{1,\ldots,C\}} |e_c(i)|^2,\ e(i) = e_{c_{\text{opt}}}(i),\ \mathbf{P}(i) = \mathbf{P}_{c_{\text{opt}}}. \tag{3.14}$$

As shown in (3.12) and (3.13), the position matrices are distinguished by the values of $z_{c,d}$. The optimal way for selecting $z_{c,d}$ is to test all the possibilities of the position matrices and choose a structure which corresponds to the minimum squared error. However, in the DS-UWB system, the number of possible positions is $(M-q)^D$, where M is much larger than q and D, say $M = 112$ and $q = D = 3$. Therefore, it is too expensive to find the optimal position matrix from such a huge number of possibilities. Hence, we design a small number of C pre-stored position matrices that enables us to find a sub-optimum instantaneous position matrix that provides an attractive tradeoff between performance and complexity. Note that the number C can be considered as a system parameter for the designer, increasing the number of position matrices will benefit the performance but also increase the complexity. In section 3.6.1, we propose a branch number selection algorithm to determine the C within a given range to decrease the averaged required number of branches while maintaining the performance.

For designing the pre-stored matrices, we propose a simple deterministic way to set

the values of $z_{c,d}$ as follows

$$z_{c,d} = \lfloor \frac{M}{D} \rfloor \times (d-1) + (c-1)q, \tag{3.15}$$

where $c = 1, \ldots, C$ and $d = 1, \ldots, D$. Bearing in mind the matrix form shown in (3.12) and (3.13), the first MD-by-qD position matrix $\mathbf{P}_1$ can be expressed as

$$\mathbf{P}_1 = \begin{bmatrix} \mathbf{I}_q & & & & \\ \mathbf{0}_{M-q} & & & & \\ & \mathbf{0}_{\lfloor \frac{M}{D} \rfloor} & & & \\ & \mathbf{I}_q & & & \\ & \mathbf{0}_{M-q-\lfloor \frac{M}{D} \rfloor} & & & \\ & & \ddots & & \\ & & & \mathbf{0}_{\lfloor \frac{M}{D} \rfloor (D-1)} & \\ & & & \mathbf{I}_q & \\ & & & \mathbf{0}_{M-q-\lfloor \frac{M}{D} \rfloor (D-1)} & \end{bmatrix}, \tag{3.16}$$

where all the zero and identity matrices have q columns and the subscripts denote the number of rows of these matrices. We remark that the proposed approach arranges the q-by-q identity matrices in a simple fixed sliding pattern. This then allows efficient generation of the remaining position matrices. For example, the second projection matrix $\mathbf{P}_2$ can be considered as a shifted version of $\mathbf{P}_1$, in which each column has been shifted down by q elements. It should be noted that the pre-stored position matrices can also be generated randomly, in which approach the values of $z_{c,d}$ are set randomly. However, the random method will require extra storage space for all the pre-stored matrices and the performance of this method is inferior to the proposed deterministic method.

3.4.2 Filter Design

After determining the position matrix $\mathbf{P}(i)$, the LS design of the reduced-rank filter and the projection vector can be developed to minimize the following cost function

$$\mathbf{J}_{\mathrm{LS}}(\bar{\mathbf{w}}(i), \boldsymbol{\psi}(i)) = \sum_{j=1}^{i} \lambda^{i-j} |d(j) - \bar{\mathbf{w}}^H(i) \mathbf{R}_{\mathrm{in}}(j) \mathbf{P}(i) \boldsymbol{\psi}(i)|^2, \tag{3.17}$$

where λ is a forgetting factor. Firstly, we calculate the gradient of (3.17) with respect to $\bar{\mathbf{w}}(i)$, which is

$$\mathbf{g}_{\mathrm{LS}\bar{w}^*(i)} = -\bar{\mathbf{p}}_{w_{\mathrm{LS}}}(i) + \bar{\mathbf{R}}_{w_{\mathrm{LS}}}(i) \bar{\mathbf{w}}(i), \tag{3.18}$$

where $\bar{\mathbf{p}}_{w_{\mathrm{LS}}}(i) = \sum_{j=1}^{i} \lambda^{i-j} d^*(j)\bar{\mathbf{r}}(j)$ and $\bar{\mathbf{R}}_{w_{\mathrm{LS}}}(i) = \sum_{j=1}^{i} \lambda^{i-j}\bar{\mathbf{r}}(j)\bar{\mathbf{r}}^H(j)$. Assuming that $\boldsymbol{\psi}(i)$ is fixed, the LS solution of the reduced-rank filter is

$$\bar{\mathbf{w}}_{\mathrm{LS}}(i) = \bar{\mathbf{R}}^{-1}_{w_{\mathrm{LS}}}(i)\bar{\mathbf{p}}_{w_{\mathrm{LS}}}(i). \tag{3.19}$$

Secondly, we examine the gradient of (3.17) with respect to $\boldsymbol{\psi}(i)$, which is

$$\mathbf{g}_{\mathrm{LS}\psi^*(i)} = -\mathbf{p}_{\psi_{LS}}(i) + \mathbf{R}_{\psi_{\mathrm{LS}}}(i)\boldsymbol{\psi}(i), \tag{3.20}$$

where $\mathbf{p}_{\psi_{\mathrm{LS}}}(i) = \sum_{j=1}^{i} \lambda^{i-j} d(j)\mathbf{r}_{\psi}(j)$, $\mathbf{R}_{\psi_{\mathrm{LS}}}(i) = \sum_{j=1}^{i} \lambda^{i-j}\mathbf{r}_{\psi}(j)\mathbf{r}^H_{\psi}(j)\boldsymbol{\psi}(i)$ and $\mathbf{r}_{\psi}(j) = \mathbf{P}^H(j)\mathbf{R}^H_{\mathrm{in}}(j)\bar{\mathbf{w}}(j)$. With the assumption that $\bar{\mathbf{w}}(i)$ is fixed, the LS solution of the projection vector is

$$\boldsymbol{\psi}_{\mathrm{LS}}(i) = \mathbf{R}^{-1}_{\psi_{\mathrm{LS}}}(i)\mathbf{p}_{\psi_{\mathrm{LS}}}(i). \tag{3.21}$$

Finally, (3.19) and (3.21) summarize the LS design of the reduced-rank filter and the projection vector in the SAABF scheme. A discussion on the optimization of the SAABF scheme is presented in appendix B.

3.5 Adaptive Algorithms

In this section, joint LMS and RLS algorithms are developed for estimating the reduced-rank filter and the projection vector. The complexity analysis is also given to compare the computational load of existing and the proposed algorithms. We remark that in the SAABF scheme, when a number of branches are implemented, the joint adaptation only requires one iteration for each time instant.

3.5.1 The LMS Version

The joint LMS version of the SAABF scheme is developed to minimize the MSE cost function:

$$\mathbf{J}_{\mathrm{MSE}}(\bar{\mathbf{w}}(i), \boldsymbol{\psi}(i)) = E[|d(i) - \bar{\mathbf{w}}^H(i)\mathbf{R}_{\mathrm{in}}(i)\mathbf{P}(i)\boldsymbol{\psi}(i)|^2], \tag{3.22}$$

where $\mathbf{P}(i)$ is the instantaneous position matrix. The MMSE solution of the SAABF scheme is shown in the appendix A.

At the i-th time instant, we firstly determine the instantaneous position matrix with the selection rule (3.14). Then, the reduced-rank filter weight vector $\bar{\mathbf{w}}(i)$ can be updated with the LMS algorithm [26]. Taking the gradient vector of (3.22) with respect to $\bar{\mathbf{w}}(i)$

and using the instantaneous values of the gradient vector, the adaptation equation for the reduced-rank filter is given by

$$\bar{\mathbf{w}}(i+1) = \bar{\mathbf{w}}(i) + \mu_w \mathbf{R}_{\text{in}}(i)\mathbf{P}(i)\boldsymbol{\psi}(i)e^*(i), \tag{3.23}$$

where μ_w is the step size. With the knowledge of the updated reduced-rank filter, the projection vector can be adapted to minimize the cost function (3.22). Taking the gradient vector of (3.22) with respect to $\boldsymbol{\psi}(i)$ and using the instantaneous estimate of the gradient vector, the adaptation equation for the projection vector is obtained as

$$\boldsymbol{\psi}(i+1) = \boldsymbol{\psi}(i) + \mu_\psi \mathbf{P}^H(i)\mathbf{R}_{\text{in}}^H(i)\bar{\mathbf{w}}(i+1)e(i), \tag{3.24}$$

where μ_ψ is the step size. We summarize the LMS version of the SAABF scheme in Table 3.1.

Tab. 3.1: Proposed adaptive algorithms for SAABF scheme.

LMS :	
Step 1:	Initialization: $\boldsymbol{\psi}(0)$=ones(qD, 1) and $\bar{\mathbf{w}}(0)$=zeros(D, 1) Set values for μ_w and μ_ψ Generate the position matrices $\mathbf{P}_1, \ldots, \mathbf{P}_C$
Step 2:	For i=0, 1, 2, ... (1) Compute the error signals $e_c(i)$ for each branch, (2) Select the branch $c_{\text{opt}} = \arg\min_{c\in\{1,\ldots,C\}} \lvert e_c(i)\rvert^2$, (3) Set the instantaneous position matrix $\mathbf{P}(i)$=$\mathbf{P}_{c_{\text{opt}}}$, (4) Update $\bar{\mathbf{w}}(i+1)$ using (3.23) (5) Update $\boldsymbol{\psi}(i+1)$ using (3.24).
RLS :	
Step 1:	Initialization: $\boldsymbol{\psi}(0)$=ones(qD, 1) and $\bar{\mathbf{w}}(0)$=zeros(D, 1) $\bar{\mathbf{R}}_{w_{\text{LS}}}^{-1}(0)$=$\mathbf{I}_D/\delta_w$ and $\mathbf{R}_{\psi_{\text{LS}}}^{-1}(0)$=$\mathbf{I}_{qD}/\delta_\psi$ Set values for λ, δ_w and δ_ψ Generate the position matrices $\mathbf{P}_1, \ldots, \mathbf{P}_C$
Step 2:	For i=1, 2, ... (1) Compute the error signals $e_c(i)$ for each branch, (2) Select the branch $c_{\text{opt}} = \arg\min_{c\in\{1,\ldots,C\}} \lvert e_c(i)\rvert^2$, (3) Set the instantaneous position matrix $\mathbf{P}(i)$=$\mathbf{P}_{c_{\text{opt}}}$, (4) Update $\bar{\mathbf{w}}(i) = \bar{\mathbf{w}}(i-1) + \mathbf{K}_w(i)e^*(i)$, (5) Update $\bar{\mathbf{R}}_{w_{\text{LS}}}^{-1}(i)$ using (3.25), (6) Update $\boldsymbol{\psi}(i) = \boldsymbol{\psi}(i-1) + \mathbf{K}_\psi(i)e(i)$, (7) Update $\mathbf{R}_{\psi_{\text{LS}}}^{-1}(i)$ using (3.30).

3.5.2 The RLS Version

Let us consider the RLS design of the SAABF scheme, which can be developed to minimize the cost function shown in (3.17). The instantaneous position matrix is determined with the selection rule (3.14). The reduced-rank filter will be updated first. The gradient of (3.17) with respect to $\bar{\mathbf{w}}(i)$ is shown in (3.18). By applying the matrix inversion lemma to $\bar{\mathbf{R}}_{w_{\mathrm{LS}}}(i)$, we obtain its inverse matrix in a recursive way as

$$\bar{\mathbf{R}}_{w_{\mathrm{LS}}}^{-1}(i) = \lambda^{-1}\bar{\mathbf{R}}_{w_{\mathrm{LS}}}^{-1}(i-1) - \lambda^{-1}\mathbf{K}_w(i)\bar{\mathbf{r}}^H(i)\bar{\mathbf{R}}_{w_{\mathrm{LS}}}^{-1}(i-1), \tag{3.25}$$

where

$$\mathbf{K}_w(i) = \frac{\bar{\mathbf{R}}_{w_{\mathrm{LS}}}^{-1}(i-1)\bar{\mathbf{r}}(i)}{\lambda + \bar{\mathbf{r}}^H(i)\bar{\mathbf{R}}_{w_{\mathrm{LS}}}^{-1}(i-1)\bar{\mathbf{r}}(i)}. \tag{3.26}$$

In order to obtain a recursive update equation, we express the vector $\bar{\mathbf{p}}_{w_{\mathrm{LS}}}(i)$ as

$$\bar{\mathbf{p}}_{w_{\mathrm{LS}}}(i) = \lambda\bar{\mathbf{p}}_{w_{\mathrm{LS}}}(i-1) + d^*(i)\bar{\mathbf{r}}(i). \tag{3.27}$$

By substituting (3.25) and (3.27) into (3.18) and setting the gradient to zero, we obtain the RLS adaptation equation for the reduced-rank filter as

$$\bar{\mathbf{w}}(i) = \bar{\mathbf{w}}(i-1) + \mathbf{K}_w(i)e^*(i). \tag{3.28}$$

With the knowledge of the updated reduced-rank filter, we can adapt the projection vector to minimize the cost function (3.17). The gradient of (3.17) with respect to $\boldsymbol{\psi}(i)$ is shown in (3.20).

In order to obtain the recursive update equation for the projection vector, we express $\mathbf{p}_{\psi_{\mathrm{LS}}}(i)$ in a recursive form as:

$$\mathbf{p}_{\psi_{\mathrm{LS}}}(i) = \lambda\mathbf{p}_{\psi_{\mathrm{LS}}}(i-1) + d(i)\mathbf{r}_\psi(i), \tag{3.29}$$

where $\mathbf{r}_\psi(j) = \mathbf{P}^H(j)\mathbf{R}_{\mathrm{in}}^H(j)\bar{\mathbf{w}}(j)$.

Applying the matrix inversion lemma to $\mathbf{R}_{\psi_{\mathrm{LS}}}(i)$, we obtain its inverse recursively

$$\mathbf{R}_{\psi_{\mathrm{LS}}}^{-1}(i) = \lambda^{-1}\mathbf{R}_{\psi_{\mathrm{LS}}}^{-1}(i-1) - \lambda^{-1}\mathbf{K}_\psi(i)\mathbf{r}_\psi^H(i)\mathbf{R}_{\psi_{\mathrm{LS}}}^{-1}(i-1), \tag{3.30}$$

where

$$\mathbf{K}_\psi(i) = \frac{\mathbf{R}_{\psi_{\mathrm{LS}}}^{-1}(i-1)\mathbf{r}_\psi(i)}{\lambda + \mathbf{r}_\psi^H(i)\mathbf{R}_{\psi_{\mathrm{LS}}}^{-1}(i-1)\mathbf{r}_\psi(i)}, \tag{3.31}$$

By substituting (3.29) and (3.30) into (3.20) and setting the gradient to zero, we obtain

Tab. 3.2: Complexity analysis for the MMSE based algorithms

Algorithm	Complex Additions	Complex Multiplications
Full-Rank LMS	$2M$	$2M+1$
Full-Rank RLS	$3M^2+M$	$4(M^2+M)$
MSWF-LMS	$DM^2+(D+2)M$	$(D+1)M^2+(3D+2)M$ $+2D+1$
MSWF-RLS	$DM^2+(D+2)M$ $+3D^2-D$	$(D+1)M^2+(3D+2)M$ $+4(D^2+D)$
AVF	$(3D+1)M^2+M$ $-2D-1$	$(5D+2)M^2+(D+1)M$
SAABF(C,D,q)-LMS	$qD(C+1)-CD$ $+C+D$	$DM+2Dq(C+1)+D+2$
SAABF(C,D,q)-RLS	$4(qD)^2+CD(q-1)$ $+3D^2+C+D$	$DM+5(qD)^2+2CDq+4D^2$ $+3Dq+3D$

the RLS adaptation equation for the projection vector

$$\boldsymbol{\psi}(i)=\boldsymbol{\psi}(i-1)+\mathbf{K}_{\psi}(i)e(i). \tag{3.32}$$

The RLS version of the SAABF scheme is summarized in Table 3.1.

3.5.3 Complexity Analysis

The computational complexity for different adaptive algorithms with respect to the number of complex additions and complex multiplications for each processed data bit is shown in Table 3.2. We compare the complexity of the full-rank LMS and RLS, the LMS and RLS versions of the MSWF, the AVF and the proposed SAABF scheme. The quantity M is the length of the full-rank filter, D is the dimension of the subspace, C is the number of branches in the SAABF scheme and q is the length of the inner function. In Fig.3.2, the number of complex multiplications of the linear adaptive algorithms are shown as a function of M. We remark that the complexity of the receiver with the proposed SAABF scheme is linearly proportional to the length of the received signal and is much lower than the existing reduced-rank schemes in the large signal length scenarios. It should be noted that for each time instant the SAABF scheme requires one simple search procedure, which will select the minimum squared-error from a C-dimensional error vector.

There is an extremely simple configuration of the proposed scheme that can be expressed as SAABF (C,D,1), in which the length of the inner function is only 1 and the

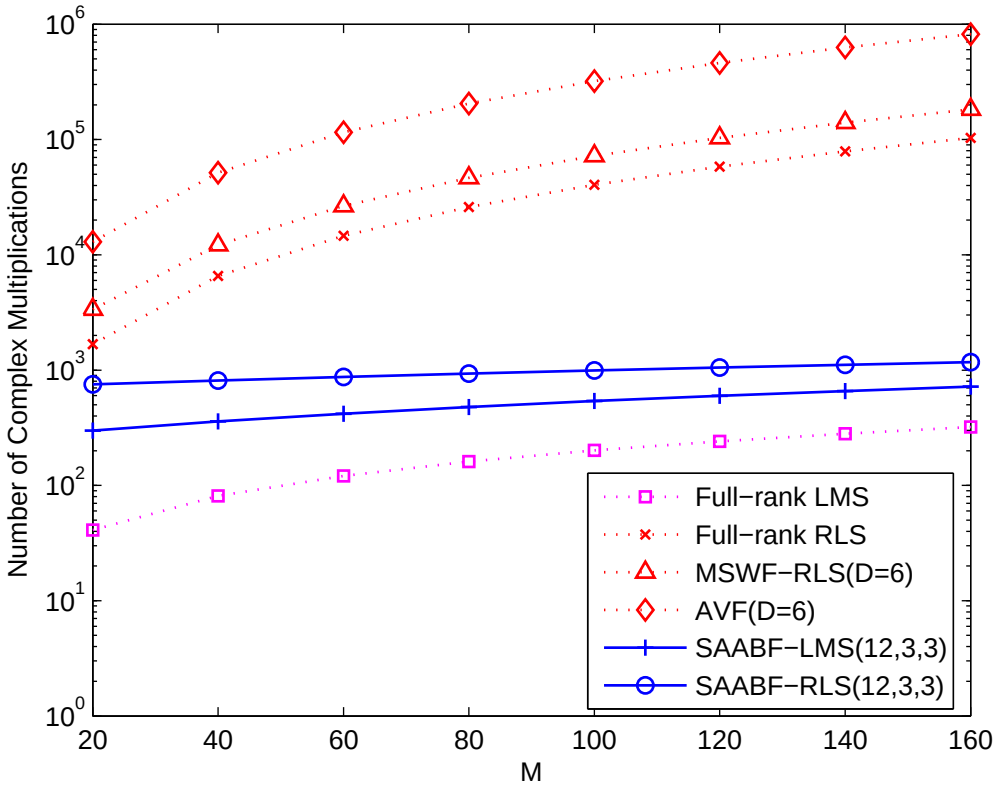

Fig. 3.2: The computational complexity of the linear adaptive algorithms.

projection vector $\boldsymbol{\psi}(i)$ is fixed to its initial value of $\boldsymbol{\psi}(i) = \mathrm{ones}(\mathrm{D}, 1)$. This feature significantly reduces the complexity of the SAABF scheme and the performance of this configuration will be illustrated with simulation results.

3.6 Model Order and Parameter Adaptation

In the SAABF (C,D,q) scheme, the computational complexity and the performance are highly dependent on the values of the parameter C and the model order D and q. Although we can set suitable values for these parameters in a specific operation environment with some performance requirements, the best tradeoffs between the complexity and performance usually can not be obtained. In order to choose these parameters automatically and effectively in different environments, we propose adaptive algorithms as follows.

3.6.1 Branch Number Selection

The algorithm for selecting the most appropriate branch number is developed with the observations: all the branches will be used at least once but there are some branches that are more likely to be selected; for a target squared-error, with a given number of branches, it is unnecessary to test all of them at each time instant, we can choose the first one that assures the target. With these observations and assuming that D and q are fixed, we propose an algorithm to select the number of branches. Firstly, we set a minimum and a maximum number of branches, denoted as $C_{\min}$ and $C_{\max}$, respectively. Then, we define a threshold γ that is related to the MMSE. For each time instant, we test the first $C_{\min}$ branches, if the MSE target is not assured, we test the $(C_{\min}+1)$-th branch and so on. We stop the search when the target is achieved or the maximum allowed number of branches $C_{\max}$ is reached. The proposed algorithm can be expressed as

$$C_{\mathrm{r}}(i) = \arg \min_{c \in \{C_{\min},\ldots,C_{\max}\}} [|e_c^2(i) - e_{\mathrm{MMSE}}^2| < \gamma], \tag{3.33}$$

where $e_c(i) = d(i) - \bar{\mathbf{w}}^H(i)\mathbf{R}_{\mathrm{in}}(i)\mathbf{P}_c\boldsymbol{\psi}(i)$ is the error signal corresponding to the c-th branch and $C_{\mathrm{r}}(i)$ represents the required number of branches at the i-th time instant. Note that the e_{MMSE} is the ideal minimum error signal and we can replace it with a given value for the target environment. The aim of this selection algorithm is to reduce the average number of used branches while maintaining the BER (or MSE) performance.

3.6.2 Rank Adaptation

The computational complexity and the performance of the novel SAABF reduced-rank scheme is sensitive to the determined rank D. Unlike prior work that used the approach proposed in [42], we develop a rank adaptation algorithm based on the *a posteriori* LS cost function to estimate the MSE, which is a function of the parameters $\bar{\mathbf{w}}_D^H(i)$, $\mathbf{R}_{\mathrm{in},D}(i)$, $\mathbf{P}_D(i)$ and $\boldsymbol{\psi}_D(i)$

$$\mathscr{C}_D(i) = \sum_{n=0}^{i} \lambda_D^{i-n} |d(i) - \bar{\mathbf{w}}_D^H(i)\mathbf{R}_{\mathrm{in},D}(i)\mathbf{P}_D(i)\boldsymbol{\psi}_D(i)|^2, \tag{3.34}$$

where λ_D is a forgetting factor. Since the optimal rank can be considered as a function of the time index i [42], the forgetting factor is required and allows us to track the optimal rank. We assume that the number of branches C and the length of the inner function q are fixed. For each time instant, we update a reduced-rank filter $\bar{\mathbf{w}}_{\mathrm{M}}(i)$ and a projection

vector $\boldsymbol{\psi}_M(i)$ with the maximum rank $D_{\max}$, which can be expressed as

$$\begin{aligned}\bar{\mathbf{w}}_{\mathrm{M}}(i) &= [\bar{w}_{\mathrm{M},1}(i), \ldots, \bar{w}_{\mathrm{M},D}(i), \ldots, \bar{w}_{\mathrm{M},D_{\max}}(i)]^T \\ \boldsymbol{\psi}_{\mathrm{M}}(i) &= [\psi_{\mathrm{M},1}(i), \ldots, \psi_{\mathrm{M},qD}(i), \ldots, \psi_{\mathrm{M},qD_{\max}}(i)]^T.\end{aligned} \tag{3.35}$$

After the adaptation, we test values of D within the range $D_{\min}$ to $D_{\max}$. For each tested rank, we use the following estimators

$$\begin{aligned}\bar{\mathbf{w}}_D(i) &= [\bar{w}_{\mathrm{M},1}(i), \ldots, \bar{w}_{\mathrm{M},D}(i)]^T \\ \boldsymbol{\psi}_D(i) &= [\psi_{\mathrm{M},1}(i), \ldots, \psi_{\mathrm{M},qD}(i)]^T.\end{aligned} \tag{3.36}$$

The position matrices for different model orders can be pre-stored and the instantaneous position matrix $\mathbf{P}_D(i)$ can be determined by the decision rule as shown in (3.14). After selecting the position matrix and given the input data matrix, we substitute (4.60) into (4.58) to obtain the value of $\mathscr{C}_D(i)$, where $D \in \{D_{\min}, \ldots, D_{\max}\}$. The proposed algorithm can be expressed as

$$D_{\mathrm{opt}}(i) = \arg \min_{D \in \{D_{\min}, \ldots, D_{\max}\}} \mathscr{C}_D(i). \tag{3.37}$$

We remark that the complexity of updating the reduced-rank filter and the projection vector in the proposed rank adaptation algorithm is the same as the SAABF (C,$\mathrm{D}_{\max}$,q), since we only adapt the $\bar{\mathbf{w}}_{\mathrm{M}}(i)$ and $\boldsymbol{\psi}_{\mathrm{M}}(i)$ for each time instant. However, additional computations are required for calculating the values of $\mathscr{C}_D(i)$ and selecting the minimum value of a $(D_{\max} - D_{\min} + 1)$-dimensional vector that corresponds to a simple search and comparison.

3.6.3 Inner Function Length Selection

In the SAABF scheme, the length of the inner function is also a sensitive parameter that affects the complexity and the overall performance. In this work, we apply a similar idea used for the rank adaptation, to select the optimal value of q. The criterion to choose q_{opt} is that it minimizes the following cost function

$$\mathscr{C}_q(i) = \sum_{n=0}^{i} \lambda_q^{i-n} |d(i) - \bar{\mathbf{w}}^H(i) \mathbf{R}_{\mathrm{in}}(i) \mathbf{P}_q(i) \boldsymbol{\psi}_q(i)|^2, \tag{3.38}$$

where the forgetting factor λ_q is applied, since we observe that in the SAABF scheme, the length of q plays a similar role as the rank D and the optimal q can change as a function of the time index i.

When the model order D and the branch number C are fixed, for each time instant,

we adapt a D-by-1 reduced-rank filter $\bar{\mathbf{w}}(i)$ jointly with a $Dq_{\max}$-by-1 projection vector $\boldsymbol{\psi}_{\mathrm{Q}}(i) = [\psi_{\mathrm{Q},1}(i), \ldots, \psi_{\mathrm{Q},Dq}(i), \ldots, \psi_{\mathrm{Q},Dq_{\max}}(i)]^T$. For different values of q, we use the estimate

$$\boldsymbol{\psi}_q(i) = [\boldsymbol{\psi}_{q,1}^T(i), \ldots, \boldsymbol{\psi}_{q,D}^T(i)]^T, \tag{3.39}$$

where the vectors of $\boldsymbol{\psi}_{q,d}(i)$, $d = 1, \ldots, D$, can be expressed as

$$\boldsymbol{\psi}_{\mathrm{q,d}}(i) = [\psi_{\mathrm{Q},(d-1)q_{\max}+1}(i), \ldots, \psi_{\mathrm{Q},(d-1)q_{\max}+q}(i)]^T. \tag{3.40}$$

At the i-th moment, we search from $q_{\min}$ to $q_{\max}$ and determine the q_{opt} using the following algorithm

$$q_{\mathrm{opt}}(i) = \arg \min_{q \in \{q_{\min}, \ldots, q_{\max}\}} \mathscr{C}_q(i). \tag{3.41}$$

The computational complexity of updating the reduced-rank filter and the projection vector in this algorithm is the same as the SAABF (C,D,$\mathrm{q}_{\max}$). Since we only adapt a D-by-1 reduced-rank filter and a $Dq_{\max}$-by-1 projection vector for all tested values of q. Additional computations are needed to compute the values of $\mathscr{C}_q(i)$ and search the minimum value in a $(q_{\max} - q_{\min} + 1)$-dimensional vector.

3.7 Simulations

In this section, we apply the proposed generic and SAABF schemes to the uplink of a multiuser BPSK DS-UWB system and evaluate their performance against existing reduced-rank and full-rank methods. In all numerical simulations, all the users are assumed to be transmitting continuously at the same power level. The pulse shape adopted is the RRC pulse with the pulse-width 0.375ns. The spreading codes are generated randomly for each user in each independent simulation with a spreading gain of 32 and the data rate of the communication is approximately 83Mbps. The standard IEEE 802.15.4a channel model for the NLOS indoor environment is employed [23] and we assume that the channel is constant during the whole transmission. The channel delay spread is $T_{DS} = 30ns$ that is much larger than the symbol duration, which is $T_s = 12ns$. Hence, the severe ISI from $2G = 6$ neighbor symbols are taken into the account for the simulations. The sampling rate at the receiver is assumed to be 2.67GHz and the length of the discrete time received signal is $M = 112$. For all the simulations, the adaptive filters are initialized as null vectors. This allows a fair comparison between the analyzed techniques for their convergence performance. In practice, the filters can be initialized with prior knowledge about the spreading code or the channel to accelerate the convergence. In this work, we present the uncoded bit error rate (BER) for all the comparisons. All the curves are obtained by averaging 200 independent simulations.

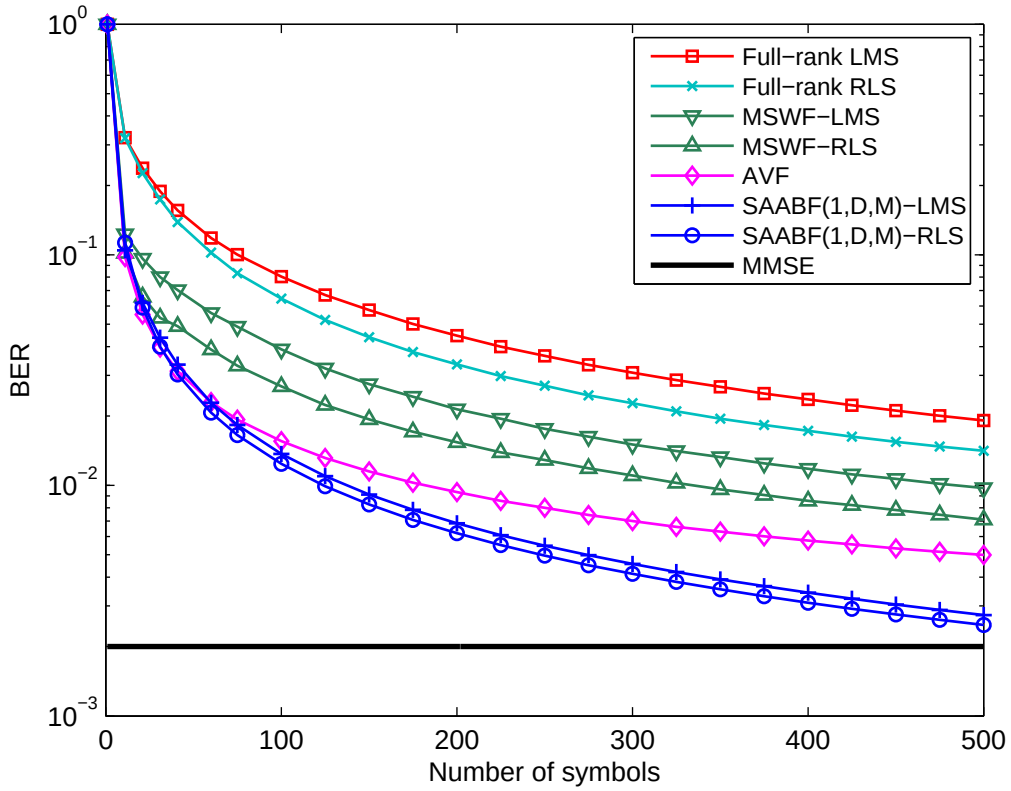

Fig. 3.3: BER performance of different algorithms for a SNR=20dB and 8 users. The following parameters were used: full-rank LMS ($\mu = 0.075$), full-rank RLS ($\lambda = 0.998$, $\delta = 10$), MSWF-LMS ($D = 6$, $\mu = 0.075$), MSWF-RLS ($D = 6$, $\lambda = 0.998$), AVF ($D = 6$), SAABF (1,3,M)-LMS ($\mu_w = 0.15$, $\mu_\psi = 0.15$, 3 iterations) and SAABF (1,3,M)-RLS ($\lambda = 0.998$, $\delta = 10$, 3 iterations).

The first experiment we perform is to compare the uncoded BER performance of the generic reduced-rank scheme, which is denoted as SAABF (1,D,M), with the full-rank LMS and RLS algorithms, the LMS and RLS versions of the MSWF, and the AVF method. We consider the scenario with a signal-to-noise ratio (SNR) of 20dB, 8 users. Fig.3 shows the BER performance of different schemes as a function of training symbols transmitted. The proposed generic scheme outperforms all the other methods with 3 iterations. In the generic scheme, the joint RLS algorithm could converge faster than the joint LMS algorithm with the same number of iterations. However, in the SAABF (C,D,q) scheme, when a sufficient number of branches are employed, both versions of the joint adaptive algorithm can achieve excellent performance with only one iteration for each input data.

Fig.3.4 shows the uncoded BER performance of the RLS version of the novel SAABF scheme with different number of branches in the same scenario as in the first experiment. In this experiment, the performance of the simple configuration SAABF (C,D,1) is com-

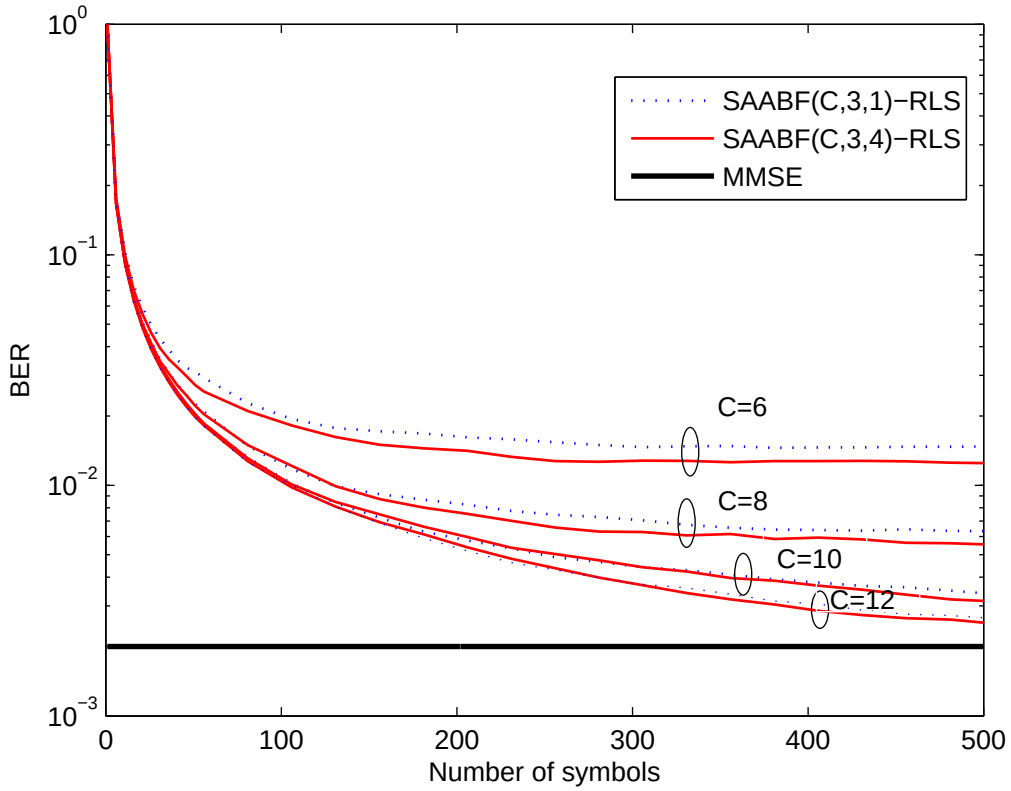

Fig. 3.4: BER performance of the proposed SAABF scheme versus the number of training symbols for a SNR=20dB. The number of users is 8 and the following parameters were used: SAABF-RLS ($\lambda = 0.998$, $\delta = 10$).

pared with SAABF (C,D,q), where $q = 4$. Note that, in SAABF (C,D,1), the projection vector $\boldsymbol{\psi}(i)$ is no longer updated, we use its initial value for the whole transmission. In the SAABF (C,D,q) scheme, when a sufficient number of branches are employed, both versions of the joint adaptive algorithm can achieve excellent performance with only one iteration for each input data. It is shown that increasing the number of branches, the performance approaches that of the full-rank MMSE filter that assumes given the knowledge of the noise variance, the channels and the spreading codes for all the users. The SAABF (C,D,1) scheme can achieve a similar convergence speed to the SAABF (C,D,q), but the steady-state performance of the SAABF (C,D,q) is better than the SAABF (C,D,1). The RLS version of the SAABF scheme performs slightly better than the LMS version. The results of the LMS version are not included in the figure for the sake of clarity.

Fig.3.5 (a) and (b) show the uncoded BER performances of algorithms with different SNRs in a 8 users communication and with different numbers of users in a 18dB scenario, respectively. It should be noted that if the number of training symbols is sufficient, the performance of the full-rank algorithms and the reduced-rank algorithms will approach

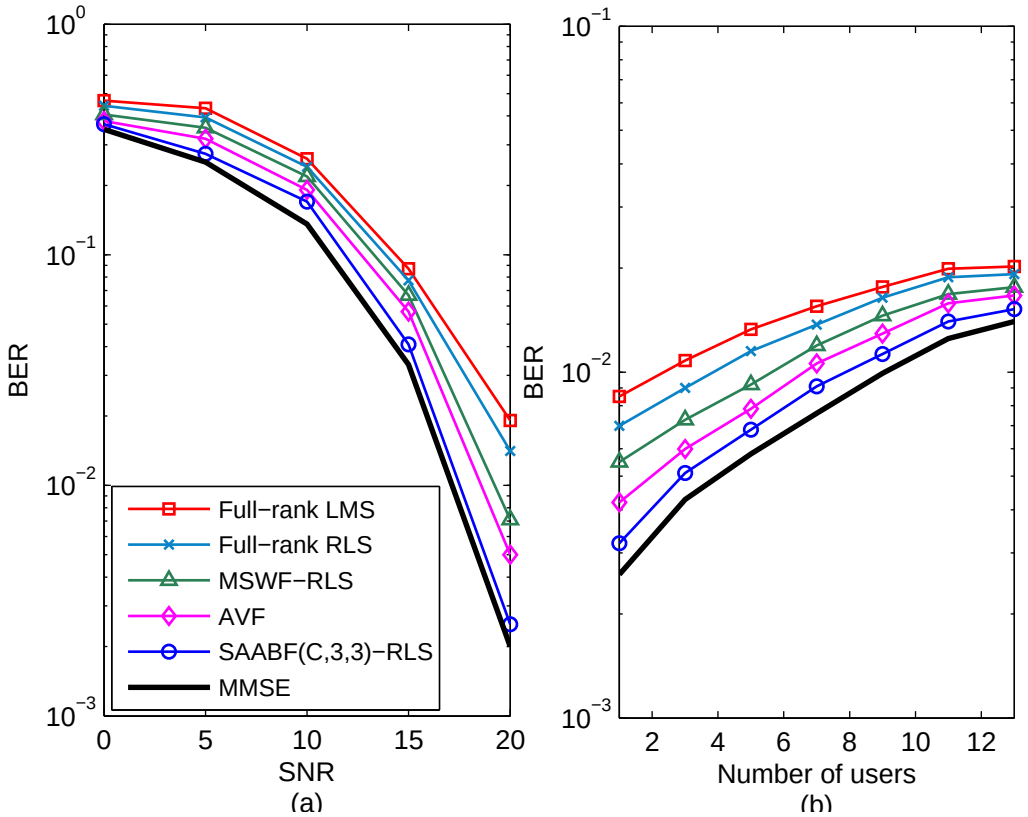

Fig. 3.5: BER performance of the proposed scheme with different SNRs and number of users.

the performance of the full-rank MMSE filter. However, for short data support the reduced rank algorithms outperform the full-rank algorithms due to their faster training. In these experiments, 500 symbols are transmitted for each tested environment in each independent simulation. The SAABF (C,3,3)-RLS is employed with C in the range of 2 to 12. For different scenarios, the minimum number of branches that enables the proposed scheme to approach the linear MMSE performance is chosen. We remark that in this experiment, the number of coefficients required to be updated in the SAABF scheme is significantly smaller than the received signal length. The novel SAABF scheme outperforms all other schemes in all the simulated scenarios. In the scenario with 8 users, the SAABF-RLS can save over 1dB in comparison with the AVF scheme and save approximately 4dB in comparison with the full-rank LMS algorithm for a BER around 0.02. When the SNR is 18dB, the SAABF-RLS scheme can support 1 additional user in comparison with the AVF and up to 7 additional users in comparison with the full-rank LMS algorithm for a BER of 0.01.

The uncoded BER performance of the proposed RLS version of the SAABF scheme with the implementation of the branch number selection algorithm is shown in Fig.3.6.

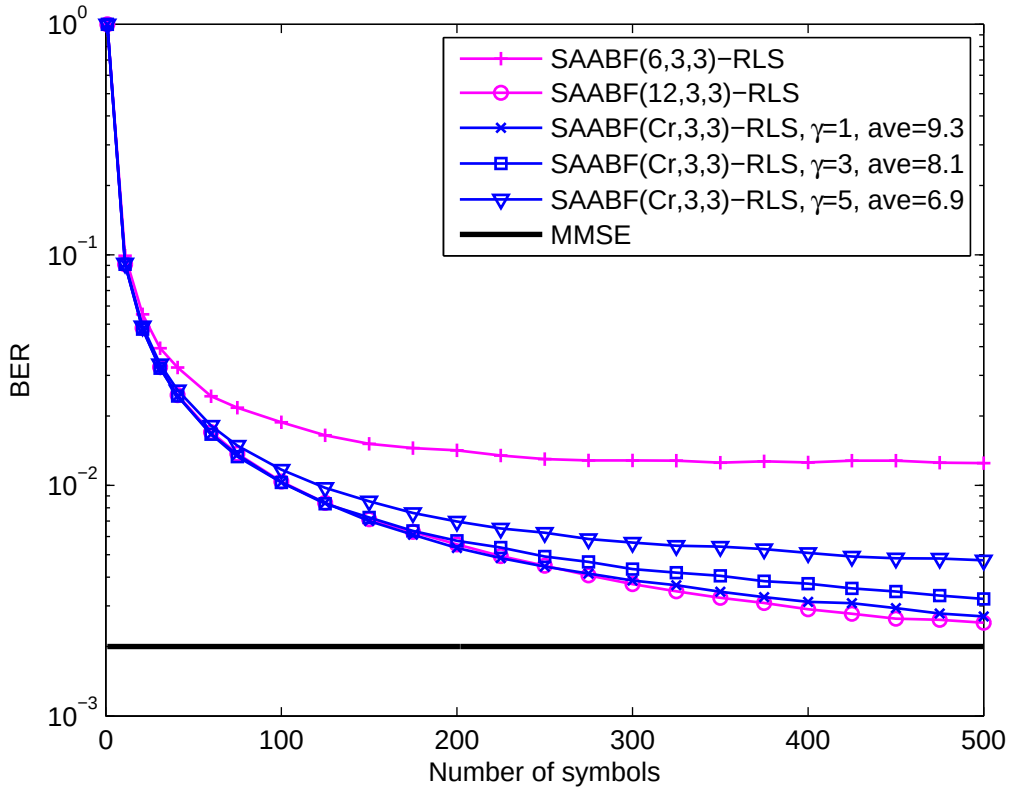

Fig. 3.6: BER performance of the SAABF scheme with branch-number selection. The scenario of 20dB and 8 users are considered. The parameters used: SAABF-RLS ($\lambda = 0.998$, $\delta = 10$). For branch-number selection algorithm: $C_{\min} = 6$ and $C_{\max} = 12$, threshold γ is in the unit of dB.

The proposed algorithm instantaneously chooses the number of branches C_r using (3.33), from the range $C_{\min} = 6$ to $C_{\max} = 12$. As the threshold γ increasing, the average required number of branches C_r and the overall complexity are reducing, but the performance degrading. For a 1dB threshold, the performance of the branch number selection SAABF (C_r,D,q) is very close to the SAABF ($C_{\max}$,D,q), while the average branch number C_r is only 9.3, which is considerably lower than the $C_{\max} = 12$. Hence, with the branch number selection algorithm we obtain a solution which has lower complexity and similar performance to that when the $C_{\max}$ is used.

Fig.3.7 compares the BER performance of the SAABF-LMS using the rank-adaptation algorithm with $C = 5$ and $q = 3$. The results using a fixed-rank of 3 and 8 are also shown in Fig.3.7 for comparison purposes and illustration of the sensitivity of the SAABF scheme to the rank D. The rank-adaptation solution selects the optimal rank $D_o(i)$ using (4.61) for each time instant, from the range $D_{\min} = 3$ to $D_{\max} = 8$. The BER performance of the SAABF scheme with the rank-adaptation algorithm outperforms the fixed-rank

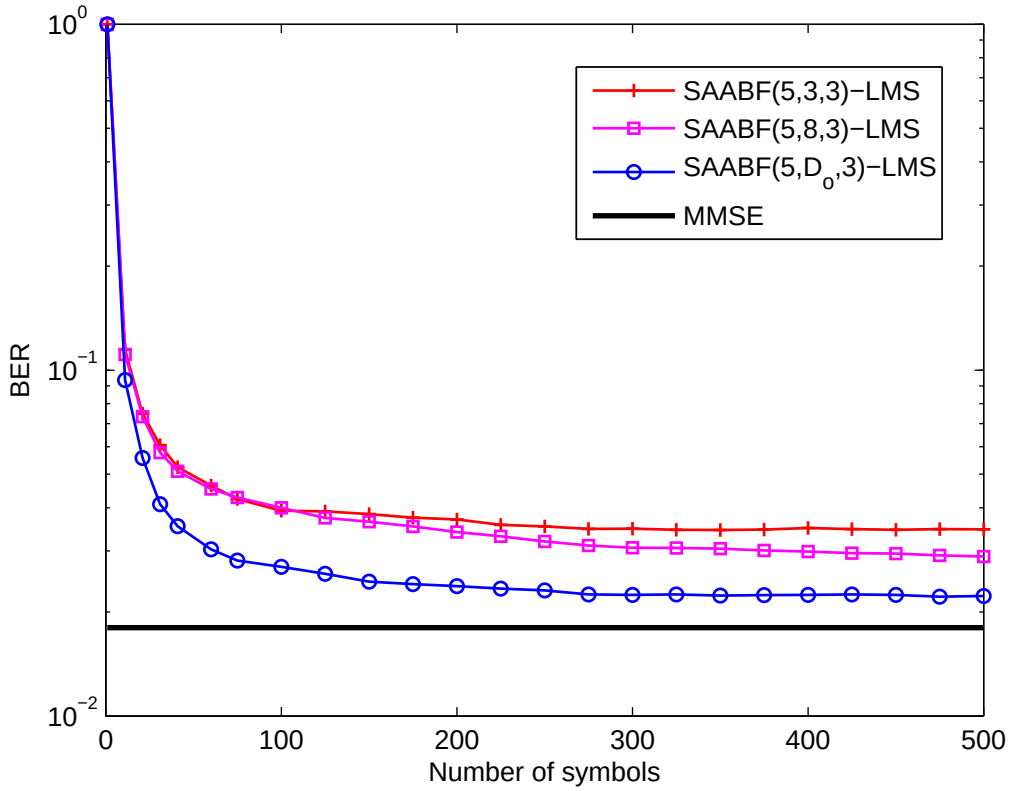

Fig. 3.7: BER performance of the SAABF scheme with rank adaptation. The scenario of 16dB and 8 users are considered. The parameters used: SAABF-LMS ($\mu_w = 0.15$, $\mu_\psi = 0.15$). For rank-adaptation algorithm: $D_{\min} = 3$, $D_{\max} = 8$ and $\lambda_D = 0.998$.

SAABF scheme with $D_{\min}$ or $D_{\max}$. In this environment, $D = 8$ has better steady-state performance than $D = 3$, with both cases showing the same convergence speed.The rank-adaptation algorithm provides a better tradeoff between the convergence speed and the steady-state performance.

Fig.3.8 shows the BER behavior of the SAABF-RLS scheme with the adaptive algorithm determining q, which is the length of the inner function. The value of $q_o(i)$ for each time instant is determined by (3.41), we set $q_{\min} = 3$ and $q_{\max} = 8$ and the forgetting factor is set to $\lambda_q = 0.998$. A clear improvement is shown when the algorithm that selects q is used. It also can be seen that, in the cases with fixed q, smaller values of q could lead to faster convergence, however it introduces losses to the steady-state performance.

In the last experiment, we conduct a comparison of the proposed and existing linear receiver structures as shown in Fig. 3.9. In a system with 8 users, we examine the performance of the traditional RAKE receiver with the maximal-ratio combining (MRC), the reduced-order multiuser detection (RMUD) [36] with 15 taps, the generic algorithm (GA)

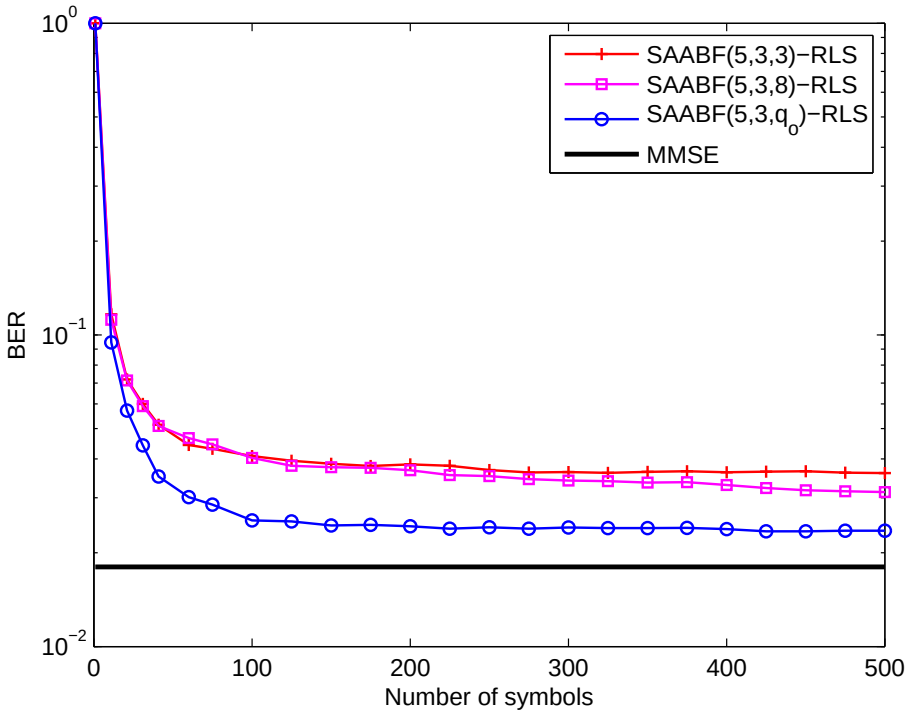

Fig. 3.8: BER performance of the SAABF scheme with adaptive short function length. The scenario of 16dB and 8 users are considered. The parameters used: SAABF-RLS ($\lambda = 0.998$, $\delta = 10$). $q_{\min} = 3$, $q_{\max} = 8$ and $\lambda_q = 0.998$.

based RAKE-MMSE receiver [32] with 25 fingers and 20 iterations and the proposed SAABF-RLS scheme (the parameters are the same as in Fig.3.5). For each independent run, 500 symbols are transmitted. The receiver with the SAABF-RLS scheme outperforms other receiver structures especially in high SNR scenarios. Compared with the GA-RAKE-MMSE scheme, a 2dB gain is obtained for a BER around 10^{-2}. The proposed SAABF scheme is able to suppress the interference efficiently without the knowledge of the channel, the noise variance and the spreading codes.

3.8 Conclusions

In this chapter, we have introduced a generic reduced-rank scheme for interference suppression, which jointly updates the projection vector and the reduced-rank filter. Then, by constraining the design of the projection vector in the generic scheme, we investigated a novel reduced-rank interference suppression scheme based on switched approximations of adaptive basis function (SAABF) for DS-UWB system. LMS and RLS algorithms were developed for adaptive estimation of the parameters of the SAABF scheme. The uncoded

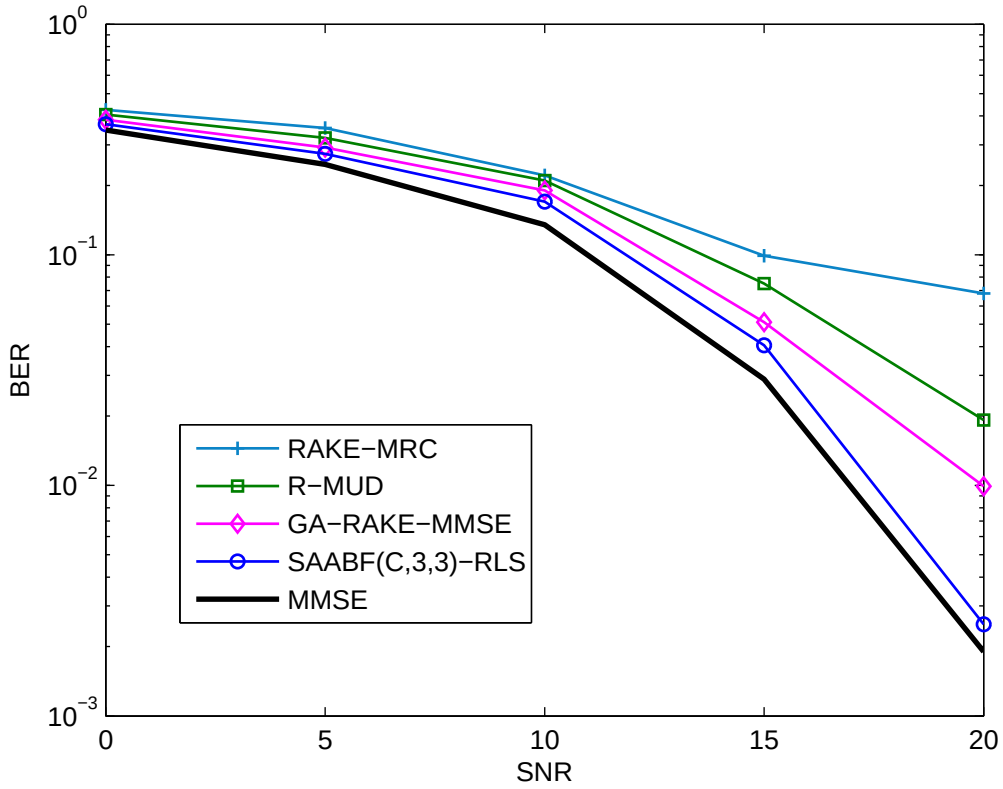

Fig. 3.9: BER performance against SNR of different receiver structures in a system with 8 users.

BER performance of the novel receiver structure was then evaluated in various scenarios with severe MAI and ISI. With a low complexity, the SAABF scheme outperforms other reduced-rank schemes and full-rank schemes. A discussion of the global optimality of the reduced-rank filter was presented, and the relationships between the SAABF and the generic scheme and the full-rank scheme were established and are shown in the Appendices A and B.

4. BLIND REDUCED-RANK ADAPTIVE RECEIVERS FOR DS-UWB SYSTEMS BASED ON THE JIO AND CCM CRITERION

Contents

4.1 Introduction

Blind adaptive linear receivers have high spectrum efficiency and low complexity designs can be obtained by solving constrained optimization problems based on the CCM or CMV criterion [56], [59]. The CCM criterion-based receivers have shown better performance and increased robustness against signature mismatch over the CMV based approaches [56], [58]. Recently, CCM based blind full-rank SG and RLS adaptive filters have been proposed for multiuser detection in DS-UWB communications [59], [60]. In order to achieve faster convergence and increase the robustness against the interference, reduced-rank filtering techniques can be implemented. In [61], a blind subspace multiuser detection scheme is proposed for UWB systems which requires the expensive eigendecomposition of the covariance matrix of the received signal.

In this chapter, a low-complexity CCM based joint iterative optimization (JIO) blind reduced-rank receiver is proposed. A projection matrix and a reduced-rank filter construct the proposed receiver and they are updated jointly and iteratively to minimize the CM cost function subject to a constraint. The constraint is adopted to avoid the undesired local minima. Adaptive NSG and RLS algorithms are developed for the JIO receiver.

In the NSG version, a low-complexity leakage SG channel estimator that was proposed in [64] is adopted. Applying an approximation of the covariance matrix of the received signal, the RLS channel estimator proposed in [64] is modified for the proposed JIO-RLS with reduced complexity. Since each column of the projection matrix can be considered as a direction vector on one dimension of the subspace, we update the projection matrix column by column to achieve a better representation of the projection procedure in the JIO-RLS. The main contributions of this chapter are summarized as follows:

- A novel linear blind JIO reduced-rank receiver based on the CCM criterion is proposed for interference suppression in DS-UWB systems.

- NSG algorithms, which are able to facilitate the setting of step sizes in multiuser scenarios, are developed for the proposed reduced-rank receivers.

- RLS algorithms are developed to jointly update the columns of the projection matrix and the reduced-rank filter with low complexity.

- A rank adaptation algorithm is developed to achieve a better tradeoff between the convergence speed and the steady state performance.

- The convergence properties of the CM cost function with a constraint are discussed.

- Simulations are performed with the IEEE 802.15.4a channel model and severe ISI and MAI are assumed for the evaluation of the proposed scheme against existing techniques.

The rest of this chapter is structured as follows. The design of the JIO CCM blind receiver is detailed in Section 4.2. The proposed NSG and RLS versions of the blind JIO receiver are described in Section 4.3 and 4.4, respectively. In Section 4.5, a complexity analysis for the proposed receiver versions is detailed and a rank adaptation algorithm is developed for the JIO receiver. Simulation results are shown in Section 4.6 and conclusions are drawn in Section 4.7.

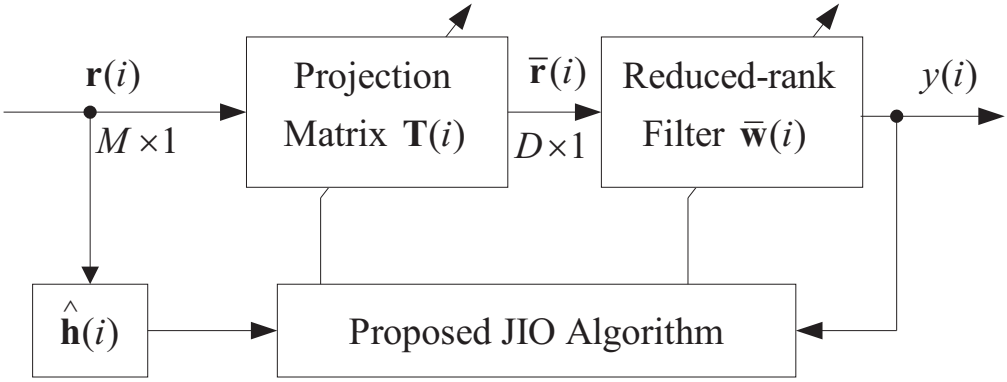

Fig. 4.1: Block diagram of the proposed blind reduced-rank receiver.

4.2 Proposed Blind JIO Reduced-Rank Receiver Design

In this section, we firstly detail the design of the proposed JIO reduced-rank receiver that is able to recover the data symbol from the noisy received signal as shown in (2.5) with only the knowledge of the spreading code of the desired user and the timing. Then, a blind channel estimation algorithm is detailed.

4.2.1 Blind JIO Reduced-Rank Receiver

The block diagram of the proposed receiver is shown in Fig.4.1. In the JIO blind linear receiver, the reduced-rank received signal can be expressed as

$$\bar{\mathbf{r}}(i) = \mathbf{T}^H(i)\mathbf{r}(i), \tag{4.1}$$

where $\mathbf{T}(i)$ is the M-by-D (where $D \ll M$) projection matrix. After the projection, $\bar{\mathbf{r}}(i)$ is fed into the reduced-rank filter $\bar{\mathbf{w}}(i)$ and the output signal is given by

$$y(i) = \bar{\mathbf{w}}^H(i)\bar{\mathbf{r}}(i). \tag{4.2}$$

The decision of the desired data symbol is defined as

$$\hat{b}(i) = \mathrm{sign}(\Re[y(i)]). \tag{4.3}$$

where $\mathrm{sign}(\cdot)$ is the algebraic sign function and $\Re(\cdot)$ represents the real part of a complex number.

The optimization problem to be solved can be expressed as

$$[\bar{\mathbf{w}}(i), \mathbf{T}(i)] = \arg \min_{\bar{\mathbf{w}}(i), \mathbf{T}(i)} \mathbf{J}_{\mathrm{JIO}}\big(\bar{\mathbf{w}}(i), \mathbf{T}(i)\big), \tag{4.4}$$

subject to the constraint

$$\bar{\mathbf{w}}^H(i)\mathbf{T}^H(i)\mathbf{p} = \nu, \tag{4.5}$$

where $\mathbf{p} = \mathbf{P}_r\mathbf{S}_e\mathbf{h}$ is defined as the effective signature vector for the desired user and ν is a real-valued constant to ensure the convexity of the CM cost function

$$\mathbf{J}_{\mathrm{JIO}}\big(\bar{\mathbf{w}}(i), \mathbf{T}(i)\big) = \frac{1}{2}E\left[(|y(i)|^2 - 1)^2\right]. \tag{4.6}$$

The convergence properties of the CM cost function subject to a constraint are discussed in Appendix C.

Let us now consider the problem through the Lagrangian

$$\mathcal{L}_{\mathrm{JIO}}\big(\bar{\mathbf{w}}(i), \mathbf{T}(i)\big) = \frac{1}{2}E\left[(|y(i)|^2 - 1)^2\right] + \Re[\lambda(i)(\bar{\mathbf{w}}^H(i)\mathbf{T}^H(i)\mathbf{p} - \nu)], \tag{4.7}$$

where $\lambda(i)$ is a complex-valued Lagrange multiplier. In order to obtain the adaptation equation of $\mathbf{T}(i)$, we firstly assume that $\bar{\mathbf{w}}(i)$ is fixed and the gradient of the Lagrangian with respect to $\mathbf{T}(i)$ is given by

$$\nabla_T\mathcal{L}_{\mathrm{JIO}} = E\left[e(i)y^*(i)\mathbf{r}(i)\bar{\mathbf{w}}^H(i)\right] + \frac{\lambda_T(i)}{2}\mathbf{p}\bar{\mathbf{w}}^H(i), \tag{4.8}$$

where $\lambda_T(i)$ is the complex-valued Lagrange multiplier for updating the projection matrix and $e(i) = |y(i)|^2 - 1$ is defined as a real-valued error signal. Recalling the relationship $y^*(i) = \mathbf{r}^H(i)\mathbf{T}(i)\bar{\mathbf{w}}(i)$ and setting (4.8) to a zero matrix, we obtain

$$\mathbf{T}_{\mathrm{opt}} = \mathbf{R}_Y^{-1}\left(\mathbf{D}_T - \frac{\lambda_T(i)}{2}\mathbf{p}\bar{\mathbf{w}}^H(i)\right)\mathbf{R}_w^{-1}, \tag{4.9}$$

where $\mathbf{R}_Y = E[|y(i)|^2\mathbf{r}(i)\mathbf{r}^H(i)]$, $\mathbf{D}_T = E[y^*(i)\mathbf{r}(i)\bar{\mathbf{w}}^H(i)]$ and $\mathbf{R}_w = E[\bar{\mathbf{w}}(i)\bar{\mathbf{w}}^H(i)]$. Using the constraint $\bar{\mathbf{w}}^H(i)\mathbf{T}_{\mathrm{opt}}^H\mathbf{p} = \nu$, we obtain the Lagrange multiplier

$$\lambda_T(i) = 2\left(\frac{\bar{\mathbf{w}}^H(i)\mathbf{R}_w^{-1}\mathbf{D}_T\mathbf{R}_Y^{-1}\mathbf{p} - \nu}{\bar{\mathbf{w}}^H(i)\mathbf{R}_w^{-1}\bar{\mathbf{w}}(i)\mathbf{p}^H\mathbf{R}_Y^{-1}\mathbf{p}}\right)^*. \tag{4.10}$$

Finally, the expression for $\mathbf{T}_{\mathrm{opt}}$ is given by

$$\mathbf{T}_{\mathrm{opt}} = \mathbf{R}_Y^{-1}\left(\mathbf{D}_T - \left(\frac{\bar{\mathbf{w}}^H(i)\mathbf{R}_w^{-1}\mathbf{D}_T\mathbf{R}_Y^{-1}\mathbf{p} - \nu}{\bar{\mathbf{w}}^H(i)\mathbf{R}_w^{-1}\bar{\mathbf{w}}(i)\mathbf{p}^H\mathbf{R}_Y^{-1}\mathbf{p}}\right)^*\mathbf{p}\bar{\mathbf{w}}^H(i)\right)\mathbf{R}_w^{-1}. \tag{4.11}$$

Now, we assume that $\mathbf{T}(i)$ is fixed in (4.7) and calculate the gradient of the Lagrangian with respect to $\bar{\mathbf{w}}(i)$ which is given by

$$\nabla_w \mathcal{L}_{\text{JIO}} = E\left[e(i)\mathbf{T}^H(i)\mathbf{r}(i)y^*(i)\right] + \frac{\lambda_w(i)}{2}\mathbf{T}^H(i)\mathbf{p}, \tag{4.12}$$

where $\lambda_w(i)$ is the complex-valued Lagrange multiplier for updating the reduced-rank filter. Rearranging the terms, we obtain

$$\bar{\mathbf{w}}_{\text{opt}} = \mathbf{R}_{\bar{y}}^{-1}\left(\mathbf{d}_{\bar{r}} - \frac{\lambda_w(i)}{2}\mathbf{T}^H(i)\mathbf{p}\right), \tag{4.13}$$

where $\mathbf{R}_{\bar{y}} = E[|y(i)|^2\bar{\mathbf{r}}(i)\bar{\mathbf{r}}^H(i)]$ and $\mathbf{d}_{\bar{r}} = E[y^*(i)\bar{\mathbf{r}}(i)]$. Using the constraint $\bar{\mathbf{w}}_{\text{opt}}^H\mathbf{T}^H(i)\mathbf{p} = \mathbb{v}$, we obtain the Lagrange multiplier

$$\lambda_w(i) = 2\left(\frac{\mathbf{d}_{\bar{r}}^H\mathbf{R}_{\bar{y}}^{-1}\mathbf{T}^H(i)\mathbf{p} - \mathbb{v}}{\mathbf{p}^H\mathbf{T}(i)\mathbf{R}_{\bar{y}}^{-1}\mathbf{T}^H(i)\mathbf{p}}\right)^*. \tag{4.14}$$

Finally, the expression for $\bar{\mathbf{w}}_{\text{opt}}$ is given by

$$\bar{\mathbf{w}}_{\text{opt}} = \mathbf{R}_{\bar{y}}^{-1}\left(\mathbf{d}_{\bar{r}} - \left(\frac{\mathbf{d}_{\bar{r}}^H\mathbf{R}_{\bar{y}}^{-1}\mathbf{T}^H(i)\mathbf{p} - \mathbb{v}}{\mathbf{p}^H\mathbf{T}(i)\mathbf{R}_{\bar{y}}^{-1}\mathbf{T}^H(i)\mathbf{p}}\right)^*\mathbf{T}^H(i)\mathbf{p}\right). \tag{4.15}$$

With the solutions of $\mathbf{T}_{\text{opt}}$ and $\bar{\mathbf{w}}_{\text{opt}}$, the NSG and RLS adaptive versions of the JIO receiver will be developed in the following sections, in which the direct matrix inversions are not required and the computational complexity is reduced. Note that when adaptive algorithms are implemented to estimate $\mathbf{T}_{\text{opt}}$ and $\bar{\mathbf{w}}_{\text{opt}}$, $\mathbf{T}(i)$ is a function of $\bar{\mathbf{w}}(i)$ and $\bar{\mathbf{w}}(i)$ is a function of $\mathbf{T}(i)$. Thus, the optimal CCM design is not in a closed form and one possible solution for such optimization problem is to jointly and iteratively adapt these two quantities. The joint update means for the i-th time instant, $\mathbf{T}(i)$ is updated with the knowledge of $\mathbf{T}(i-1)$ and $\bar{\mathbf{w}}(i-1)$, then $\bar{\mathbf{w}}(i)$ is updated with $\mathbf{T}(i)$ and $\bar{\mathbf{w}}(i-1)$. Each iterative update can be considered as one repetition of the joint update.

4.2.2 Blind Channel Estimation

It should also be noted that the blind JIO receiver design requires the knowledge of the effective signature vector of the desired user, or equivalently, the channel parameters. In this work, the channel coefficients are not given and must be estimated.

In order to facilitate the development of the blind channel estimation, we rearrange the

term and express the received signal as

$$\mathbf{r}(i) = \sum_{k=1}^{K} \sqrt{E_k}\mathbf{P}_r\mathbf{S}_{e,k}\mathbf{h}_k b_k(i) + \boldsymbol{\eta}(i) + \mathbf{n}(i) = \sum_{k=1}^{K} \mathbf{x}_k(i) + \boldsymbol{\eta}(i) + \mathbf{n}(i), \qquad (4.16)$$

where $\mathbf{S}_{e,k}$ is the Toeplitz matrix with the first column being the vector $\mathbf{s}_{e,k} = \mathbf{P}_t\mathbf{s}_k$ zero-padded to length M_H. The matrix $\mathbf{P}_r$ represents the MF and chip-rate sampling with the size M-by-M_H. $\mathbf{P}_t$ denotes the (T_s/T_τ)-by-N_c pulse shaping matrix.

Let us perform singular value decomposition (SVD) on the covariance matrix $\mathbf{R}$ as in [62]:

$$\mathbf{R} = E[\mathbf{r}(i)\mathbf{r}^H(i)] = [\mathbf{V}_s\ \mathbf{V}_n] \begin{bmatrix} \boldsymbol{\Lambda}_s + \sigma^2\mathbf{I} & \mathbf{0} \\ \mathbf{0} & \sigma^2\mathbf{I} \end{bmatrix} [\mathbf{V}_s\ \mathbf{V}_n]^H \qquad (4.17)$$

where $\mathbf{V}_s$ and $\mathbf{V}_n$ are the signal (includes the ISI) and the noise subspaces, respectively. Because of the orthogonality of the signal subspace and the noise subspace [63], [64], we have $\mathbf{V}_n^H\mathbf{x}_k(i) = \mathbf{V}_n^H\mathbf{P}_r\mathbf{S}_{e,k}\mathbf{h}_k = \mathbf{0}$ and hence we have

$$\Upsilon = \mathbf{h}_k^H\mathbf{S}_{e,k}^H P_r^H\mathbf{V}_n\mathbf{V}_n^H\mathbf{P}_r\mathbf{S}_{e,k}\mathbf{h}_k = \mathbf{0}. \qquad (4.18)$$

Assuming that $\mathbf{V}_n$ is given, it suffices to consider only Υ, which allows the recovery of $\mathbf{h}_k$ as the eigenvector corresponding to the smallest eigenvalue of the matrix $\mathbf{S}_{e,k}^H P_r^H\mathbf{V}_n\mathbf{V}_n^H\mathbf{P}_r\mathbf{S}_{e,k}$. A traditional approach to obtain the noise subspace $\mathbf{V}_n$ and its rank is to do the SVD on the covariance matrix $\mathbf{R}$, which is computational expensive. To avoid the SVD on $\mathbf{R}$, the following lemma is adopted [62]:

Lemma: Consider the SVD on $\mathbf{R}$ as in (4.17), then we have:

$$\lim_{p\to\infty} (\mathbf{R}/\sigma^2)^{-m} = \mathbf{V}_n\mathbf{V}_n^H. \qquad (4.19)$$

Hence, the channel coefficients for the desired user can be obtained by the optimization:

$$\hat{\mathbf{h}}(i) = \arg\min_{\hat{\mathbf{h}}(i)}\ \hat{\mathbf{h}}^H(i)\mathbf{S}_e^H P_r^H\hat{\mathbf{R}}^{-m}\mathbf{P}_r\mathbf{S}_e\hat{\mathbf{h}}(i), \qquad (4.20)$$

subject to $\|\hat{\mathbf{h}}(i)\| = 1$, where m is an integer and $\hat{\mathbf{R}}(i)$ is the estimated covariance matrix. The solution of the $\hat{\mathbf{h}}(i)$ is the eigenvector corresponding to the minimum eigenvalue of the matrix $\mathbf{S}_e^H P_r^H\hat{\mathbf{R}}^{-m}\mathbf{P}_r\mathbf{S}_e$ that can be obtained using SVD. Note that the scalar quantity $(\sigma^2)^m$ is discarded in this optimization problem because it does not affect the subspace determination problem [64]. The performance of the estimator can be improved by increasing m even though our studies reveal that it suffices to use powers up to $m = 3$. In order to achieve further complexity reduction, we employ the variant of the power method

introduced in [64] to avoid the SVD of the matrix $\mathbf{S}_e^H P_r^H \hat{\mathbf{R}}^{-m} \mathbf{P}_r \mathbf{S}_e$. Hence, we have

$$\hat{\mathbf{h}}(i) = \left(\mathbf{I} - \hat{\mathbf{V}}(i)/tr[\hat{\mathbf{V}}(i)] \right) \hat{\mathbf{h}}(i-1), \tag{4.21}$$

where the L-by-L matrix is defined as

$$\hat{\mathbf{V}}(i) = \mathbf{S}_e^H \mathbf{P}_r^H \mathbf{R}^{-m}(i) \mathbf{P}_r \mathbf{S}_e, \tag{4.22}$$

and $\mathbf{I}$ is the identity matrix, $tr[\cdot]$ stands for trace and we make $\hat{\mathbf{h}}(i) \leftarrow \hat{\mathbf{h}}(i)/\|\hat{\mathbf{h}}(i)\|$ to normalize the channel. $\mathbf{R}(i) = \sum_{j=1}^{i} \alpha^{i-j} \mathbf{r}(j) \mathbf{r}^H(j)$ and m is a finite power. The estimate of the matrix $\mathbf{R}^{-1}(i)$ is obtained recursively via the matrix inversion lemma [26] and is given by

$$\hat{\mathbf{R}}^{-1}(i) = \frac{1}{\alpha} \left(\hat{\mathbf{R}}^{-1}(i-1) - (\phi(i) \boldsymbol{\kappa}(i)) \boldsymbol{\kappa}^H(i) \right), \tag{4.23}$$

where α is the forgetting factor, $\boldsymbol{\kappa}(i) = \hat{\mathbf{R}}^{-1}(i-1)\mathbf{r}(i)$ and $\phi(i) = \left(\alpha + \mathbf{r}^H(i) \boldsymbol{\kappa}(i) \right)^{-1}$. The estimator of the inversion of the covariance matrix requires $3M^2 + 2M + 1$ multiplications and $2M^2$ additions. Equation (4.22) requires $(m+1)M^2L$ multiplications and $(m+1)M^2L - (m+1)ML$ additions, while equation (4.21) requires L^2 multiplications and $L^2 + L - 1$ additions (the multiplications and additions in this work are both complex-valued operations). Note that, the matrix $\mathbf{P}_r \mathbf{S}_e$ is assumed given at the receiver.

The estimate of the effective signature vector can be finally obtained as

$$\hat{\mathbf{p}}(i) = \mathbf{P}_r \mathbf{S}_e \hat{\mathbf{h}}(i), \tag{4.24}$$

where $\hat{\mathbf{h}}(i)$ is given in (4.21).

4.3 Proposed JIO-NSG Algorithms

In this section, we develop the NSG algorithm to jointly and iteratively update $\mathbf{T}(i)$ and $\bar{\mathbf{w}}(i)$. The blind channel estimator based on the leakage SG algorithm that is proposed in [64] is implemented to provide the channel coefficients.

4.3.1 JIO-NSG Algorithms

The optimization problem to be solved in the NSG version is given by

$$[\bar{\mathbf{w}}(i), \mathbf{T}(i)] = \arg \min_{\bar{\mathbf{w}}(i), \mathbf{T}(i)} \mathbf{J}_{\mathrm{JIO}}\big(\bar{\mathbf{w}}(i), \mathbf{T}(i)\big), \tag{4.25}$$

subject to $\bar{\mathbf{w}}^H(i)\mathbf{T}^H(i)\hat{\mathbf{p}}(i) = \mathbb{v}$, where $\hat{\mathbf{p}}(i)$ is the estimated signature vector obtained via blind channel estimation that will be detailed in Section 4.3.2 and $\mathbb{v}$ is a real-valued constant to ensure the convexity of the cost function

$$\mathbf{J}_{\mathrm{JIO-NSG}}\big(\bar{\mathbf{w}}(i), \mathbf{T}(i)\big) = \frac{1}{2} E\left[(|y(i)|^2 - 1)^2\right]. \tag{4.26}$$

Here, we consider the problem through the Lagrangian

$$\mathcal{L}_{\mathrm{JIO-NSG}}\big(\bar{\mathbf{w}}(i), \mathbf{T}(i)\big) = \frac{1}{2} E\left[(|y(i)|^2 - 1)^2\right] + \Re[\lambda_N(i)(\bar{\mathbf{w}}^H(i)\mathbf{T}^H(i)\hat{\mathbf{p}}(i) - \mathbb{v})], \tag{4.27}$$

where $\lambda_N(i)$ is a complex-valued Lagrange multiplier. For each time instant, we firstly update $\mathbf{T}(i)$ while assuming that $\bar{\mathbf{w}}(i)$ is fixed. Then we adapt $\bar{\mathbf{w}}(i)$ with the updated $\mathbf{T}(i)$.

The gradient of the Lagrangian with respect to $\mathbf{T}(i)$ is given by

$$\nabla_T \mathcal{L}_{\mathrm{JIO-NSG}} = E\left[e(i)y^*(i)\mathbf{r}(i)\bar{\mathbf{w}}^H(i)\right] + \frac{1}{2}\lambda_{NT}(i)\hat{\mathbf{p}}(i)\bar{\mathbf{w}}^H(i),$$

where $\lambda_{NT}(i)$ is the complex-valued Lagrange multiplier for updating the projection matrix and $e(i) = |y(i)|^2 - 1$ is defined as a real-valued error signal. Using the instantaneous estimator to the gradient vector, the SG update equation is given by

$$\mathbf{T}(i+1) = \mathbf{T}(i) - \mu_T \left(e(i)y^*(i)\mathbf{r}(i) + \frac{\lambda_{NT}(i)}{2}\hat{\mathbf{p}}(i)\right)\bar{\mathbf{w}}^H(i), \tag{4.28}$$

where μ_T is the step size for the SG algorithm that updates the projection matrix. Using the constraint of $\bar{\mathbf{w}}^H(i)\mathbf{T}^H(i+1)\hat{\mathbf{p}}(i) = \mathbb{v}$, we obtain that

$$\lambda_{NT}(i) = 2\frac{\hat{\mathbf{p}}^H(i)\mathbf{T}(i)\bar{\mathbf{w}}(i) - \mu_T e(i)y^*(i)\|\bar{\mathbf{w}}(i)\|^2\hat{\mathbf{p}}^H(i)\mathbf{r}(i) - \mathbb{v}}{\mu_T\|\bar{\mathbf{w}}(i)\|^2\|\hat{\mathbf{p}}(i)\|^2}. \tag{4.29}$$

The NSG algorithm aims at minimizing the cost function

$$\mathbf{J}_{\mathrm{JIO-NSG}}(\mu_T) = \frac{1}{2}\left[\left|\bar{\mathbf{w}}^H(i)\mathbf{T}^H(i+1)\mathbf{r}(i)\right|^2 - 1\right]^2. \tag{4.30}$$

Substituting (4.28) and (4.29) into (4.30) and setting the gradient vector of (4.30) with

respect to μ_T to zeros, we obtain the solutions

$$\mu_{T,1} = \frac{|y(i)| - 1}{|y(i)|e(i)A_{T,1}},\ \mu_{T,2} = \frac{|y(i)| + 1}{|y(i)|e(i)A_{T,1}},$$

$$\mu_{T,3} = \mu_{T,4} = \frac{1}{e(i)A_{T,1}},$$

where the real-valued scale term $A_{T,1}$ is defined as

$$A_{T,1} = \|\bar{\mathbf{w}}(i)\|^2 \left[\|\mathbf{r}(i)\|^2 - \frac{|\mathbf{r}^H(i)\hat{\mathbf{p}}(i)|^2}{\|\hat{\mathbf{p}}(i)\|^2}\right].$$

By examining the second derivative of (4.30) with respect to μ_T, we conclude that $\mu_{T,1}$ and $\mu_{T,2}$ are the solutions that correspond to the minima. In this work, the $\mu_{T,1}$ is used and a positive real scaling factor $\mu_{T,0}$ is implemented that will not change the direction of the tap-weight vector. Finally, the NSG update function of $\mathbf{T}(i)$ is given by

$$\mathbf{T}(i+1) = \mathbf{T}(i) - y^*(i)\mu_{T,0}\mathbf{A}_{T,2} - A_{T,3}\hat{\mathbf{p}}(i)\bar{\mathbf{w}}^H(i). \tag{4.31}$$

where

$$\mathbf{A}_{T,2} = \frac{|y(i)| - 1}{|y(i)|A_{T,1}}\left(\mathbf{r}(i)\bar{\mathbf{w}}^H(i) - \frac{\hat{\mathbf{p}}^H(i)\mathbf{r}(i)}{\|\hat{\mathbf{p}}(i)\|^2}\hat{\mathbf{p}}(i)\bar{\mathbf{w}}^H(i)\right),$$

$$A_{T,3} = \left(\|\bar{\mathbf{w}}(i)\|^2\|\hat{\mathbf{p}}(i)\|^2\right)^{-1}\left(\hat{\mathbf{p}}^H(i)\mathbf{T}(i)\bar{\mathbf{w}}(i) - \mathbb{v}\right).$$

Now, let us adapt $\bar{\mathbf{w}}(i)$ while assuming $\mathbf{T}(i)$ is fixed. The gradient of the Lagrangian with respect to $\bar{\mathbf{w}}(i)$ is given by $\nabla_w \mathcal{L}_{\mathrm{JIO-NSG}} = E\left[e(i)y^*(i)\mathbf{T}^H(i)\mathbf{r}(i)\right] + \frac{1}{2}\lambda_{Nw}(i)\hat{\mathbf{p}}(i)\bar{\mathbf{w}}^H(i)$, where $\lambda_{Nw}(i)$ is the complex-valued Lagrange multiplier for updating the reduced-rank filter. By using the instantaneous estimator of the gradient vector, the SG adaptation equation is given by

$$\bar{\mathbf{w}}(i+1) = \bar{\mathbf{w}}(i) - \mu_w e(i)y^*(i)\mathbf{T}^H(i)\mathbf{r}(i) - \mu_w\frac{\lambda_{Nw}(i)}{2}\mathbf{T}^H(i)\hat{\mathbf{p}}(i). \tag{4.32}$$

Using the constraint $\bar{\mathbf{w}}^H(i+1)\mathbf{T}^H(i)\hat{\mathbf{p}}(i) = \mathbb{v}$, we have

$$\lambda_{Nw}(i) = 2\frac{\hat{\mathbf{p}}^H(i)\mathbf{T}(i)\bar{\mathbf{w}}(i) - \mu_w e(i)y^*(i)\hat{\mathbf{p}}^H(i)\mathbf{T}(i)\mathbf{T}^H(i)\mathbf{r}(i) - \mathbb{v}}{\mu_w\|\mathbf{T}^H(i)\hat{\mathbf{p}}(i)\|^2}. \tag{4.33}$$

The NSG algorithm for updating the reduced-rank filter aims at minimizing the cost function

$$\mathbf{J}_{\mathrm{JIO-NSG}}(\mu_w) = \frac{1}{2}\left[\left|\bar{\mathbf{w}}^H(i+1)\mathbf{T}^H(i)\mathbf{r}(i)\right|^2 - 1\right]^2. \tag{4.34}$$

Substituting (4.32) and (4.33) into (4.34), the solutions of μ_w that correspond to a null

gradient vector of (4.34) are given by

$$\mu_{w,1} = \frac{|y(i)|-1}{|y(i)|e(i)A_{w,1}},\ \mu_{w,2} = \frac{|y(i)|+1}{|y(i)|e(i)A_{w,1}},$$

$$\mu_{w,3} = \mu_{w,4} = \frac{1}{e(i)A_{w,1}},$$

where the scale term is given by

$$A_{w,1} = \|\mathbf{T}^H(i)\mathbf{r}(i)\|^2 - \frac{|\mathbf{r}^H(i)\mathbf{T}(i)\mathbf{T}^H(i)\hat{\mathbf{p}}(i)|^2}{\|\mathbf{T}^H(i)\hat{\mathbf{p}}(i)\|^2}$$

By examining the second derivative of (4.34) with respect to μ_w, only $\mu_{w,1}$ and $\mu_{w,2}$ correspond to the minima of the cost function (4.34). Finally, by applying a positive real scaling factor $\mu_{w,0}$ to control the tap-weight vector, the adaptation equation by using $\mu_{w,1}$ is given by

$$\bar{\mathbf{w}}^H(i+1) = \bar{\mathbf{w}}^H(i) - y^*(i)\mu_{w,0}\mathbf{A}_{w,2} - A_{w,3}\mathbf{T}^H(i)\hat{\mathbf{p}}(i). \tag{4.35}$$

where

$$\mathbf{A}_{w,2} = \frac{|y(i)|-1}{|y(i)|A_{w,1}}\left(\mathbf{T}^H(i)\mathbf{r}(i) - \frac{\hat{\mathbf{p}}^H(i)\mathbf{T}(i)\mathbf{T}^H(i)\mathbf{r}(i)}{\|\mathbf{T}^H(i)\hat{\mathbf{p}}(i)\|^2}\mathbf{T}^H(i)\hat{\mathbf{p}}(i)\right),$$

$$A_{w,3} = \left(\|\mathbf{T}^H(i)\hat{\mathbf{p}}(i)\|^2\right)^{-1}\left(\hat{\mathbf{p}}^H(i)\mathbf{T}(i)\bar{\mathbf{w}}(i) - \mathbb{v}\right).$$

In the proposed JIO-NSG scheme, $\mathbf{T}(i)$ and $\bar{\mathbf{w}}(i)$ are computed jointly and iteratively. Let c denote the iteration number and define c_{max} as the total number of iterations for each time instant. We have $\mathbf{T}_0(i) = \mathbf{T}_{c_{max}}(i-1)$ and $\bar{\mathbf{w}}_0(i) = \bar{\mathbf{w}}_{c_{max}}(i-1)$. For the c-th iteration, $\mathbf{T}_c(i)$ is updated with $\mathbf{T}_{c-1}(i)$ and $\bar{\mathbf{w}}_{c-1}(i)$ using (4.31), then $\bar{\mathbf{w}}_c(i)$ is trained with $\mathbf{T}_c(i)$ and $\bar{\mathbf{w}}_{c-1}(i)$ via (4.35).

It is interesting to note that the complexity of the JIO-NSG scheme could be lower than the full-rank NSG algorithm because there are many entries that are frequently reused in the update equations, for example, the scalar term $\hat{\mathbf{p}}^H(i)\mathbf{r}(i)$, the vectors of $\mathbf{T}^H(i)\hat{\mathbf{p}}(i)$ and $\mathbf{T}^H(i)\mathbf{r}(i)$. However, the price we pay for the complexity reduction is the requirement of extra storage space at the receiver.

4.3.2 Blind Channel Estimator for the NSG Version

For the JIO-NSG receiver, we rearrange the equation (4.22) as

$$\hat{\mathbf{V}}(i) = \mathbf{S}_e^H \mathbf{P}_r^H \hat{\mathbf{W}}(i) \tag{4.36}$$

where $\hat{\mathbf{W}}(i) = \mathbf{R}^{-m}(i)\mathbf{P}_r\mathbf{S}_e$. Here, we implement the Leakage SG algorithm to estimate $\hat{\mathbf{W}}(i)$, which can be expressed as [64]

$$\hat{\mathbf{W}}_l(i) = \lambda_v \hat{\mathbf{W}}_l(i-1) + \mu_v(\hat{\mathbf{W}}_{l-1}(i) - \mathbf{r}(i)\mathbf{r}^H(i)\hat{\mathbf{W}}_l(i-1)), \tag{4.37}$$

where $l = 1, \ldots, m$ is defined as the iteration index, λ_v is the leakage factor and μ_v is the step size. Using (4.36), we obtain the leakage SG blind channel estimator that is given by

$$\hat{\mathbf{h}}(i) = \hat{\mathbf{h}}(i-1) - \left(\hat{\mathbf{V}}(i)\hat{\mathbf{h}}(i-1)\right)/tr[\hat{\mathbf{V}}(i)], \tag{4.38}$$

Finally, the effective signature vector of the desired user is given by

$$\hat{\mathbf{p}}(i) = \mathbf{P}_r\mathbf{S}_e\hat{\mathbf{h}}(i) \tag{4.39}$$

In terms of the computational complexity, we need $4mML$ multiplications and $3mML - mL$ additions for all the recursions in (4.37); L^2M multiplications and $L^2M - L^2$ additions for (4.36).

The JIO-NSG version is summarized in Table. 4.1.

4.4 Proposed JIO-RLS Algorithms

In this section we detail the RLS version of the proposed JIO scheme. In the JIO scheme, the M-by-D (where $D \ll M$) projection matrix can be expressed as

$$\mathbf{T}(i) = [\mathbf{t}_1(i), \mathbf{t}_2(i), \ldots, \mathbf{t}_D(i)]. \tag{4.40}$$

Note that the reduced-rank received signal can be expressed as $\bar{\mathbf{r}}(i) = \mathbf{T}^H(i)\mathbf{r}(i)$, whose d-th element is $\bar{r}_d(i) = \mathbf{t}_d^H(i)\mathbf{r}(i)$. Since the projection matrix projects the received signal onto a small-dimensional subspace, these vectors $\mathbf{t}_d(i)$ can be considered as the direction vectors on each dimension of the subspace. For each time instant, we compute these M-dimensional vectors $\mathbf{t}_d(i)$ (where $d = 1, 2, \ldots, D$) one by one. One of the advantages of this method in the RLS version is that the complexity of training the projection ma-

Tab. 4.1: NSG version of the Proposed JIO-CCM Receiver.

NSG version:

Initialization:

$\bar{\mathbf{w}}(1) = [1, 1, 1, \ldots, 1]$, D-by-1 vector ; $\mathbf{T}(1) = [\mathbf{I}_D \mid \mathbf{0}]^T$, M-by-D matrix.

for $i = 1, 2, \ldots$

1: Pre-adaptation:

$\bar{\mathbf{r}}(i) = \mathbf{T}^H(i)\mathbf{r}(i)$, $y(i) = \bar{\mathbf{w}}^H(i)\bar{\mathbf{r}}(i)$,

Calculate $\hat{\mathbf{V}}(i)$ and $\hat{\mathbf{h}}(i)$ using (4.36) and (4.38), respectively,

Calculate $\hat{\mathbf{p}}(i)$ using (4.39),

Set $\mathbf{T}_0(i+1) = \mathbf{T}_{c_{max}}(i)$ and $\bar{\mathbf{w}}_0(i+1) = \bar{\mathbf{w}}_{c_{max}}(i)$.

2: Adaptation of $\mathbf{T}(i+1)$ and $\bar{\mathbf{w}}(i+1)$:

for $c = 1, 2, \ldots, c_{max}$

Update $\mathbf{T}_c(i+1)$ using (4.31) with $\mathbf{T}_{c-1}(i+1)$ and $\bar{\mathbf{w}}_{c-1}(i+1)$,

Update $\bar{\mathbf{w}}_c(i+1)$ using (4.35) with $\mathbf{T}_c(i+1)$ and $\bar{\mathbf{w}}_{c-1}(i+1)$,

end

Set $\mathbf{T}(i+1) = \mathbf{T}_{c_{max}}(i+1)$ and $\bar{\mathbf{w}}(i+1) = \bar{\mathbf{w}}_{c_{max}}(i+1)$

3: Make Decision for the i-th data bit:

$\hat{b}(i) = \mathrm{sign}(\Re(y(i)))$

trix could be reduced with an approximation which will be shown soon. In addition, this method provides a better representation of the projection matrix and leads to better performance than the approach that updates all the columns of the projection matrix together. It should be noted that, the NSG version can also be modified to update the columns of the projection matrix one by one, but the limited improved performance in the NSG version is not worth the payment of the increased complexity.

After the projection, $\bar{\mathbf{r}}(i)$ is fed into the reduced-rank filter $\bar{\mathbf{w}}(i)$ and the output signal is given by

$$y(i) = \bar{\mathbf{w}}^H(i)\mathbf{T}^H(i)\mathbf{r}(i) = \bar{\mathbf{w}}^H(i)\sum_{d=1}^{D}\mathbf{t}_d^H(i)\mathbf{r}(i)\mathbf{q}_d,$$

where $\mathbf{q}_d$ (where $d = 1, 2, \ldots, D$) are the vectors whose d-th elements are ones, while all the other elements are zeros. In this section, an adaptive blind channel estimation is employed and $\mathbf{t}_d(i)$ are optimized jointly and iteratively with $\bar{\mathbf{w}}(i)$ via RLS algorithms.

4.4.1 JIO-RLS Algorithms

In the JIO-RLS scheme, we need to solve the optimization problem

$$[\bar{\mathbf{w}}(i), \mathbf{t}_1(i), \ldots, \mathbf{t}_D(i)] = \arg \min_{\mathbf{w}(i), \mathbf{t}_1(i), \ldots, \mathbf{t}_D(i)} \mathbf{J}_{JIO-RLS}\big(\bar{\mathbf{w}}(i), \mathbf{t}_1(i), \ldots, \mathbf{t}_D(i)\big), \quad (4.41)$$

subject to the constraint $\bar{\mathbf{w}}^H(i) \sum_{d=1}^{D} \mathbf{t}_d^H(i)\hat{\mathbf{p}}(i)\mathbf{q}_d = \mathbb{v}$, where $\hat{\mathbf{p}}(i)$ is the estimated signature vector obtained via blind channel estimation that will be detailed in Section 4.4.2, and $\mathbb{v}$ is a real-valued constant to ensure the convexity of the CM cost function given by

$$\mathbf{J}_{JIO-RLS}\big(\bar{\mathbf{w}}(i), \mathbf{t}_1(i), \ldots, \mathbf{t}_D(i)\big) = \frac{1}{2} \sum_{j=1}^{i} \alpha^{i-j} \left(|y(j)|^2 - 1\right)^2,$$

where $0 < \alpha \leq 1$ is the forgetting factor and $y(i)$ is the output signal at the i-th time instant. Let us now consider the problem through the Lagrangian

$$\begin{aligned} \mathcal{L}_{JIO-RLS}\big(\bar{\mathbf{w}}(i), \mathbf{t}_1(i), \ldots, \mathbf{t}_D(i)\big) &= \frac{1}{2} \sum_{j=1}^{i} \alpha^{i-j} \left(|y(j)|^2 - 1\right)^2 \\ &+ \Re \left[\lambda_R(i) \big(\bar{\mathbf{w}}^H(i) \sum_{d=1}^{D} \mathbf{t}_d^H(i)\hat{\mathbf{p}}(i)\mathbf{q}_d - \mathbb{v} \big) \right], \end{aligned} \quad (4.42)$$

where $\lambda_R(i)$ is a complex-valued Lagrange multiplier. In the proposed JIO-RLS scheme, for each time instant, we firstly update the vectors $\mathbf{t}_d(i)$ (where $d = 1, 2, \ldots, D$) while assuming that $\bar{\mathbf{w}}(i)$ and other column vectors are fixed. Then we adapt the reduced-rank filter with the updated projection matrix.

For the update of the column vectors of the projection matrix, we can divide the output signal as follows

$$y(i) = \bar{\mathbf{w}}^H(i) \sum_{d=1}^{D} \mathbf{t}_d^H(i)\mathbf{r}(i)\mathbf{q}_d = \bar{w}_d^*(i)\bar{r}_d(i) + \bar{\mathbf{w}}^H(i)\bar{\mathbf{r}}_e(i),$$

where the D-dimensional vector $\bar{\mathbf{r}}_e(i)$ can be obtained by calculating the reduced-rank received signal $\bar{\mathbf{r}}(i)$ and setting its d-th element to zero. By computing the gradient term of (4.42) with respect to $\mathbf{t}_d(i)$ and setting it to a null vector, we have

$$\begin{aligned} &\nabla_{t_d} \mathcal{L}_{JIO-RLS} \\ &= \sum_{j=1}^{i} \alpha^{i-j} e(j)\mathbf{r}(j)\big(|\bar{w}_d(j)|^2 \mathbf{r}^H(j)\mathbf{t}_d(i) + \bar{w}_d^*(j)\bar{\mathbf{r}}_e^H(j)\bar{\mathbf{w}}(j)\big) + \frac{1}{2}\lambda_{t,d}(i)\bar{w}_d^*(i)\hat{\mathbf{p}}(i) = 0, \end{aligned}$$

where $e(i) = |y(i)|^2 - 1$ and $\lambda_{t,d}(i)$ is the complex-valued Lagrange multiplier for updating the d-th column vector in the projection matrix. Rearranging the terms we obtain

$$\mathbf{t}_d(i) = -\mathbf{R}_{\mathrm{d}}^{-1}(i)\left(\frac{\lambda_{t,d}(i)}{2}\bar{w}_d^*(i)\hat{\mathbf{p}}(i) + \mathbf{v}_r(i)\right), \tag{4.43}$$

where we define the M-dimensional vector

$$\mathbf{v}_r(i) = \sum_{j=1}^{i}\alpha^{i-j}\bar{w}_d^*(j)\mathbf{r}(j)\big(e(j)\mathbf{r}_e^H(j)\bar{\mathbf{w}}(j) - \bar{w}_d(j)\bar{r}_d^*(j)\big) \tag{4.44}$$

and the M-by-M matrix

$$\mathbf{R}_{\mathrm{d}}(i) = \sum_{j=1}^{i}\alpha^{i-j}|\bar{w}_d(j)|^2|y(j)|^2\mathbf{r}(j)\mathbf{r}^H(j). \tag{4.45}$$

Note that, $\mathbf{R}_{\mathrm{d}}(i)$ is dependent on $\bar{w}_d(i)$, which is the d-th element of the reduced-rank filter. Hence, for updating each $\mathbf{t}_d(i)$, we need to calculate the corresponding $\mathbf{R}_{\mathrm{d}}^{-1}(i)$ and that leads to high computational complexity. Assuming that $\bar{w}_d(i) \approx \bar{w}_d(i+1)$, we devise an approximation

$$\mathbf{R}_{\mathrm{d}}(i) \approx |\bar{w}_d(i)|^2\sum_{j=1}^{i}\alpha^{i-j}|y(j)|^2\mathbf{r}(j)\mathbf{r}^H(j) = |\bar{w}_d(i)|^2\mathbf{R}_y(i). \tag{4.46}$$

Then we adopt the matrix inversion lemma [26] to recursively estimate $\mathbf{R}_y^{-1}(i)$ as follows

$$\begin{aligned}
\boldsymbol{\kappa}_y(i) &= \hat{\mathbf{R}}_y^{-1}(i-1)y(i)\mathbf{r}(i),\\
\phi_y(i) &= \frac{1}{\alpha + y^*(i)\mathbf{r}^H(i)\boldsymbol{\kappa}_y(i)},\\
\hat{\mathbf{R}}_y^{-1}(i) &= \frac{1}{\alpha}\left(\hat{\mathbf{R}}_y^{-1}(i-1) - (\phi(i)\boldsymbol{\kappa}_y(i))\boldsymbol{\kappa}_y^H(i)\right),
\end{aligned} \tag{4.47}$$

where $\hat{\mathbf{R}}_y^{-1}(i)$ is the estimate of $\mathbf{R}_y^{-1}(i)$. We use $\hat{\mathbf{R}}_y^{-1}(i)$ for all the adaptations of $\mathbf{t}_d(i)$ to avoid the estimation of the $\mathbf{R}_{\mathrm{d}}^{-1}(i)$ (where $d = 1, 2, \ldots, D$) and the new update equation is given by

$$\mathbf{t}_d(i) = -\frac{\hat{\mathbf{R}}_y^{-1}(i)}{|\bar{w}_d(i)|^2}\left(\frac{\lambda_{t,d}(i)}{2}\bar{w}_d^*(i)\hat{\mathbf{p}}(i) + \mathbf{v}_r(i)\right). \tag{4.48}$$

Using the constraint $\bar{\mathbf{w}}^H(i)\sum_{d=1}^{D}\mathbf{t}_d^H(i)\hat{\mathbf{p}}(i)\mathbf{q}_d = \mathbb{v}$, we obtain the expression of the Lagrange multiplier as

$$\lambda_{t,d}(i) = 2\left[\frac{\bar{w}_d^*(i)\mathbf{v}_r^H(i)\hat{\mathbf{R}}_y^{-1}(i)\hat{\mathbf{p}}(i) + \big(\mathbb{v} - \bar{\mathbf{w}}^H(i)\hat{\mathbf{p}}_d(i)\big)|\bar{w}_d(i)|^2}{-|\bar{w}_d(i)|^2\hat{\mathbf{p}}^H(i)\hat{\mathbf{R}}_y^{-1}(i)\hat{\mathbf{p}}(i)}\right]^*, \tag{4.49}$$

where $\hat{\mathbf{p}}_d(i)$ can be obtained by calculating the vector $\mathbf{T}^H(i)\hat{\mathbf{p}}(i)$ and setting its d-th element to zero. Note that in the update equation (4.48), small values of $|\bar{w}_d(i)|^2$ may cause numerical problems for the later calculation. This issue can be addressed by normalizing the column vector after each adaptation, which is given by $\mathbf{t}_d(i) \leftarrow \mathbf{t}_d(i)/\|\mathbf{t}_d(i)\|$.

After updating the projection matrix column by column, now we are going to adapt the reduced-rank filter $\bar{\mathbf{w}}(i)$. By assuming that the projection matrix is fixed, we can express the output signal in a simpler way as

$$y(i) = \bar{\mathbf{w}}^H(i)\mathbf{T}^H(i)\mathbf{r}(i), \tag{4.50}$$

where $\mathbf{T}(i) = [\mathbf{t}_1(i), \ldots, \mathbf{t}_D(i)]$ and the constraint can be expressed as $\bar{\mathbf{w}}^H(i)\mathbf{T}^H(i)\hat{\mathbf{p}}(i) = \mathbb{v}$. Hence, the Lagrangian becomes

$$\mathcal{L}_{JIO-RLS}\big(\bar{\mathbf{w}}(i), \mathbf{T}(i)\big) = \frac{1}{2}\sum_{j=1}^{i}\alpha^{i-j}\left(|y(j)|^2 - 1\right)^2 + \Re[\lambda_R(i)\big(\bar{\mathbf{w}}^H(i)\mathbf{T}^H(i)\hat{\mathbf{p}}(i) - \mathbb{v}\big)]. \tag{4.51}$$

By taking the gradient term of (4.51) with respect to $\bar{\mathbf{w}}(i)$ and setting it to a null vector, we have

$$\nabla_{\mathbf{w}}\mathcal{L}_{JIO-RLS} = \sum_{j=1}^{i}\alpha^{i-j}e(j)\mathbf{T}^H(j)\mathbf{r}(j)\mathbf{r}^H(j)\mathbf{T}(j)\bar{\mathbf{w}}(i) + \frac{1}{2}\lambda_{Rw}(i)\mathbf{T}^H(i)\hat{\mathbf{p}}(i) = 0,$$

where the real-valued error is $e(i) = (|y(i)|^2 - 1)$ and $\lambda_{Rw}(i)$ is the complex-valued Lagrange multiplier for updating the reduced-rank filter, rearranging the terms we obtain

$$\bar{\mathbf{w}}(i) = \mathbf{R}_{\mathrm{T}}^{-1}(i)\left(-\frac{\lambda_{Rw}(i)}{2}\mathbf{T}^H(i)\hat{\mathbf{p}}(i) + \bar{\mathbf{d}}(i)\right), \tag{4.52}$$

where $\mathbf{R}_{\mathrm{T}}(i) = \sum_{j=1}^{i}\alpha^{i-j}|y(j)|^2\bar{\mathbf{r}}(j)\bar{\mathbf{r}}^H(j)$ and $\bar{\mathbf{d}}(i) = \sum_{j=1}^{i}\alpha^{i-j}\bar{\mathbf{r}}(j)y^*(j) = \bar{\mathbf{d}}(i-1) + \alpha\bar{\mathbf{r}}(i)y^*(i)$. The matrix inversion lemma [26] is used again to recursively estimate the inversion matrix $\mathbf{R}_{\mathrm{T}}^{-1}(i)$ as follows

$$\begin{aligned}
\boldsymbol{\kappa}_{\mathrm{T}}(i) &= \hat{\mathbf{R}}_{\mathrm{T}}^{-1}(i-1)\bar{\mathbf{r}}(i)y(i), \\
\phi_{\mathrm{T}}(i) &= \frac{1}{\alpha + y(i)^*\bar{\mathbf{r}}^H(i)\boldsymbol{\kappa}_{\mathrm{T}}(i)}, \\
\hat{\mathbf{R}}_{\mathrm{T}}^{-1}(i) &= \frac{1}{\alpha}\left(\hat{\mathbf{R}}_{\mathrm{T}}^{-1}(i-1) - (\phi_{\mathrm{T}}(i)\boldsymbol{\kappa}_{\mathrm{T}}(i))\boldsymbol{\kappa}_{\mathrm{T}}^H(i)\right),
\end{aligned} \tag{4.53}$$

where $\hat{\mathbf{R}}_{\mathrm{T}}^{-1}(i)$ is the estimate of $\mathbf{R}_{\mathrm{T}}^{-1}(i)$. For calculating the Lagrange multiplier, we use

Tab. 4.2: RLS version of the Proposed JIO-CCM Receiver.

RLS version:

Initialization:

$\bar{\mathbf{w}}(1) = [1, 1, 1, \ldots, 1]$, D-by-1 vector ; $\hat{\mathbf{R}}_{\mathrm{T}}^{-1}(0) = \mathbf{I}_D/\delta$, D-by-D matrix;
$\mathbf{t}_d(1) = [1, 0, 0, \ldots, 0]$ ($d = 1, 2, \ldots, D$), D-by-1 vectors;
$\bar{\mathbf{d}}(0) = [0, 0, \ldots, 0]$, D-by-1 vector ; $\hat{\mathbf{R}}_{y}^{-1}(0) = \mathbf{I}_M/\delta$, M-by-M matrix;

for $i = 1, 2, \ldots$

1: Pre-adaptation:

$\bar{\mathbf{r}}(i) = \mathbf{T}^H(i)\mathbf{r}(i)$, $y(i) = \bar{\mathbf{w}}^H(i)\bar{\mathbf{r}}(i)$, $\bar{\mathbf{d}}(i) = \bar{\mathbf{d}}(i-1) + \alpha\bar{\mathbf{r}}(i)y^*(i)$,
Estimate $\hat{\mathbf{R}}_{y}^{-1}(i)$ and $\hat{\mathbf{R}}_{\mathrm{T}}^{-1}(i)$ using (4.47) and (4.53), respectively,
Calculate $\hat{\mathbf{V}}(i)$ and $\hat{\mathbf{h}}(i)$ using (4.56) and (4.55), respectively,
Calculate $\hat{\mathbf{p}}(i)$ using (4.57).

2: Adaptation of $\mathbf{t}_d(i)$:

for $d = 1, 2, \cdots, D$
Calculate $\lambda_{t,d}(i)$ using (4.49), Update $\mathbf{t}_d(i)$ using (4.48),
Normalize $\mathbf{t}_d(i) \leftarrow \mathbf{t}_d(i)/ \parallel \mathbf{t}_d(i) \parallel$.

3: Adaptation of $\bar{\mathbf{w}}(i)$:

Calculate $\lambda_{Rw}(i)$ using (4.54), Update $\bar{\mathbf{w}}(i)$ using (4.52),

4: Make Decision for the i-th data bit:

$\hat{b}(i) = \mathrm{sign}(\Re(y(i)))$

the constraint $\bar{\mathbf{w}}^H(i)\mathbf{T}^H(i)\hat{\mathbf{p}}(i) = \mathbb{v}$ and obtain

$$\lambda_{Rw}(i) = 2\left[\frac{\bar{\mathbf{d}}^H(i)\mathbf{R}_{\mathrm{T}}^{-1}(i)\mathbf{T}^H(i)\hat{\mathbf{p}}(i) - \mathbb{v}}{\hat{\mathbf{p}}^H(i)\mathbf{T}(i)\mathbf{R}_{\mathrm{T}}^{-1}(i)\mathbf{T}^H(i)\hat{\mathbf{p}}(i)}\right]^*. \tag{4.54}$$

4.4.2 Blind Channel Estimator for the RLS version

In the JIO-RLS algorithm, the estimation of the covariance matrix $\mathbf{R}_y(i) = \sum_{j=1}^{i}\alpha^{i-j}|y(j)|^2\mathbf{r}(j)\mathbf{r}^H(j)$ and its inversion are obtained in the stage of adapting the projection matrix. It should be noted that $|y(j)|^2$ tends to 1 as the number of received signal increasing. Hence, by replacing the inverse matrix $\mathbf{R}^{-1}(i)$ in (4.22) with $\mathbf{R}_y^{-1}(i)$, we obtain

$$\hat{\mathbf{h}}(i) = \hat{\mathbf{h}}(i-1) - \left(\hat{\mathbf{V}}(i)\hat{\mathbf{h}}(i-1)\right)/tr[\hat{\mathbf{V}}(i)], \tag{4.55}$$

where the L-by-L matrix is defined as

$$\hat{\mathbf{V}}(i) = \mathbf{S}_e^H \mathbf{P}_r^H \mathbf{R}_y^{-m}(i) \mathbf{P}_r \mathbf{S}_e, \tag{4.56}$$

and the effective signature vector of the desired user is given by

$$\hat{\mathbf{p}}(i) = \mathbf{P}_r \mathbf{S}_e \hat{\mathbf{h}}(i) \tag{4.57}$$

Using $\mathbf{R}_y^{-1}(i)$ instead of $\mathbf{R}^{-1}(i)$ can save $\mathcal{O}(M^2)$ in terms of computational complexity for the JIO-RLS version and simulation results will demonstrate later that the performance will not be degraded with this replacement. The JIO-RLS version is summarized in Table. 4.2.

4.5 Complexity Analysis and Rank Adaptation Algorithm

In this section, a complexity analysis is presented to compare the two versions of the JIO receiver, the full-rank NSG and RLS schemes, the NSG and RLS versions of the MSWF. The computational complexity of the blind channel estimators that are implemented in this work are also analyzed. A rank adaptation algorithm is detailed in this section which is able to select the rank adaptively and can achieve better tradeoffs between the convergence speed and the steady state performances.

4.5.1 Complexity Analysis

As shown in Table. 4.3, the complexity of the analyzed blind CCM full-rank NSG and RLS, MSWF-NSG and MSWF-RLS [56] and the proposed NSG and RLS versions of the JIO scheme is compared with respect to the number of complex additions and complex multiplications for each time instant. The complexity of the conventional blind channel estimator (BCE) that is described in Section 4.2 is compared with the BCEs for the JIO-NSG and JIO-RLS that are described in Section 4.3.2 and Section 4.4.2, respectively.

For the analysis of the adaptive algorithms, the quantity M is the length of the full-rank filter, D is the dimension of reduced-rank filter and c_{max} is the number of iterations for the JIO-NSG version in each time instant. Note that, only one iteration is required in the JIO-RLS version for each time instant. For the analysis of the BCEs, the quantity L is the length of the CIR and m is the power of the inverse covariance matrix. In this work, M is the minimum integer that is larger than the scalar term $(T_s/T_\tau + T_{DS}/T_\tau - 1)/(T_c/T_\tau) =$

Tab. 4.3: Complexity analysis for the blind algorithms

	Complex Additions	Complex Multiplications
Full-Rank NSG	$M^2 + 3M - 1$	$2M^2 + 4M + 5$
Full-Rank RLS	$5M^2 + 2M + 1$	$5M^2 + 3M + 1$
MSWF-NSG	$DM^2 + (2D + 2)M$ $-2D^2 - 2$	$(D + 1)M^2 + (4D + 2)M$ $-2D^2 + 4D + 5$
MSWF-RLS	$DM^2 + (2D + 2)M$ $+2D^2 - D$	$(D + 1)M^2 + (4D + 2)M$ $+2D^2 + 3D + 1$
JIO-NSG	$c_{max}(6DM + 3M + 4D - 2)$	$c_{max}(8DM + 4M + 7D + 11)$
JIO-RLS	$DM^2 + 3DM + 4D^2 - 4D$	$DM^2 + 6DM + 4D^2$ $+15D + 1$
Conventional BCE	$(m + 1)M^2L - (m + 1)ML$ $+2M^2 + L^2 + L - 1$	$(m + 1)M^2L + 3M^2 + L^2$ $+2M + 1$
BCE for JIO-NSG	$L^2M + 3mML - (m - 1)L - 1$	$L^2M + 4mML + L^2$
BCE for JIO-RLS	$(m + 1)M^2L - (m + 1)ML$ $+L^2 + L - 1$	$(m + 1)M^2L + L^2$

$(T_s + T_{DS} - T_\tau)/T_c$ and $L = T_{DS}/T_\tau$. Since T_τ is set to $0.125ns$ as for the standard IEEE802.15.4a channel model, symbol duration T_s and chip duration T_c are assumed given for the designer. Hence, M and L are both related to the channel delay spread T_{DS}. In this work, the parameters are set as follows: $T_s = 12ns$, $T_c = 0.375ns$, $m = 3$ and $c_{max} = 3$. As shown in Fig. 4.2, the number of complex multiplications required for different algorithms are compared as a function of channel delay spread T_{DS}. The JIO-RLS algorithm with $D = 3$ has lower complexity than the MSWF algorithms and the full-rank RLS. It will be demonstrated by the simulation results that the JIO-RLS algorithm can achieve fast convergence with a very small rank ($D < 5$). The proposed JIO-NSG algorithm has lower complexity than the full-rank NSG algorithm in the long channel delay spread scenarios. As discussed in Section 4.3.1, the price we pay for such a complexity reduction is the extra storage space at the receiver.

The complexity of the BCEs for the JIO versions is shown in Fig. 4.3, in which the number of complex multiplications is shown as a function of channel delay spread T_{DS}. The complexity of the BCE for the JIO-NSG version has lower complexity than the BCE for the JIO-RLS version in all the analyzed scenarios.

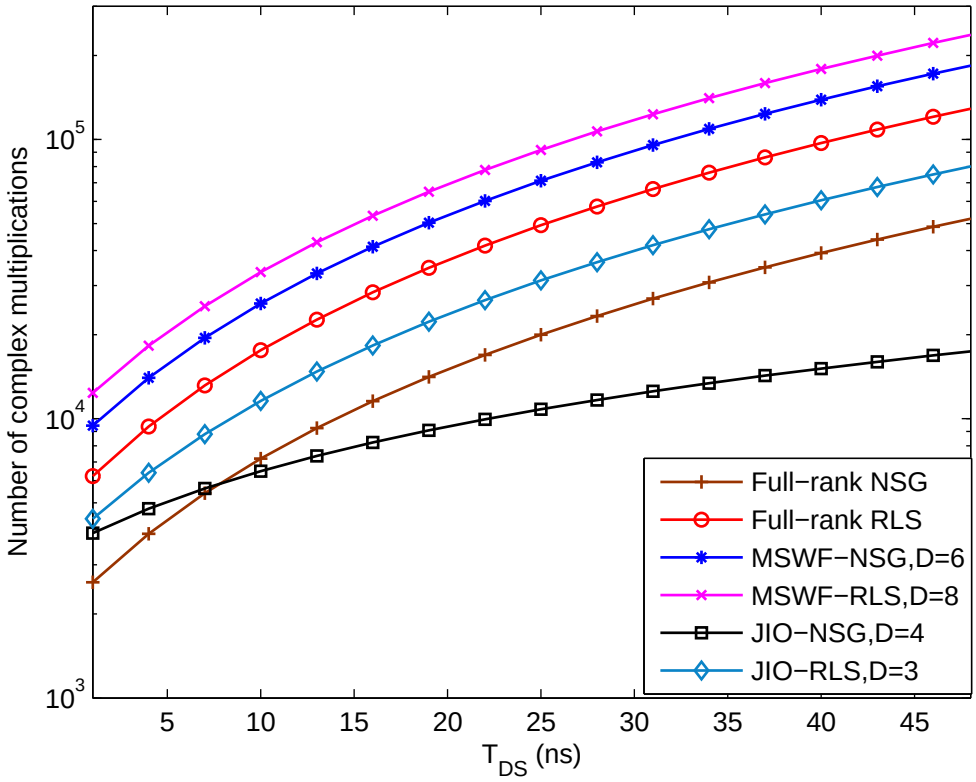

Fig. 4.2: Number of multiplications required for different blind algorithms.

4.5.2 Rank Adaptation

In the proposed blind JIO reduced-rank receiver, the computational complexity and the performance are sensitive to the determined rank D. In this section, a rank adaptation algorithm is employed to achieve better tradeoffs between the performance and the complexity of the JIO receiver. The rank adaptation algorithm is based on the *a posteriori* LS cost function to estimate the MSE, which is a function of $\bar{\mathbf{w}}_D(i)$ and $\mathbf{T}_D(i)$ and can be expressed as

$$\mathscr{C}_D(i) = \sum_{n=0}^{i} \lambda_D^{i-n} \left(|\bar{\mathbf{w}}_D^H(n)\mathbf{T}_D^H(n)\mathbf{r}(n)|^2 - 1 \right)^2, \tag{4.58}$$

where λ_D is a forgetting factor. Since the optimal rank can be considered as a function of the time interval i [42], the forgetting factor is required and allows us to track the optimal rank. For each time instant, we update a projection matrix $\mathbf{T}_{\mathrm{M}}(i)$ and a reduced-rank filter $\bar{\mathbf{w}}_{\mathrm{M}}(i)$ with the maximum rank $D_{\max}$, which can be expressed as

$$\begin{aligned} \mathbf{T}_{\mathrm{M}}(i) &= [\mathbf{t}_{\mathrm{M},1}(i), \ldots, \mathbf{t}_{\mathrm{M},D}(i), \ldots, \mathbf{t}_{\mathrm{M},D_{\max}}(i)]^T \\ \bar{\mathbf{w}}_{\mathrm{M}}(i) &= [\bar{w}_{\mathrm{M},1}(i), \ldots, \bar{w}_{\mathrm{M},D}(i), \ldots, \bar{w}_{\mathrm{M},D_{\max}}(i)]^T \end{aligned} \tag{4.59}$$

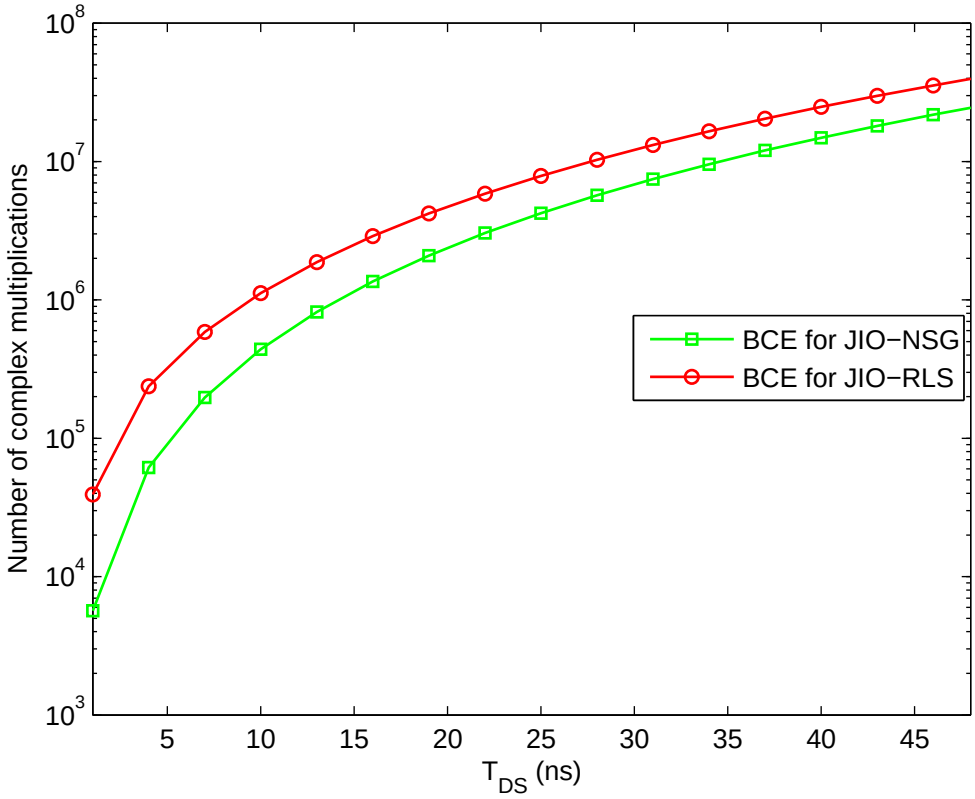

Fig. 4.3: Number of multiplications required for BCEs.

After the adaptation, we test values of D within the range $D_{\min}$ to $D_{\max}$. For each tested rank, we use the following estimators

$$\begin{aligned} \mathbf{T}_D(i) &= [\mathbf{t}_{\mathrm{M},1}(i), \ldots, \mathbf{t}_{\mathrm{M},D}(i)]^T \\ \bar{\mathbf{w}}_D(i) &= [\bar{w}_{\mathrm{M},1}(i), \ldots, \bar{w}_{\mathrm{M},D}(i)]^T \end{aligned} \tag{4.60}$$

and substitute (4.60) into (4.58) to obtain the value of $\mathscr{C}_D(i)$, where $D \in \{D_{\min}, \ldots, D_{\max}\}$. The proposed algorithm can be expressed as

$$D_{\mathrm{opt}}(i) = \arg \min_{D \in \{D_{\min}, \ldots, D_{\max}\}} \mathscr{C}_D(i). \tag{4.61}$$

We remark that the complexity of updating the reduced-rank filter and the projection matrix in the proposed rank adaptation algorithm is the same as the receiver with rank $D_{\max}$, since we only adapt the $\mathbf{T}_{\mathrm{M}}(i)$ and $\bar{\mathbf{w}}_{\mathrm{M}}(i)$ for each time instant. However, additional computations are required for calculating the values of $\mathscr{C}_D(i)$ and selecting the minimum value of a $(D_{\max} - D_{\min} + 1)$-dimensional vector that corresponds to a simple search and comparison.

4.6 Simulations

In this section, the proposed NSG and RLS versions of the blind JIO adaptive receivers are applied to the uplink of a multiuser BPSK DS-UWB system. The uncoded BER performance of the proposed receivers are compared with the NSG and RLS versions of the full-rank schemes and the MSWF. The RAKE receiver with the maximal-ratio combining (MRC) is also included for comparison. Note that, the blind channel estimation described in 4.2.2 is implemented to provide channel coefficients to the RAKE receiver and its BER performance is averaged for comparison purposes. In all simulations, all the users are assumed to be transmitting continuously at the same power level as the desired user. The pulse shape adopted is the RRC pulse with the pulse-width 0.375ns. The spreading codes are generated randomly for each user with a spreading gain of 32 and the data rate of the communication is approximately 83Mbps. The standard IEEE 802.15.4a channel model for the NLOS indoor environment is employed [23] and we assume that the channel is constant during the whole transmission. The channel delay spread is T_{DS} = 10ns and the ISI from 2 neighbor symbols are taken into account for the simulations. The sampling rate at the receiver is assumed to be 2.67GHz and the length of the discrete time received signal is M = 59. For all the experiments, all the adaptive receivers are initialized as vectors with all the elements equal to 1. This allows a fair comparison between the analyzed techniques for their convergence performance. In practice, the filters can be initialized with prior knowledge about the spreading code or the channel to accelerate the convergence. In all the simulations, the phase $\mathbf{h}(0)$ is used as a reference to remove the phase ambiguity derived from the blind channel estimates. All the curves shown in this section are obtained by averaging 200 independent runs.

The first experiment we perform is to compare the uncoded BER performance of the proposed JIO receivers with the full-rank NSG and RLS algorithms the MSWF-NSG and MSWF-RLS. We consider a 7-user scenario with a signal-to-noise ratio (SNR) of 20dB. For each independent simulation, 2000 symbols are transmitted. Fig.4.4 shows the BER performance of different algorithms as a function of symbols transmitted. The proposed JIO-RLS algorithm converges faster than other algorithms. The JIO-NSG algorithm outperforms the MSWF versions and the full-rank versions with a low-complexity. A noticeable improvement on the BER performance is obtained for the JIO receivers.

Fig.4.5 and Fig. 4.6 show the uncoded BER performances of algorithms with different SNRs in a 7-user scenario and with different number of users in a 20dB SNR scenario, respectively. The parameters set for all the adaptive algorithms are the same as in the first experiment. For all the tested environments, 2000 symbols are transmitted for each independent run. The proposed JIO versions show better MAI and ISI canceling capabil-

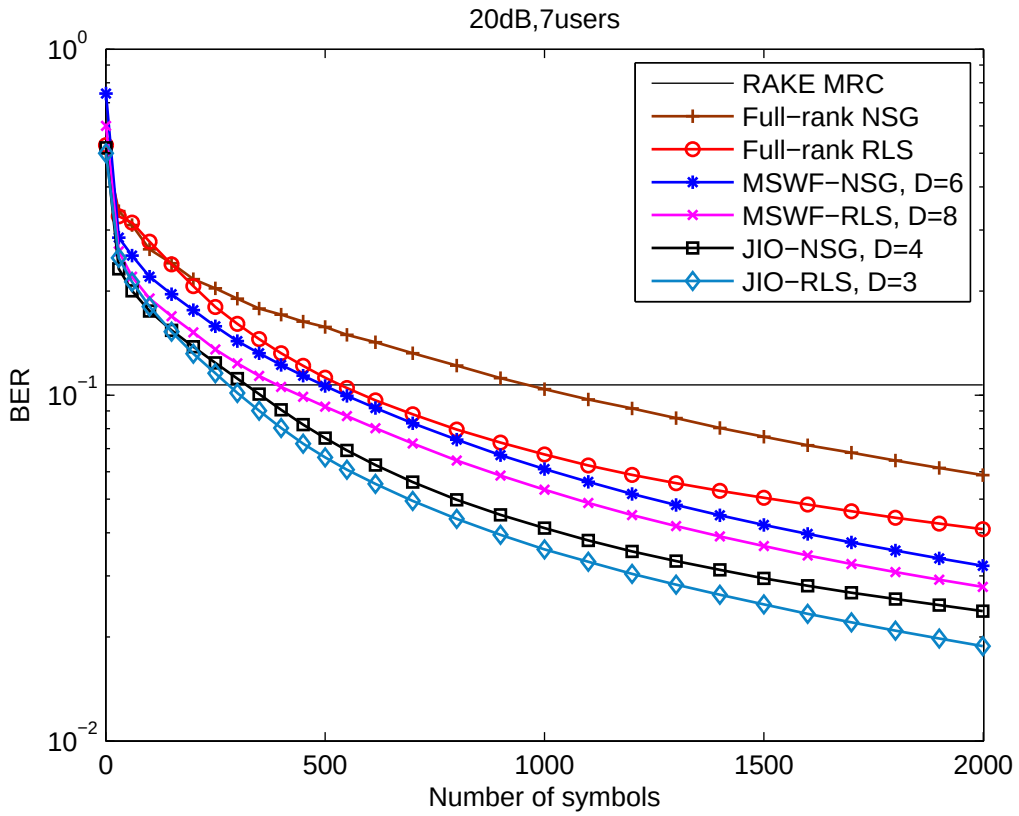

Fig. 4.4: BER performance of different algorithms. For full-rank NSG: $\mu = 0.025$, full-rank RLS: $\delta = 10$, $\lambda = 0.9998$. For MSWF-NSG, $D = 6$, $\mu = 0.025$; MSWF-RLS: $D = 8$, $\lambda = 0.998$. For JIO-NSG $D = 4$, $c_{max} = 3$, $\nu = 1$, $\mu_{T,0} = 0.075$, $\mu_{w,0} = 0.005$; JIO-RLS: $D = 3$, $\lambda = 0.9998$, $\delta = 10$, $\nu = 0.5$.

ity in all the simulated scenarios. In Fig.4.5, for a BER around 0.02, JIO-RLS can save around 3dB in comparison with the MSWF-RLS and the JIO-NSG can save about 2dB in comparison with the MSWF-NSG. In Fig.4.6, the JIO-RLS scheme can support about 3 additional users in comparison with the MSWF-RLS and around 7 additional users in comparison with the full-rank LMS algorithm for a BER of 0.03.

Fig.4.7 compares the BER performance of the JIO-RLS using the rank-adaptation algorithm given by (4.61) with $D_{\max} = 8$ and $D_{\min} = 3$. The results using a fixed-rank of 3 and 8 are also shown for comparison purposes and illustration of the sensitivity of the JIO scheme to the rank D. The forgetting factor is $\lambda_D = 0.998$. It can be seen that the BER performance of the JIO-RLS scheme with the rank-adaptation algorithm outperforms the fixed-rank scenarios with $D_{\min} = 3$ and $D_{\max} = 8$. In this experiment, $D = 3$ has better steady state performance than $D = 8$, with both cases showing the similar convergence speed. The rank-adaptation algorithm provides a better solution than the fixed rank approaches.

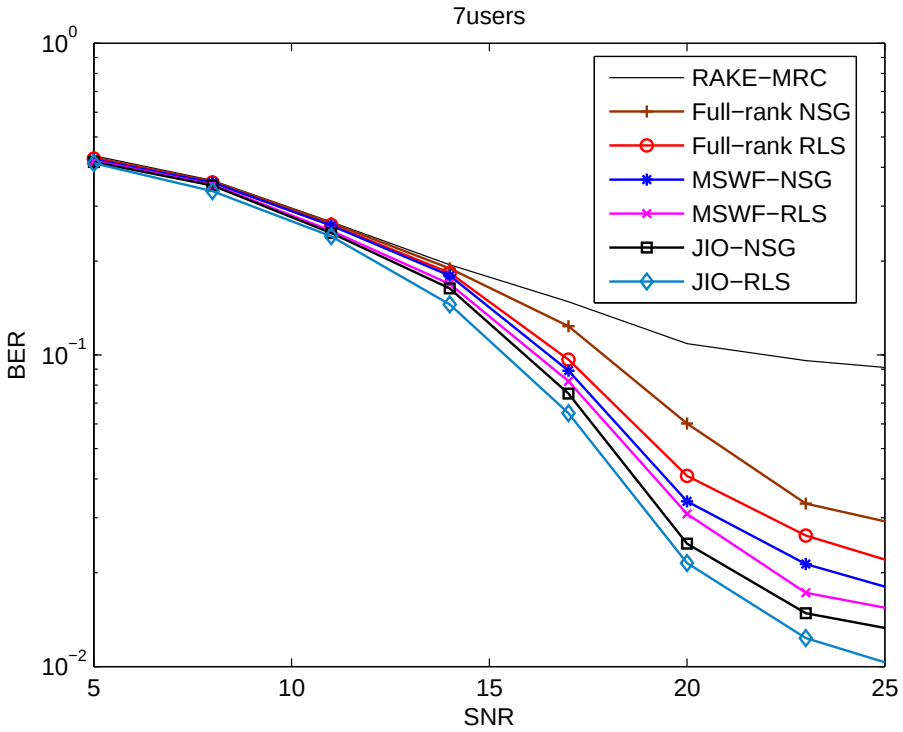

Fig. 4.5: BER performance of the proposed JIO-CCM scheme with different SNRs.

In the last experiment, we examine the blind adaptive algorithms with an additional narrow band interference (NBI), which is modeled as a single-tone signal (complex base-band) [79]:

$$J(t) = \sqrt{P_j} e^{(2\pi f_d t + \theta_j)}, \tag{4.62}$$

where P_j is the NBI power, f_d is the frequency difference between the carrier frequency of the UWB signal and the one of the NBI and θ_j is the random phase which is uniformly distributed in $[0, \pi)$. Here, the received signal can be expressed as

$$z(t) = \sum_{k=1}^{K} \sum_{l=0}^{L-1} h_{k,l} x^{(k)}(t - lT_\tau) + n(t) + J(t). \tag{4.63}$$

Note that, in this experiment, the receivers are required to suppress the ISI, MAI and NBI together blindly. In Fig. 4.8, in a 7-user system with SNR=20dB, the BER performance of the RLS versions are compared with different signal to NBI ratio (SIR). The algorithms are set with the same parameters as in the first experiment and 2000 symbols are transmitted in each tested point for each independent run. With the NBI, the eigenvalue spread of the covariance matrix of the received signal is increased and this change slows down the convergence rate of the full-rank scheme. However, the proposed JIO receiver shows a better ability to cope with this change and the performance gain over the full-rank scheme

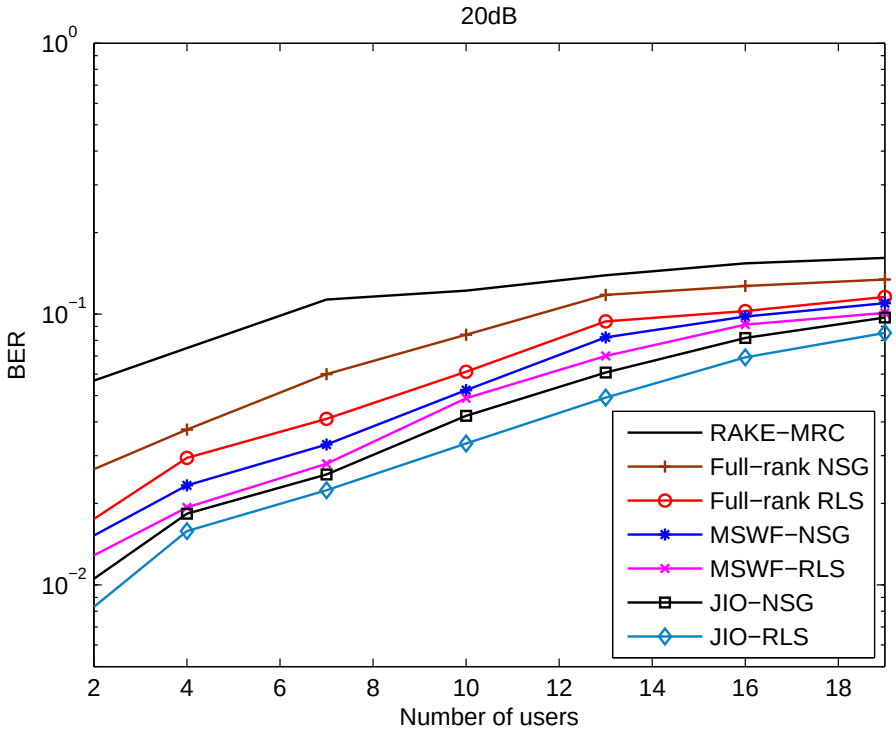

Fig. 4.6: BER performance of the proposed JIO-CCM scheme with different number of users.

is increased compared to the NBI free scenarios.

4.7 Conclusion

A novel blind reduced-rank receiver is proposed based on JIO and the CCM criterion. The novel receiver consists of a projection matrix and a reduced-rank filter. The NSG and RLS adaptive algorithms are developed for updating its parameters. In DS-UWB systems, both versions (NSG and RLS) of the proposed blind reduced-rank receivers outperform the analyzed CCM based full-rank and existing reduced-rank adaptive schemes with a low complexity. The robustness of the proposed receivers has been demonstrated in the scenario that the blind receivers are required to suppress the ISI, MAI and NBI together. Note that the proposed blind receivers can be employed in spread-spectrum systems which encounter large filter problems and suffer from severe interferences.

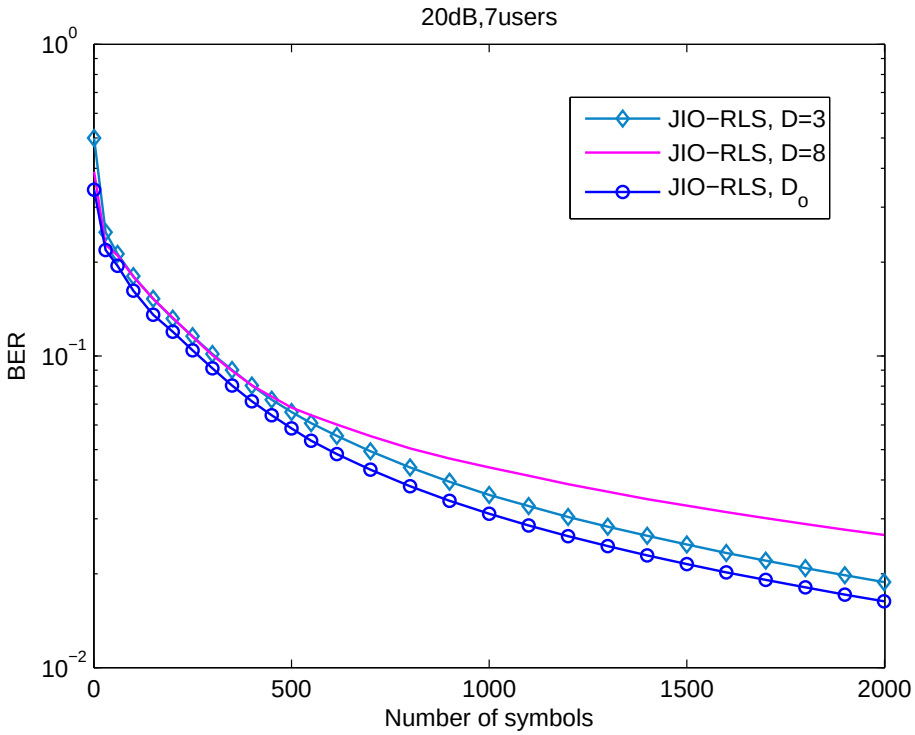

Fig. 4.7: BER performance of the rank-adaptation algorithm in JIO-CCM scheme.

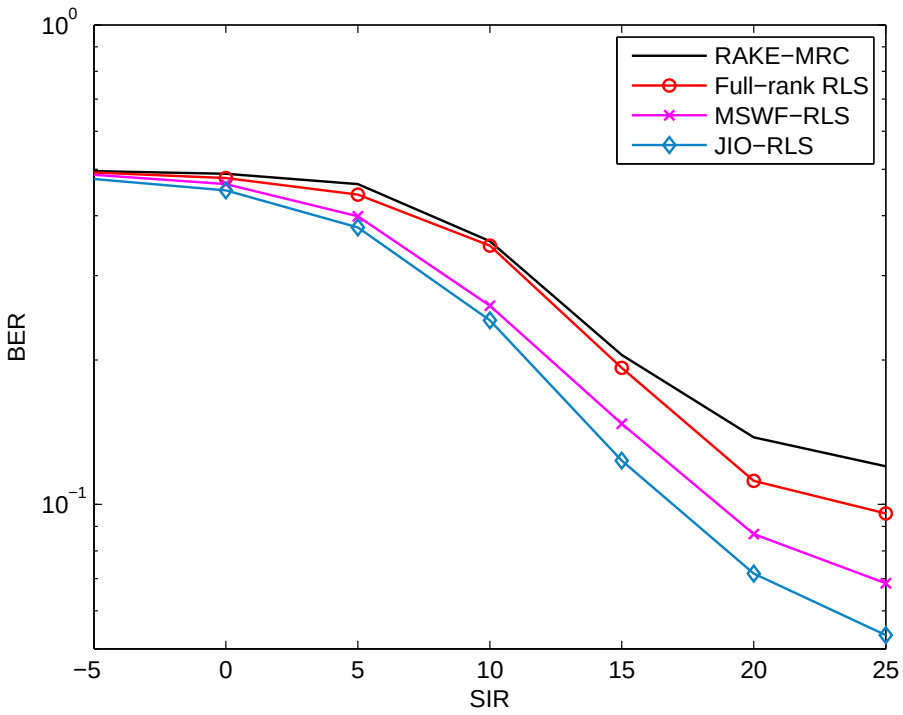

Fig. 4.8: BER performance of the blind adaptive algorithm with NBI. For NBI, $f_d = 23MHz$.

5. FREQUENCY DOMAIN ADAPTIVE DETECTORS FOR SC-FDE IN MULTIUSER DS-UWB SYSTEMS

Contents

5.1 Introduction

In this chapter, we propose two adaptive detection schemes based on single-carrier frequency domain equalization (SC-FDE) for multiuser direct-sequence ultra-wideband (DS-UWB) systems, which are termed structured channel estimation (SCE) and direct adaptation (DA). Both schemes use the minimum mean square error (MMSE) linear detection strategy and employ a cyclic prefix. Least-mean squares (LMS), recursive least squares (RLS) and conjugate gradient (CG) adaptive algorithms are then developed for both schemes. A complexity analysis compares the computational complexity of the proposed algorithms and schemes, and simulation results illustrate their performance.

The main contributions of this chapter are listed below.

- Two adaptive detection schemes are developed and compared for SC-FDE in multiuser DS-UWB systems. For both schemes, the LMS, RLS and CG algorithms are developed.

- In the first scheme, named SCE, adaptive algorithms are developed for estimating the channel coefficients and algorithms for computing the noise variance and the number of active users are also proposed.

- In the second scheme, named DA, a new signal model is adopted to enable simplified adaptive implementation. A low-complexity RLS algorithm is then obtained.

- The performance and complexity of LMS, RLS and CG algorithms are compared for both schemes.

The rest of this chapter is structured as follows. The detection schemes for the SC-FDE in DS-UWB system are introduced in section 5.2. The proposed adaptive algorithms for SCE and DA schemes are described in section 5.3 and section 5.4, respectively. The complexity analysis for the adaptive algorithms and the schemes are presented in section 5.5. In section 5.6, the approaches for estimating the noise variance and the number of active users is detailed. Simulations results of the proposed schemes are shown in section 5.7 and section 5.8 draws the conclusions.

5.2 Proposed Linear MMSE Detection Schemes

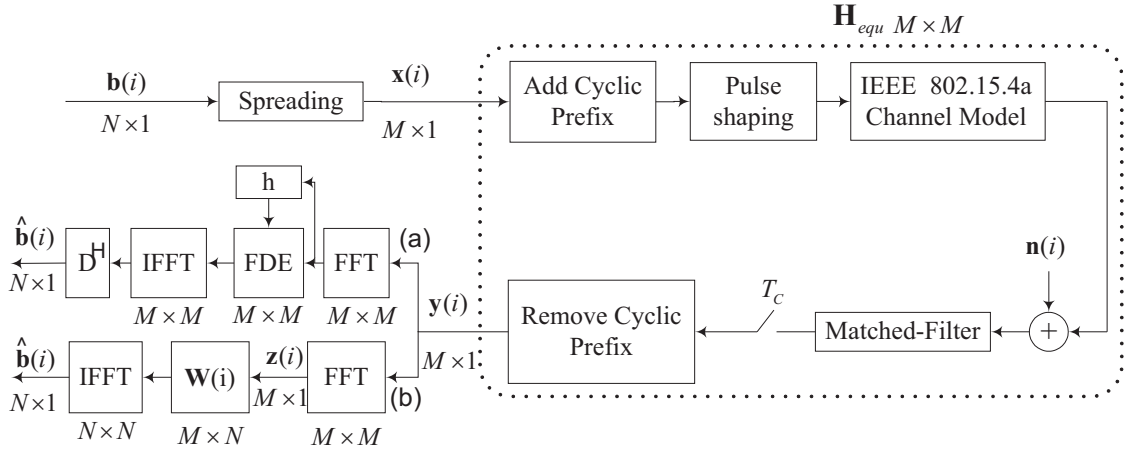

Fig. 5.1: Block diagram of SC-FDE schemes in DS-UWB system, (a) Structured channel estimation (SCE) and (b) Direct adaptation (DA).

5.2.1 Problem Statement

After the DFT, the frequency domain detectors are implemented to recover the original data vector from the received signal that is shown in (2.12) As shown in Fig.5.1, we propose two detection schemes, named SCE and DA, respectively. The SCE scheme explicitly performs the channel estimation in the frequency domain, the detection with the estimated channel coefficients, and finally carries out despreading in the time domain. The DA scheme implicitly estimates the channel and suppresses the ISI and MAI together with only one filter and has a simpler structure than the SCE scheme. Without loss of generality, we consider user 1 as the desired user and bypass the subscript of this user for simplicity.

We define the estimated signal as $\hat{\mathbf{b}}(i)$ and the final recovered signal as $\hat{\mathbf{b}}_r(i)$. Hence, for the SCE scheme, the recovered signal can be expressed as

$$\hat{\mathbf{b}}_r(i) = \mathrm{sign}(\Re(\hat{\mathbf{b}}(i)) = \mathrm{sign}(\Re(\mathbf{D}^{\mathrm{H}}\mathbf{F}^{\mathrm{H}}\mathbf{C}^{\mathrm{H}}\mathbf{z}(i))), \tag{5.1}$$

where$(\cdot)^H$ denotes the Hermitian transpose, $\mathrm{sign}(\cdot)$ is the algebraic sign function and $\Re(\cdot)$ represents the real part of a complex number. $\mathbf{C}$ denotes the frequency domain equalizer. The despreading is denoted as $\mathbf{D}^H$ which can be considered as the Hermitian transpose of the spreading matrix.

For the DA scheme, the final recovered signal can be expressed as

$$\hat{\mathbf{b}}_r(i) = \mathrm{sign}(\Re(\hat{\mathbf{b}}(i)) = \mathrm{sign}(\Re(\mathbf{F}_N^{\mathrm{H}}\mathbf{W}^{\mathrm{H}}\mathbf{z}(i))), \tag{5.2}$$

where $\mathbf{W}$ represents the frequency domain filter that is in an M-by-N matrix form. $\mathbf{F}_N$ is the N-by-N DFT matrix. In this scheme, the channel estimation and the despreading is fulfilled implicitly together in the filter $\mathbf{W}$.

In what follows, the MMSE designs of the matrix $\mathbf{C}$ in the SCE scheme and the $\mathbf{W}$ in the DA scheme will be detailed. In general, these two detection schemes are based on the same MMSE problem which aims at minimizing $E[\|\mathbf{b}(i) - \hat{\mathbf{b}}(i)\|^2]$, but they use different approaches to perform linear detection. For each scheme, some simplifications and approximations for the later adaptive implementations will also be presented.

5.2.2 Detector with Structured Channel Estimation (SCE)

The block diagram of the detector with SCE is shown as the branch (a) in Fig.5.1. Expanding (2.12), we have

$$\mathbf{z}(i) = \mathbf{F}\mathbf{H}_{\text{equ}} \sum_{k=1}^{K} \mathbf{x}_k(i) + \mathbf{F}\mathbf{n}(i) = \mathbf{F}\mathbf{H}_{\text{equ}}\mathbf{F}^H\mathbf{F} \sum_{k=1}^{K} \mathbf{x}_k(i) + \mathbf{F}\mathbf{n}(i), \tag{5.3}$$

Bearing in mind the circulant Toeplitz form of the equivalent channel matrix, we have a diagonal matrix

$$\mathbf{\Lambda}_{\text{H}} = \mathbf{F}\mathbf{H}_{\text{equ}}\mathbf{F}^H, \tag{5.4}$$

whose a-th diagonal entry can be expressed as $\tilde{h}_a = \sum_{l=0}^{L-1} h_l \exp\{-j(2\pi/M)al\}$. Let us express it in a more convenient matrix form as

$$\tilde{\mathbf{h}} = \sqrt{M}\mathbf{F}_{M,L}\mathbf{h}_{\text{equ}}, \tag{5.5}$$

where $\tilde{\mathbf{h}} = [\tilde{h}_0, \tilde{h}_1, \ldots, \tilde{h}_{M-1}]^T$ is called frequency domain CIR and $\mathbf{F}_{M,L}$ is an M-by-L matrix that is structured with the first L columns of the DFT matrix $\mathbf{F}$. In order to simplify the expression of this scheme in later adaptive developments, we include the constant $\sqrt{M}$ into the $\mathbf{F}_{M,L}$, that is

$$\mathbf{F}_{M,L} \Longleftarrow \sqrt{M}\mathbf{F}_{M,L}. \tag{5.6}$$

The equations (5.5) and (5.6) are important for the development of the adaptive algorithms in the SCE scheme which will be detailed later. Here, we develop the MMSE detector $\mathbf{C}$ to minimize the following cost function

$$\mathbf{J}_{\text{MSE-SCE}}(i) = E[\left\|\mathbf{b}(i) - \mathbf{D}^H\mathbf{F}^H\mathbf{C}^H\mathbf{z}(i))\right\|^2]. \tag{5.7}$$

Substituting (5.3) and (5.4) into (5.7) and assuming that the noise sequence and the signal sequences are uncorrelated to each other, we can obtain the expression of the detector as

$$\mathbf{C}_{\text{MMSE}} = \left(\mathbf{\Lambda}_{\text{H}}\mathbf{F}\mathbf{D}_{\text{all}}\mathbf{D}_{\text{all}}^H\mathbf{F}^H\mathbf{\Lambda}_{\text{H}}^H + \sigma^2\mathbf{I}_{\text{M}}\right)^{-1}\mathbf{\Lambda}_{\text{H}}, \tag{5.8}$$

where the M-by-NK block diagonal matrix $\mathbf{D}_{\text{all}}$ contains the information of the spreading codes for all the users and can be expressed as

$$\mathbf{D}_{\text{all}} = \begin{bmatrix} \mathbf{s}_1 \ldots \mathbf{s}_K & & & \\ & \mathbf{s}_1 \ldots \mathbf{s}_K & & \\ & & \ddots & \\ & & & \mathbf{s}_1 \ldots \mathbf{s}_K \end{bmatrix}. \tag{5.9}$$

For the adaptive implementation, the downlink terminal usually does not have the information of the spreading codes of other users. Hence, in this work, we adopted the approximation $\mathbf{D}_{\text{all}}\mathbf{D}_{\text{all}}^{H} \approx (K/N_c)\mathbf{I}_{\text{M}}$ for the development of the adaptive algorithms. This approximation can also lead to a diagonal MMSE detector that can be considered as a sub-optimal solution [71]

$$\hat{\mathbf{C}} = \left(\frac{K}{N_c}\mathbf{\Lambda}_{\text{H}}\mathbf{\Lambda}_{\text{H}}^{H} + \sigma_e^2\mathbf{I}_{\text{M}}\right)^{-1}\mathbf{\Lambda}_{\text{H}}. \tag{5.10}$$

From the expression of (5.10), it is clear that the remaining tasks of the SCE scheme for the adaptive implementation are to estimate the channel coefficients $\tilde{\mathbf{h}}$, the noise variance σ_e^2 and the number of active users K. The proposed algorithms for estimating these parameters will be presented in later sections.

5.2.3 Detector with Direct Adaptation (DA)

The block diagram of the DA scheme is shown as the branch (b) in Fig.5.1. This scheme has much simpler system structure than the SCE scheme. However, if we go directly with the signal model used for the SCE scheme, the resulting adaptive filter for DA schemes will be in an M-by-N matrix form which means very high complexity. Thanks to the new signal model proposed in [68], we can explore the structure of the MMSE detector in SC-FDE systems more efficiently. In this work, we adopt this new signal model and extend it to simplify the design of the adaptive filters. It will be clear soon how the new signal model we adopted can significantly reduce the complexity of the adaptive filter implementation in the DA scheme.

Firstly, we can express the transmitted signal from the k-th user as

$$\mathbf{x}_k(i) = \mathbf{S}_k\mathbf{b}_{k,\text{e}}(i), \tag{5.11}$$

where the M-by-M ($M = N \times N_c$) spreading matrix $\mathbf{S}_k$ has a circulant Toeplitz form as [68]

$$\mathbf{S}_k = \begin{bmatrix} s_k(1) & & & s_k(2) \\ s_k(2) & s_k(1) & & \vdots \\ \vdots & s_k(2) & & s_k(N_c) \\ s_k(N_c) & \vdots & \ddots & \\ & s_k(N_c) & \ddots & \\ & & \ddots & \\ & & & s_k(1) \end{bmatrix},$$

The equivalent M-dimensional expanded data vector is

$$\mathbf{b}_{k,\mathrm{e}}(i) = [b_k(1), \mathbf{0}_{N_c-1}, b_k(2), \mathbf{0}_{N_c-1}, \cdots, b_k(N), \mathbf{0}_{N_c-1}]^T,$$

where $(\cdot)^T$ is the transpose. Hence, with the new signal model, the frequency domain received signal becomes

$$\mathbf{z}(i) = \mathbf{F}\mathbf{y}(i) = \sum_{k=1}^{K} \mathbf{F}\mathbf{H}_{\mathrm{equ}}\mathbf{S}_k\mathbf{b}_{k,\mathrm{e}}(i) + \mathbf{F}\mathbf{n}(i), \tag{5.12}$$

Since both $\mathbf{H}_{\mathrm{equ}}$ and $\mathbf{S}_k$ are circulant Toeplitz matrices, their product also has the circulant Toeplitz form. This feature makes $\mathbf{\Lambda}_k = \mathbf{F}\mathbf{H}_{\mathrm{equ}}\mathbf{S}_k\mathbf{F}^H$ a diagonal matrix. Hence, we have

$$\mathbf{z}(i) = \sum_{k=1}^{K} \mathbf{F}\mathbf{H}_{\mathrm{equ}}\mathbf{S}_k\mathbf{F}^H\mathbf{F}\mathbf{b}_{k,\mathrm{e}}(i) + \mathbf{F}\mathbf{n}(i) = \sum_{k=1}^{K} \mathbf{\Lambda}_k\mathbf{F}\mathbf{b}_{k,\mathrm{e}}(i) + \mathbf{F}\mathbf{n}(i). \tag{5.13}$$

We can further expand $\mathbf{F}\mathbf{b}_{k,\mathrm{e}}(i)$ as [68]

$$\mathbf{F}\mathbf{b}_{k,\mathrm{e}}(i) = (1/\sqrt{N_c})\mathbf{I}_{\mathrm{e}}\mathbf{F}_N\mathbf{b}_k(i), \tag{5.14}$$

where $\mathbf{F}_N$ denotes the N-by-N DFT matrix and the M-by-N matrix $\mathbf{I}_{\mathrm{e}}$ are structured as

$$\mathbf{I}_{\mathrm{e}} = [\underbrace{\mathbf{I}_N, \cdots, \mathbf{I}_N}_{N_c}]^T. \tag{5.15}$$

where $\mathbf{I}_N$ denotes the N-by-N identity matrix. Finally, the frequency domain received signal $\mathbf{z}(i)$ is expressed as

$$\mathbf{z}(i) = \sum_{k=1}^{K} (1/\sqrt{N_c})\mathbf{\Lambda}_k\mathbf{I}_{\mathrm{e}}\mathbf{F}_N\mathbf{b}_k(i) + \mathbf{F}\mathbf{n}(i). \tag{5.16}$$

In the DA scheme, an M-by-N MMSE filter $\mathbf{W}(i)$ can be developed via the following cost function:

$$\mathbf{J}_{\mathrm{MSE-DA}}(i) = E[\left\|\mathbf{b}(i) - \mathbf{F}_N^H\mathbf{W}^H(i)\mathbf{z}(i)\right\|^2]. \tag{5.17}$$

The MMSE solution of (5.17) is

$$\mathbf{W}_{\mathrm{MMSE}} = \mathbf{R}^{-1}\mathbf{P}, \tag{5.18}$$

where

$$\mathbf{R} = E[\mathbf{z}(i)\mathbf{z}^H(i)] = (1/N_c)\sum_{k=1}^{K}\mathbf{\Lambda}_k\mathbf{I}_{\rm e}\mathbf{I}_{\rm e}^H\mathbf{\Lambda}_k^H + \sigma^2\mathbf{I};\ \ \mathbf{P} = E[\mathbf{z}(i)\mathbf{b}^H(i)] = (1/\sqrt{N_c})\mathbf{\Lambda}_k\mathbf{I}_{\rm e}. \tag{5.19}$$

Expanding (5.18), the MMSE solution can be expressed as

$$\mathbf{W}_{\rm MMSE} = \left(\frac{1}{N_c}\sum_{k=1}^{K}\mathbf{\Lambda}_k\mathbf{I}_{\rm e}\mathbf{I}_{\rm e}^H\mathbf{\Lambda}_k^H + \sigma^2\mathbf{I}\right)^{-1}\frac{\mathbf{\Lambda}_k\mathbf{I}_{\rm e}}{\sqrt{N_c}} = \mathbf{V}\mathbf{I}_{\rm e}, \tag{5.20}$$

where the M-by-M matrix $\mathbf{V}$ is

$$\mathbf{V} = \frac{1}{\sqrt{N_c}}\left(\frac{1}{N_c}\sum_{k=1}^{K}\mathbf{\Lambda}_k\mathbf{I}_{\rm e}\mathbf{I}_{\rm e}^H\mathbf{\Lambda}_k^H + \sigma^2\mathbf{I}\right)^{-1}\mathbf{\Lambda}_k. \tag{5.21}$$

Note that the matrix $\mathbf{V}$ can be expressed as N_c-by-N_c block matrices $\mathbf{v}_{ij}$, $i,j \in \{1, N_c\}$, each $\mathbf{v}_{ij}$ is a N-by-N diagonal matrix. Hence, we take a closer look at the product of $\mathbf{V}$ and $\mathbf{I}_{\rm e}$:

$$\begin{aligned}\mathbf{V}\mathbf{I}_e &= \begin{bmatrix}\mathbf{v}_{1,1} & \mathbf{v}_{1,2} & \cdots & \mathbf{v}_{1,N_c}\\ \mathbf{v}_{2,1} & \mathbf{v}_{2,2} & \cdots & \mathbf{v}_{2,N_c}\\ \vdots & \vdots & \vdots & \vdots\\ \mathbf{v}_{N_c,1} & \mathbf{v}_{N_c,2} & \cdots & \mathbf{v}_{N_c,N_c}\end{bmatrix}\begin{bmatrix}\mathbf{I}_N\\ \mathbf{I}_N\\ \vdots\\ \mathbf{I}_N\end{bmatrix} = \begin{bmatrix}\sum_{j=1}^{N_c}\mathbf{v}_{1,j}\\ \sum_{j=1}^{N_c}\mathbf{v}_{2,j}\\ \vdots\\ \sum_{j=1}^{N_c}\mathbf{v}_{N_c,j}\end{bmatrix}\\ &= \begin{bmatrix}\hat{\mathbf{w}}_1 & & & \\ & \hat{\mathbf{w}}_2 & & \\ & & \ddots & \\ & & & \hat{\mathbf{w}}_{N_c}\end{bmatrix}\begin{bmatrix}\mathbf{I}_N\\ \mathbf{I}_N\\ \vdots\\ \mathbf{I}_N\end{bmatrix} = \hat{\mathbf{W}}\mathbf{I}_{\rm e},\end{aligned} \tag{5.22}$$

where $\hat{\mathbf{w}}_i = \sum_{j=1}^{N_c}\mathbf{v}_{i,j}$, $i = 1, \ldots, N_c$, are diagonal matrices. Hence, the product of $\mathbf{V}$ and $\mathbf{I}_{\rm e}$ can be converted into a product of a M-by-M ($M = N \times N_c$) diagonal matrix $\hat{\mathbf{W}}$ and $\mathbf{I}_{\rm e}$, where the entries of $\hat{\mathbf{W}}$ are $\hat{w}_l$, $l = 1, \ldots, M$, equals the sum of all entries in the l-th row of matrix $\mathbf{V}$. Finally, we express the MMSE design as

$$\mathbf{W}_{\rm MMSE} = \hat{\mathbf{W}}\mathbf{I}_{\rm e} = {\rm diag}(\hat{\mathbf{w}}_{\rm e})\mathbf{I}_{\rm e}, \tag{5.23}$$

where $\hat{\mathbf{w}}_{\rm e} = (\hat{w}_1, \hat{w}_2, \ldots, \hat{w}_M)$ is an equivalent filter with M taps.

The design of the MMSE filter in DA scheme can be expressed as either in (5.18) or (5.23). We remark that the expression shown in (5.23) enables us to design an M-dimensional adaptive filter rather than an M-by-N matrix form adaptive filter to estimate the MMSE solution. This simplification significantly reduced the complexity of this

scheme.

5.3 Adaptive Algorithms for SCE

In this section, we develop the LMS, RLS and CG adaptive algorithms for the frequency domain channel estimation in multiuser DS-UWB communications.

5.3.1 SCE-LMS

Substituting (5.5) and (5.6) into (5.3) and defining a diagonal matrix $\mathbf{X}_{\mathrm{a}}(i) = \mathrm{diag}[\mathbf{F}\sum_{\mathrm{k}=1}^{\mathrm{K}}\mathbf{x}_{\mathrm{k}}(\mathrm{i})]$, the rearranged frequency domain received signal becomes

$$\mathbf{z}(i) = \mathbf{X}_{\mathrm{a}}(i)\tilde{\mathbf{h}} + \mathbf{F}\mathbf{n}(i) = \mathbf{X}_{\mathrm{a}}(i)\mathbf{F}_{M,L}\mathbf{h}_{\mathrm{equ}} + \mathbf{F}\mathbf{n}(i). \tag{5.24}$$

In the SCE, we take into account the fact that the length of the equivalent CIR $\mathbf{h}_{\mathrm{equ}}$ is typically smaller than the received signal size [72]. For example, we assume that the DS-UWB channel in the time domain has 100 sample-spaced taps. This length of the standard channel contains more than 85 percent of the total energy and can be considered as an upper bound of the channel length. In the scenario where the received signal has a length of $M = 256$ chips and we assume that each chip was sampled 3 times, hence the length of the $\mathbf{h}_{\mathrm{equ}}$ is equal to $L = 34$ chips that is much smaller than M. As shown in (5.5), we can estimate the L-dimensional vector $\mathbf{h}_{\mathrm{equ}}$ rather than the M-dimensional vector $\tilde{\mathbf{h}}$. The SCE-LMS aims at minimizing the MSE cost function

$$\mathbf{J}_{\mathrm{SCE-LMS}}(\hat{\mathbf{h}}_{\mathrm{equ}}(i)) = E[||\mathbf{z}(i) - \mathbf{X}(i)\mathbf{F}_{M,L}\hat{\mathbf{h}}_{\mathrm{equ}}(i)||^2], \tag{5.25}$$

where the frequency domain received signal $\mathbf{z}(i)$ is shown in (5.24) and $\mathbf{X}(i) = \mathrm{diag}[\mathbf{F}\mathbf{x}(\mathrm{i})]$, $\mathbf{x}(i)$ is the pilot signal from the desired user. The gradient of (5.25) with respect to $\hat{\mathbf{h}}_{\mathrm{equ}}(i)$ is

$$\mathbf{g}_{\mathrm{h}}(i) = -E[\mathbf{F}_{M,L}^H\mathbf{X}^H(i)\mathbf{z}(i)] + E[\mathbf{F}_{M,L}^H\mathbf{X}^H(i)\mathbf{X}(i)\mathbf{F}_{M,L}]\hat{\mathbf{h}}_{\mathrm{equ}}(i), \tag{5.26}$$

This leads to the SCE-LMS algorithm

$$\hat{\mathbf{h}}_{\mathrm{equ}}(i+1) = \hat{\mathbf{h}}_{\mathrm{equ}}(i) + \mu_h\mathbf{F}_{M,L}^H\mathbf{X}^H(i)\mathbf{e}_{\mathrm{h}}(i), \tag{5.27}$$

where $\mathbf{e}_{\mathrm{h}}(i) = \mathbf{z}(i) - \mathbf{X}(i)\mathbf{F}_{M,L}\hat{\mathbf{h}}_{\mathrm{equ}}(i)$ denotes the L-dimensional error vector and the constant μ_h is the step size of the SCE-LMS algorithm.

5.3.2 SCE-RLS

The SCE-RLS algorithm is developed to minimize the least squares (LS) cost function

$$\mathbf{J}_{\mathrm{SCE-RLS}}(\hat{\mathbf{h}}_{\mathrm{equ}}(i)) = \sum_{j=1}^{i} \lambda_h^{i-j} \left|\left|\mathbf{z}(j) - \mathbf{X}(j)\mathbf{F}_{M,L}\hat{\mathbf{h}}_{\mathrm{equ}}(i)\right|\right|^2, \tag{5.28}$$

where λ_h is the forgetting factor. Computing the gradient of (5.28) with respect to $\hat{\mathbf{h}}_{\mathrm{equ}}(i)$ and setting it to zero, the LS solution is

$$\mathbf{h}_{\mathrm{equ,LS}}(i) = \mathbf{R}_{\mathrm{h}}^{-1}(i)\mathbf{p}_{\mathrm{h}}(i) \tag{5.29}$$

where

$$\mathbf{R}_{\mathrm{h}}(i) = \sum_{j=1}^{i} \lambda_h^{i-j}\mathbf{F}_{M,L}^H\mathbf{X}^H(j)\mathbf{X}(j)\mathbf{F}_{M,L} \;\; ; \;\; \mathbf{p}_{\mathrm{h}}(i) = \sum_{j=1}^{i} \lambda_h^{i-j}\mathbf{F}_{M,L}^H\mathbf{X}^H(j)\mathbf{z}(j).$$

Note that there is an inversion of an L-by-L matrix $\mathbf{R}_{\mathrm{h}}(i)$ in this solution. The matrix $\mathbf{R}_{\mathrm{h}}(i)$ can be computed in a recursive way via the recursion

$$\mathbf{R}_{\mathrm{h}}(i) = \lambda_h\mathbf{R}_h(i-1) + \mathbf{F}_{M,L}^H\mathbf{X}^H(i)\mathbf{X}(i)\mathbf{F}_{M,L}. \tag{5.30}$$

There is no recursive way to simplify the inversion of this matrix and hence, we apply the adaptation equation shown in [72], that is

$$\hat{\mathbf{h}}_{\mathrm{equ}}(i+1) = \hat{\mathbf{h}}_{\mathrm{equ}}(i) + \mathbf{R}_{\mathrm{h}}^{-1}(i)\mathbf{F}_{M,L}^H\mathbf{X}^H(i)\mathbf{e}_{\mathrm{h}}(i), \tag{5.31}$$

where $\mathbf{e}_{\mathrm{h}}(i) = \mathbf{z}(i) - \mathbf{X}(i)\mathbf{F}_{M,L}\hat{\mathbf{h}}_{\mathrm{equ}}(i)$ is the M-dimensional error vector. For the L-by-L matrix $\mathbf{R}_{\mathrm{h}}(i)$, computing its inverse matrix with Gauss-Jordan elimination requires L^3 of complex multiplications [80]. This problem makes the SCE-RLS a high complexity algorithm and for this reason the performance of the RLS algorithm has not been discussed in [72]. For this paper, our goal is to implement this approach and assess its performance against the performance of the proposed SCE-CG algorithm.

5.3.3 SCE-CG

The SCE-CG aims at minimizing the MSE cost function

$$\mathbf{J}_{\mathrm{SCE-CG}}(\hat{\mathbf{h}}_{\mathrm{equ}}(i)) = E[||\mathbf{z}(i) - \mathbf{X}(i)\mathbf{F}_{M,L}\hat{\mathbf{h}}_{\mathrm{equ}}(i)||^2], \tag{5.32}$$

where the frequency domain input signal $\mathbf{z}(i)$ is shown in (5.24) and $\mathbf{X}(i) = \mathrm{diag}[\mathbf{Fx(i)}]$, $\mathbf{x}(i)$ is the pilot signal from the desired user. The instantaneous estimate of the gradient of (5.32) with respect to $\hat{\mathbf{h}}_{\mathrm{equ}}(i)$ is

$$\hat{\mathbf{g}}_{\mathrm{h}}(i) = -\mathbf{F}_{M,L}^{H}\mathbf{X}^{H}(i)\mathbf{e}_{\mathrm{h}}(i), \tag{5.33}$$

where $\mathbf{e}_{\mathrm{h}}(i) = \mathbf{z}(i) - \mathbf{X}(i)\mathbf{F}_{M,L}\hat{\mathbf{h}}_{\mathrm{equ}}(i)$ denotes the error vector. For each input data vector, a number of iterations is required for the CG method. Let us denote the iteration index as c. For the $(c+1)$-th iteration, the estimated $\hat{\mathbf{h}}_{\mathrm{equ}}(i)$ is updated as

$$\hat{\mathbf{h}}_{\mathrm{equ,c+1}}(i) = \hat{\mathbf{h}}_{\mathrm{equ,c}}(i) + \alpha_{\mathrm{h,c}}(i)\mathbf{d}_{\mathrm{h,c}}(i), \tag{5.34}$$

where $\alpha_{\mathrm{h,c}}(i)$ is the optimum step size and $\mathbf{d}_{h,c}(i)$ is the direction vector for the c-th iteration. With the new estimator $\hat{\mathbf{h}}_{\mathrm{equ,c+1}}(i)$, the error vector is updated as

$$\begin{aligned}\mathbf{e}_{\mathrm{h,c+1}}(i) &= \mathbf{z}(i) - \mathbf{X}(i)\mathbf{F}_{M,L}\hat{\mathbf{h}}_{\mathrm{equ,c+1}}(i) \\ &= \mathbf{e}_{\mathrm{h,c}}(i) - \alpha_{\mathrm{h,c}}(i)\mathbf{X}(i)\mathbf{F}_{M,L}\mathbf{d}_{\mathrm{h,c}}(i).\end{aligned} \tag{5.35}$$

Since the direction vector $\mathbf{d}_{\mathrm{h,c}}(i)$ is orthogonal to the inverse gradient vector after the c-th iteration [28], we have

$$\mathbf{d}_{\mathrm{h,c}}^{H}(i)[-\hat{\mathbf{g}}_{\mathrm{h,c+1}}(i)] = 0, \tag{5.36}$$

where $\hat{\mathbf{g}}_{\mathrm{h,c+1}}(i) = -\mathbf{F}_{M,L}^{H}\mathbf{X}^{H}(i)\mathbf{e}_{\mathrm{h,c+1}}(i)$.

Substituting (5.35) into (5.36), we obtain the expression for the optimum step size

$$\alpha_{\mathrm{h,c}}(i) = \frac{-\mathbf{d}_{\mathrm{h,c}}^{H}(i)\hat{\mathbf{g}}_{\mathrm{h,c}}(i)}{\mathbf{d}_{\mathrm{h,c}}^{H}\mathbf{F}_{M,L}^{H}\mathbf{X}^{H}(i)\mathbf{X}(i)\mathbf{F}_{M,L}\mathbf{d}_{\mathrm{h,c}}(i)}. \tag{5.37}$$

In the CG methods, the direction vector for each iteration can be obtained by

$$\mathbf{d}_{\mathrm{h,c+1}}(i) = -\hat{\mathbf{g}}_{\mathrm{h,c+1}}(i) + \beta_{\mathrm{h,c}}\mathbf{d}_{\mathrm{h,c}}(i), \tag{5.38}$$

where the constant $\beta_{\mathrm{h,c}}$ is determined to fulfill the convergence requirement for the direction vectors that these vectors are mutually conjugate [27], [28], [31]. We adopt the

expression for $\beta_{\mathrm{h,c}}$ as in [28]

$$\beta_{\mathrm{h,c}} = \frac{\hat{\mathbf{g}}^H_{\mathrm{h,c+1}}(i)\hat{\mathbf{g}}_{\mathrm{h,c+1}}(i)}{-\mathbf{d}^H_{\mathrm{h,c}}(i)\hat{\mathbf{g}}_{\mathrm{h,c}}(i)}. \tag{5.39}$$

Substituting (5.38) into the term $\mathbf{d}^H_{\mathrm{h,c}}(i)\hat{\mathbf{g}}_{\mathrm{h,c}}(i)$ in (5.39) and taking the conjugate feature of the direction vectors into account, that is $\mathbf{d}^H_{\mathrm{h,c-1}}(i)\hat{\mathbf{g}}_{\mathrm{h,c}}(i) = 0$, we can find that

$$-\mathbf{d}^H_{\mathrm{h,c}}(i)\hat{\mathbf{g}}_{\mathrm{h,c}}(i) = \hat{\mathbf{g}}^H_{\mathrm{h,c}}(i)\hat{\mathbf{g}}_{\mathrm{h,c}}(i). \tag{5.40}$$

We remark that the relationship obtained in (5.40) can reduce the complexity of the SCE-CG algorithm by $\mathcal{O}(cL)$, where c is the number of iterations and L is the length of the equivalent CIR. This is because we have to compute the scalar term $\hat{\mathbf{g}}^H_{\mathrm{h,c+1}}(i)\hat{\mathbf{g}}_{\mathrm{h,c+1}}(i)$ in (5.39) for the c-th iteration. However, with the relationship shown in (5.40), this scalar term can be used directly in the $(c+1)$-th iteration to save the computation for the scalar term $-\mathbf{d}^H_{\mathrm{h,c+1}}(i)\hat{\mathbf{g}}_{\mathrm{h,c+1}}(i)$.

For the SCE scheme, the CG algorithm has lower computational complexity than the RLS algorithm while performing better than the LMS algorithm.

The proposed adaptive algorithms for the SCE scheme are summarized in the first column of Table 5.1.

5.4 Adaptive Algorithms for DA

In this section, we develop the LMS, RLS and CG adaptive algorithms for the DA scheme with the new signal model presented in section 5.2.3. For multiuser block transmission systems, these techniques can be implemented with a simple receiver structure.

5.4.1 DA-LMS

With the expression in (5.23), we can estimate the data vector as

$$\hat{\mathbf{b}}(i) = \mathbf{F}^H_N\mathbf{I}^H_{\mathrm{e}}\hat{\mathbf{W}}^H(i)\mathbf{z}(i) = \mathbf{F}^H_N\mathbf{I}^H_{\mathrm{e}}\hat{\mathbf{Z}}(i)\hat{\mathbf{w}}(i), \tag{5.41}$$

Tab. 5.1: Adaptive Algorithms For The Proposed Frequency domain Detection Schemes

SCE-Scheme	DA-Scheme
1. Initialization: $\hat{\mathbf{h}}_{\mathrm{equ}}(1) = L$-by-1 zero-vector For $\quad i = 1, 2, \ldots$	**1. Initialization:** $\hat{\mathbf{w}}(1) = M$-by-1 zero-vector For $\quad i = 1, 2, \ldots$
2.1 SCE-LMS $\mathbf{e}_{\mathrm{h}}(i) = \mathbf{z}(i) - \mathbf{X}(i)\mathbf{F}_{M,L}\hat{\mathbf{h}}_{\mathrm{equ}}(i)$ $\hat{\mathbf{h}}_{\mathrm{equ}}(i+1) = \hat{\mathbf{h}}_{\mathrm{equ}}(i) + \mu_h \mathbf{F}_{M,L}^H \mathbf{X}^H(i)\mathbf{e}_{\mathrm{h}}(i)$	**2.1 DA-LMS** $\mathbf{e}_{\mathrm{w}}(i) = \mathbf{b}(i) - \mathbf{Y}(i)\hat{\mathbf{w}}(i)$ $\hat{\mathbf{w}}(i+1) = \hat{\mathbf{w}}(i) + \mu_{\mathrm{w}} \mathbf{Y}^H(i)\mathbf{e}_{\mathrm{w}}(i)$
2.2 SCE-RLS $\mathbf{R}_{\mathrm{h}}(i) = \lambda_h \mathbf{R}_{\mathrm{h}}(i-1) + \mathbf{F}_{M,L}^H \mathbf{X}^H(i)\mathbf{X}(i)\mathbf{F}_{M,L}$ $\mathbf{e}_{\mathrm{h}}(i) = \mathbf{z}(i) - \mathbf{X}(i)\mathbf{F}_{M,L}\hat{\mathbf{h}}_{\mathrm{equ}}(i)$ $\hat{\mathbf{h}}_{\mathrm{equ}}(i+1) = \hat{\mathbf{h}}_{\mathrm{equ}}(i) + \mathbf{R}_{\mathrm{h}}^{-1}(i)\mathbf{F}_{M,L}^H \mathbf{X}^H(i)\mathbf{e}_{\mathrm{h}}(i)$	**2.2 DA-RLS** $\mathbf{R}_{\mathrm{w}}(i) = \lambda_w \mathbf{R}_{\mathrm{w}}(i-1) + \mathbf{Y}^H(i)\mathbf{Y}(i)$ $\mathbf{e}_{\mathrm{aw}}(i) = \mathbf{b}(i) - \mathbf{Y}(i)\hat{\mathbf{w}}(i)$ $\hat{\mathbf{w}}(i+1) = \hat{\mathbf{w}}(i) + \mathbf{R}_{\mathrm{w}}^{-1}(i)\mathbf{Y}^H(i)\mathbf{e}_{\mathrm{aw}}(i).$
2.3 SCE-CG **STEP 1: Initialization for iterations** $\hat{\mathbf{h}}_{\mathrm{equ},0}(i) = \hat{\mathbf{h}}_{\mathrm{equ}}(i),$ $\mathbf{e}_{\mathrm{h},0}(i) = \mathbf{z}(i) - \mathbf{X}(i)\mathbf{F}_{M,L}\hat{\mathbf{h}}_{\mathrm{equ},0}(i),$ $\mathbf{d}_{\mathrm{h},0}(i) = -\hat{\mathbf{g}}_{\mathrm{h},0}(i) = \mathbf{F}_{M,L}^H \mathbf{X}^H(i)\mathbf{e}_{\mathrm{h},0}(i).$ For $\quad c = 0, 1, 2, \ldots, (c_{\max} - 1)$ **STEP 2: Update the channel estimation:** $\alpha_{\mathrm{h,c}}(i) = \frac{\hat{\mathbf{g}}_{\mathrm{h,c}}^H(i)\hat{\mathbf{g}}_{\mathrm{h,c}}(i)}{\mathbf{d}_{\mathrm{h,c}}^H \mathbf{F}_{M,L}^H \mathbf{X}^H(i)\mathbf{X}(i)\mathbf{F}_{M,L}\mathbf{d}_{\mathrm{h,c}}(i)},$ $\hat{\mathbf{h}}_{\mathrm{equ,c+1}}(i) = \hat{\mathbf{h}}_{\mathrm{equ,c}}(i) + \alpha_{\mathrm{h,c}}(i)\mathbf{d}_{\mathrm{h,c}}(i),$ $\mathbf{e}_{\mathrm{h,c+1}}(i) = \mathbf{e}_{\mathrm{h,c}}(i) - \alpha_{\mathrm{h,c}}(i)\mathbf{X}(i)\mathbf{F}_{M,L}\mathbf{d}_{\mathrm{h,c}}(i),$ $\hat{\mathbf{g}}_{\mathrm{h,c+1}}(i) = -\mathbf{F}_{M,L}^H \mathbf{X}^H(i)\mathbf{e}_{\mathrm{h,c+1}}(i).$ **STEP 3: Adapt the direction vector:** $\beta_{\mathrm{h,c}} = \frac{\hat{\mathbf{g}}_{\mathrm{h,c+1}}^H(i)\hat{\mathbf{g}}_{\mathrm{h,c+1}}(i)}{\hat{\mathbf{g}}_{\mathrm{h,c}}^H(i)\hat{\mathbf{g}}_{\mathrm{h,c}}(i)},$ $\mathbf{d}_{\mathrm{h,c+1}}(i) = -\hat{\mathbf{g}}_{\mathrm{h,c+1}}(i) + \beta_{\mathrm{h,c}}\mathbf{d}_{\mathrm{h,c}}(i).$ $\hat{\mathbf{h}}_{\mathrm{equ}}(i+1) = \hat{\mathbf{h}}_{\mathrm{equ,c_{max}}}(i).$	**2.3 DA-CG** **STEP 1: Initialization for iterations** $\hat{\mathbf{w}}_0(i) = \hat{\mathbf{w}}(i),$ $\mathbf{e}_{\mathrm{w},0}(i) = \mathbf{b}(i) - \mathbf{Y}(i)\hat{\mathbf{w}}_0(i),$ $\mathbf{d}_{\mathrm{w},0}(i) = -\hat{\mathbf{g}}_{\mathrm{w},0}(i) = \mathbf{Y}^H(i)\mathbf{e}_{\mathrm{w},0}(i).$ For $\quad c = 0, 1, 2, \ldots, (c_{max} - 1)$ **STEP 2: Update the filter weights:** $\alpha_{\mathrm{w,c}}(i) = \frac{\hat{\mathbf{g}}_{\mathrm{w,c}}^H(i)\hat{\mathbf{g}}_{\mathrm{w,c}}(i)}{\mathbf{d}_{\mathrm{w,c}}^H \mathbf{Y}^H(i)\mathbf{Y}(i)\mathbf{d}_{\mathrm{w,c}}(i)},$ $\hat{\mathbf{w}}_{c+1}(i) = \hat{\mathbf{w}}_c(i) + \alpha_{\mathrm{w,c}}(i)\mathbf{d}_{\mathrm{w,c}}(i),$ $\mathbf{e}_{\mathrm{w,c+1}}(i) = \mathbf{e}_{\mathrm{w,c}}(i) - \alpha_{\mathrm{w,c}}(i)\mathbf{Y}(i)\mathbf{d}_{\mathrm{w,c}}(i),$ $\hat{\mathbf{g}}_{\mathrm{w,c+1}}(i) = -\mathbf{Y}^H(i)\mathbf{e}_{\mathrm{w,c+1}}(i).$ **STEP 3: Adapt the direction vector:** $\beta_{\mathrm{w,c}} = \frac{\hat{\mathbf{g}}_{\mathrm{w,c+1}}^H(i)\hat{\mathbf{g}}_{\mathrm{w,c+1}}(i)}{\hat{\mathbf{g}}_{\mathrm{w,c}}^H(i)\hat{\mathbf{g}}_{\mathrm{w,c}}(i)},$ $\mathbf{d}_{\mathrm{w,c+1}}(i) = -\hat{\mathbf{g}}_{\mathrm{w,c+1}}(i) + \beta_{\mathrm{w,c}}\mathbf{d}_{\mathrm{w,c}}(i).$ $\hat{\mathbf{w}}(i+1) = \hat{\mathbf{w}}_{\mathrm{c_{max}}}(i)$
3. Estimate the data vector $\mathbf{\Lambda}_{\mathrm{H}}(i) = \mathrm{diag}\left(\mathbf{F}_{M,L}\hat{\mathbf{h}}_{\mathrm{equ}}(i)\right),$ $\hat{\mathbf{C}}(i) = \left(\frac{\hat{K}}{N_c}\mathbf{\Lambda}_{\mathrm{H}}(i)\mathbf{\Lambda}_{\mathrm{H}}^H(i) + \hat{\sigma}_e^2 \mathbf{I}_{\mathrm{M}}\right)^{-1}\mathbf{\Lambda}_{\mathrm{H}}$ $\hat{\mathbf{b}}_r(i) = \mathrm{sign}(\Re(\mathbf{D}^{\mathrm{H}}\mathbf{F}^{\mathrm{H}}\hat{\mathbf{C}}(i)\mathbf{z}(i))).$	**3. Estimate the data vector** $\hat{\mathbf{b}}_r(i) = \mathrm{sign}(\Re(\mathbf{Y}(i)\hat{\mathbf{w}}(i))).$

where $\hat{\mathbf{Z}}(i) = \mathrm{diag}(\mathbf{z}(i))$ and $\hat{\mathbf{w}}(i) = \hat{\mathbf{w}}_{\mathrm{e}}^{*}(i)$ is the adaptive filter weight vector. Since $\mathbf{F}_N$ and $\mathbf{I}_{\mathrm{e}}$ are fixed, we consider the equivalent N-by-M received data matrix as

$$\mathbf{Y}(i) = \mathbf{F}_N^H \mathbf{I}_{\mathrm{e}}^H \hat{\mathbf{Z}}(i), \tag{5.42}$$

and express the estimated data vector as

$$\hat{\mathbf{b}}(i) = \mathbf{Y}(i)\hat{\mathbf{w}}(i). \tag{5.43}$$

Hence, the cost function for developing the DA-LMS algorithm can be expressed as

$$\mathbf{J}_{\mathrm{DA-LMS}}(\hat{\mathbf{w}}(i)) = E[||\mathbf{b}(i) - \mathbf{Y}(i)\hat{\mathbf{w}}(i)||^2]. \tag{5.44}$$

The gradient of (5.44) with respect to $\hat{\mathbf{w}}(i)$ is

$$\mathbf{g}_{\mathrm{w}}(i) = -E[\mathbf{Y}^H(i)\mathbf{b}(i)] + E[\mathbf{Y}^H(i)\mathbf{Y}(i)]\mathbf{w}(i).$$

Using the instantaneous estimates of the expected values in the gradient, we obtain the DA-LMS as

$$\hat{\mathbf{w}}(i+1) = \hat{\mathbf{w}}(i) + \mu_{\mathrm{w}}\mathbf{Y}^H(i)\mathbf{e}_{\mathrm{w}}(i), \tag{5.45}$$

where $\mathbf{e}_{\mathrm{w}}(i) = \mathbf{b}(i) - \mathbf{Y}(i)\hat{\mathbf{w}}(i)$ is the N-dimensional error vector and μ_{w} is the step size for DA-LMS.

5.4.2 DA-RLS

The DA-RLS algorithm is developed to minimize the least square (LS) cost function

$$\mathbf{J}_{\mathrm{DA-RLS}}(\hat{\mathbf{w}}(i)) = \sum_{j=1}^{i} \lambda_w^{i-j} \left|\left|\mathbf{b}(j) - \mathbf{Y}(j)\hat{\mathbf{w}}(i)\right|\right|^2, \tag{5.46}$$

where λ_w is the forgetting factor. Computing the gradient of (5.46) with respect to $\hat{\mathbf{w}}(i)$ and setting it to zero, the LS solution is

$$\mathbf{w}_{\mathrm{LS}}(i) = \mathbf{R}_{\mathrm{w}}^{-1}(i)\mathbf{p}_{\mathrm{w}}(i), \tag{5.47}$$

where $\mathbf{R}_{\mathrm{w}}(i) = \sum_{j=1}^{i} \lambda_w^{i-j}\mathbf{Y}^H(j)\mathbf{Y}(j)$ and $\mathbf{p}_{\mathrm{w}}(i) = \sum_{j=1}^{i} \lambda_w^{i-j}\mathbf{Y}^H(j)\mathbf{b}(j)$. We can express the M-by-M (where $M = NN_c$) matrix $\mathbf{R}_{\mathrm{w}}(i)$ and the M-dimensional vector $\mathbf{p}_{\mathrm{w}}(i)$ recursively as

$$\mathbf{R}_{\mathrm{w}}(i) = \lambda_w \mathbf{R}_{\mathrm{w}}(i-1) + \mathbf{Y}^H(i)\mathbf{Y}(i), \tag{5.48}$$

$$\mathbf{p}_{\mathrm{w}}(i) = \lambda_w \mathbf{p}_{\mathrm{w}}(i-1) + \mathbf{Y}^H(i)\mathbf{b}(i). \tag{5.49}$$

With the expression of the received data matrix shown in (5.42), we can explore the structure of the matrix $\mathbf{R}_{\mathrm{w}}(i)$, since

$$\mathbf{Y}^H(i)\mathbf{Y}(i) = \hat{\mathbf{Z}}^H(i)\mathbf{I}_{\mathrm{e}}\mathbf{F}_N\mathbf{F}_N^H\mathbf{I}_{\mathrm{e}}^H\hat{\mathbf{Z}}(i) = \hat{\mathbf{Z}}^H(i)\left(\mathbf{I}_{\mathrm{e}}\mathbf{I}_{\mathrm{e}}^H\right)\hat{\mathbf{Z}}(i), \tag{5.50}$$

the M-by-M sparse matrix $\left(\mathbf{I}_{\mathrm{e}}\mathbf{I}_{\mathrm{e}}^H\right)$ is structured with N_c-by-N_c block matrices and each block matrix is an N-by-N identity matrix. Bearing in mind that the matrix $\hat{\mathbf{Z}}(i)$ is a diagonal matrix, we conclude that $\mathbf{R}_{\mathrm{w}}(i)$ is an M-by-M symmetric sparse matrix which consists of N_c-by-N_c block matrices and each block matrix is an N-by-N diagonal matrix. The number of nonzero elements in $\mathbf{R}_{\mathrm{w}}(i)$ equals MN_c. With Gauss-Jordan elimination [80], the inversion of each N-by-N diagonal matrix has the complexity $\mathcal{O}(N)$ and the inversion of N_c-by-N_c such block matrices requires the complexity $\mathcal{O}(NN_c^3)$, which equals $\mathcal{O}(MN_c^2)$. Hence, for the single user case, where $N_c = 1$, the complexity of computing $\mathbf{R}_{\mathrm{w}}^{-1}(i)$ is only $\mathcal{O}(M)$. In addition, equation (5.50) shows that the complexity of the recursion to obtain $\mathbf{R}_{\mathrm{w}}(i)$ is low. Since the matrix $\left(\mathbf{I}_{\mathrm{e}}\mathbf{I}_{\mathrm{e}}^H\right)$ can be pre-stored at the receiver, for each time instant, the computation complexity to obtain $\mathbf{R}_{\mathrm{w}}(i)$ is only $\mathcal{O}(MN_c)$. With these properties, we can investigate a low-complexity RLS algorithm to update the filter vector recursively. In order to obtain such a recursion, we apply the method that is proposed in the appendix B in [72]. We have the relationship

$$\mathbf{R}_{\mathrm{w}}(i)\hat{\mathbf{w}}(i+1) = \mathbf{p}_{\mathrm{w}}(i). \tag{5.51}$$

Replacing $\hat{\mathbf{w}}(i+1)$ with $[\hat{\mathbf{w}}(i+1) - \hat{\mathbf{w}}(i) + \hat{\mathbf{w}}(i)]$ in (5.51) and using (5.48) and (5.49) obtains

$$\mathbf{R}_{\mathrm{w}}(i)[\hat{\mathbf{w}}(i+1) - \hat{\mathbf{w}}(i)] + [\lambda_w \mathbf{R}_{\mathrm{w}}(i-1) + \mathbf{Y}^H(i)\mathbf{Y}(i)]\hat{\mathbf{w}}(i) = \lambda_w \mathbf{p}_{\mathrm{w}}(i-1) + \mathbf{Y}^H(i)\mathbf{b}(i). \tag{5.52}$$

Since $\mathbf{R}_{\mathrm{w}}(i-1)\hat{\mathbf{w}}(i) = \mathbf{p}_{\mathrm{w}}(i-1)$, (5.52) becomes

$$\mathbf{R}_{\mathrm{w}}(i)[\hat{\mathbf{w}}(i+1) - \hat{\mathbf{w}}(i)] = \mathbf{Y}^H(i)\mathbf{e}_{\mathrm{aw}}(i), \tag{5.53}$$

where $\mathbf{e}_{\mathrm{aw}}(i) = \mathbf{b}(i) - \mathbf{Y}(i)\hat{\mathbf{w}}(i)$ is the N-dimensional error vector. Finally, the recursion for updating the filter vector is

$$\hat{\mathbf{w}}(i+1) = \hat{\mathbf{w}}(i) + \mathbf{R}_{\mathrm{w}}^{-1}(i)\mathbf{Y}^H(i)\mathbf{e}_{\mathrm{aw}}(i). \tag{5.54}$$

We remark that the DA-RLS only consists of (5.48) and (5.54). The complexity of this algorithm is only $\mathcal{O}(MN_c^2)$, which is comparable to the DA-CG in multiuser scenarios and for the single user scenario where $N_c = 1$, it reduces to the level of the DA-LMS.

5.4.3 DA-CG

The cost function for developing a CG algorithm for the DA scheme can be expressed as

$$\mathbf{J}_{\mathrm{DA-CG}}(\hat{\mathbf{w}}(i)) = E[||\mathbf{b}(i) - \mathbf{Y}(i)\hat{\mathbf{w}}(i)||^2]. \tag{5.55}$$

The gradient of (5.55) with respect to $\hat{\mathbf{w}}(i)$ is

$$\mathbf{g}_{\mathrm{w}}(i) = -E[\mathbf{Y}^H(i)\mathbf{b}(i)] + E[\mathbf{Y}^H(i)\mathbf{Y}(i)]\hat{\mathbf{w}}(i).$$

We can use the instantaneous estimates of the expected values and obtain an estimate of the gradient vector as

$$\hat{\mathbf{g}}_{\mathrm{w}}(i) = -\mathbf{Y}^H(i)\mathbf{e}_{\mathrm{w}}(i), \tag{5.56}$$

where $\mathbf{e}_{\mathrm{w}}(i) = \mathbf{b}(i) - \mathbf{Y}(i)\hat{\mathbf{w}}(i)$ is the error vector. Here, we also define the iteration index as c. For the $(c+1)$-th iteration, the error vector is

$$\mathbf{e}_{\mathrm{w,c+1}}(i) = \mathbf{b}(i) - \mathbf{Y}(i)\hat{\mathbf{w}}_{\mathrm{c+1}}(i), \tag{5.57}$$

where the filter weight vector is updated as

$$\hat{\mathbf{w}}_{\mathrm{c+1}}(i) = \hat{\mathbf{w}}_{\mathrm{c}}(i) + \alpha_{\mathrm{w,c}}(i)\mathbf{d}_{\mathrm{w,c}}(i), \tag{5.58}$$

where $\mathbf{d}_{\mathrm{w,c}}(i)$ is the direction vector at the c-th iteration. The step size $\alpha_{\mathrm{w,c}}(i)$ is determined to minimize the cost function (5.55) [28], [31]. Substituting (5.58) in (5.57), the error vector can be expressed as

$$\mathbf{e}_{\mathrm{w,c+1}}(i) = \mathbf{e}_{\mathrm{w,c}}(i) - \alpha_{\mathrm{w,c}}(i)\mathbf{Y}(i)\mathbf{d}_{\mathrm{w,c}}(i). \tag{5.59}$$

Since the direction vector $\mathbf{d}_{\mathrm{w,c}}(i)$ is orthogonal to the inverse gradient vector after the c-th iteration [28], we have $\mathbf{d}^H_{\mathrm{w,c}}(i)[-\hat{\mathbf{g}}_{\mathrm{w,c+1}}(i)] = 0$, where $\hat{\mathbf{g}}_{\mathrm{w,c+1}}(i) = -\mathbf{Y}^H(i)\mathbf{e}_{\mathrm{w,c+1}}(i)$. Hence, from (5.59), the optimum step size is

$$\alpha_{\mathrm{w,c}}(i) = \frac{-\mathbf{d}^H_{\mathrm{w,c}}(i)\hat{\mathbf{g}}_{\mathrm{w,c}}(i)}{\mathbf{d}^H_{\mathrm{w,c}}\mathbf{Y}^H(i)\mathbf{Y}(i)\mathbf{d}_{\mathrm{w,c}}(i)}. \tag{5.60}$$

The adaptation equation for the direction vector can be expressed as

$$\mathbf{d}_{\mathrm{w,c+1}}(i) = -\hat{\mathbf{g}}_{\mathrm{w,c+1}}(i) + \beta_{\mathrm{w,c}}\mathbf{d}_{\mathrm{w,c}}(i), \tag{5.61}$$

where the constant $\beta_{\mathrm{w,c}}$ is determined to fulfill the convergence requirement for the direction vectors that these vectors are mutually conjugate [27], [28], [31]. We adopt the

Tab. 5.2: Complexity analysis for the frequency domain adaptive algorithms

Algorithm	Complex Additions	Complex Multiplications
SCE-LMS	$2ML$	$2ML + 2M + L$
SCE-RLS	$2L^3 + 2ML - 2L^2$	$2L^3 + 3ML + (2+M)L^2$
SCE-CG	$(2ML + M + 3L - 3)c$	$(2ML + 4M + 4L + 1)c$
DA-LMS	$2MN$	$2MN + N$
DA-RLS	$M(N_c^2 + 2N_c + 2N - 2)$	$M(N_c^2 + 6N_c + 2N - 1)$
DA-CG	$(2MN + 2M - 2)c$	$(2MN + 2M + N + 2)c$

expression for $\beta_{\mathrm{w,c}}$ as in [28]

$$\beta_{\mathrm{w,c}} = \frac{\hat{\mathbf{g}}_{\mathrm{w,c+1}}^H(i)\hat{\mathbf{g}}_{\mathrm{w,c+1}}(i)}{-\mathbf{d}_{\mathrm{w,c}}^H(i)\hat{\mathbf{g}}_{\mathrm{w,c}}(i)}, \tag{5.62}$$

If we substitute (5.61) into the term $\mathbf{d}_{\mathrm{w,c}}^H(i)\hat{\mathbf{g}}_{\mathrm{w,c}}(i)$ in (5.62) and take the conjugate feature of the direction vectors into account, we can find that

$$-\mathbf{d}_{\mathrm{w,c}}^H(i)\hat{\mathbf{g}}_{\mathrm{w,c}}(i) = \hat{\mathbf{g}}_{\mathrm{w,c}}^H(i)\hat{\mathbf{g}}_{\mathrm{w,c}}(i). \tag{5.63}$$

As explained for (5.40), the relationship obtained in (5.63) can save the computational complexity by $\mathcal{O}(cM)$ for the DA-CG algorithm, where c is the number of iterations and M is the length of the received signal.

The proposed adaptive algorithms for the DA scheme are summarized in the second column of Table 5.1.

5.5 Complexity Analysis

In this section, we discuss the complexity of the proposed adaptive algorithms and the detection schemes.

Table 5.2 shows the complexity for the proposed algorithms with respect to the number of complex additions and complex multiplications for each time instant, where M is the length of the received signal, N is the length of the data block and L is the length of the equivalent CIR. For the CG algorithms, the iteration number is denoted as c, which is much smaller than M, say $M = 256$, $c = 8$. In this work, the complexity of the FFT and IFFT, which is $\mathcal{O}(M\log_2 M)$, is common to all the techniques and is not shown in this table.

It is important to note that for the adaptive algorithms in the SCE scheme, the complexity is determined by M and L, while in the DA scheme it is determined by M and N, bearing in mind that the spreading gain N_c equals M/N. Hence, we compare the complexity of the algorithms with the system parameters that will be used in the simulation section, say $L = 34$ and $N = 32$, with different spreading gain N_c (which leads to different received signal length M, since $M = N_c N$). Fig. 5.2 shows the number of complex multiplications for adaptive algorithms versus different spreading gains. The complexity of the CG algorithms with iteration number of 2 and 8 are shown in this figure for comparison. With these system parameters, the SCE-LMS has a similar complexity to the DA-LMS, and the SCE-CG has a similar complexity to the DA-CG. However, the SCE-RLS is the most complex adaptive algorithm while the DA-RLS has much lower complexity. For the SCE scheme, the SCE-CG algorithm is significantly simpler than the SCE-RLS. It will be illustrated by the simulation results that with 8 iterations, the performance of the SCE-CG algorithm is very close to the SCE-RLS. For the DA scheme, in the single user scenario where $N_c = 1$, the DA-RLS has the same complexity level as the DA-LMS. In the multiuser case, the complexity of the DA-RLS is comparable to the DA-CG. With small spreading gains, the DA-RLS has lower complexity than the DA-CG with only 2 iterations. However, the complexity of the DA-RLS will be boosted when the spreading gain increases. It will be illustrated by simulations that the performance of the DA-CG is comparable to the DA-RLS, hence, for multiuser scenarios with different values of N_c, the designer can choose either RLS or CG for the DA scheme.

After discussing the complexity of the adaptive algorithms, let us consider the complexity of the detection schemes. For the DA scheme, where only one adaptive filter is implemented and the complexity shown in Table 5.2 can be considered as the whole scheme's complexity. However, for the SCE scheme, the complexity shown in the table is only for the adaptive channel estimation. The complexity of estimating the noise variance $\mathcal{O}(ML^2)$, the number of active users $\mathcal{O}(M)$, performing the MMSE detection $\mathcal{O}(M)$ and the time domain despreading $\mathcal{O}(N^2)$ should also be included. Hence, we conclude that the DA scheme is simpler than the SCE scheme in both structure and the computational complexity. However, the SCE scheme, which will be shown later, has better performance than the DA scheme.

5.6 Noise Variance and Number of Active Users Estimation

For the SCE scheme, the MMSE detector is generated as (5.10), which requires the knowledge of the noise variance σ_e^2 and the number of active users K. In this section,

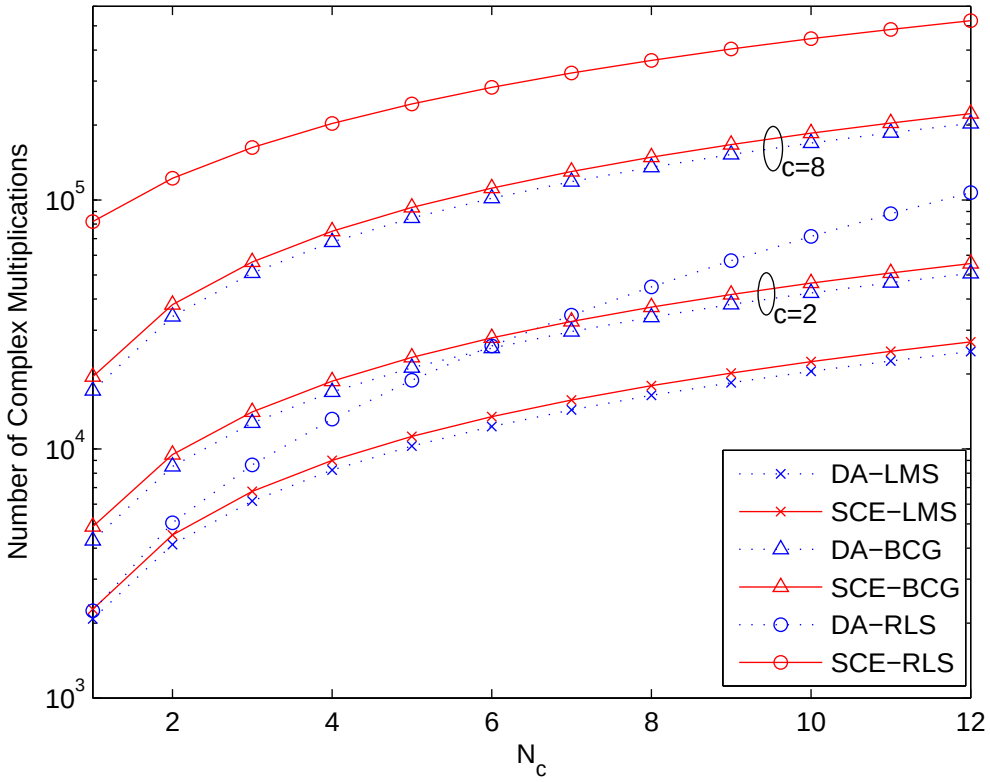

Fig. 5.2: Complexity comparison of the proposed schemes for SC-FDE.

we propose an ML estimation algorithm that extends [72] for estimating σ_e^2 in the DS-UWB system. We consider multiuser communication and the pilot sequence is generated randomly for each time instant.

The most popular active users number detection schemes for symbol by symbol transmission systems that are based on the eigenvalue decomposition have been proposed in [81]- [83]. These schemes have very high complexity and require high SNR to work in our block transmission system. In this work, we propose a simple approach to estimate the number of users based on the idea that the power of the received signal will reflect the number of active users. So firstly, we develop the relationship between the received signal power, the noise variance, the estimated channel coefficients and the number of active users. Then we obtain a simple algorithm to estimate K with these relationships.

5.6.1 Noise Variance Estimation

Revisiting (5.24), we have the frequency domain received signal as

$$\mathbf{z}(i) = \mathbf{X}_{\mathrm{a}}(i)\mathbf{F}_{M,L}\mathbf{h}_{\mathrm{equ}} + \mathbf{F}\mathbf{n}(i), \tag{5.64}$$

where the diagonal matrix $\mathbf{X}_{\mathrm{a}}(i) = \mathrm{diag}[\sum_{\mathrm{k}=1}^{\mathrm{K}} \mathbf{F}\mathbf{x}_{\mathrm{k}}(\mathrm{i})]$. We assume that the first user is the desired user and define $\mathbf{X}(i) = \mathrm{diag}[\mathbf{F}\mathbf{x}(\mathrm{i})]$. The uncorrelated additive noise is assumed to be Gaussian distributed with zero mean and variance of σ_e^2. The ML estimator aims at estimating $\sigma_e^2(i)$ and $\mathbf{h}_{\mathrm{equ}}(i)$ by maximizing the log-likelihood function, that is

$$\left[\hat{\sigma}_e^2(i), \hat{\mathbf{h}}_{\mathrm{equ}}(i)\right] = \arg \max_{\sigma_e^2(i), \mathbf{h}_{\mathrm{equ}}(i)} \mathbf{\Lambda}(\sigma_e^2(i), \mathbf{h}_{\mathrm{equ}}(i)), \tag{5.65}$$

where

$$\mathbf{\Lambda}(\sigma_e^2(i), \mathbf{h}_{\mathrm{equ}}(i)) = -M\ln(\sigma_e^2(i)) - \frac{\|\mathbf{z}(i) - \mathbf{B}(i)\mathbf{h}_{\mathrm{equ}}(i)\|^2}{\sigma_e^2(i)}, \tag{5.66}$$

where $\mathbf{B}(i) = \mathbf{X}(i)\mathbf{F}_{M,L}$. To solve this joint optimization problem, we firstly fix $\sigma_e^2(i)$ and find the optimum $\hat{\mathbf{h}}_{\mathrm{equ}}(i)$. By calculating the gradient of (5.66) with respect to $\mathbf{h}_{\mathrm{equ}}(i)$ and setting it to zero, we obtain

$$\hat{\mathbf{h}}_{\mathrm{equ,ML}}(i) = \left(\mathbf{B}^H(i)\mathbf{B}(i)\right)^{-1}\mathbf{B}^H(i)\mathbf{z}(i). \tag{5.67}$$

Substituting (5.67) into (5.66), and calculating the gradient of (5.66) with respect to $\sigma_e^2(i)$ and setting it to zero, we obtain the ML estimate of $\sigma_e^2(i)$

$$\hat{\sigma}_{e,\mathrm{ML}}^2(i) = \frac{1}{M}\left\|\mathbf{z}(i) - \mathbf{B}(i)\hat{\mathbf{h}}_{\mathrm{equ,ML}}(i)\right\|^2. \tag{5.68}$$

In the training stage of the SCE scheme, we estimate the noise variance via (5.67) and (5.68), where the number of complex multiplications required is $ML^2 + L^3 + 2ML + L^2 + M + 1$. The cost of this estimator is high and it is possible to obtain a simplified estimate with the complexity of $\mathcal{O}(ML)$ by replacing the ML estimate $\hat{\mathbf{h}}_{\mathrm{equ,ML}}(i)$ with the estimated channel $\hat{\mathbf{h}}_{\mathrm{equ}}(i)$ that is obtained in section 5.3. However, this will introduce noticeable degradation of the estimation performance in multiuser scenarios. Since in our SCE scheme, the noise variance estimator is used for both users number estimation and the MMSE detection, the degradation of the $\hat{\sigma}^2$ will affect the final performance.

5.6.2 Number of Active Users Estimation

In order to obtain the relationship of the active users number and the received signal power, let us consider the expected value of the frequency domain received signal power

$$\begin{aligned} E[\mathbf{z}^H(i)\mathbf{z}(i)] &= E\left[\left(\mathbf{X}_{\mathrm{a}}(i)\tilde{\mathbf{h}} + \mathbf{F}\mathbf{n}(i)\right)^H \left(\mathbf{X}_{\mathrm{a}}(i)\tilde{\mathbf{h}} + \mathbf{F}\mathbf{n}(i)\right)\right] \\ &= \tilde{\mathbf{h}}^H E[\mathbf{X}_{\mathrm{a}}^H(i)\mathbf{X}_{\mathrm{a}}(i)]\tilde{\mathbf{h}} + \sigma_e^2 M, \end{aligned} \tag{5.69}$$

where $\mathbf{z}(i)$ is shown in (5.24). Since the M-by-M diagonal matrix $\mathbf{X}_{\mathrm{a}}(i) = \mathrm{diag}[\mathbf{F}\sum_{\mathrm{k}=1}^{\mathrm{K}}\mathbf{x}_{\mathrm{k}}(i)]$, the l-th entry of the main diagonal can be expressed as

$$\mathrm{X}_{\mathrm{a},l}(i) = \mathbf{F}_l \sum_{k=1}^{K} \mathbf{x}_k(i), \tag{5.70}$$

where $l = 1, 2, \ldots, M$ and $\mathbf{F}_l$ is the l-th row of the DFT matrix $\mathbf{F}$. Bearing in mind the fact that $\mathbf{F}_l\mathbf{F}_l^H = 1$. Hence, the expected entry in (5.69) can be expressed as

$$E[\mathbf{X}_{\mathrm{a}}^H(i)\mathbf{X}_{\mathrm{a}}(i)] = \mathrm{diag}\left(\mathrm{E}[\mathrm{X}_{\mathrm{a},1}^2, \mathrm{X}_{\mathrm{a},2}^2, \ldots, \mathrm{X}_{\mathrm{a},M}^2]\right), \tag{5.71}$$

where

$$\begin{aligned} E\left[\mathrm{X}_{\mathrm{a},l}^2\right] &= E\left[\mathbf{F}_l \left(\sum_{k=1}^{K}\mathbf{x}_k(i)\right)\left(\sum_{k=1}^{K}\mathbf{x}_k(i)\right)^H \mathbf{F}_l^H\right] \\ &= E\left[\mathbf{F}_l\mathbf{D}_{\mathrm{all}}\mathbf{D}_{\mathrm{all}}^H\mathbf{F}_l^H\right] \approx \frac{K}{N_c}, \end{aligned} \tag{5.72}$$

where $\mathbf{D}_{\mathrm{all}}$ is shown in (5.9) and the approximation used here is the same as in (5.10), that is $\mathbf{D}_{\mathrm{all}}\mathbf{D}_{\mathrm{all}}^H \approx (K/N_c)\mathbf{I}_{\mathrm{M}}$.

Finally, substituting (5.71) into (5.69) with the approximation shown in (5.72), we obtain the relationship which can be expressed as

$$E[\mathbf{z}^H(i)\mathbf{z}(i)] \approx \frac{K}{N_c}\tilde{\mathbf{h}}^H\tilde{\mathbf{h}} + \sigma_e^2 M, \tag{5.73}$$

where K is the number of active users, σ_e^2 is the noise variance and $\tilde{\mathbf{h}}$ is the frequency domain channel coefficients. In this work, we have already obtained the estimator for σ_e^2 and $\mathbf{h}_{\mathrm{equ}}$. The expected received signal power can be estimated via time-averaging, that is

$$\hat{\mathrm{P}}_{\mathrm{r}}(i) = \frac{1}{T}\sum_{i=1}^{T}\mathbf{z}^H(i)\mathbf{z}(i). \tag{5.74}$$

Hence, the algorithm for estimating K can be expressed as

$$\hat{K}(i) = \left(\hat{\mathrm{P}}_{\mathrm{r}}(i) - \hat{\sigma}_e^2(i)M\right) \frac{N_c}{\hat{\mathrm{P}}_{\mathrm{h}}(i)}, \tag{5.75}$$

where

$$\hat{\mathrm{P}}_{\mathrm{h}}(i) = (\mathbf{F}_{M,L}\hat{\mathbf{h}}_{\mathrm{equ}}(i))^H(\mathbf{F}_{M,L}\hat{\mathbf{h}}_{\mathrm{equ}}(i)). \tag{5.76}$$

In order to obtain the integer estimated values, we can set $\hat{K}(i)$ to the nearest integer towards zero.

We remark that this proposed algorithm is efficient to estimate the number of active users in the downlink of our block data transmission system with very low complexity. The only parameter that is required to compute for this algorithm is the average received signal power.

5.7 Simulation Results

In this section, we apply the proposed SC-FDE schemes and algorithms to the downlink of a multiuser BPSK DS-UWB system. The pulse shape adopted in this work is the RRC pulse with the pulse-width $T_c = 0.375ns$. The length of the data block is set to $N = 32$ symbols. The Walsh spreading code with a spreading gain $N_c = 8$ is generated for the simulations and we assume that the maximum number of active users is 7. The channel has been simulated according to the standard IEEE 802.15.4a channel model for the NLOS indoor environment as shown in [23]. We assume that the channel is constant during the whole transmission and the time domain CIR has 100 taps. The sampling rate of the standard channel model is $8GHz$. The CP guard interval has the length of 35 chips, which has the equivalent length of 105 samples and it is enough to eliminate the IBI. The uncoded data rate of the communication is approximately $293\mathrm{Mbps}$. For all the simulations, the adaptive filters are initialized as null vectors. This allows a fair comparison between the analyzed techniques of their convergence performance. In practice, the filters can be initialized with *prior* knowledge about the spreading code or the channel to accelerate the convergence. All the curves are obtained by averaging 100 independent simulations.

The first experiment we perform is to compare the uncoded bit error rate (BER) performance of the proposed adaptive algorithms in SCE and DA schemes. We consider the scenario with a signal-to-noise ratio (SNR) of 16dB, 3 users, and 1000 training blocks. Fig.5.3 shows the BER performance of different algorithms as a function of blocks trans-

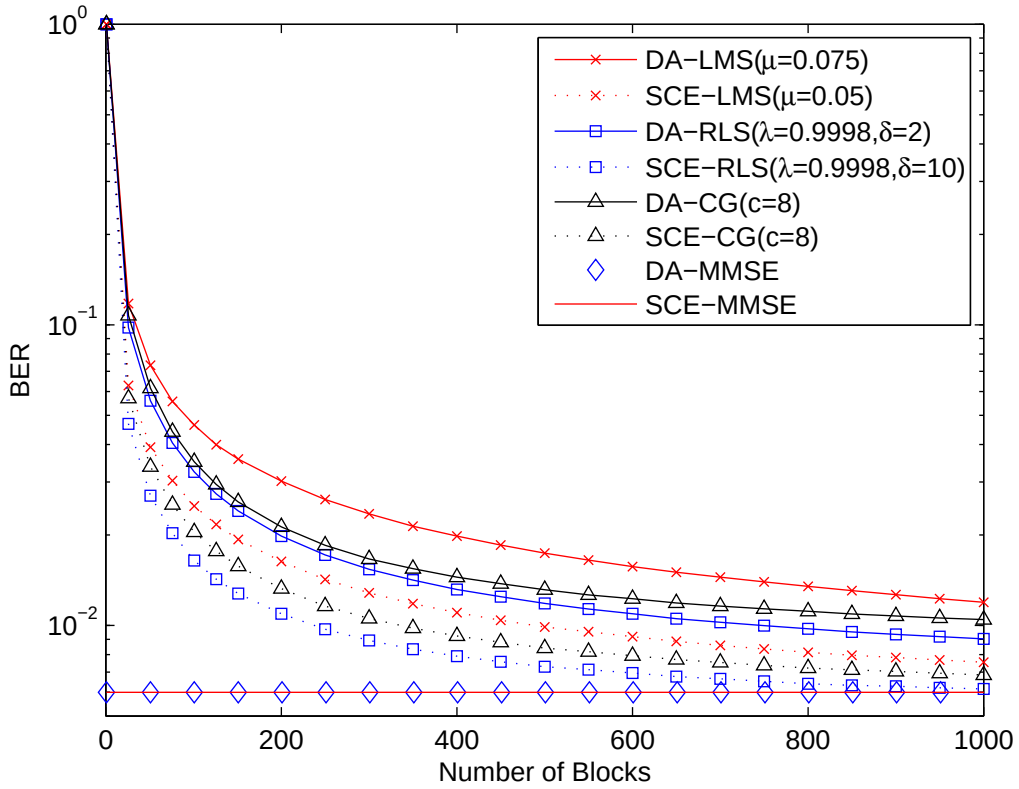

Fig. 5.3: BER performance of the proposed SC-FDE detection schemes versus the number of training blocks for a SNR=16dB. The number of users is 3.

mitted. In this experiment, the knowledge of the number of users K and the noise variance σ_e^2 are given for MMSE detection in the SCE scheme. It will be shown later, the perfectly known K and σ_e^2 does not produce significant improvements in the BER performance compared with using the estimated values. In both schemes, with only 8 iterations, the proposed CG algorithms outperform the LMS algorithms and perform close to the RLS algorithms. Since the filtering step in the SCE scheme which takes into the account that L is smaller than M provides some performance gain, the adaptive algorithms in SCE scheme performs better than in the DA scheme. However, the DA scheme has simpler structure and lower computational complexity. The MMSE curves are obtained with the knowledge of the channel, the spreading codes of all the users and the noise variance. It can be found that, the MMSE performances of the proposed schemes are exactly the same. This is because these two schemes can be considered as two different approaches to solve the same MMSE problem.

Fig.5.4 shows the performances of the ML estimators of the noise variance in different SNRs. For each SNR scenario, the estimated values of the noise variances for 1, 3 and 5 users are compared with the values in theory. For the multiuser case, the ML estimators

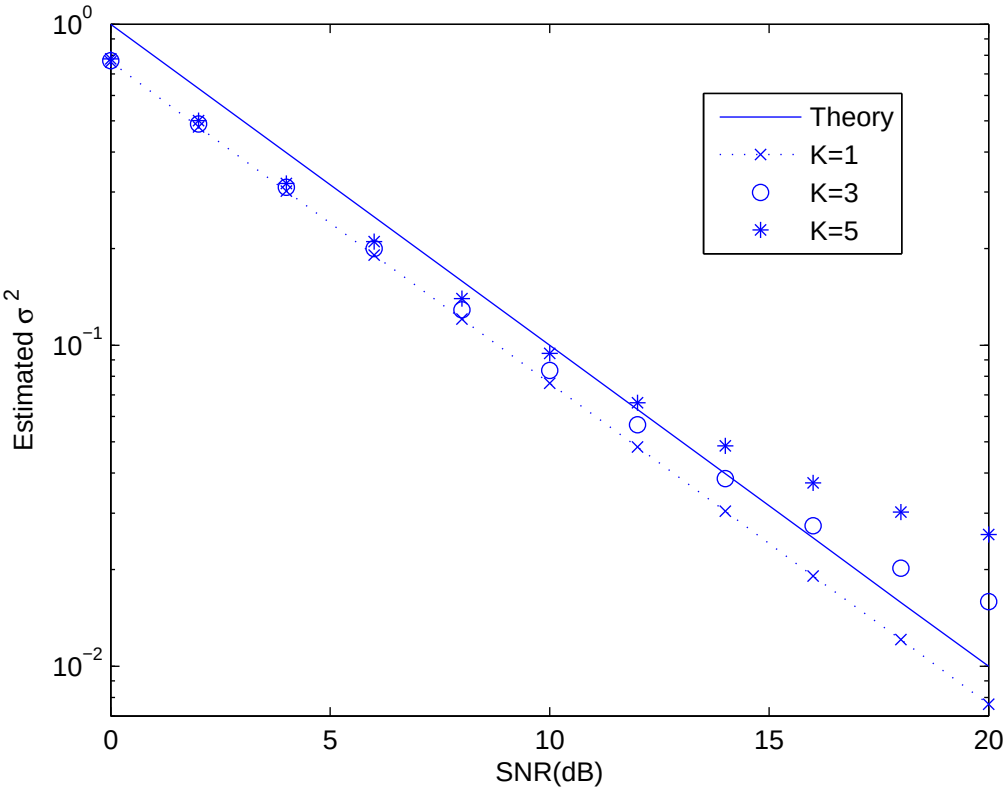

Fig. 5.4: Performance of the noise variance estimator.

are not very accurate in the high SNR environments. However, it will be demonstrated soon by simulations that this inaccuracy will only lead to very limited BER performance reduction.

Fig.5.5 illustrates the performance of the estimators of the number of active users in a $16dB$ environment with SCE-CG algorithm and we consider the multiuser cases of 2 to 4 users. The number of users is determined by the received signal power $\mathrm{P_r}(i)$, the noise variance $\sigma_e^2(i)$ and the channel power $\mathrm{P_h}(i)$ as shown in (5.75). Firstly, we show the performance of this estimator with the knowledge of $\sigma_e^2(i)$ and $\mathrm{P_h}(i)$. Because of an approximation used in (5.73), the values of the estimated users number have gaps to the real values. For example, in 2 and 3 users cases, these gaps are around 0.5 users. Secondly, we assess the performance of the users number estimator with the estimated noise variance $\hat{\sigma}_e^2(i)$ and the adaptive channel coefficients. It should be noted that the channel estimation is started with a null vector, which means very small $\hat{\mathrm{P}}_\mathrm{h}(i)$ at the beginning stage and this leads to very large $\hat{K}$. Hence, we set $\hat{K} = 7$ as an upper maximum for this estimator. The estimated values of $\hat{K}$ approaches the curves which are obtained with the knowledge of noise variance and the channel power. For the cases of 3 and 4 users, the curves fit

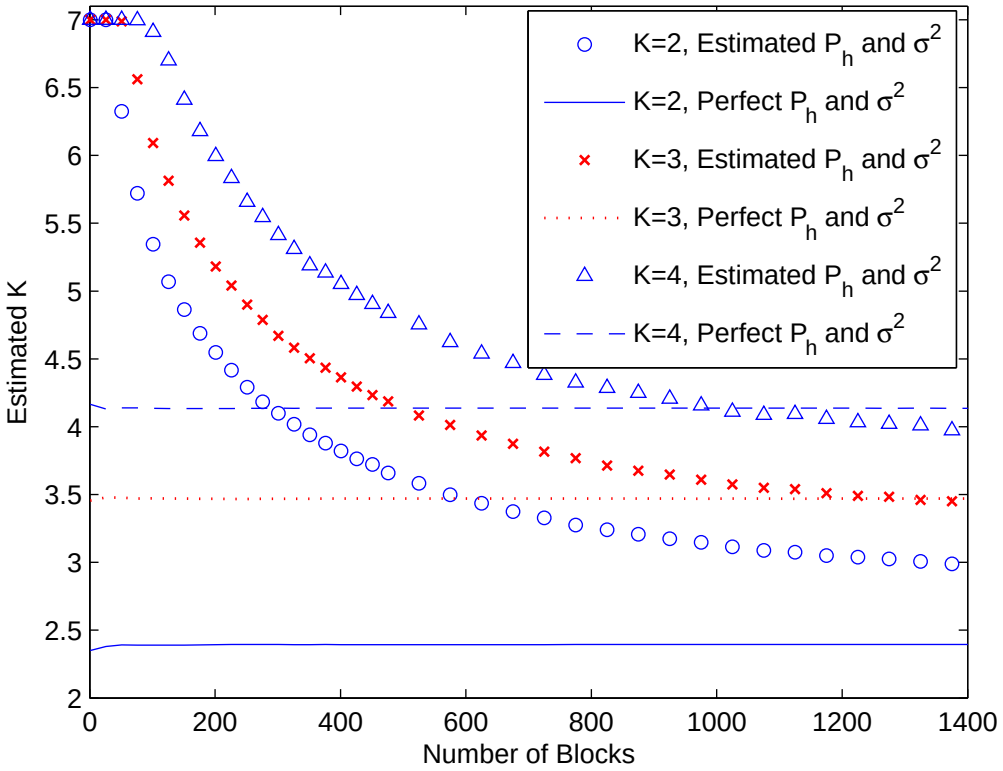

Fig. 5.5: Performance of the active users number estimator.

well but there is a mismatch when the users number is 2. This mismatch is caused by the estimation errors of $\hat{\sigma}_e^2(i)$ and $\hat{\mathrm{P}}_{\mathrm{h}}(i)$. However, later simulations will indicate that the mismatches introduced by the approximation and the estimation errors will not noticeably affect the BER performance.

Fig.5.6 shows the uncoded BER performance of the proposed CG algorithms with different number of iterations for each adaptation. For both schemes, the CG algorithms perform better as the number of iterations increases. However, using more than 8 iterations will only produce very limited improvement in the BER performance for both schemes but increase significantly the computational complexity. In our system, a good choice for the number of iterations is $c = 8$. In this figure, all the dotted curves for the SCE scheme are obtained with the knowledge of σ_e^2 and K. We also include a dashed curve to show the performance of the SCE-CG with 8 iterations that is using the estimated values of $\hat{\sigma}_e^2$ and $\hat{K}$. It is shown that using the estimated values will not affect the convergence rate but only lead to a small reduction at the steady-state performance.

Fig.5.7 illustrates the uncoded BER performance of different algorithms in a scenario

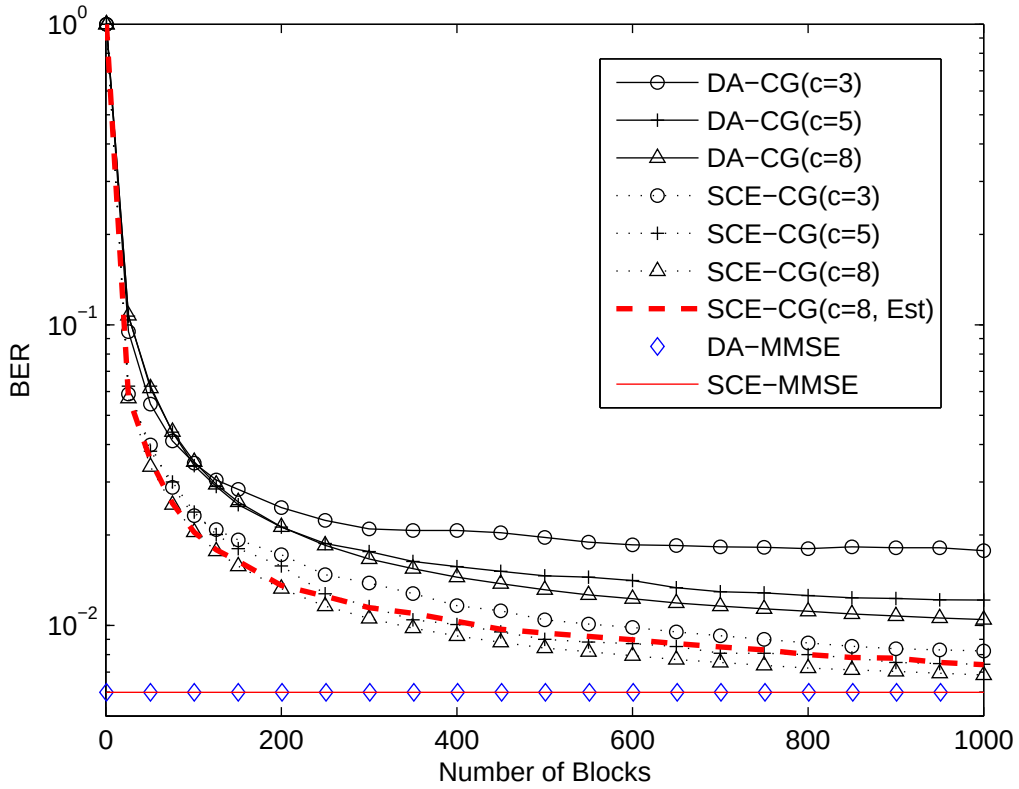

Fig. 5.6: BER performance of the proposed CG algorithms versus the number of training blocks for a SNR=16dB. The number of users is 3.

with 3 users and different SNRs. In this experiment, 500 training blocks are transmitted at each SNR and for the SCE scheme, the estimated $\hat{\sigma}_e^2$ and $\hat{K}$ are used. For all the simulated SNRs, the proposed CG algorithms outperform the LMS algorithms and are very close to the RLS algorithms.

Fig.5.8 shows the uncoded BER performance of different algorithms in a $16dB$ scenario, with different numbers of active users. The parameters for the adaptive algorithms are the same as those used to obtain Fig.5.7 and we use the estimated values of $\hat{\sigma}_e^2$ and $\hat{K}$ for the SCE scheme. For both schemes, the CG algorithms can support about 2 additional users in comparison with the LMS algorithms and the RLS algorithms can support about 1 additional user in comparison with the CG algorithms.

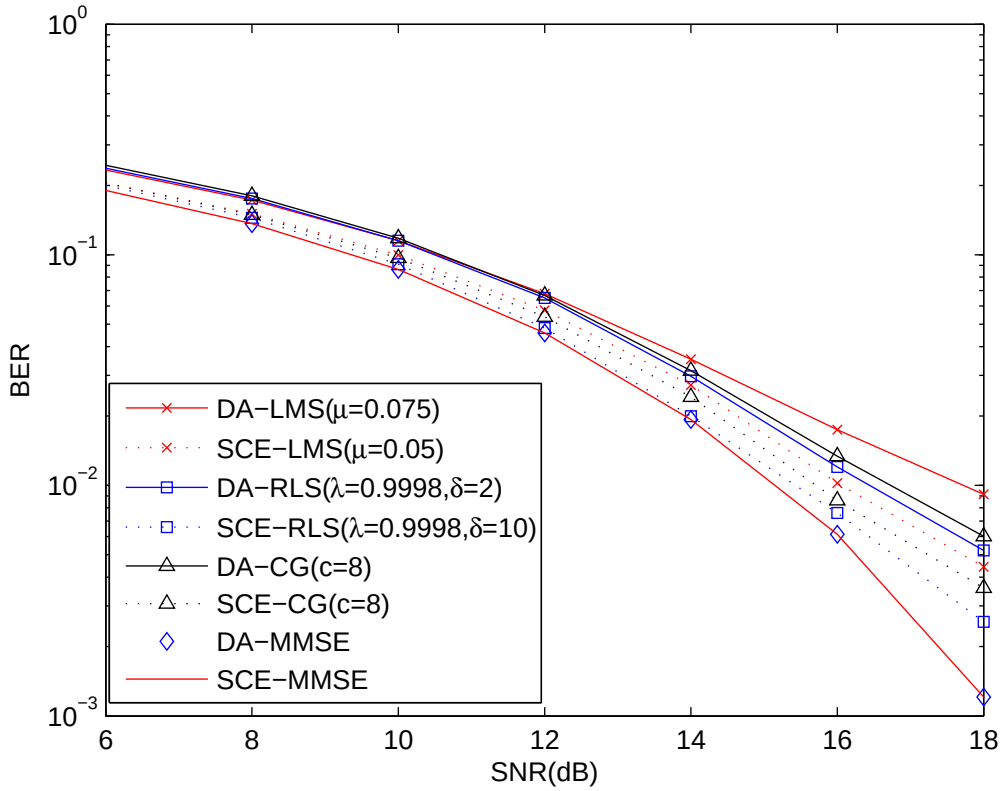

Fig. 5.7: BER performance of the proposed SC-FDE detection schemes versus the SNR. The number of users is 3.

5.8 Conclusion

In this chapter, two adaptive detection schemes are proposed for the multiuser DS-UWB communications based on the SC-FDE. These schemes can be considered as two approaches to solve the MMSE detection problem in the block by block transmission SC systems. The first scheme, named SCE, adaptively estimates the channel coefficients in the frequency domain and then performs the detection and despreading separately. In addition, the MMSE detection in SCE scheme requires the knowledge of the noise variance and the number of active users. To this purpose, we proposed simple algorithms to estimate these values. The second scheme, named DA, updates one filter in the frequency domain to suppress both the MAI and the ISI. The DA scheme has a simpler structure and a lower complexity but the SCE scheme performs better. For both schemes, we developed LMS, RLS and CG adaptive algorithms. For the SCE scheme, the CG algorithm has much lower complexity than the RLS algorithm while performing better than the LMS algorithm. For the DA scheme, a low complexity RLS algorithm is obtained which has the complexity comparable to the CG algorithm in the multiuser scenarios. In the single

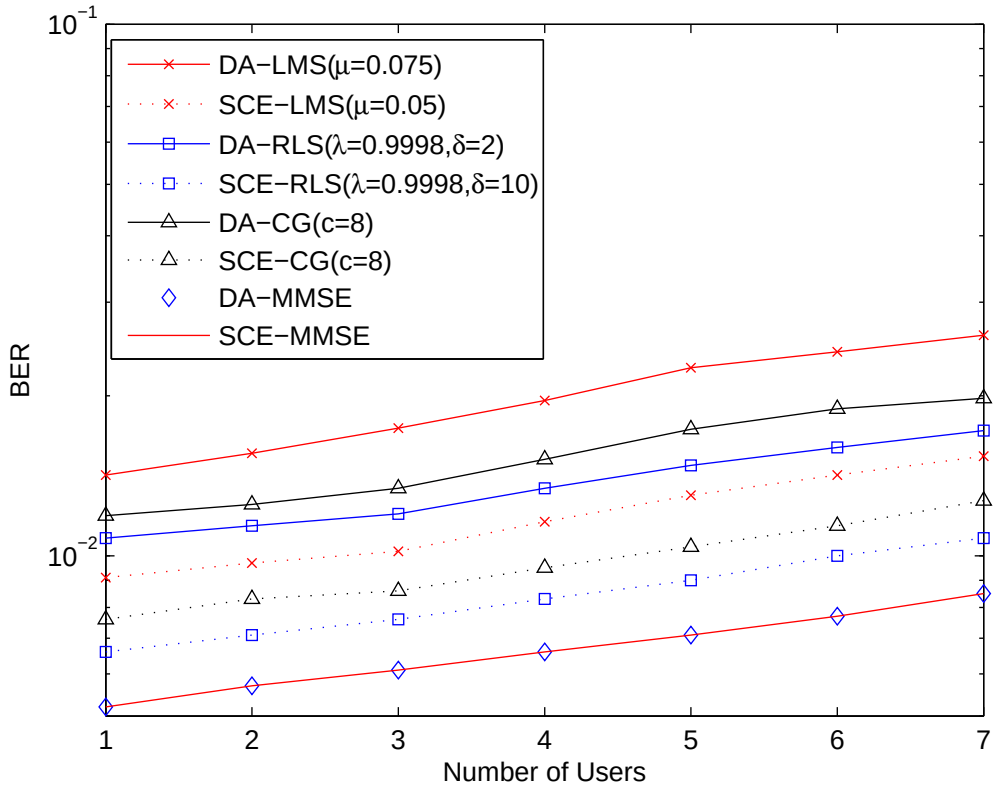

Fig. 5.8: BER performance of the proposed SC-FDE detection schemes versus number of Users in the scenario with a 16dB SNR.

user system, the complexity of DA-RLS is reduced to the same level as the DA-LMS.

6. ADAPTIVE PARAMETER ESTIMATION AND INTERFERENCE SUPPRESSION WITH BIAS IN THE FREQUENCY DOMAIN

Contents

6.1 Introduction

A common estimation problem in communications engineering is to estimate a parameter vector from noisy observations. In this chapter, we consider the deterministic estimation problem with additive white Gaussian noise (AWGN) in two scenarios: parameter estimation and interference suppression. In the parameter estimation scenario, the M-dimensional observation vector is given by $\mathbf{y} = \mathbf{X}\mathbf{h} + \mathbf{n}$, where $\mathbf{X}$ is a given M-by-L matrix and $\mathbf{n}$ is the M-dimensional vector that presents the AWGN with zero mean. The L-dimensional parameter vector $\mathbf{h}$ is the target parameter vector to be estimated. In the interference suppression scenario, the M-dimensional observation vector is given by $\mathbf{z} = \mathbf{H}\mathbf{b} + \mathbf{n}$, where $\mathbf{H}$ is an unknown M-by-N matrix that can represent the channel and/or the spreading codes and the M-dimensional vector $\mathbf{n}$ is the AWGN. Instead of given $\mathbf{H}$, a training sequence is transmitted and an equalizer whose parameters are organized in the vector $\mathbf{w}$ is estimated to recover the N-dimensional date vector $\mathbf{b}$.

A classical approach to solving these problems is the least-square (LS) method, which will lead to minimum variance unbiased estimators (MVUE) [84]. The unbiasness is usually considered as a good property for an estimator. Indeed, the unbiased estimators will obtain the true value of the unknown parameter on average [84]. However, in some

scenarios the LS method is not directly related to the MSE associated with the target parameter vector and it has been found that a lower MSE can be achieved by adding an appropriately chosen bias to the conventional LS estimators [85]- [92]. The biased estimation has shown its ability to outperform the existing estimators especially in the low signal-to-noise ratios (SNR) and/or short data records [86].

In the parameter estimation scenario, the typical objective is to minimize the estimation error $(\mathbf{h}-\hat{\mathbf{h}})$, rather than minimize the the Euclidian norm of the error $(\mathbf{y}-\hat{\mathbf{y}})$, where $\hat{\mathbf{y}} = \mathbf{X}\hat{\mathbf{h}}$ is the transformed estimator [85]. Some biased estimators have been proposed to achieve a smaller estimation error than the LS solutions by removing the unbiasedness of the conventional estimators with a shrinkage factor in the parameter estimation scenario. The earliest shrinkage estimators that reduce the MSE over MVUE include the well known James-Stein estimator [87] and the work of Thompson [88]. Some extensions of the James-Stein estimator have been proposed in [89]- [92]. In [93], blind minimax estimation (BME) techniques have been proposed, in which the biased estimators were developed to minimize the worst case MSE among all possible values of $\mathbf{h}$ within a parameter set. If a spherical parameter set is assumed, the shrinkage estimator obtained is named spherical BME (SBME) [93].

For the interference suppression scenario, the LS solution of the equalizer is obtained to minimize the Euclidian norm of the error $(\mathbf{b}-\hat{\mathbf{b}})$ and results in an unbiased estimator of $\mathbf{w}$. In this scenario, biased estimators can be implemented to achieve lower estimation error between $\mathbf{w}$ and $\hat{\mathbf{w}}$, which is a more accurate approach to estimate the equalizer itself. The shrinkage estimators thus are promising to perform better in the interference suppression scenario with short training data support and in long filter scenarios.

To the best of our knowledge, the shrinkage estimators are rarely implemented into real communication systems. One possible reason is that some assumptions required for the signal model may not be found, for example, in the TH-UWB systems, the MAI cannot be accurately approximated by a Gaussian distribution for some values of SNR and SIR [94]- [95]. Another possible reason is that the existing shrinkage estimators usually require some statistical information such as the noise variance and the norm of the real parameter vector. In this chapter, we propose adaptive bias shrinkage estimators, which do not require this information and are able to improve the performance of the RLS adaptive algorithms in the scenarios of parameter estimation and interference suppression. The considered schemes corresponding to these scenarios are the RLS versions of the structured channel estimation (SCE) and the direct adaptation (DA) in SC-FDE for DS-UWB systems that are proposed in Chapter 5. With additional complexity that is linearly dependent on the filter size, considerable performance improvement can be obtained especially

in the low SNR and short data support environments. In the parameter estimation scenario, the proposed biased estimator performs better than the conventional RLS-based SCE in terms of the MSE between the estimated parameter vector and the true vector. Note that the SCE structure has some performance gain in comparison with the unstructured channel estimation [72] and the RLS version of the SCE performs better than other adaptive versions that are studied in Chapter 5.3. We remark that with the proposed biased estimator, further improvement of the SCE-RLS is obtained in terms of MSE. In the interference suppression scenario, the proposed biased estimator brings some initialization gain for the DA-RLS scheme that is introduced in Chapter 5.4.2. The convergence of the DA-RLS scheme is accelerated because of the bias and a more accurate equalizer estimation is achieved. An extended CRLB is calculated to examine the MSE performance of the proposed shrinkage biased estimators. A study of the proposed algorithms in the presence of UWB signals is carried out.

The main contributions of this chapter are listed below.

- Shrinkage estimators are developed to improve the performance of the frequency domain RLS algorithms in the applications of parameter estimation and interference suppression in DS-UWB systems.

- LMS based adaptive algorithms are developed in both scenarios to obtain the shrinkage factors.

- The biased CRLB that constitutes a fundamental estimation limit of the shrinkage estimators is calculated and we extend it to a lower bound for the MSE performance of the shrinkage estimators.

- The performance of the proposed biased estimators are examined in SC-FDE of DS-UWB systems with IEEE 802.15.4a channel model and severe ISI and MAI.

The rest of this chapter is structured as follows. Section 6.2 presents the LS solution for the parameter estimation scenario and the proposed shrinkage estimator that can achieve a lower estimation error. Section 6.3 presents the LS solution for the interference suppression scenario and the proposed shrinkage estimator that is aiming to improve the performance of the RLS algorithm with short data records. The biased CRLB is calculated in Section 6.4. In Section 6.5, the proposed biased estimators are equipped in SC-FDE of DS-UWB systems and the simulation results demonstrate their better performance than the RLS algorithms. Section 6.6 draws the conclusions.

6.2 Parameter Estimation

In this section, the LS design for the parameter estimation scenario is detailed and the proposed shrinkage estimator is developed to improve the MSE performance of the LS solution.

6.2.1 LS solution Parameter Estimation

The linear estimation problem we discussed in this section can be expressed as

$$\mathbf{y} = \mathbf{X}\mathbf{h} + \mathbf{n}, \tag{6.1}$$

where the M-by-L data matrix $\mathbf{X}$ and the M-dimensional received signal $\mathbf{y}$ are given, $\mathbf{n}$ is additive white Gaussian noise (AWGN) with zero mean and variance σ^2. Note that, the structured channel estimation (SCE) problem we solved in Chapter 5.3 is a typical example of the parameter estimation scenario. In such scenario, we are aiming at estimating the L-dimensional channel vector $\mathbf{h}$ based on the MMSE criterion. The MSE consists of the variance and the bias of the estimator, which can be expressed as

$$\mathrm{E}[\|\mathbf{h} - \hat{\mathbf{h}}\|^2] = \mathrm{E}[(\hat{\mathbf{h}} - \mathrm{E}[\hat{\mathbf{h}}])^H(\hat{\mathbf{h}} - \mathrm{E}[\hat{\mathbf{h}}])] + \mathrm{E}[\|\mathrm{E}[\hat{\mathbf{h}}] - \mathbf{h}\|^2], \tag{6.2}$$

For the unbiased estimators, the MSE becomes

$$\mathrm{E}[\|\mathbf{h} - \hat{\mathbf{h}}_u\|^2] = \mathrm{E}[(\hat{\mathbf{h}}_u - \mathbf{h})^H(\hat{\mathbf{h}}_u - \mathbf{h})] = var(\mathbf{h}, \hat{\mathbf{h}}_u), \tag{6.3}$$

To solve the parameter estimation problem, the conventional LS channel estimation can be obtained by minimizing the following cost function

$$\mathbf{J}_{\mathrm{LS}}(\mathbf{h}) = \|\mathbf{y} - \mathbf{X}\mathbf{h}\|^2, \tag{6.4}$$

assuming that the matrix $\mathbf{X}^H\mathbf{X}$ is a full rank matrix, then the LS solution is given by

$$\hat{\mathbf{h}}_{\mathrm{LS}} = (\mathbf{X}^H\mathbf{X})^{-1}\mathbf{X}^H\mathbf{y}. \tag{6.5}$$

Assuming the AWGN with zero mean and variance σ^2, the LS estimator is an unbiased

estimator because $\mathrm{E}[\hat{\mathbf{h}}_{\mathrm{LS}}] = \mathbf{h}$. Hence, the MSE for the LS estimator is

$$\mathrm{E}[\|\mathbf{h} - \hat{\mathbf{h}}_{\mathrm{LS}}\|^2] = \mathrm{E}[(\hat{\mathbf{h}}_{\mathrm{LS}} - \mathbf{h})^H(\hat{\mathbf{h}}_{\mathrm{LS}} - \mathbf{h})] = var(\mathbf{h}, \hat{\mathbf{h}}_{\mathrm{LS}}). \tag{6.6}$$

Defining $v = var(\mathbf{h}, \hat{\mathbf{h}}_{\mathrm{LS}})$, we have

$$\begin{aligned} v &= \mathrm{E}[(\hat{\mathbf{h}}_{\mathrm{LS}} - \mathbf{h})^H(\hat{\mathbf{h}}_{\mathrm{LS}} - \mathbf{h})] = \mathrm{E}[\big((\mathbf{X}^H\mathbf{X})^{-1}\mathbf{X}^H\mathbf{n}\big)^H\big((\mathbf{X}^H\mathbf{X})^{-1}\mathbf{X}^H\mathbf{n}\big)] \\ &= tr\{\mathrm{E}[\big((\mathbf{X}^H\mathbf{X})^{-1}\mathbf{X}^H\mathbf{n}\big)^H\big((\mathbf{X}^H\mathbf{X})^{-1}\mathbf{X}^H\mathbf{n}\big)]\} \\ &= \mathrm{E}[tr\{\big((\mathbf{X}^H\mathbf{X})^{-1}\mathbf{X}^H\mathbf{n}\big)^H\big((\mathbf{X}^H\mathbf{X})^{-1}\mathbf{X}^H\mathbf{n}\big)\}] \\ &= \mathrm{E}[tr\{\big((\mathbf{X}^H\mathbf{X})^{-1}\mathbf{X}^H\mathbf{n}\big)\big((\mathbf{X}^H\mathbf{X})^{-1}\mathbf{X}^H\mathbf{n}\big)^H\}] \\ &= tr\{\sigma^2(\mathbf{X}^H\mathbf{X})^{-1}\} \end{aligned} \tag{6.7}$$

In section 6.4, the Cramér-Rao Lower Bound (CRLB) for the unbiased and the biased estimators are calculated. We can conclude that the unbiased CRLB is achieved by the LS estimator, which indicates that the LS estimator is an MVUE, or equivalently, the LS estimator achieves minimum MSE among all the unbiased estimators. In what follows, a shrinkage factor is equipped to the unbiased LS estimator that is able to improve the performance in terms of MSE.

6.2.2 Shrinkage Factor Estimation in Parameter Estimation

Let us define the biased estimator as

$$\hat{\mathbf{h}}_{\mathrm{b}} = (1 + \alpha)\hat{\mathbf{h}}_{\mathrm{LS}}, \tag{6.8}$$

where α is a real-valued variable and $(1 + \alpha)$ is defined as the shrinkage factor. The MSE that is introduced by such a biased estimator is given by

$$\mathrm{E}[\|\mathbf{h} - \hat{\mathbf{h}}_{\mathrm{b}}\|^2] = (1 + \alpha)^2 v + \alpha^2\|\mathbf{h}\|^2, \tag{6.9}$$

where $v = var(\mathbf{h}, \hat{\mathbf{h}}_{\mathrm{LS}})$.

Recalling the target of the biased estimation that is to reduce the MSE of the $\hat{\mathbf{h}}_{\mathrm{LS}}$, we can express the objective as

$$\mathrm{E}[\|\mathbf{h} - \hat{\mathbf{h}}_{\mathrm{b}}\|^2] \leq \mathrm{E}[\|\mathbf{h} - \hat{\mathbf{h}}_{\mathrm{LS}}\|^2]. \tag{6.10}$$

Substituting (6.9) and (6.7) into the left hand side and the right hand side of (6.10), re-

spectively, and rearranging the terms, we have the objective equation

$$(1+\alpha)^2 v + \alpha^2 \|\mathbf{h}\|^2 - v \leq 0. \tag{6.11}$$

Note that the value of $\|\mathbf{h}\|^2$ is not given, we make the assumption that $\|\mathbf{h}\|^2 \leq P_{\mathrm{m}}$, where P_{m} is a positive real-valued constant. Hence, the problem to be solved becomes

$$f(\alpha) = (1+\alpha)^2 v + \alpha^2 P_{\mathrm{m}} - v \leq 0. \tag{6.12}$$

The solutions for $f(\alpha) = 0$ are

$$\alpha_1 = 0 \ \text{ and } \ \alpha_2 = \frac{-2v}{v + P_{\mathrm{m}}}. \tag{6.13}$$

Since v and P_{m} are both nonnegative quantities, we have $f(\alpha) < 0$ for all the values of $\alpha \in (\alpha_2, \alpha_1)$. By computing the gradient of $f(\alpha)$ with respect to α and setting it to zero, the optimal solution is given by

$$\alpha_{\mathrm{opt}} = \frac{-v}{v + P_{\mathrm{m}}}. \tag{6.14}$$

In this work, the LS channel estimator is recursively computed by the RLS adaptive algorithm that is detailed in Chapter 5.3.2. The value of P_{m} and the variance of the LS estimator are both unknown and must be estimated. To the best of our knowledge, this problem has not been addressed in the literature. In this work, we propose the following LMS-based algorithm to update the value of α.

The gradient of $f(\alpha)$ with respect to α is given by

$$g_\alpha = (1+\alpha)v + \alpha P_{\mathrm{m}}, \tag{6.15}$$

and the LMS update equation can be expressed as

$$\alpha(i+1) = \alpha(i) - \mu \hat{g}_\alpha(i), \tag{6.16}$$

where μ is the step size and the estimated gradient of $f(\alpha)$ with respect to α is given by

$$\hat{g}_\alpha(i) = \big(1 + \alpha(i)\big)\hat{v}(i) + \alpha(i)\hat{P}_{\mathrm{m}}(i), \tag{6.17}$$

in which the instantaneous estimator is employed as $\hat{v}(i) = \big(\hat{\mathbf{h}}_{\mathrm{RLS}}(i) - \mathbf{h}(i)\big)^H \big(\hat{\mathbf{h}}_{\mathrm{RLS}}(i) -$

$\mathbf{h}(i)\big)$, and $\mathbf{h}$ is replaced by the time averaged RLS channel estimator, that is $\mathbf{h}(i) = \frac{1}{i}\sum_{j=1}^{i}\hat{\mathbf{h}}_{\mathrm{RLS}}(j)$.

In order to determine the values of $\hat{P}_{\mathrm{m}}(i)$, two approaches are developed. In the first approach, which is named estimator based (EB) method, the values of $\hat{P}_{\mathrm{m}}(i)$ is simply replaced by $\hat{\mathbf{h}}_{\mathrm{RLS}}^{H}(i)\hat{\mathbf{h}}_{\mathrm{RLS}}(i)$. Note that in this case, the equation (6.14) has the same expression as the SBME that is proposed in [93]. However, the knowledge of the noise variance is not required in our work. In the second approach, which is named automatic tuning (AT) method, an LMS-based algorithm is proposed to update the values of $\hat{P}_{\mathrm{m}}(i)$ within a given range. In this method, $\hat{P}_{\mathrm{m}}(i)$ is considered as a variable of the following function

$$f(\hat{P}_{\mathrm{m}}(i)) = \big(1+\alpha_{\mathrm{o}}(i)\big)^{2}v + \alpha_{\mathrm{o}}(i)^{2}\hat{P}_{\mathrm{m}}(i) - v, \tag{6.18}$$

where $\alpha_{\mathrm{o}}(i) = -v/\big(v+\hat{P}_{\mathrm{m}}(i)\big)$. Then the LMS algorithm is employed to update the values of $\hat{P}_{\mathrm{m}}(i)$ as follows

$$\begin{aligned}\hat{P}_{\mathrm{m}}(i+1) &= \hat{P}_{\mathrm{m}}(i) - \mu_p\hat{g}_p(i) \\ &= \hat{P}_{\mathrm{m}}(i) + \mu_p\left(\frac{2\hat{v}(i)\big(\hat{v}(i)+\hat{v}(i)\alpha(i)+\alpha(i)\hat{P}_{\mathrm{m}}(i)\big)}{\big(\hat{v}(i)+\hat{P}_{\mathrm{m}}(i)\big)^{2}} - \alpha^{2}(i)\right),\end{aligned} \tag{6.19}$$

where μ_p is a small positive constant defined as the step size and $\hat{g}_p(i)$ is the estimated gradient of the function $f(\hat{P}_{\mathrm{m}}(i))$ with respect to $\hat{P}_{\mathrm{m}}(i)$. Recalling the equation (6.13), the range of the α is given as $\alpha \in (\alpha_2, \alpha_1)$ and it is dependent on the positive constant P_{m}. If $P_{\mathrm{m}} \to 0$, the range approaches $(-2, 0)$. If $P_{\mathrm{m}} \to \infty$, the range approaches a null set. Also note that P_{m} is assumed to be a constant that is larger than the value of $\mathbf{h}^{H}\mathbf{h}$. Hence, for the second approach, we set lower and upper limits for the values of $\hat{P}_{\mathrm{m}}(i)$. If the value of $\hat{P}_{\mathrm{m}}(i)$ goes beyond these limitations, it is set to the medium value of the thresholds and continues the adaptation.

For the implementation of the proposed shrinkage estimator, the SCE problem discussed in Chapter 5.3.2 is considered. The RLS solution of the channel estimation, which is represented as an L-dimensional vector $\hat{\mathbf{h}}_{\mathrm{RLS}}(i)$, is obtained by using Equation (5.31). In Table 6.1, the proposed biased estimators with two approaches to calculate $\hat{P}_{\mathrm{m}}(i)$ are summarized. Note that, the biased estimator with the EB approach, in which $\hat{P}_{\mathrm{m}}(i) = \hat{\mathbf{h}}_{\mathrm{RLS}}^{H}(i)\hat{\mathbf{h}}_{\mathrm{RLS}}(i)$, requires $4L+3$ complex multiplications and $4L+2$ complex additions. For the AT approach, in which $\hat{P}_{\mathrm{m}}(i)$ is updated by using equation (6.19), the number of complex multiplications required is $3L+9$ and the number of complex additions required is $3L+8$. It will be demonstrated by the simulations that the performance of the AT approach is better than the EB approach, but there is no need to set the upper and lower limits for the values of $\hat{P}_{\mathrm{m}}(i)$ in the EB approach.

Tab. 6.1: Biased Estimation for SCE-RLS in SC-FDE DS-UWB Systems

Proposed EB	Proposed AT
1. Initialization:	**1. Initialization:**
$\alpha(1) = 0$	$\alpha(1) = 0, \hat{P}_{\mathrm{m}}(1) = 0.05$
Set value of μ	Set values of μ, μ_p, $\hat{P}_{\mathrm{m,min}}$ and $\hat{P}_{\mathrm{m,max}}$
2. Calculate the biased estimator:	**2. Calculate the biased estimator:**
For $i = 1, 2, \ldots$	For $i = 1, 2, \ldots$
$\hat{\mathbf{h}}_{\mathrm{b}}(i) = (1 + \alpha(i))\hat{\mathbf{h}}_{\mathrm{RLS}}(i)$	$\hat{\mathbf{h}}_{\mathrm{b}}(i) = (1 + \alpha(i))\hat{\mathbf{h}}_{\mathrm{RLS}}(i)$
3. Calculate the shrinkage factor:	**3. Calculate the shrinkage factor:**
$\mathbf{h}(i) = \frac{1}{i}\sum_{j=1}^{i} \hat{\mathbf{h}}_{\mathrm{RLS}}(j)$	$\mathbf{h}(i) = \frac{1}{i}\sum_{j=1}^{i} \hat{\mathbf{h}}_{\mathrm{RLS}}(j)$,
$\hat{v}(i) = \big(\hat{\mathbf{h}}_{\mathrm{RLS}}(i) - \mathbf{h}(i)\big)^H \big(\hat{\mathbf{h}}_{\mathrm{RLS}}(i) - \mathbf{h}(i)\big)$	$\hat{v}(i) = \big(\hat{\mathbf{h}}_{\mathrm{RLS}}(i) - \mathbf{h}(i)\big)^H \big(\hat{\mathbf{h}}_{\mathrm{RLS}}(i) - \mathbf{h}(i)\big)$
$\hat{P}_{\mathrm{m}}(i) = \hat{\mathbf{h}}_{\mathrm{RLS}}^H(i)\hat{\mathbf{h}}_{\mathrm{RLS}}(i)$	$\hat{P}_{\mathrm{m}}(i+1)$ is computed by using (6.19)
	If $\hat{P}_{\mathrm{m}}(i+1) < \hat{P}_{\mathrm{m,min}}$ or $> \hat{P}_{\mathrm{m,max}}$
$\hat{g}_\alpha(i) = \big(1 + \alpha(i)\big)\hat{v}(i) + \alpha(i)\hat{P}_{\mathrm{m}}(i),$	$\hat{P}_{\mathrm{m}}(i+1) = \frac{1}{2}(\hat{P}_{\mathrm{m,min}} + \hat{P}_{\mathrm{m,max}})$ End If
	$\hat{g}_\alpha(i) = \big(1 + \alpha(i)\big)\hat{v}(i) + \alpha(i)\hat{P}_{\mathrm{m}}(i)$
$\alpha(i+1) = \alpha(i) - \mu\hat{g}_\alpha(i)$	$\alpha(i+1) = \alpha(i) - \mu\hat{g}_\alpha(i)$

6.3 Interference Suppression

In this section, we discuss the LS estimator and the biased estimator for the interference suppression scenario.

6.3.1 LS Solution for Interference Suppression

The linear estimation problem to be solved in this section can be expressed as

$$\mathbf{z} = \mathbf{H}\mathbf{b} + \mathbf{n}, \tag{6.20}$$

where the M-by-N matrix $\mathbf{H}$ is an unknown matrix, $\mathbf{z}$ is the M-dimensional received signal, $\mathbf{b}$ is the N-dimensional transmitted data vector and $\mathbf{n}$ is the AWGN with zero mean and unknown variance σ^2. Note that, the direct adaptation (DA) problem we solved in Chapter 5.4 is a typical example of the interference suppression scenario. Assuming the first user is the desired user and the MAI is Gaussian distributed, the expression of the received signal as shown in (5.16) can be rewritten as

$$\mathbf{z} = (1/\sqrt{N_c})\mathbf{\Lambda}_1\mathbf{I}_{\mathrm{e}}\mathbf{F}_N\mathbf{b}_1 + \mathbf{n}. \tag{6.21}$$

Note that, if we consider the M-by-N matrix $(1/\sqrt{N_c})\mathbf{\Lambda}_1\mathbf{I}_{\rm e}\mathbf{F}_N$ as matrix $\mathbf{H}$, then this signal model has the same expression as (6.20).

Now, follow the expression as in equation (5.43), a linear equalizer $\mathbf{w}$ can be implemented to estimate the data vector as

$$\hat{\mathbf{b}} = \mathbf{Y}\mathbf{w}, \tag{6.22}$$

where $\mathbf{Y} = \mathbf{F}_{\rm N}^H\mathbf{I}_{\rm e}^H\mathbf{Z}$ and $\mathbf{Z} = \mathrm{diag}(\mathbf{z})$. The cost function for the development of the LS estimation is given by

$$\mathbf{J}_{\rm LS} = \|\mathbf{b} - \mathbf{Y}\mathbf{w}\|^2, \tag{6.23}$$

and the LS design of the linear equalizer can be expressed as

$$\hat{\mathbf{w}}_{\rm LS} = (\mathbf{Y}^H\mathbf{Y})^{-1}\mathbf{Y}^H\mathbf{b} = \mathbf{R}_{\rm LS}^{-1}\mathbf{p}_{\rm LS}, \tag{6.24}$$

where matrix $\mathbf{R}_{\rm LS}$ is defined as $(\mathbf{Y}^H\mathbf{Y})$ and $\mathbf{p}_{\rm LS}$ represents the vector $\mathbf{Y}^H\mathbf{b}$.

Note that, the data vector can be expressed as

$$\mathbf{b} = \mathbf{Y}\mathbf{w}_{\rm o} + \epsilon_{\rm o}, \tag{6.25}$$

where $\mathbf{w}_{\rm o}$ is the optimal solution of the equalizer and $\epsilon_{\rm o}$ is the measurement error. Assuming that $\epsilon_{\rm o}$ has zero mean and covariance of $\sigma_e^2\mathbf{I}$, we can obtain

$$E[\hat{\mathbf{w}}_{\rm LS}] = \mathbf{w}_{\rm o}, \tag{6.26}$$

which indicates that the LS estimator of the equalizer is an unbiased estimator. Now, let us have a look at the following MSE:

$$\mathrm{E}[\|\mathbf{w}_{\rm o} - \hat{\mathbf{w}}_{\rm LS}\|^2] = \mathrm{E}[(\mathbf{w}_{\rm o} - \hat{\mathbf{w}}_{\rm LS})^H(\mathbf{w}_{\rm o} - \hat{\mathbf{w}}_{\rm LS})] = var(\mathbf{w}_{\rm o}, \hat{\mathbf{w}}_{\rm LS}). \tag{6.27}$$

Defining $v_w = var(\mathbf{w}_{\rm o}, \hat{\mathbf{w}}_{\rm LS})$ and using the similar derivation in (6.7), we have

$$v_w = tr\{\sigma_e^2(\mathbf{Y}^H\mathbf{Y})^{-1}\}. \tag{6.28}$$

In the interference suppression scenario, the unbiased LS estimator is obtained for the equalizer. It is possible to introduce the biased estimation to reduce the MSE between the optimal equalizer $\mathbf{w}_{\rm o}$ and the LS estimator $\hat{\mathbf{w}}_{\rm LS}$. Note that, for the interference suppression scenario, the typical objective is to minimize the overall performance which is determined as the MSE of $\mathrm{E}[\|\mathbf{b} - \hat{\mathbf{b}}\|^2]$, rather than to minimize the MSE of $\mathrm{E}[\|\mathbf{w}_{\rm o} - \hat{\mathbf{w}}_{\rm LS}\|^2]$.

Hence, different from the objective of biased estimator in parameter estimation scenario, the main motivation to introduce the bias in the interference suppression scenario is to provide some initialization gain for the overall performance when the adaptive filtering techniques are employed and the training data is limited. This can also help with tracking problems and with robustness against interference.

6.3.2 Shrinkage Factor Estimation in Interference Suppression Schemes

The biased estimator of the equalizer with a shrinkage factor can be expressed as

$$\hat{\mathbf{w}}_{\mathrm{b}} = (1+\alpha)\hat{\mathbf{w}}_{\mathrm{LS}}, \tag{6.29}$$

and the MSE of the biased estimator is given by

$$\mathrm{E}[\|\mathbf{w}_{\mathrm{o}} - \hat{\mathbf{w}}_{\mathrm{b}}\|^2] = (1+\alpha)^2 v_w + \alpha^2 \|\mathbf{w}_{\mathrm{o}}\|^2. \tag{6.30}$$

The objective of the biased estimation is to achieve a smaller MSE between $\mathbf{w}_{\mathrm{o}}$ and $\hat{\mathbf{w}}_{\mathrm{LS}}$, which can be expressed as

$$\mathrm{E}[\|\mathbf{w}_{\mathrm{o}} - \hat{\mathbf{w}}_{\mathrm{b}}\|^2] \leq \mathrm{E}[\|\mathbf{w}_{\mathrm{o}} - \hat{\mathbf{w}}_{\mathrm{LS}}\|^2]. \tag{6.31}$$

Substituting (6.30) and (6.28) into the left hand side and the right hand side of (6.10), respectively, and rearranging the terms, we have the objective equation

$$(1+\alpha)^2 v_w + \alpha^2 \|\mathbf{w}_{\mathrm{o}}\|^2 - v_w \leq 0. \tag{6.32}$$

Note that the value of $\|\mathbf{w}_{\mathrm{o}}\|^2$ is not given. We make the assumption that $\|\mathbf{w}_{\mathrm{o}}\|^2 \leq P_{\mathrm{w}}$, where P_{w} is a positive real-valued constant. Hence, the problem to be solved becomes

$$f(\alpha) = (1+\alpha)^2 v_w + \alpha^2 P_{\mathrm{w}} - v_w \leq 0. \tag{6.33}$$

The problem to be solved here has the similar expression as the problem solved in the previous section 6.2.2. Using the similar derivation to obtain (6.14), the optimal solution here is given by

$$\alpha_{\mathrm{opt}} = \frac{-v_w}{v_w + P_{\mathrm{w}}}. \tag{6.34}$$

It is necessary to examine the effect of the shrinkage factor to the overall MSE performance, which can be examined by calculating the MSE difference as follows:

$$\mathrm{E}[\|\mathbf{b}-\hat{\mathbf{b}}_{\mathrm{b}}\|^2]-\mathrm{E}[\|\mathbf{b}-\hat{\mathbf{b}}_{\mathrm{LS}}\|^2]=\mathrm{E}[\|\mathbf{b}-(1+\alpha)\mathbf{Y}\hat{\mathbf{w}}_{\mathrm{LS}}\|^2]-\mathrm{E}[\|\mathbf{b}-\mathbf{Y}\hat{\mathbf{w}}_{\mathrm{LS}}\|^2] \quad (6.35)$$

Recalling the equation (6.24), we have

$$\mathrm{E}[\|\mathbf{b}-\mathbf{Y}\hat{\mathbf{w}}_{\mathrm{LS}}\|^2]=\|\mathbf{b}\|^2-\mathbf{p}_{\mathrm{LS}}^{\mathrm{H}}\mathbf{R}_{\mathrm{LS}}^{-1}\mathbf{p}_{\mathrm{LS}},$$

and

$$\mathrm{E}[\|\mathbf{b}-(1+\alpha)\mathbf{Y}\hat{\mathbf{w}}_{\mathrm{LS}}\|^2]=\|\mathbf{b}\|^2+\big(\alpha^2-1\big)\mathbf{p}_{\mathrm{LS}}^{\mathrm{H}}\mathbf{R}_{\mathrm{LS}}^{-1}\mathbf{p}_{\mathrm{LS}}.$$

Hence,

$$\mathrm{E}[\|\mathbf{b}-\hat{\mathbf{b}}_{\mathrm{b}}\|^2]-\mathrm{E}[\|\mathbf{b}-\hat{\mathbf{b}}_{\mathrm{LS}}\|^2]=\alpha^2\mathbf{p}_{\mathrm{LS}}^{\mathrm{H}}\mathbf{R}_{\mathrm{LS}}^{-1}\mathbf{p}_{\mathrm{LS}}\geq 0. \quad (6.36)$$

Although the biased equalizer will have a closer Euclidean distance to the optimal equalizer, equation (6.36) indicates that the shrinkage factor actually will increase the MSE between the data vector $\mathbf{b}$ and its estimator. Hence, in the interference suppression scenario, the price to obtain a better presentation of the equalizer is the increased overall MSE performance. We remark that the biased estimators can be utilized here to accelerate the convergence rate or they can bring an initial gain for the RLS adaptive algorithm that is aiming at estimating the LS solution recursively.

In this section, the LS estimator of the equalizer is approached by the RLS adaptive algorithm that is detailed in Chapter 5.4.2. After calculating the $\hat{\mathbf{w}}_{\mathrm{RLS}}(i)$ by using equation (5.54), the value of P_w and the variance of the LS estimator must be estimated. Using a similar derivation as in subsection 6.2.2, the LMS-based update equation for $\alpha(i)$ in interference suppression scenario is given by

$$\alpha(i+1)=\alpha(i)-\mu\left(\big(1+\alpha(i)\big)\hat{v}_w(i)+\alpha(i)\hat{P}_{\mathrm{w}}(i)\right), \quad (6.37)$$

where μ is the step size and the instantaneous estimator for the variance is given by

$$\hat{v}_w(i)=\big(\hat{\mathbf{w}}_{\mathrm{RLS}}(i)-\mathbf{w}_{\mathrm{o}}(i)\big)^H\big(\hat{\mathbf{w}}_{\mathrm{RLS}}(i)-\mathbf{w}_{\mathrm{o}}(i)\big), \quad (6.38)$$

where $\mathbf{w}_{\mathrm{o}}$ is replaced by the time averaged RLS equalizer estimator, that is $\mathbf{w}_{\mathrm{o}}(i)=\frac{1}{i}\sum_{j=1}^{i}\hat{\mathbf{w}}_{\mathrm{RLS}}(j)$.

In order to determine the values of $\hat{P}_{\mathrm{w}}(i)$, the proposed EB and AT approaches are employed. In the EB method, we set $\hat{P}_{\mathrm{w}}(i)=\hat{\mathbf{w}}_{\mathrm{RLS}}^H(i)\hat{\mathbf{w}}_{\mathrm{RLS}}(i)$. In the AT approach, we

Tab. 6.2: Biased Estimation for DA-RLS in SC-FDE DS-UWB Systems

Proposed EB	Proposed AT
1. Initialization:	**1. Initialization:**
$\alpha(1) = 0$	$\alpha(1) = 0, \hat{P}_{\mathrm{w}}(1) = 10$
Set value of μ	Set values of μ, μ_p, $\hat{P}_{\mathrm{w,min}}$ and $\hat{P}_{\mathrm{w,max}}$
2. Calculate the biased estimator:	**2. Calculate the biased estimator:**
For $i = 1, 2, \ldots$	For $i = 1, 2, \ldots$
$\hat{\mathbf{w}}_{\mathrm{b}}(i) = (1 + \alpha(i))\hat{\mathbf{w}}_{\mathrm{RLS}}(i)$	$\hat{\mathbf{w}}_{\mathrm{b}}(i) = (1 + \alpha(i))\hat{\mathbf{w}}_{\mathrm{RLS}}(i)$
$\hat{\mathbf{b}}_{\mathrm{b}}(i) = \mathbf{Y}(i)\hat{\mathbf{w}}_{\mathrm{b}}(i)$	$\hat{\mathbf{b}}_{\mathrm{b}}(i) = \mathbf{Y}(i)\hat{\mathbf{w}}_{\mathrm{b}}(i)$
3. Calculate the shrinkage factor:	**3. Calculate the shrinkage factor:**
$\mathbf{w}_{\mathrm{o}}(i) = \frac{1}{i}\sum_{j=1}^{i} \hat{\mathbf{w}}_{\mathrm{RLS}}(j)$	$\mathbf{w}_{\mathrm{o}}(i) = \frac{1}{i}\sum_{j=1}^{i} \hat{\mathbf{w}}_{\mathrm{RLS}}(j),$
$\hat{v}_w(i)$ is calculated by using (6.38)	$\hat{v}_w(i)$ is calculated by using (6.38)
$\hat{P}_{\mathrm{w}}(i) = \hat{\mathbf{w}}^H_{\mathrm{RLS}}(i)\hat{\mathbf{w}}_{\mathrm{RLS}}(i)$	$\hat{P}_{\mathrm{w}}(i+1)$ is computed by using (6.39)
	If $\hat{P}_{\mathrm{w}}(i+1) < \hat{P}_{\mathrm{w,min}}$ or $> \hat{P}_{\mathrm{w,max}}$
$\hat{g}_\alpha(i) = \big(1 + \alpha(i)\big)\hat{v}(i) + \alpha(i)\hat{P}_{\mathrm{w}}(i),$	$\hat{P}_{\mathrm{w}}(i+1) = \frac{1}{2}(\hat{P}_{\mathrm{w,min}} + \hat{P}_{\mathrm{w,max}})$ End If
	$\hat{g}_\alpha(i) = \big(1 + \alpha(i)\big)\hat{v}(i) + \alpha(i)\hat{P}_{\mathrm{w}}(i)$
$\alpha(i+1) = \alpha(i) - \mu\hat{g}_\alpha(i)$	$\alpha(i+1) = \alpha(i) - \mu\hat{g}_\alpha(i)$

employ the recursive equation

$$\hat{P}_{\mathrm{w}}(i+1) = \hat{P}_{\mathrm{w}}(i) + \mu_p \left(\frac{2\hat{v}_w(i)\big(\hat{v}_w(i) + \hat{v}_w(i)\alpha(i) + \alpha(i)\hat{P}_{\mathrm{w}}(i)\big)}{\big(\hat{v}_w(i) + \hat{P}_{\mathrm{w}}(i)\big)^2} - \alpha^2(i) \right), \quad (6.39)$$

where μ_p is a small positive constant defined as the step size and similar to the algorithm in the parameter estimation scenario, we also set upper and lower limits for the values of $\hat{P}_{\mathrm{w}}(i)$. For the implementation of the proposed shrinkage estimator, the DA problem discussed in Chapter 5.4.2 is considered. The RLS solution of the equalizer, which is represented as an M-dimensional vector $\hat{\mathbf{w}}_{\mathrm{RLS}}(i)$, is obtained by using equation (5.54). In Table 6.2, the proposed biased estimators with two approaches to calculate $\hat{P}_{\mathrm{w}}(i)$ are summarized. Note that, the EB approach requires $4M + 3$ complex multiplications and $4M + 2$ complex additions. For the AT method, in which $\hat{P}_{\mathrm{m}}(i)$ is updated by using equation (6.39), the number of complex multiplications required is $3M+9$ and the number of complex additions required is $3M + 8$. Simulation results will demonstrate that in the interference suppression scenario, both approaches will introduce initialization gain to the DA-RLS scheme. The AT method has faster convergence rate than the EB method, but EB method will introduce less MSE loss for the overall performance.

6.4 The Cramér-Rao Lower Bound and Its Extension

The Cramér-Rao Lower Bound (CRLB) is the minimal variance that an unbiased estimator can achieve [96], [97]. For biased estimators, a biased CRLB can be calculated to indicate the lower bound of the variance of biased estimators [97]. In this section, CRLB for the biased estimators equipped with shrinkage factors is examined and the parameter estimation scenario is employed to show the derivations.

For the estimation problem $\mathbf{y} = \mathbf{X}\mathbf{h} + \mathbf{n}$, where $\mathbf{X}$ is a given matrix and $\mathbf{n}$ is the AWGN with zero mean and variance σ^2. We define $p(\mathbf{y};\mathbf{h})$ as the probability density function (PDF) of the received signal $\mathbf{y}$, which is characterized by $\mathbf{h}$. Assuming that $p(\mathbf{y};\mathbf{h})$ satisfies the regularity condition [96], which is given by $\mathrm{E}[\partial p(\mathbf{y};\mathbf{h})/\partial \mathbf{h}] = 0$, for all $\mathbf{h}$. In this work, we consider the shrinkage estimator which is given in (6.8) and we have

$$\mathrm{E}[\hat{\mathbf{h}}_{\mathrm{b}}] = \mathbf{h} + \alpha\mathbf{h} = \mathbf{h} + \mathbf{B}(\mathbf{h}), \tag{6.40}$$

where $\mathbf{B}(\mathbf{h}) = \alpha\mathbf{h}$ represents the bias which is a function of $\mathbf{h}$. Then, the biased CRLB for the shrinkage estimator is given by

$$\mathrm{E}[(\hat{\mathbf{h}}_b - \mathrm{E}[\hat{\mathbf{h}}_b])^H(\hat{\mathbf{h}}_b - \mathrm{E}[\hat{\mathbf{h}}_b])] \geq \frac{\left(1 + \frac{d\mathbf{B}(\mathbf{h})}{d\mathbf{h}}\right)^2}{-\mathrm{E}\left[\frac{\partial^2 \ln p(\mathbf{y};\mathbf{h})}{\partial \mathbf{h}^2}\right]}, \tag{6.41}$$

Bearing in mind that the noise is assumed to be white Gaussian and its covariance is defined as $\sigma^2\mathbf{I}$, we have

$$-\mathrm{E}\left[\frac{\partial^2 \ln p(\mathbf{y};\mathbf{h})}{\partial \mathbf{h}^2}\right] = tr\{\frac{1}{\sigma^2}\mathbf{X}^H\mathbf{X}\}. \tag{6.42}$$

Finally, the CRLB for the variance of the shrinkage estimators with bias $\mathbf{B}(\mathbf{h})$ is given by

$$\mathrm{E}[(\hat{\mathbf{h}}_b - \mathrm{E}[\hat{\mathbf{h}}_b])^H(\hat{\mathbf{h}}_b - \mathrm{E}[\hat{\mathbf{h}}_b])] \geq (1+\alpha)^2 tr\{\sigma^2(\mathbf{X}^H\mathbf{X})^{-1}\}. \tag{6.43}$$

The CRLB for the unbiased estimator can be expressed as

$$\mathrm{E}[(\hat{\mathbf{h}}_u - \mathrm{E}[\hat{\mathbf{h}}_u])^H(\hat{\mathbf{h}}_u - \mathrm{E}[\hat{\mathbf{h}}_u])] \geq tr\{\sigma^2(\mathbf{X}^H\mathbf{X})^{-1}\}. \tag{6.44}$$

It must be noted that the biased CRLB shown in (6.43) gives the minimum variance that a shrinkage estimator can achieve and indicates that the shrinkage estimators attain this lower bound. However, it is not as meaningful as the CRLB for the unbiased estimator that is shown in (6.44). The main reason is that for the unbiased estimator, the variance is equal to the MSE of the estimator and hence the CRLB can also be considered as the lower bound of the MSE performance. However, for the biased estimators, recalling the equation (6.9), the MSE performance is determined not only by the variance of the estimator but also the bias, which is $\alpha^2\|\mathbf{h}\|^2$ in our case. In addition, there is an unknown variable α in (6.43) and the derivation in this section so far is not able to give an optimal solution of α that leads to minimum MSE. Hence, we extend the analysis here to obtain a lower bound for the MSE performance of the biased estimators. The MSE of a shrinkage biased estimator is given by

$$\mathrm{E}[\|\mathbf{h}-\hat{\mathbf{h}}_{\mathrm{b}}\|^2] = var(\mathbf{h},\hat{\mathbf{h}}_b)+bias(\mathbf{h},\hat{\mathbf{h}}_b) = (1+\alpha)^2 tr\{\sigma^2(\mathbf{X}^H\mathbf{X})^{-1}\}+\alpha^2\|\mathbf{h}\|^2. \quad (6.45)$$

If we consider the MSE expression as a function of α, then the optimal solution of α that corresponds to the minimum MSE can be obtained by computing the gradient with respect to α and setting it to zero. The optimal α can be expressed as

$$\alpha_{\mathrm{opt}} = \frac{-tr\{\sigma^2(\mathbf{X}^H\mathbf{X})^{-1}\}}{tr\{\sigma^2(\mathbf{X}^H\mathbf{X})^{-1}\}+\|\mathbf{h}\|^2}. \quad (6.46)$$

Hence, the lower bound for the MSE performance of the shrinkage estimator is

$$\begin{aligned}\mathrm{E}[\|\mathbf{h}-\hat{\mathbf{h}}_{\mathrm{b}}\|^2] &\geq (1+\alpha_{\mathrm{opt}})^2 tr\{\sigma^2(\mathbf{X}^H\mathbf{X})^{-1}\}+\alpha_{\mathrm{opt}}^2\|\mathbf{h}\|^2 \\ &= \frac{tr\{\sigma^2(\mathbf{X}^H\mathbf{X})^{-1}\}\|\mathbf{h}\|^2}{tr\{\sigma^2(\mathbf{X}^H\mathbf{X})^{-1}\}+\|\mathbf{h}\|^2} \\ &= \frac{1}{\left(tr\{\sigma^2(\mathbf{X}^H\mathbf{X})^{-1}\}/\|\mathbf{h}\|^2\right)+1} tr\{\sigma^2(\mathbf{X}^H\mathbf{X})^{-1}\}.\end{aligned} \quad (6.47)$$

The equation (6.47) is the extended CRLB for the shrinkage estimators and it indicates the followings:

1: The value of the scalar term $\frac{1}{(tr\{\sigma^2(\mathbf{X}^H\mathbf{X})^{-1}\}/\|\mathbf{h}\|^2)+1}$ is always smaller than 1 and larger than 0, which means the lower bound of the shrinkage MSE is always lower than the CRLB for the unbiased estimators that is given in (6.44).

2: The distance between the bounds of unbiased estimators (in (6.44)) and the extended CRLB for shrinkage estimators (in (6.47)) is dependent on the noise variance σ^2. Interestingly, in the low SNR scenarios where σ^2 is large, the distance between the bounds

becomes larger than in the high SNR scenarios. Actually, if the SNR is high and $\sigma^2 \to 0$, then these two bounds tend to be the same. The simulation results will also demonstrate this phenomenon as the gain of the shrinkage estimator over the unbiased LS solution is increasing as the SNR reduces.

3: If the white Gaussian is assumed and the shrinkage estimator is obtained based on a minimum variance unbiased estimator (MVUE), then the optimal α is given in (6.46) and the lower bound shown in (6.47) is achieved.

6.5 Simulations

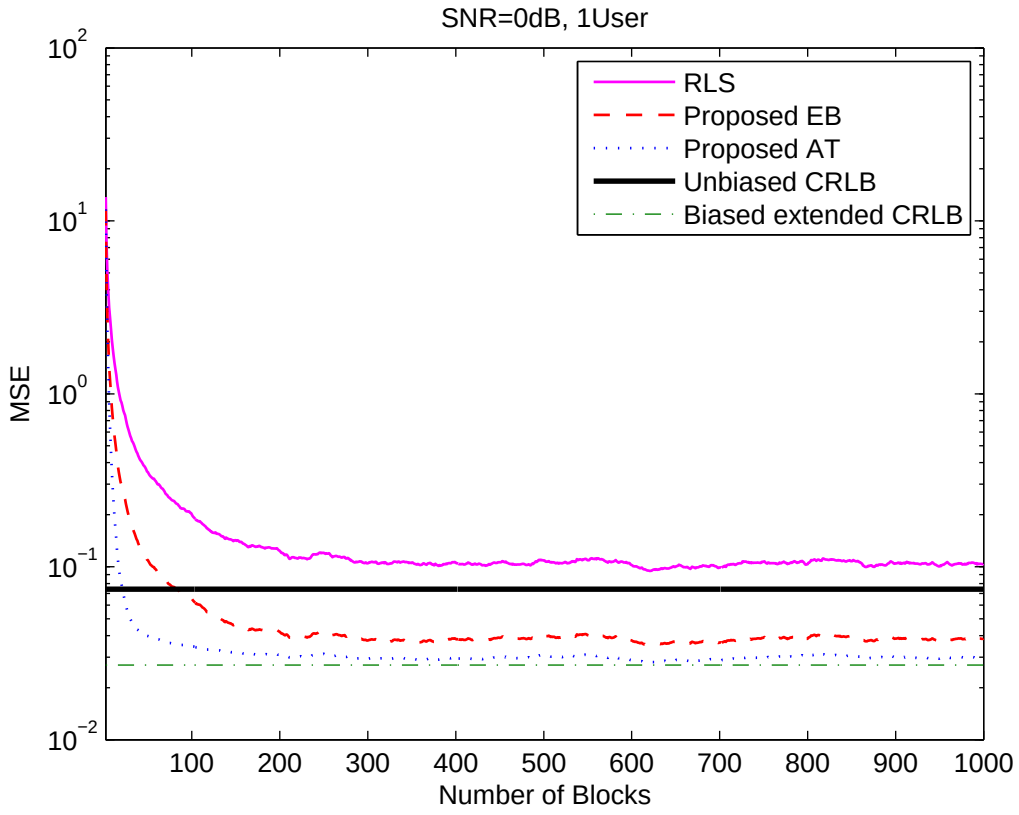

Fig. 6.1: MSE performance ($\|\mathbf{h} - \hat{\mathbf{h}}\|^2$) of the biased structured channel estimation (SCE). The parameters used: RLS ($\lambda = 0.998$, $\delta = 10$). Proposed EB: $\mu = 0.075$ and proposed AT: $\mu = 0.075$, $\mu_p = 0.05$, $\hat{P}_{\mathrm{m,min}} = 0.05$, $\hat{P}_{\mathrm{m,max}} = 0.15$.

In this section, the biased estimators are employed in the SCE and DA detectors that are developed in Chapter 5 and their MSE performance are compared with the conventional SCE-RLS and DA-RLS algorithms, respectively. The simulation environment is set to

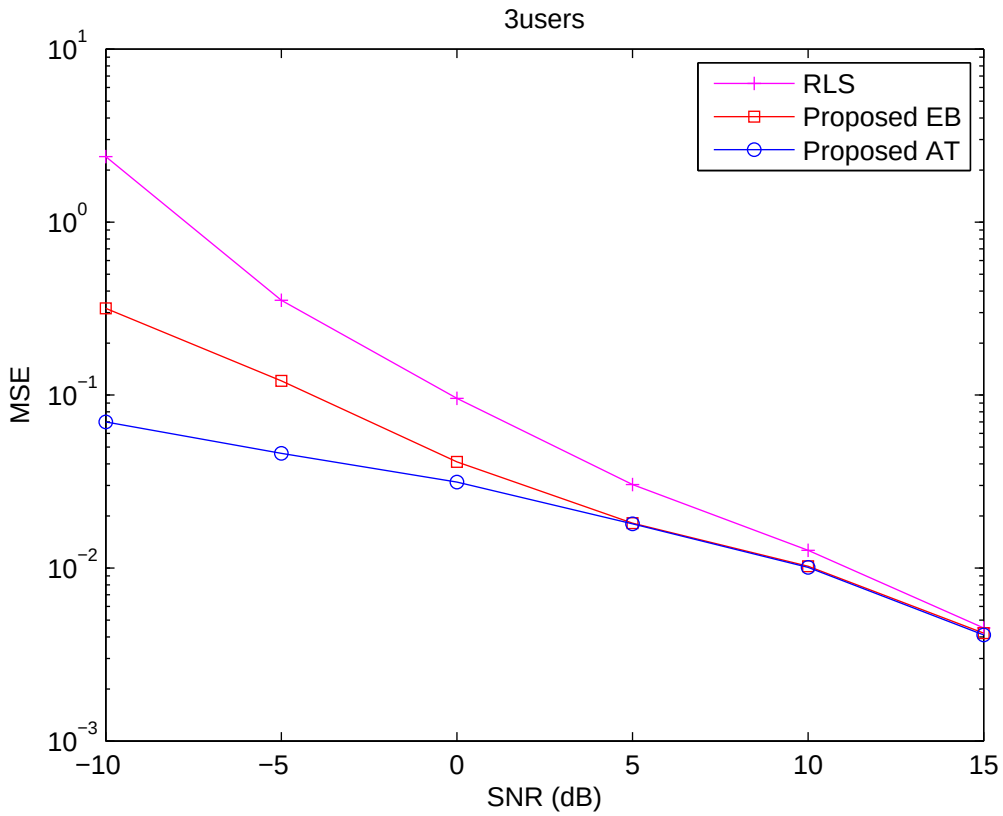

Fig. 6.2: MSE performance ($\|\mathbf{h} - \hat{\mathbf{h}}\|^2$) of the biased SCE with different SNRs.

the same as in Chapter 5. The pulse shape adopted is the RRC pulse with the pulse-width $T_c = 0.375ns$. The length of the data block is set to $N = 32$ symbols. The Walsh spreading code with a spreading gain $N_c = 8$ is generated for the simulations and we assume that the maximum number of active users is 7. The channel has been simulated according to the standard IEEE 802.15.4a channel model for the NLOS indoor environment as shown in [23]. We assume that the channel is constant during the whole transmission and the time domain CIR has 100 taps. The sampling rate of the standard channel model is $8GHz$. The CP guard interval has the length of 35 chips, which has the equivalent length of 105 samples and it is enough to eliminate the IBI. The uncoded data rate of the communication is approximately 293Mbps. For all the simulations, the adaptive filters are initialized as null vectors. All the curves are obtained by averaging 200 independent simulations.

In the first experiment, we examine the proposed biased estimators for the SCE in a single user system with 0dB SNR. In Fig. 6.1, the MSE performance of the channel estimators are compared as a function of number of blocks transmitted. The RLS algorithm approaches the unbiased CRLB given in (6.44) while the proposed biased estimators ap-

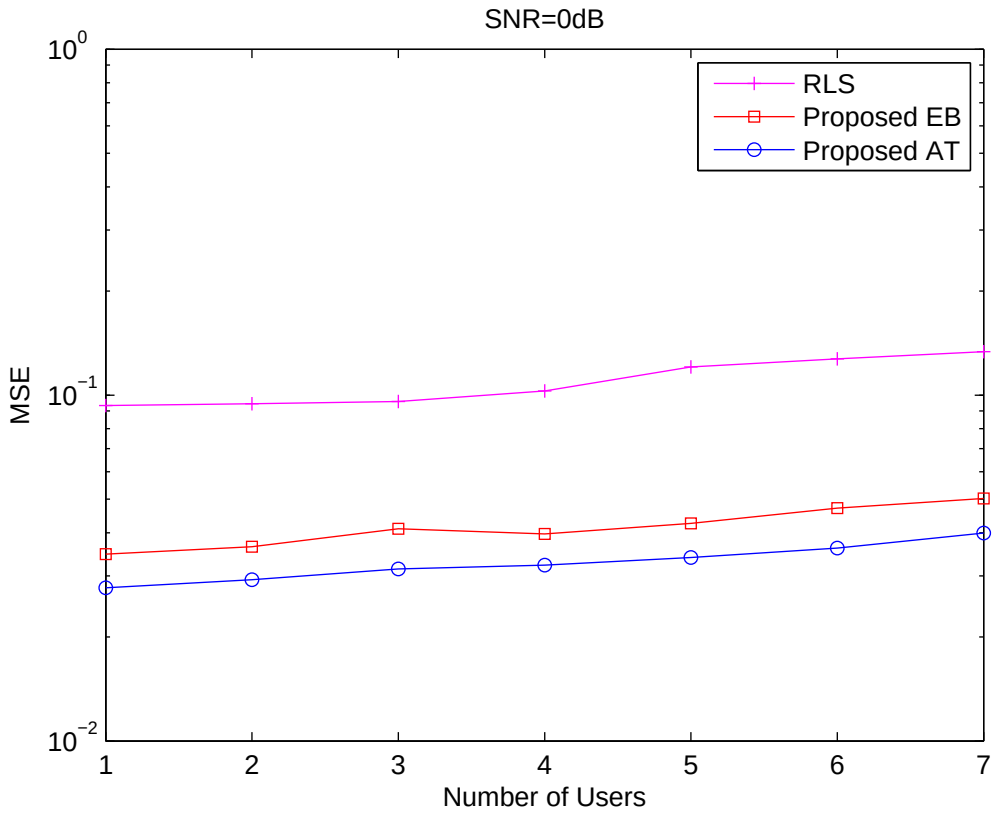

Fig. 6.3: MSE performance ($\|\mathbf{h} - \hat{\mathbf{h}}\|^2$) of the biased SCE with different number of users.

proach the extended CRLB as given in (6.47). The proposed estimators converge faster than the RLS algorithm and the stead-state performance is also improved. The proposed AT algorithm in this scenario performs the best. Note that the additional complexity to employ the biased estimation techniques increases linearly with the length of the channel.

Fig. 6.2 illustrates the MSE performance of different channel estimators in a scenario with 3 users and different SNRs. The parameters for the adaptive algorithms are the same as those used to obtain Fig. 6.1 and 200 training blocks are transmitted for each run. For all the simulated SNRs, the proposed biased algorithms outperform the RLS algorithm. In low SNR scenarios, the gain achieved by the biased estimator is larger than in the high SNR scenarios.

Fig. 6.3 shows the MSE performance of different channel estimators in a 0dB scenario, with different numbers of active users. The parameters for the adaptive algorithms are the same as those used to obtain Fig. 6.1 and 200 training blocks are transmitted for each run. The proposed biased algorithms outperform RLS algorithm in all the scenarios.

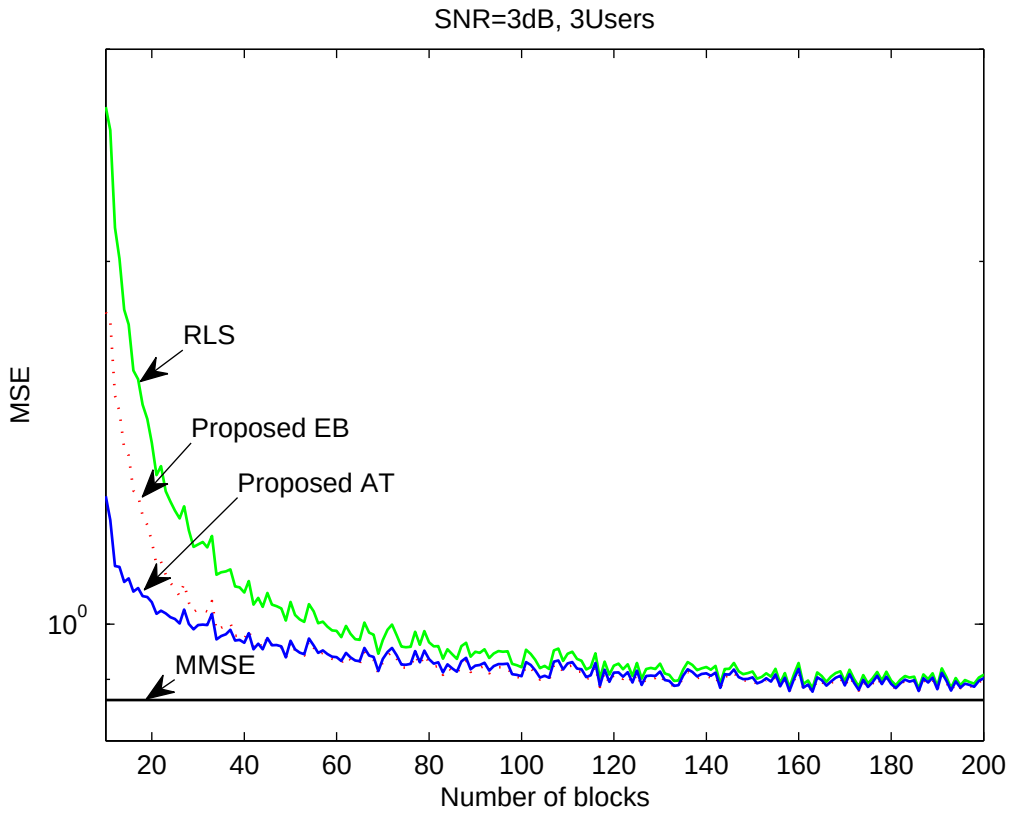

Fig. 6.4: MSE performance ($\|\mathbf{b} - \hat{\mathbf{b}}\|^2$) of the biased estimator in DA-RLS scheme with 3users in 3dB SNR. The parameters used: RLS ($\lambda = 0.998$, $\delta = 2$). Proposed EB: $\mu = 0.0075$ and proposed AT: $\mu = 0.0075$, $\mu_p = 0.005$, $\hat{P}_{\mathrm{m,min}} = 10$, $\hat{P}_{\mathrm{m,max}} = 20$.

In Fig. 6.4, the MSE performance of the estimators in the DA scheme are compared as a function of number of blocks transmitted. There is an initial gain achieved by the biased estimators and the proposed AT algorithm performs best with 200 transmitted training blocks. Note that the MSE performance compared here is the overall MSE performance that is given by $\|\mathbf{b} - \hat{\mathbf{b}}\|^2$. As discussed in Chapter 6.3.2, although the biased equalizer will have a closer Euclidean distance to the optimal equalizer, equation (6.36) indicates that the shrinkage factor actually will increase the overall MSE between the data vector $\mathbf{b}$ and its estimator. Hence, in the DA scheme, the main idea to employ the biased estimators is to achieve an initial gain for the RLS adaptive algorithm.

In Fig. 6.5, we examine the MSE performance of the estimators in the DA scheme in a short data support scenario. For a 3-user communications with 3 dB SNR, the number of training blocks is set to 50. The parameters for the adaptive algorithms are the same as those used to obtain Fig. 6.4. After the training stage, all the adaptive algorithms are operated in steady-state stage. In this experiment, we show that the biased estimators in the interference suppression scenario (DA scheme as an example) can be employed in the

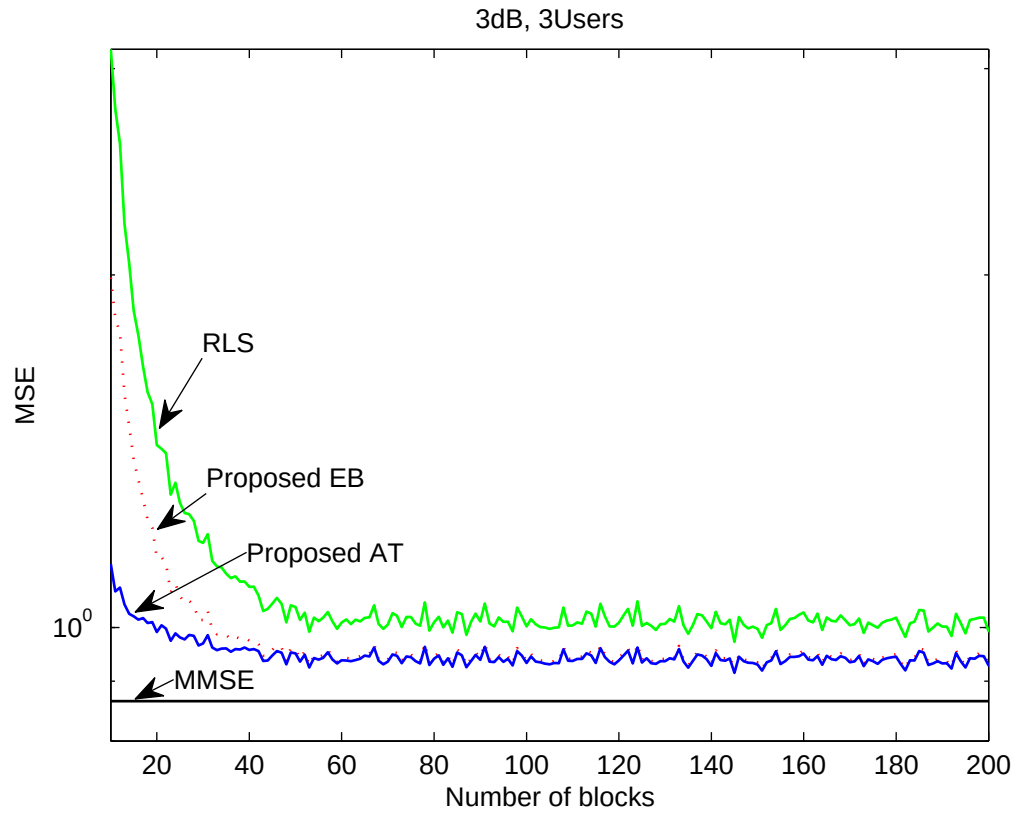

Fig. 6.5: MSE performance ($\|\mathbf{b} - \hat{\mathbf{b}}\|^2$) of the biased estimator in short data support DA-RLS scheme with 3users in a scenario with SNR=3dB.

systems with short training sequence and the initial gain can be maintained.

In Fig. 6.6, we examine the MSE performance of the estimators in the DA scheme in a 10dB SNR scenario. The proposed estimators still have an initial gain over the conventional RLS algorithm. In this scenario, the overall MSE performance loss introduced by the proposed AT algorithm can be spotted after around 40 blocks transmitted. However, for the EB algorithm, the performance is still better than the RLS with 200 training blocks.

In Fig. 6.7, we examine the uncoded BER performance of the biased estimators in the SCE scheme in a system with 3 users in different SNRs. In this experiment, the parameters for the adaptive algorithms are the same as those used to obtain Fig. 6.1 and only 50 training blocks are transmitted for each run. The proposed biased estimators achieve a BER gain around 1dB at the low SNR scenarios. The proposed AT scheme outperforms the EB and conventional RLS algorithm in the tested scenarios. As the SNR increases, the difference between the BER performance of these algorithms become smaller. For the DA scheme, the similar performance gain can be obtained for the proposed biased

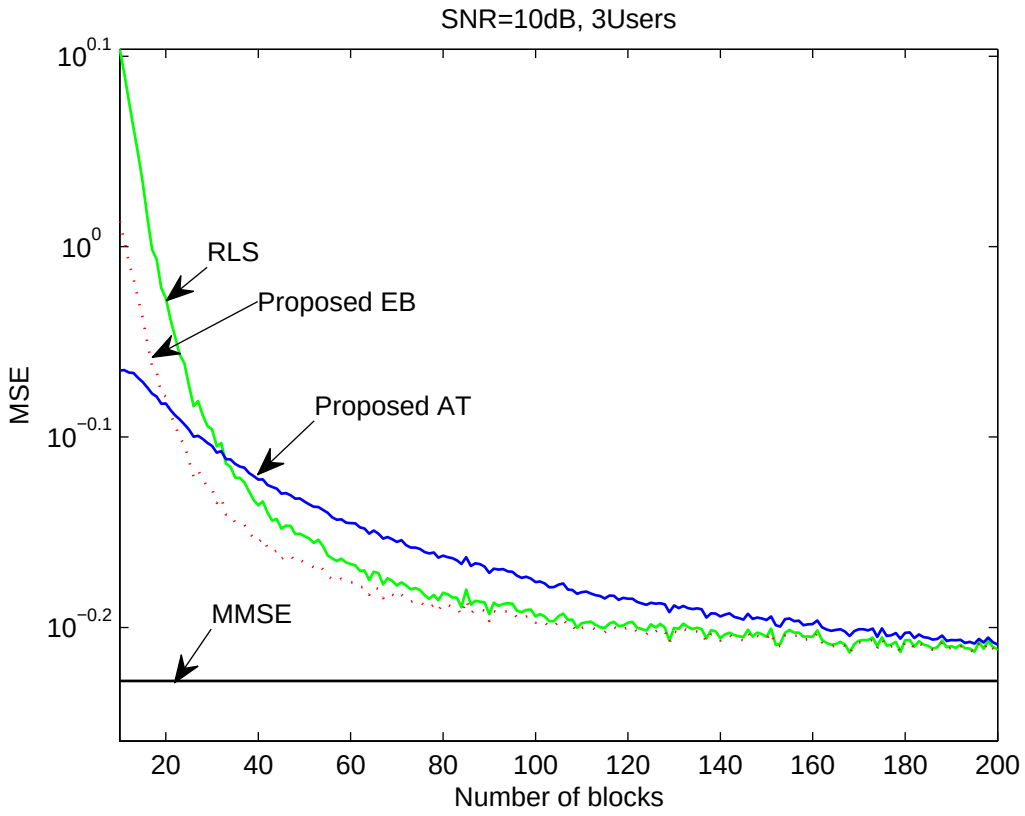

Fig. 6.6: MSE performance ($\|\mathbf{b} - \hat{\mathbf{b}}\|^2$) of the biased estimator in DA-RLS scheme with 3users in a scenario with SNR=10dB.

estimators and the results is not included in the figure for the sake of clarity.

6.6 Conclusion

In this Chapter, shrinkage biased estimators are developed in the scenarios of parameter estimation and interference suppression. LMS-based adaptive algorithms are devised to obtain the shrinkage factors. The biased CRLB has been computed and we have extended it to obtain a lower bound for the MSE performance of the shrinkage biased estimators. The incorporation of the proposed estimators has been considered in the detection schemes of SCE and DA as introduced in Chapter 5. The simulation results demonstrate the improved MSE performance of the biased estimators in different scenarios.

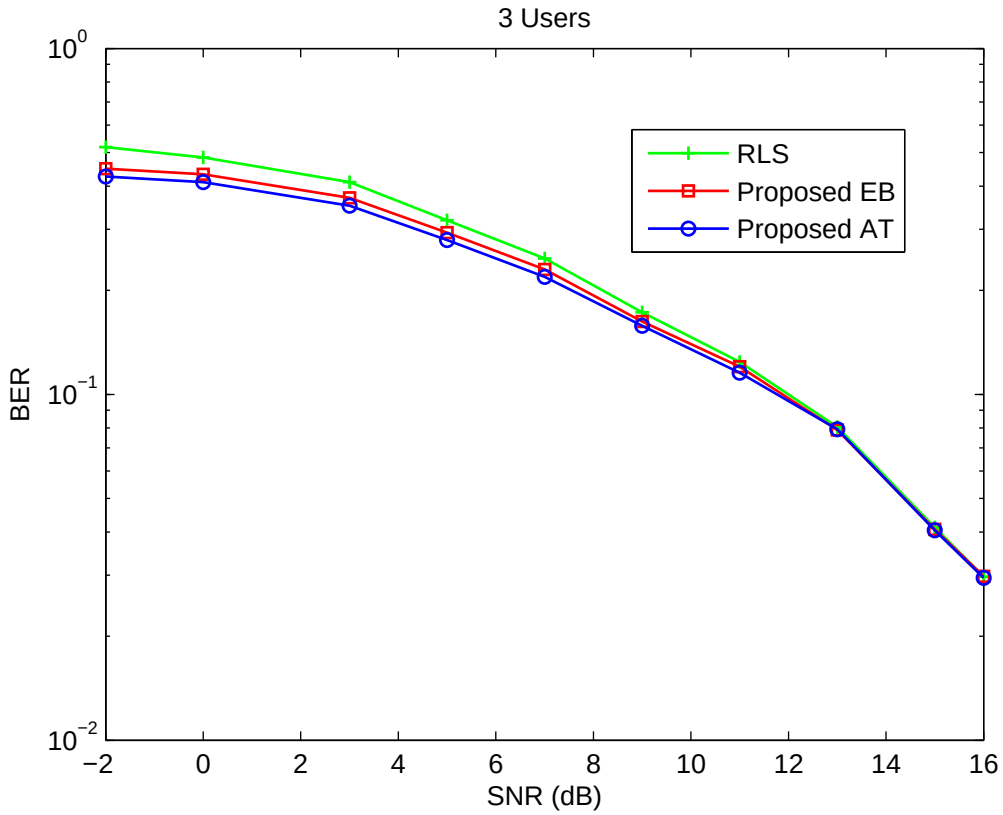

Fig. 6.7: BER performance in SCE scheme with different SNRs in a 3 user scenario.

7. CONCLUSIONS AND FUTURE WORK

Contents

7.1 Summary of Work

In this thesis, we have investigated interference suppression adaptive algorithms for the multiuser DS-UWB systems. These algorithms are implemented in the time domain in symbol by symbol transmission systems and in the frequency domain in block by block transmission systems. Reduced-rank adaptive algorithms are proposed for the time domain interference suppression tasks, a novel generic reduced-rank receiver and SAABF scheme are proposed with LMS and RLS adaptive algorithms that are developed based on the MMSE criterion (Chapter 3), blind reduced-rank receivers are proposed based on the CCM criterion and NSG and RLS versions are developed (Chapter 4). The LMS, RLS and CG-based adaptive detectors are developed for SC-FDE in DS-UWB systems (Chapter 5) and shrinkage estimators are proposed to improve the performance of the RLS versions of the frequency domain detectors (Chapter 6). The proposed reduced-rank receivers can be employed in spread-spectrum systems which encounter large filter problems and suffer from severe interferences. The adaptive algorithms that is developed in SC-FDE systems can also be used in OFDM systems.

In Chapter 3, firstly, a generic reduced-rank scheme that jointly updates the projection vector and the reduced-rank filter is proposed. We pointed out that although this generic scheme outperforms the existing reduced-rank schemes in the multiuser DS-UWB systems, it still has high computational complexity. Hence, a novel reduced-rank interference suppression scheme is investigated and named SAABF, in which the design of the projection vector in the generic scheme is constrained with a multi-branch structure and the significant complexity reduction is achieved. Simulation results demonstrate that the performance of the generic scheme is maintained in the SAABF scheme. Then, LMS and

RLS algorithms were developed for adaptive implementation of the SAABF scheme. A discussion of the global optimality of the reduced-rank filter was presented, and the relationships between the SAABF and the generic scheme and the full-rank scheme were established. We remark that the proposed SAABF scheme is a promising low-complexity solution for the communication systems that encounter large filter problems and severe interferences.

In Chapter 4, blind reduced-rank adaptive receivers based on the JIO and CCM criterion are proposed for the multiuser DS-UWB systems. The NSG and RLS adaptive algorithms are developed for the proposed blind receiver. In the RLS version, the columns of the projection matrix are updated one by one. We found that the performance of the blind reduced-rank scheme can be improved by calculating the columns of the projection matrix individually. This is because the columns of the projection matrix can be considered as the direction vectors on the dimensions of the subspace and a better representation of the projection procedure can be obtained via using the column-by-column adaptation. However, the computational complexity will be increased by using the column-by-column adaptation. In order to reduce the complexity, an approximation is devised for the RLS version. The robustness of the proposed receivers has been demonstrated in the scenario that the blind receivers are required to suppress the ISI, MAI and NBI together. Compared to the SAABF scheme proposed in Chapter 3, the proposed blind reduced-rank receivers offer higher spectrum efficiency while only requiring the time synchronization and the spreading code of the desired user.

In Chapter 5, two adaptive detection schemes are proposed based on the MMSE linear detection strategy for SC-FDE in DS-UWB systems, which are termed SCE and DA. Cyclic prefix is employed in both schemes. LMS, RLS and CG adaptive algorithms are developed for the adaptive implementations. For the SCE scheme, the channel estimation is carried out in the frequency domain and the estimated channel coefficients are then substituted into the expression of the MMSE detector. It should be noted that the noise variance and the number of users are required in the expression of the MMSE detector. For this purpose, we estimate the noise variance via the maximum likelihood (ML) method and develop a low-complexity algorithm to estimate the number of active users. For the DA scheme, only one filter is implemented in the frequency domain to suppress the interference. A new signal model is employed in the DA scheme and is extended to the adaptive implementations that enables a simplified linear adaptive filter design. Simulation results illustrate that the SCE scheme outperforms the DA scheme in the multiuser DS-UWB systems, while the DA scheme has a simpler receiver structure and lower complexity.

In Chapter 6, biased adaptive estimation techniques based on shrinkage estimators are devised and incorporated into RLS versions of the SCE and DA schemes that are proposed in Chapter 5. LMS-based adaptive algorithms are proposed to recursively compute the shrinkage factors. For the SCE scheme, the biased estimator achieves a lower MSE of the channel estimation than the SCE-RLS. For the DA scheme, the biased estimator is developed to reduce the MSE of the estimated equalizer. Note that to equip these biased estimators, the additional complexity required increases linearly with the length of the estimated parameter vector. In this chapter, the biased CRLB that constitutes a fundamental estimation limit of the shrinkage estimators is computed and we extend it to a lower bound for the MSE performance of the shrinkage estimators. Simulations are carried out in multiuser DS-UWB systems and the performance improvements are achieved in low SNR scenarios and with short data support. The biased estimators obtained in this work are developed in general expressions for the scenarios of parameter estimation and interference suppression. Hence, they can be implemented into other communication systems to improve the performance of the unbiased LS solutions, especially for the systems that operate in low SNR and with short data support.

7.2 Future Work

Some suggestions for future work based on this thesis are given below.

In Chapter 3, novel reduced-rank algorithms are proposed based on the JIO and switching. One possible future implementation scenario of the proposed schemes is the cooperative UWB communication systems. In a cooperative transmission system, data is transmitted or relayed from the terminals or users to the destination user or terminal. The main reason to employ the cooperative communication is to transmit information through an optimally selected or combined route from all the possibilities such that the communication resources can be fully utilized and systems can perform with increased reliability, lower transmit power, larger coverage and higher transmission rate [98]- [101]. For DS-UWB systems, cooperative communications have the potential to increase the coverage and the data rate while requiring low transmitted power. In Chapter 3, the proposed SAABF scheme is a promising technique to the cooperative communications because of its low-complexity and remarkable interference suppression ability. Another possible implementation of the SAABF scheme is to modify it to achieve timing acquisition. For the UWB systems, accurate timing acquisition is required and the performance may loss dramatically if the timing errors larger than a small fraction of nanosecond [102]. In [103], a near-far-resistant demodulator with symbol-level timing acquisition scheme is proposed

based on MMSE criterion for CDMA systems in AWGN channel. We can modify the SAABF scheme to solve the MMSE synchronization problem as modeled in [103] for DS-UWB systems.

In Chapter 4, blind reduced-rank algorithms are proposed for DS-UWB systems based on CCM and JIO criterion. The BER performance can be improved by including coding techniques such as turbo and low-density parity-check (LDPC) coding. An iterative (turbo) equalizer has been proposed for MSWF-based reduced-rank scheme in [104], in which the performance of the coded reduced-rank scheme is significantly better than the uncoded schemes. We can also employ channel coding into the blind reduced-rank algorithms in the future work. Since the performance of the proposed JIO-CCM schemes outperforms the MSWF algorithms in the uncoded systems, a large coding gain can be expected from the proposed scheme.

In Chapter 5, the adaptive frequency domain detection schemes have been proposed for SC-FDE in DS-UWB systems. In fact, the signal model employed and the adaptive algorithms developed in this chapter can be modified to operate in OFDM-based block by block transmission systems. In Chapter 6, biased estimators are proposed to improve the performance of the RLS versions of the frequency domain equalizers that are introduced in Chapter 5. A further development of the biased estimation can be achieved by introducing a matrix-form shrinkage factor. For example, the biased estimator in parameter estimation scenario proposed in Chapter 6 is given by $\hat{\mathbf{h}}_{\mathrm{b}} = (1+\alpha)\hat{\mathbf{h}}_{\mathrm{u}}$, where a scalar shrinkage factor is employed for all the parameters in the L-dimensional vector $\hat{\mathbf{h}}_{\mathrm{u}}$. For a further development, the biased estimator can be expressed as $\hat{\mathbf{h}}_{\mathrm{b}} = (\mathbf{I}+\mathbf{M})\hat{\mathbf{h}}_{\mathrm{u}}$, where $\mathbf{M}$ is a diagonal matrix and its diagonal vector is $\mathbf{m} = [\alpha_1, \alpha_2, \ldots, \alpha_L]$. This method will allow a better way to assign the bias for each parameter in the vector $\hat{\mathbf{h}}_{\mathrm{u}}$.

APPENDIX

A. PROOF OF THE EQUIVALENCE OF THE SCHEMES

In this section, we prove that the SAABF (1,D,M) is equivalent to the the generic scheme and the SAABF (1,1,M) is equivalent to the full-rank scheme.

Firstly, we express the MMSE solutions for the SAABF scheme as

$$\bar{\mathbf{w}}_{\mathrm{MMSE}} = \bar{\mathbf{R}}^{-1}\bar{\mathbf{p}},\ \boldsymbol{\psi}_{\mathrm{MMSE}} = \mathbf{R}_{\psi}^{-1}\mathbf{p}_{\psi} \tag{A.1}$$

where $\bar{\mathbf{R}} = E[\mathbf{R}_{\mathrm{in}}(i)\mathbf{P}(i)\boldsymbol{\psi}(i)\boldsymbol{\psi}^H(i)\mathbf{P}^H(i)\mathbf{R}_{\mathrm{in}}^H(i)]$, $\bar{\mathbf{p}} = E[d^*(i)\mathbf{R}_{\mathrm{in}}(i)\mathbf{P}(i)\boldsymbol{\psi}(i)]$, $\mathbf{R}_{\psi} = E[\mathbf{P}^H(i)\mathbf{R}_{\mathrm{in}}^H(i)\bar{\mathbf{w}}(i+1)\bar{\mathbf{w}}^H(i+1)\mathbf{R}_{\mathrm{in}}(i)\mathbf{P}(i)]$ and $\mathbf{p}_{\psi} = E[d(i)\mathbf{P}^H(i)\mathbf{R}_{\mathrm{in}}^H(i)\bar{\mathbf{w}}(i+1)]$. Revisit the expression of the basis functions in the SAABF scheme in (3.12). In SAABF (1,D,M), the length of the inner function equals to the length of the basis function and the position matrix in (3.13) becomes an MD-by-MD identity matrix. Hence, the MMSE solutions of the generic scheme shown in (3.10) are the same as (A.1) when $\mathbf{P}(i)$ is an identity matrix, which means the SAABF (1,D,M) is equivalent to the generic scheme.

Secondly, we prove that the SAABF (1,1,M), or the generic scheme with D=1, is equivalent to the full-rank scheme in the sense that they have the same MMSE corresponding to the optimum solutions. Here, we expand the cost function of the generic scheme that is shown in (3.9)

$$\begin{aligned}\mathbf{J}_{\mathrm{G}} = \sigma_d^2 &- E[d(i)\mathbf{t}^H(i)\mathbf{R}_{\mathrm{in}}^H(i)\bar{\mathbf{w}}(i)] - E[d^*(i)\bar{\mathbf{w}}^H(i)\mathbf{R}_{\mathrm{in}}(i)\mathbf{t}(i)] \\ &+ E[\bar{\mathbf{w}}^H(i)\mathbf{R}_{\mathrm{in}}(i)\mathbf{t}(i)\mathbf{t}^H(i)\mathbf{R}_{\mathrm{in}}^H(i)\bar{\mathbf{w}}(i)].\end{aligned} \tag{A.2}$$

In the case of D=1, the input data matrix $\mathbf{R}_{\mathrm{in}}(i)$=$\mathbf{r}^T(i)$ becomes a 1-by-M vector, the reduced-rank filter has only one tap and hence the $\bar{w}_{\mathrm{opt}}$ is a scalar term and we can find the relationship between $\mathbf{t}_{\mathrm{opt}}$ and $\bar{w}_{\mathrm{opt}}$ as

$$\mathbf{t}_{\mathrm{opt}} = (E[\mathbf{r}^*(i)\mathbf{r}^T(i)]\bar{w}_{\mathrm{opt}}\bar{w}_{\mathrm{opt}}^*)^{-1}E[d(i)\mathbf{r}^*(i)]\bar{w}_{\mathrm{opt}} = (\mathbf{R}^T)^{-1}\mathbf{p}^*(\bar{w}_{\mathrm{opt}}^*)^{-1}$$

Hence, the second term in (A.2) becomes

$$E[d(i)\mathbf{t}^H(i)\mathbf{R}_{\text{in}}^H(i)\bar{\mathbf{w}}(i)] = \mathbf{t}_{\text{opt}}^H E[d(i)\mathbf{r}^*(i)]\bar{w}_{\text{opt}} = [(\mathbf{R}^T)^{-1}\mathbf{p}^*(\bar{w}_{\text{opt}}^*)^{-1}]^H\mathbf{p}^*\bar{w}_{\text{opt}} \\ = \mathbf{p}^T(\mathbf{R}^T)^{-1}\mathbf{p}^* = (\mathbf{p}^H\mathbf{R}^{-1}\mathbf{p})^T = \mathbf{p}^H\mathbf{R}^{-1}\mathbf{p}. \tag{A.3}$$

Note that here we use the fact that the transpose of the scale term $\mathbf{p}^H\mathbf{R}^{-1}\mathbf{p}$ is itself and $(\mathbf{R}^T)^H = \mathbf{R}^T$. Since the third scalar term in (A.2) is the conjugate of the second term, we have $E[d^*(i)\bar{\mathbf{w}}^H(i)\mathbf{R}_{\text{in}}(i)\mathbf{t}(i)] = (\mathbf{p}^H\mathbf{R}^{-1}\mathbf{p})^H = \mathbf{p}^H\mathbf{R}^{-1}\mathbf{p}$. The fourth term of (A.2) can be expanded as

$$E[\bar{\mathbf{w}}^H(i)\mathbf{R}_{\text{in}}(i)\mathbf{t}(i)\mathbf{t}^H(i)\mathbf{R}_{\text{in}}^H(i)\bar{\mathbf{w}}(i)] = \bar{w}_{\text{opt}}^* E[\mathbf{r}^T(i)\mathbf{t}_{\text{opt}}\mathbf{t}_{\text{opt}}^H\mathbf{r}^*(i)]\bar{w}_{\text{opt}} \\ = \bar{w}_{\text{opt}}^* E[\mathbf{t}_{\text{opt}}^H\mathbf{r}^*(i)\mathbf{r}^T(i)\mathbf{t}_{\text{opt}}]\bar{w}_{\text{opt}} = \mathbf{p}^T(\mathbf{R}^T)^{-1}\mathbf{p}^* = \mathbf{p}^H\mathbf{R}^{-1}\mathbf{p}. \tag{A.4}$$

Hence, the MMSE of the generic scheme for D=1 is $\mathbf{J}_{\text{GMMSE}} = \sigma_d^2 - \mathbf{p}^H\mathbf{R}^{-1}\mathbf{p}$, which is the same as the MMSE obtained via the full-rank Wiener filter as shown in (3.4). This completes the proof.

B. ANALYSIS OF THE OPTIMIZATION PROBLEM

In this Appendix, we discuss the optimization problem of the proposed SAABF scheme. Specially, we consider the convergence of the SAABF scheme via the computation of the Hessian matrix of the MSE cost function which can be expressed as

$$\mathbf{J}_{\mathrm{MSE}}(\bar{\mathbf{w}}(i), \boldsymbol{\psi}(i)) = E[|d(i) - \bar{\mathbf{w}}^H(i)\mathbf{R}_{\mathrm{in}}(i)\mathbf{P}(i)\boldsymbol{\psi}(i)|^2]. \tag{B.1}$$

It is known that the convexity of the function can be verified if its Hessian matrix is positive semi-definite. However, the SAABF scheme includes a discrete optimization of the position matrix and a continuous adaptation of the reduced-rank filter and the projection vector. For the position matrix selection problem, we constrain the design of the position matrix to a small number of pre-stored matrices and switch between these matrices to choose the instantaneous sub-optimum position matrix. This feature of the SAABF scheme suggests that the optimum values of the three variables of the MSE cost function may be difficult to obtain together, and that there are multiple solutions of the cost function. The convexity is only verified when we consider one of the continuously adapted variables whilst the others are kept fixed. Firstly, let us compute the D-by-D Hessian matrix for (B.1) with respect to the reduced-rank filter:

$$\mathbf{H}_{J,\bar{\mathbf{w}}} = \frac{\partial^2 \mathbf{J}_{\mathrm{MSE}}}{\partial \bar{\mathbf{w}}^H(i) \partial \bar{\mathbf{w}}(i)} = E[\mathbf{R}_{\mathrm{in}}(i)\mathbf{P}(i)\boldsymbol{\psi}(i)\boldsymbol{\psi}^H(i)\mathbf{P}^H(i)\mathbf{R}_{\mathrm{in}}^H(i)]. \tag{B.2}$$

For any D-dimensional non-zero vector $\mathbf{a}$, we discuss the following scale term

$$\mathbf{a}^H\mathbf{H}_{J,\bar{\mathbf{w}}}\mathbf{a} = E[\mathbf{a}^H\mathbf{R}_{\mathrm{in}}(i)\mathbf{P}(i)\boldsymbol{\psi}(i)\boldsymbol{\psi}^H(i)\mathbf{P}^H(i)\mathbf{R}_{\mathrm{in}}^H(i)\mathbf{a}] = E[\hat{a}(i)\hat{a}^*(i)] = E[|\hat{a}(i)|^2], \tag{B.3}$$

where $\hat{a}(i) = \mathbf{a}^H\mathbf{R}_{\mathrm{in}}(i)\mathbf{P}(i)\boldsymbol{\psi}(i)$. Assume that the position matrix $\mathbf{P}(i)$ and the projection vector $\boldsymbol{\psi}(i)$ are fixed. The scale term in (B.3) is always nonnegative. Hence, the Hessian matrix $\mathbf{H}_{J,\bar{\mathbf{w}}}$ is a positive semi-definite matrix. Similarly, the qD-by-qD Hessian matrix for (B.1) with respect to the projection vector is

$$\mathbf{H}_{J,\boldsymbol{\psi}} = E[\mathbf{P}^H(i)\mathbf{R}_{\mathrm{in}}^H(i)\bar{\mathbf{w}}(i)\bar{\mathbf{w}}^H(i)\mathbf{R}_{\mathrm{in}}(i)\mathbf{P}(i)], \tag{B.4}$$

which is also a positive semi-definite matrix if the position matrix and the reduced-rank filter are fixed.

In the SAABF scheme, after determined the position matrix, the optimization problems for the projection vector and the reduced-rank filter can be consider as a bi-convex problem [78]: by fixing one of the parameters, the other design problem is convex. In order to test the convergence of the SAABF scheme in the case of jointly updating $\bar{\mathbf{w}}(i)$ and $\boldsymbol{\psi}(i)$, we checked the impact of different initializations, which confirmed that the performance of the algorithms are not subject to degradation due to the initialization. However, the proof of the global optimum and no local minima with the joint adaptive algorithm remains an interesting open problem to be researched.

C. CONVERGENCE PROPERTIES FOR THE CCM FUNCTION

In this section, we examine the convergence properties of the cost function $\mathbf{J}_{\text{JIO}} = \frac{1}{2}E\left[(|y(i)|^2-1)^2\right]$, where $y(i) = \bar{\mathbf{w}}^H(i)\mathbf{T}^H(i)\mathbf{r}(i)$. For simplicity of the following analysis, we drop the time index (i). The received signal is given by

$$\begin{aligned}\mathbf{r} &= \sum_{k=1}^{K}\sqrt{E_k}\mathbf{P}_r\mathbf{S}_{e,k}\mathbf{h}_k b_k + \boldsymbol{\eta} + \mathbf{n}, \\ &= \sum_{k=1}^{K}\sqrt{E_k}b_k\mathbf{p}_k + \boldsymbol{\eta} + \mathbf{n} = \mathbf{P}_k\mathbf{A}_k\mathbf{b} + \boldsymbol{\eta} + \mathbf{n},\end{aligned} \tag{C.1}$$

where $\mathbf{p}_k = \mathbf{P}_r\mathbf{S}_{e,k}\mathbf{h}_k$, $k = 1,\ldots,K$, are the signature vectors of the users. $\mathbf{P}_k = [\mathbf{p}_1,\ldots,\mathbf{p}_K]$, $\mathbf{A}_k = diag(\sqrt{E_1},\ldots,\sqrt{E_K})$ and $\mathbf{b} = [b_1,\ldots,b_K]$. $\boldsymbol{\eta}$ and $\mathbf{n}$ represent the ISI and AWGN, respectively. We assume that b_k, $k = 1,\ldots,K$, are statistically independent i.i.d random variables with zero mean and unit variance and are independent to the noises. Firstly, we will discuss the noise-free scenario for the analysis, in which, the output signal of the JIO receiver is given by

$$y = \bar{\mathbf{w}}^H\mathbf{T}^H\mathbf{P}_k\mathbf{A}_k\mathbf{b} = \boldsymbol{\epsilon}^H\mathbf{b}, \tag{C.2}$$

where $\boldsymbol{\epsilon} \triangleq \mathbf{A}_k^H\mathbf{P}_k^H\mathbf{T}\bar{\mathbf{w}} = [\epsilon_1,\ldots,\epsilon_K]$. Assuming that user 1 is the desired user and recalling the constraint $\bar{\mathbf{w}}^H\mathbf{T}^H\mathbf{p}_1 = \mathbb{v}$, where $\mathbb{v}$ is a real-valued constant. We obtain that the first element of the vector $\boldsymbol{\epsilon}$ can be expressed as

$$\epsilon_1 = \sqrt{E_1}\mathbf{p}_1^H\mathbf{T}\bar{\mathbf{w}} = \sqrt{E_1}\mathbb{v}. \tag{C.3}$$

Now, let us have a closer look at the cost function,

$$\begin{aligned}\mathbf{J}_{\mathrm{JIO}} &= \frac{1}{2}E\left[|y(i)|^4 - 2|y(i)|^2 + 1\right] \\ &= \frac{1}{2}\left(E\left[(\boldsymbol{\epsilon}^H\mathbf{b}\mathbf{b}^H\boldsymbol{\epsilon})^2\right] - 2E\left[\boldsymbol{\epsilon}^H\mathbf{b}\mathbf{b}^H\boldsymbol{\epsilon}\right] + 1\right) \\ &= \frac{1}{2}\left(\sum_{k=1}^{K}\sum_{j=1}^{K}|\epsilon_k|^2|\epsilon_j|^2|b_k|^2|b_j|^2 - 2\sum_{k=1}^{K}|\epsilon_k|^2|b_k|^2 + 1\right) \\ &= \frac{1}{2}\left(\sum_{k=1}^{K}\sum_{j=1}^{K}|\epsilon_k|^2|\epsilon_j|^2 - 2\sum_{k=1}^{K}|\epsilon_k|^2 + 1\right) \\ &= \frac{1}{2}(|\epsilon_1|^2 + \tilde{\boldsymbol{\epsilon}}^H\tilde{\boldsymbol{\epsilon}})^2 - (|\epsilon_1|^2 + \tilde{\boldsymbol{\epsilon}}^H\tilde{\boldsymbol{\epsilon}}) + \frac{1}{2}\end{aligned} \tag{C.4}$$

where $\tilde{\boldsymbol{\epsilon}} = [\epsilon_2, \ldots, \epsilon_k] = \tilde{\mathbf{A}}_k^H\tilde{\mathbf{P}}_k^H\mathbf{T}\bar{\mathbf{w}}$, $\tilde{\mathbf{P}}_k = [\mathbf{p}_2, \ldots, \mathbf{p}_K]$ and $\tilde{\mathbf{A}}_k = diag(\sqrt{E_2}, \ldots, \sqrt{E_K})$. Equation (C.4) transforms the cost function of both $\mathbf{T}$ and $\bar{\mathbf{w}}$ into a function with single variable $\tilde{\boldsymbol{\epsilon}}$. We remark that $\tilde{\boldsymbol{\epsilon}}$ is a linear function of $\mathbf{T}\bar{\mathbf{w}}$ that is the blind reduced-rank receiver. Hence, the convexity properties of the cost function with respect to $\tilde{\boldsymbol{\epsilon}}$ reflects the convexity properties of the cost function with respect to $\mathbf{T}\bar{\mathbf{w}}$. To evaluate the convexity of $\mathbf{J}_{\mathrm{JIO}}$, we compute its Hessian that is given by

$$\mathbf{H}_{JIO} = \frac{\partial}{\partial\tilde{\boldsymbol{\epsilon}}^H}\frac{\partial\mathbf{J}_{\mathrm{JIO}}}{\partial\tilde{\boldsymbol{\epsilon}}} = 2\tilde{\boldsymbol{\epsilon}}\tilde{\boldsymbol{\epsilon}}^H + (|\epsilon_1|^2 - 1)\mathbf{I}. \tag{C.5}$$

It can be concluded that a sufficient condition for $\mathbf{H}_{JIO}$ to be a positive definite matrix is $|\epsilon_1|^2 > 1$, which is $E_1\mathbb{v}^2 > 1$. This condition is obtained in noiseless scenario, however, it also holds for small σ^2 that can be considered as a slight perturbation of the noise-free case [54]. For larger values of σ^2, the term $\mathbb{v}$ can be adjusted to ensure the convexity of the cost function.

BIBLIOGRAPHY

[1] R. A. Scholtz, "Multiple access with time-hopping impulse modulation," *Proc. IEEE MILCOM*, pp. 447-450, 1993.

[2] M. Z. Win and R. A. Scholtz, "Impulse radio: how it works," *IEEE Communications Letters*, vol. 2, no. 2, pp. 36-38, Feb. 1998.

[3] M. Z. Win and R. A. Scholtz, "Ultra-wide bandwidth time-hopping spread-spectrum impulse radio for wireless multiple-acess communications," *IEEE Trans. Communications*, vol. 48, no. 4, pp. 679-689, Apr. 2000.

[4] First report and order FCC-02048, Federal Communications Commission, 2002.

[5] R. C. Qiu, "A Study of the Ultra-Wideband Wireless Propagation Channel and Optimum UWB Receiver Design," *IEEE Journal on Selected Areas in Communications*, vol. 20, no. 9, pp. 1628-1637, Dec. 2002.

[6] I. Oppermann et al., *UWB Theory and Applications*, John Wiley, 2004.

[7] K. Siwiak and D. McKeown, *Ultra-wideband Radio Technology*, Wiley, Apr. 2004.

[8] F. Nekoogar, *Ultra Wideband Communications: Fundamentals and Application*, Prentice Hall, Dec. 2004.

[9] D. Tse and P. Viswanath, *Fundamentals of Wireless Communication*, Cambridge University Press, 2005.

[10] M. Ghavami, L. B. Michael and R. Kohno, *Ultra Wideband Signals and Systems in Communication Engineering*, John Wiley, 2004.

[11] D. Cassioli, M. Z. Win et al., "Low Complexity Rake Receivers in Ultra-Wideband Channels," *IEEE Trans. Wireless Communications*, vol. 6, no. 4, pp. 1265-1275, Apr. 2007.

[12] R. Fisher, R. Kohno et al., "DS-UWB Physical Layer Submission to IEEE 802.15 Task Group 3a (Doc. Number P802.15-04/0137r4)," IEEE P802.15, Jan. 2005.

[13] B. Parr, B. Cho, K. Wallace and Z. Ding, "A novel ultra-wideband pulse design algorithm," *IEEE Communications Letters*, vol. 7, no. 5, pp. 219-221, May. 2003.

[14] X. Wu, Z. Tian, T. N. Davidson and G. B. Giannakis, "Optimal Waveform Design for UWB Radios," *IEEE International Conference on Acoustics, Speech, and Signal Processing*, 2004. Proceedings.

[15] M. Z. Win, D. Dardari, A. F. Molish et al., "History and Applications of UWB," *Proceedings of the IEEE*, vol. 97, no. 2, pp 198-204, Feb. 2009.

[16] B. Mielczarek, M. Wessman and A. Svensson, "Performance of Coherent UWB Rake Receivers using different Channel Estimators," *IEEE Vehicular Technology Conference*, vol. 3, pp. 1880-1884, Oct. 2003.

[17] A. Parihar, L. Lampe, R. Schober, and C. Leung, "Equalization for DS-UWB systems–Patr I: BPSK modulation," *IEEE Trans. Communications*, vol. 55, no. 6 pp. 1164-1173, Jun. 2007.

[18] M. Hamalainen, R. Tesi, J. Iinatti and V. Hovinen, "On the Performance Comparison of Different UWB Data Modulation Schemes in AWGN Channel in the Presence of Jamming," *IEEE Radio and Wireless Conference*, 2001.

[19] I. Guvenc and H. Arslan, "On the modulation options for UWB systems," *IEEE Military Communications Conference (MILCOM)*, vol. 2, pp. 892¨C897, Oct. 2003.

[20] D. Cassioli, M. Z. Win, and A. F. Molisch, "A statistical model for the UWB indoor channel," *Proc. 53rd IEEE Vehicular Technology Conference*, vol. 2, pp. 1159¨C1163, May. 2001.

[21] D. Cassioli, M. Z. Win and A. F. Molisch, "The Ultra-Wide Bandwidth Indoor Channel: From Statistical Model to Simulations," *IEEE Journal on Selected Areas in Communications*, vol. 20, no. 6, pp 1247-1257, Aug. 2002.

[22] J. Foerster et al., "ChannelModeling Subcommittee Final Report," IEEE, Document IEEE 02490r0P802-15 SG3a, 2003.

[23] A. F. Molisch et al., "IEEE 802.15.4a Channel Model - Final Report," Tech. Rep. Doc. IEEE 802.15-0400662-02-004a, 2005.

[24] A. F. Molisch, "Ultrawideband Propagation Channels-Theory, Measurement, and Modeling," *IEEE Trans. Vehicular Technology*, vol. 54, no. 5, Sep. 2005.

[25] A. F. Molisch et al., "A Comprehensive Standardized Model for Ultrawideband Propagation Channels," *IEEE Trans. Antennas and Propagation*, vol. 54, no. 11, pp. 3151-3166, Nov. 2006.

[26] S. Haykin, *Adaptive Filter Theory,Fourth Edition*, Pearson Education, 2002.

[27] D. P. O'Leary, "The Block conjugate gradient algorithms and Related Methods," *Linear Algebra and its Applications*, vol. 29, pp. 293-322, 1980.

[28] J. S. Lim and C. K. Un, "Block conjugate gradient algorithms for adaptive filtering," *Signal Processing*, vol. 55, pp. 65-77, Nov. 1996.

[29] P. Chang and A. N. Willson,Jr., "Analysis of Conjugate Gradient Algorithms for Adaptive Filtering," *IEEE Trans. Signal Processing*, vol. 48, no. 2, pp. 409-418, Feb. 2000.

[30] H. Ge, L. L. Scharf and M. Lundberg, "Reduced-Rank Multiuser Detectors Based on Vector and Matrix Conjugate Gradient Wiener Filters," *IEEE 5th Workshop on Signal Processing in Wireless Communications*, pp. 189-193, 2004.

[31] A. S. Lalos and K. Berberidis, "An efficient conjugate gradient method in the frequency domain: Application to channel equalization," *Signal Processing*, vol. 88, pp. 99-116, Jan. 2008.

[32] S. Gezici, C. Mung, H. V. Poor and H. Kobayashi, "A genetic algorithm based finger selection scheme for UWB MMSE rake receivers," *IEEE International Conf. on UWB (ICUWB)*, pp. 164-169, Sept. 2005.

[33] J. Zhang, T. D. Abhayapala and R. A. Kennedy, "Principal components tracking algorithms for synchronization and channel identification in UWB systems," *IEEE Eighth International Symposium on Spread Spectrum Techniques and Applications (ISSSTA)*, pp. 369-373, Sept. 2004.

[34] S. H. Wu et al., "Multistage MMSE receivers for ultra-wide bandwidth impulse radio communications," *International Workshop on Ultra Wideband Systems, Joint with Conference on Ultrawideband Systems and Technologies.* pp. 16-20, May. 2004.

[35] Z. Tian, H. Ge and L. L. Scharf, "Low-complexity multiuser detection and reduced-rank Wiener filters for ultra-wideband multiple access," *IEEE International Conference on Acoustics, Speech, and Signal Processing (ICASSP)*, vol. 3, pp. 621-624, Mar. 2005.

[36] Y. Tian and C. Yang, "Reduced-order Multiuser Detection in Multi-rate DS-UWB Communications," *IEEE International Conference on Communications (ICC)*, vol.10, pp. 4746-4750, Jun. 2006.

[37] Q. Z. Ahmed and L. L. Yang, "Reduced-Rank Adaptive Multiuser Detection in Hybrid Direct-Sequence Time-Hopping Ultrawide Bandwidth Systems," *IEEE Trans. Wireless Communications*, vol. 9, no. 1, pp. 156-167, Jan. 2010.

[38] G. Kutz and D. Raphaeli, "Determination of Tap Positions for Sparse Equalizers," *IEEE Trans. Communications*, vol.55, no. 9, pp. 1712-1724, Sept. 2007.

[39] S. Burykh and K. Abed-Meraim, "Reduced-rank adaptive filtering using Krylov subspace," *EURASIP Journal on Applied Signal Processing*, vol. 12, pp. 1387-1400, 2002.

[40] A. M. Haimovich and Y. Bar-Ness, "An eigenanalysis interference canceler," *IEEE Trans. Signal Processing*, vol. 39, no. 1, pp. 76-84, Jan. 1991.

[41] J. S. Goldstein and I. S. Reed, "Reduced-rank adaptive filtering," *IEEE Trans. Signal Processing*, vol. 45, no. 2, pp. 492-496, Feb. 1997.

[42] M. L. Honig and J. S. Goldstein, "Adaptive reduced-rank interference suppression based on the multistage wiener filter," *IEEE Trans. Communications*, vol. 50, no. 6, pp. 986-994, Jun. 2002.

[43] J. D. Hiemstra, *Robust Implementations of the Multistage Wiener Filter*, PhD. thesis of Virginia Polytechnic Institute and State University, Apr. 2003.

[44] J. S. Goldstein,I. S. Reed, and L. L. Scharf, "A multistage representation of the Wiener filter based on orthogonal projections," *IEEE Trans. Information Theory*, vol. 44, no. 11, pp. 2943-2959, Nov. 1998.

[45] M. L. Honig and W. Xiao, "Performance of reduced-rank linear interference suppression," *IEEE Trans. Information Theory*, vol. 47, no. 5, pp. 1928-1946, 2001.

[46] D. A. Pados and S. N. Batalama, "Joint space-time auxiliary-vector filtering for DS/CDMA systems with antenna arrays," *IEEE Trans. Communications*, vol. 47, no. 9, pp. 1406-1415, Sep. 1999.

[47] D. A. Pados and G. N. Karystinos, "An iterative algorithm for the computation of the MVDR filter," *IEEE Trans. Signal Processing*, vol. 49, no. 2, pp. 290-300, Feb. 2001.

[48] W. Chen, U. Mitra and P. Schniter, "On the equivalence of three reduced rank linear estimators with applications to DS-CDMA," *IEEE Trans. Information Theory*, vol. 48, no. 9, pp. 2609-2614, Sep. 2002.

[49] R. C. de Lamare and R. Sampaio-Neto, "Adaptive Reduced-Rank MMSE Filtering with Interpolated FIR Filters and Adaptive Interpolators," IEEE Signal Processing Letters, vol. 12, no. 3, March 2005.

[50] R. C. de Lamare and R. Sampaio-Neto, "Adaptive reduced-rank MMSE parameter estimation based on an adaptive diversity-combined decimation and interpolation scheme," USPTO Application No.11/427.47- Patent Pending.

[51] R. C. de Lamare and R. Sampaio-Neto, "Reduced-rank adaptive filtering based on joint iterative optimization of adaptive filters," *IEEE Signal Processing Letter*, vol. 14, no. 12, pp. 980-983, Dec. 2007.

[52] M. Honig, U. Madhow and S. Verdu, "Blind adaptive multiuser detection," *IEEE Trans. Information Theory*, vol. 49, no. 9, pp. 1642-1648, Sept. 2001.

[53] R. C. de Lamare and R. Sampaio-Neto, "Low-Complexity Variable Step-Size Mechanisms for Stochastic Gradient Algorithms in Minimum Variance CDMA Receivers," *IEEE Trans. Signal Processing*, vol. 54, no. 6, pp. 2302-2317, Jun. 2006.

[54] C. Xu, G. Feng and K. S. Kwak, "A Modified Constrained Constant Modulus Approach to Blind Adaptive Multiuser Detection," *IEEE trans. Communications*, vol. 49, no. 9, pp. 1642-1648, Sept. 2001.

[55] R. C. de Lamare and R. Sampaio-Neto, "Blind Adaptive Code-Constrained Constant Modulus Algorithms for CDMA Interference Suppression in Multipath Channels," *IEEE Communications Letters*, vol. 9, no. 4, pp. 334-336, Apr. 2005.

[56] R. C. de Lamare, M. Haardt and R. Sampaio-Neto, "Blind Adaptive Constrained Reduced-Rank Parameter Estimation Based on Constant Modulus Design for CDMA Interference Suppression," *IEEE Trans. Signal Processing*, vol. 56, no. 6, pp. 2470-2482, Jun. 2008.

[57] P. Liu, and Z. Xu, "Blind MMSE-Constrained Multiuser Detection," *IEEE Trans. Vehicular Technology*, vol. 57, no. 1, pp. 608-615, Jan. 2008.

[58] J. Miguez and L. Castedo, "A Linearly Constrained Constant Modulus Approach to Blind Adaptive Multiuser Interference Suppression," *IEEE Communications Letters*, vol. 2, no. 8, pp. 217-219, Aug. 1998.

[59] G. S. Biradar, S. N. Merchant and U. B. Desai, " Performance of Constrained Blind Adaptive DS-CDMA UWB Multiuser Detector in Multipath Channel with Narrowband Interference ," *IEEE GLOBECOM 2008*, pp. 1-5 , Dec. 2008.

[60] J. Liu and Z. Liang, "Linearly Constrained Constant Modulus Algorithm Based Blind Multi-User Detection for DS-UWB Systems," *IEEE WiCom 2007*, pp. 578-581 , Sept. 2007.

[61] Z. Xu, P. Liu and J. Tang, "A Subspace Approach to BlindMultiuser Detection for Ultra-Wideband Communication Systems," *EURASIP Journal on Applied Signal Processing: Special Issue on UWB - State of the Art*, vol. 2005, no. 3, pp. 413-425, Mar. 2005.

[62] R. C. de Lamare, R. Sampaio-Neto, "Blind adaptive MIMO receivers for space-time block-coded DS-CDMA systems in multipath channels using the constant modulus criterion," *IEEE Trans. Communications*, vol. 58, no. 1, pp. 21-27, Jan. 2010.

[63] H. Liu and G. Xu, "A subspace method for signature waveform estimation in synchronous CDMA systems," *IEEE Trans. Communications*, vol. 44, pp. 1346-1354, Oct. 1996.

[64] X. G. Doukopoulos and G. V. Moustakides, "Adaptive power techniques for blind channel estimation in CDMA systems," *IEEE Trans. Signal Processing*, vol. 53, no. 3, pp. 1110-1120, Mar. 2005.

[65] P. Kaligineedi and V. K. Bhargava, "Frequency-Domain Turbo Equalization and Multiuser Detection for DS-UWB Systems," *IEEE Trans. Wireless Communications*, vol. 7, no. 9, pp. 3280-3284, Sept. 2008.

[66] Y. Wang and X. Dong, "Comparison of Frequency Offset and Timing Offset Effects on the Performance of SC-FDE and OFDM Over UWB Channels," *IEEE Trans. Vehicular Technology*, vol. 58, no. 1, pp.242-250, Jan. 2009.

[67] Y. Wang and X. Dong, "Frequency-Domain Channel Estimation for SC-FDE in UWB Communications," *IEEE Trans. Communications*, vol. 54, no. 12, pp.2155-2163, Dec. 2006.

[68] M. X. Chang and C.C. Yang, "A Novel Architecture of Single-Carrier Block Transmission DS-CDMA," in *IEEE Vehicular Technology Conference (VTC)*, Sept. 2006.

[69] H. Sato and T. Ohtsuki, "Frequency domain channel estimation and equalisation for direct sequence- ultra wideband (DS-UWB) system," *Proc. IEE Communications*, vol. 153,pp. 93-98, Feb. 2006.

[70] Y. Tang and B. Vucetic, "The FFT-based Multiuser Detection for DS-CDMA Ultra-Wideband Communication systems," in *International Workshop on Ultra Wideband*, pp.111-115, May. 2004.

[71] S. Morosi and T. Bianchi, "Frequency Domain Dectectors for Ultra-wideband Indoor Communications ," *IEEE Trans. Wireless Communications*, vol. 5, no. 10, pp. 2654-2658, Oct. 2006.

[72] M. Morelli, L. Sanguinetti and U. Mengali, "Channel Estimation for Adaptive Frequency-Domain Equalization," *IEEE Trans. Wireless Communications*, vol. 4, no. 5, pp. 2508-2518, Sep. 2005.

[73] D. G. Luenberger, *Linear and Nonlinear Programming*, 2nd ed, London:Kluwer Academic, 2003.

[74] W. M. Younis et al., "Adaptive frequency-domain equalization of space-time block-coded transmissions," in *IEEE International Conference on Acoustics, Speech, and Signal Process. (ICASSP)*, 2002.

[75] A. Parihar, L. Lampe, R. Schober and C. Leung, "Analysis of equalization for DS-UWB systems," *IEEE International Conference on UWB (ICUWB).*, pp. 170-175, Sept. 2005.

[76] M. Hamalainen et al., "On the UWB System Coexistence With GSM900, UMTS/WCDMA, and GPS," *IEEE Journal on Selected Areas in Communications*, vol. 20, no. 9, pp. 1712-1721, Dec. 2002.

[77] J. A. Wepman,"Analog-to-digital converters and their applications in radio receivers," *IEEE Communications Magazine*, vol. 33, no. 5, pp. 39-45, May. 1995.

[78] L. Xiao, M. Johansson, H. Hindi, S. Boyd, and A. Goldsmith, "Joint optimization of wireless communication and networked control systems," Chapter in Switching and Learning, Springer Lecture Notes in Computer Science 3355, pp. 248-272, Sept. 2005.

[79] X. Chu and R. D. Murch, "The effect of NBI on UWB time-hopping systems," *IEEE Trans. Wireless Communications* vol. 3, no. 5, pp. 1431-1436, Sept. 2004.

[80] C. Meyer, *Matrix Analysis and Applied Linear Algebra*, John Wiley, 2000, Chapter 3.

[81] H. Sari, G. Karam and I. Jeanclaude, "Transmission techniques for digital terrestrial TV broadcasting," *IEEE Communications Magazine*, vol. 33, no. 2, pp. 100-109, Feb. 1995.

[82] W. C. Wu and K.C. Chen, "Identification of Active Users in Synchronous CDMA Multiuser Detection," *IEEE Journal on Selected Areas Communications*, vol. 16, no. 9, pp1723-1735, Dec. 1998.

[83] R. O. Schmidt, "Multiple Emitter Location and Signal Parameter Estimation," *IEEE Trans. Antennas and Propagation*, vol. AP-34, no. 3, pp276-280, Mar. 1986.

[84] S. M. Kay, *Fundamentals of Statistical Signal Processing: Estimation Theory*, Upper Saddle River, NJ:Prentice Hall, 1993.

[85] Y. C. Eldar, A. Ben-Tal and A. Nemirovski, "Robust Mean-Squared Error Estimation in the Presence of Model Uncertainties," *IEEE Journal on Signal Processing*, vol. 53, no. 1, pp. 168-181, Jan. 2005.

[86] S. Kay and Y. C. Eldar, "Rethinking Biased Estimation," *IEEE Signal Processing Magazine*, pp. 133-136, May. 2008.

[87] W. James and C. Stein, "Estimation with quadratic loss," *Proc. 4th Berkeley Symp. Mathematical Statistics and Probability, Berkeley, CA*, vol. 1, pp.361-379, 1961.

[88] J. R. Thompson, "Some Shrinkage Techniques for Estimating the Mean," *Journal of the American Statistical Association*, vol. 63, no. 321, pp. 113-122, Mar. 1968.

[89] M. E. Bock, "Minimax estimators of the mean of a multivariate normal distribution," *The Annals of Statistics*, vol. 3, no. 1, pp. 209-218, Jan. 1975.

[90] B. Efron and C. Morris, "Data analysis using Stein's estimator and its generalizations," *Journal of the American Statistical Association*, vol. 70, no. 350, pp. 311-319, Jun. 1975.

[91] T. Kubokawa, "An approach to improving the James-Stein estimator ," *Journal of Multivariate Analysis*, vol. 36, no. 1, pp. 311-319 Jan. 1991.

[92] J. H. Manton, V. Krishnamurthy and H. V. Poor, "James-Stein State Filtering Algorithms," *IEEE Trans. Signal Processing*, vol. 46, no. 9, pp. 2431-2447, Sep. 1998.

[93] Z. Ben-Haim and Y. C. Eldar, "Blind Minimax Estimation," *IEEE Transactions on Information Theory*, vol. 53, no. 9, pp. 3145-3157, Sep. 2007.

[94] G. Durisi and S. Benedetto, "Performance evaluation of TH-PPM UWB systems in the presence of multiuser interference," *IEEE Communication Letter*, vol. 7, pp. 224-226, May 2003.

[95] N. C. Beaulieu and S. Niranjayan, "New UWB Receiver Designs Based on a Gaussian-Laplacian Noise-Plus-MAI Model," *IEEE International Conference on Communications (ICC)*, 2007.

[96] S. M. Kay, *Fundamentals of Statistical Signal Processing: Estimation Theory*, Upper Saddle River, NJ:Prentice-Hall, 1993.

[97] H. L. Van Trees, *Detection, Estimation, and Modulation Theory, Part I: Detection, Estimation, and Linear Modulation Theory*, John Wiley & Sons, 2001.

[98] J. N. Laneman, D. N. C. Tse, and G. W. Wornell, "Cooperative diversity in wireless networks: efficient protocols and outage behavior," *IEEE Trans. Information Theory*, vol. 51, no. 12, pp. 3062-3080, Dec. 2004.

[99] K. Azarian, H. El Gamal, and P. Schniter, "On the achievable diversityvs- multiplexing tradeoff in half-duplex cooperative channels," *IEEE Trans. Information Theory*, vol. 51, no. 12, pp. 4152-4172, Dec. 2005.

[100] W. P. Siriwongpairat and etc., "Employing Cooperative Diversity for Performance Enhancement in UWB Communication Systems," *IEEE Wireless Communications and Networking Conference (WCNC)*, 2006.

[101] S. Zhu, K. K. Leung, and G. Anthony, "Distributed Cooperative Data Relaying for Diversity in Impulse-Based UWB Ad-Hoc Networks," *IEEE Trans. Wireless Communications*, vol. 8, no. 8, pp. 4037-4047, Aug. 2009.

[102] V. Lottici, A. D'Andrea and U. Mengali, "Channel Estimation for Ultra-Wideband Communications," *IEEE Journal on Selected Areas in Communications*, vol. 20, no. 12, pp. 1638-1645, Dec. 2002.

[103] U. Madhow, "MMSE Interference Suppression for Timing Acquisition and Demodulation in Direct-Sequence CDMA Systems," *IEEE Trans. Communications*, vol. 46, no. 8, pp. 1065-1075, Aug. 1998.

[104] S. Yakun, V. Tripathi and M. L. Honig, "Adaptive turbo reduced-rank equalization for MIMO channels," *IEEE Trans. Wireless Communications*, vol. 4, no. 6, pp. 2789-2800, Nov. 2005.